AD-A111 590 CLARKSON COLL OF TECHNOLOGY POTSDAM NY F/G 17/9
ANALYSIS OF THE POLARIZATION DEPENDENCE OF THE INTERACTION BETW--ETC(U)
NOV 81 H R RAEMER F30602-78-C-0102
UNCLASSIFIED RADC-TR-81-244 NL

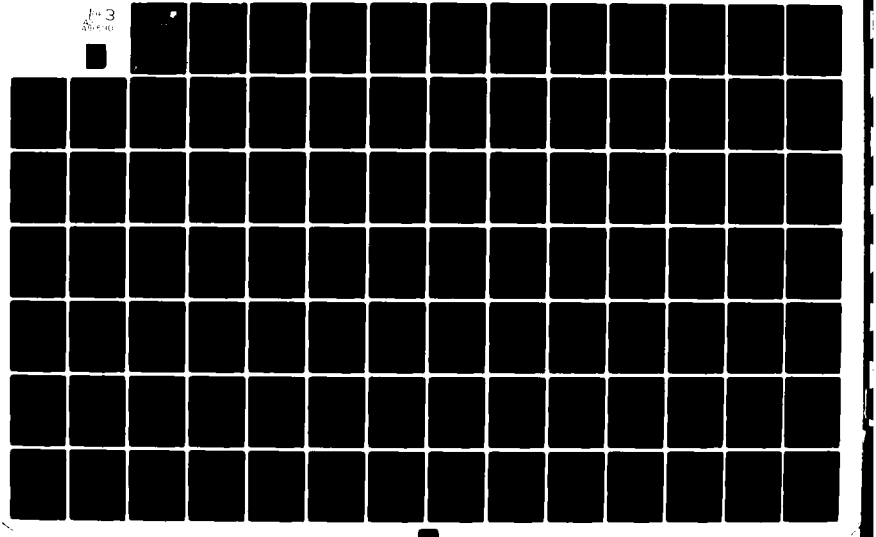

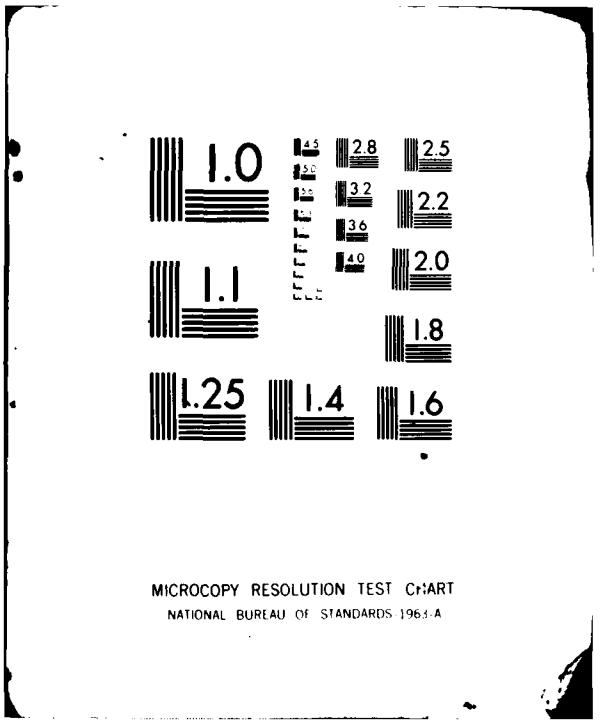
1.0
1.1
1.25
1.4
1.6
1.8
2.0
2.2
2.5
2.8
3.2
3.6
4.0
4.5
MICROCOPY RESOLUTION TEST CHART
NATIONAL BUREAU OF STANDARDS 1963-A

RADC-TR-81-244
Final Technical Report
November 1981

ANALYSIS OF THE POLARIZATION DEPENDENCE OF THE INTERACTION BETWEEN HUMAN FRAME TARGETS AND RADIO FREQUENCY SENSOR FIELDS

Clarkson College of Technology

Harold R. Raemer

This effort was sponsored by the Defense Nuclear Agency

ROME AIR DEVELOPMENT CENTER
Air Force Systems Command
Griffiss Air Force Base, New York 13441

This report has been reviewed by the RADC Public Affairs Office (PA) and is releasable to the National Technical Information Service (NTIS). At NTIS it will be releasable to the general public, including foreign nations.

RADC-TR-81-244 has been reviewed and is approved for publication.

APPROVED: Nicholas V. Karas

NICHOLAS V. KARAS
Project Engineer

APPROVED: Allan C. Schell

ALLAN C. SCHELL
Chief, Electromagnetic Sciences Division

FOR THE COMMANDER: John P. Huss

JOHN P. HUSS
Acting Chief, Plans Office

If your address has changed or if you wish to be removed from the RADC mailing list, or if the addressee is no longer employed by your organization, please notify RADC (EEC) Hanscom AFB MA 01731. This will assist us in maintaining a current mailing list.

Do not return copies of this report unless contractual obligations or notices on a specific document requires that it be returned.

UNCLASSIFIED

SECURITY CLASSIFICATION OF THIS PAGE (When Data Entered)

REPORT DOCUMENTATION PAGE		READ INSTRUCTIONS BEFORE COMPLETING FORM
1. REPORT NUMBER RADC-TR-81-244	2. GOVT ACCESSION NO.	3. RECIPIENT'S CATALOG NUMBER
4. TITLE (and Subtitle) ANALYSIS OF THE POLARIZATION DEPENDENCE OF THE INTERACTION BETWEEN HUMAN FRAME TARGETS AND RADIO FREQUENCY SENSOR FIELDS		5. TYPE OF REPORT & PERIOD COVERED Final Technical Report 8 May 79 - 16 Apr 81
		6. PERFORMING ORG. REPORT NUMBER N/A
7. AUTHOR(s) Harold R. Raemer		8. CONTRACT OR GRANT NUMBER(s) F30602-78-C-0102
9. PERFORMING ORGANIZATION NAME AND ADDRESS Clarkson College of Technology Potsdam NY 13676		10. PROGRAM ELEMENT, PROJECT, TASK AREA & WORK UNIT NUMBERS 62713H DNAR0215
11. CONTROLLING OFFICE NAME AND ADDRESS Deputy for Electronic Technology (RADC/EEC) Hanscom AFB MA 01731		12. REPORT DATE November 1981
		13. NUMBER OF PAGES 275
14. MONITORING AGENCY NAME & ADDRESS(if different from Controlling Office) Same		15. SECURITY CLASS. (of this report) UNCLASSIFIED
		15a. DECLASSIFICATION/DOWNGRADING SCHEDULE N/A

16. DISTRIBUTION STATEMENT (of this Report)

Approved for public release; distribution unlimited.

17. DISTRIBUTION STATEMENT (of the abstract entered in Block 20, if different from Report)

Same

18. SUPPLEMENTARY NOTES

RADC Project Engineer: Nicholas V. Karas (EEC)

This effort was sponsored by the Defense Nuclear Agency

19. KEY WORDS (Continue on reverse side if necessary and identify by block number)

Polarization dependence
Leaky coax
rf detection

20. ABSTRACT (Continue on reverse side if necessary and identify by block number)

An analytical model of a class of RF intrusion sensor systems was constructed. The constituents of the model are: a slotted coaxial cable laid circularly on the ground, an electromagnetic scatterer intended to simulate a human frame target in the vicinity of the cable and an antenna near the center of the circular configuration. Using the concept of a general electromagnetic field as a superposition of plane-wave fields ("plane-wave spectral representation of fields"), calculations were made

DD FORM 1 JAN 73 1473 EDITION OF 1 NOV 65 IS OBSOLETE

UNCLASSIFIED

SECURITY CLASSIFICATION OF THIS PAGE (When Data Entered)

of: (a) the fields from the cable slots as if the cable were in free space; (b) the effect of ground reflections on the fields from the slots; (c) the fields of the waves scattered from the human frame target directly toward the antenna in response to the incident wave fields [(a) plus (b)]; and (d) the effect of ground reflections on the scattered wave fields. These calculations were programmed for the VAX computer and some numerical results are presented for various orientations and positions of the human frame target.

Project Personnel

J. S. Rochefort - Principal Investigator

Harold R. Raemer - Lead Postdoctoral

Samuel Rosenthal - Scientific Programmer

Table of Contents

Section		Page
1.	Introduction	1-1 to 1-10
2.	Mathematical Modelling of RF Intrusion Sensor System	2-1 to 2-8
3.	Spectral Fields from a Rectangular Slot	3-1 to 3-6
4.	Spectral Fields from Slots in a Coaxial Cable Laid Circularly	4-1 to 4-28
5.	Plane-Wave Spectral Representation of Ground-Reflected Fields	5-1 to 5-13
6.	Fields Incident on the Scatterer-Coordinate Transformation at Input to Scattering Process	6-1 to 6-32
7.	The Barber Scattering Program	7-1 to 7-6
8.	Scattered Fields-Coordinate Transformation at Output of Scattering Process	8-1 to 8-9
9.	Effect of Ground Reflections on the Scattered Field	9-1 to 9-11
10.	Total Spectral Field at the Observation Point and Its Inverse Fourier Transform	10-1 to 10-10
11.	Numerical Results and Conclusions	11-1 to 11-89
References		R-1 to R-6
Appendix		
I.	Kirchhoff-Huyghens (or Stratton-Chu) Integral Formulas for Fields from Apertures	I-1 to I-4
II.	Plane-Wave Spectral Representation of Fields	II-1 to II-4
III.	Plane-Wave Spectral Representation of the Fields from an Aperture	III-1 to III-6
IV.	Electromagnetic Wave Propagation Along a Coaxial Cable	IV-1 to IV-19

1. INTRODUCTION

This is the final report on RADC Postdoctoral Contract No. CCT-SC-0102-442, Task Order 1. The work statement covering the portion of the project beginning May 8, 1979 and terminating on November 1, 1979 is presented below:

The objective of the project is to construct an analytical model of a class of RF intrusion sensor systems which can be used to predict their behavior under a wide range of conditions. There are a variety of RF intrusion sensor systems now in use or under development,[B-1 through B-9] but this work will be focussed on a specific configuration.[B-3,B-4,B-5,B-7] In this system a signal is generated at a point along a leaky coaxial cable[C-1 through C-14] laid out circularly on the periphery of an area to be protected.

A receiving antenna is mounted at or near the center of the area to respond to signal energy "leaking" from the small apertures placed along the cable. The entrance of an intruder perturbs the field in the vicinity of the cable and this perturbation is sensed by the antenna.

The work will be divided into four sequential tasks, as follows:

Task 1: A review of the pertinent literature to determine what analytical work has been done that is applicable to the problem. Particular attention will be focused on papers dealing with the fields generated by leaky coaxial cables[C-1 through C-14] and the perturbation of fields by various kinds of objects, including humans and animals.[D-1 through D-35]

Task 2: Generation of an analytical model for the specified configuration, using past results uncovered in Task 1 whenever they are applicable and generating new analysis if (as is already evident) the past work does not cover the entire problem. The model envisioned involves the use of theory already formulated on the fields around a leaky coaxial cable in free space, generalization

of that theory to include the effect of the ground on these fields, and finally the perturbation of the fields due to foreign objects entering the environment. Particular emphasis will be placed on the polarization characteristics of the unperturbed and perturbed fields, with a view toward the use of polarization changes as a means of identifying and tracking intruders.

Task 3: Construction of a Fortran program based on the analytical results obtained in Task 2. This program is expected to contain a large number of unspecified variables. Among those should be the radio frequency, constitutive parameters of the ground and those of foreign objects perturbing the fields, size and shape parameters of these objects, polarization characteristics of the fields and other variable parameters associated with the cable, receiving antenna and the intruding object.

Task 4: A parametric study based on the computer program constructed in Task 3 to determine the effects of various parameters on the expected behavior of the system.

*****

The contract was extended beyond November 1, 1979. However, there was a hiatus between that date and March 1980, when the second portion of the contract officially began. The extension covered the period from the above date to November 1, 1980.

The work statement for the second portion of the contract is presented below:

The objective of the project is to analyze a particular class of RF intrusion systems. Results will be used to predict their behavior under a wide range of conditions. There are a variety of RF intrusion systems now in use or under development, but this work focuses on a specific configuration. In this system a signal is generated at a point along a leaky coaxial cable

laid out circularly on the periphery of an area to be protected.

A receiving antenna is mounted at or near the center of the area to respond to signal energy "leaking" from the small apertures placed along the cable. The entrance of an intruder perturbs the field in the vicinity of the cable and this perturbation is sensed by the antenna.

Work on this problem was initiated in May 1979. A comprehensive review of the pertinent literature was completed. An analytical model was constructed which includes (a) mathematical expressions for the fields generated by the cable slots in free space, (b) the effect of ground reflections on the fields from the slots, (c) a generalized mathematical model for the scattered fields not accounting for ground reflections of these fields, and (d) a computer program for the slot-induced fields both with and without ground reflections.

The subject task constitutes an enlargement of the scope of the work to include detailed results on the fields scattered from human frame targets. The projected phases of this task are:

Phase 1: An analysis of the scattering from human frame targets, where the target is modelled as a lossy dielectric of ellipsoidal or spheroidal shape.

Phase 2: Incorporation of the scattering results of Phase 1 into the generalized mathematical model. The scattered fields obtained will include the effect of the fields from the slots impinging directly on the target and the ground-reflected slot-induced fields also incident on the target.

Phase 3: Analysis of the effect of ground-reflections on the fields obtained in Phase 2.

Phase 4: Development of a computer program incorporating the results of the analysis done in Phases 1, 2 and 3 and containing the

previously developed program [see (d) above] as a subprogram.

Phase 5: Use of the computer program developed in Phase 4 to obtain a set of numerical results showing the variation of the signals received at the antenna with key system parameters.

*****

The report describes the very extensive mathematical analysis undertaken to meet the above objectives. Numerical results are presented for a limited range of parameter values. The limitations are those of time and cost. The analytical model and the resulting computer programs are sufficiently general to include the capability of treating a much wider range of geometries and parameter variations. The outputs of the project should be considered as two-fold. First, the particular geometries for which computer results are shown are of direct importance in themselves. Secondly, the computer program should be considered as an output of the work, since it could now be used to study a wide range of cases that may be of practical interest.

The body of the report is divided into 11 sections. There are also five appendices. Section 2 contains a mathematical description of the basic model of the system. The generic configuration being analyzed consists of: (1) a set of apertures, small compared with wavelength, on which electric and magnetic fields can be specified. These apertures are placed somewhere in the vicinity of a flat ground surface; (2) an electromagnetic scatterer modelled to resemble an "intruder"; (3) an antenna, placed at an arbitrary point, which receives signals resulting from the field distributions on the apertures. The received signals are influenced by the presence of the ground and should also be influenced by the presence of the intruder. It is clear that the major objective of the work is to determine the magnitude and polarization of the fields at the receiving antenna both with and without the presence of the intruder and to

determine the effect of the intruder's presence on the magnitude and polarization of the fields.

In order to obtain numerical results, it is of course necessary to specify more tightly the set of apertures, the scatterer used to represent the intruder and the location of the antenna. Hence, in the situation actually modelled on the computer, the apertures are small slots along a coaxial cable laid along the ground surface in a circular pattern. The antenna is somewhere near, but not necessarily exactly at, the center of this circular configuration. The scatterer is a spheroid somewhere near the cable. The spheroid must have uniform constitutive parameters but aside from that constraint is not restricted, since it is in general a lossy dielectric. The frequency range of validity of the analysis is roughly from 50MHz to 500MHz, implying a wavelength range between roughly 0.6 and 6 meters. The cable diameter is less than two centimeters and the length of each slot on the cable is less than one centimeter, hence slot dimensions are always small compared with wavelength. This is a feature that simplifies the analysis somewhat.

It was not possible within the time and cost constraints of the project to model the cable fields, the scatterer and the effect of the ground in a rigorous manner. "Engineering approximations" were necessary to render the analysis feasible. Before delineating these approximations, we will first describe the basic methodology.

The electric and magnetic fields were all expressed as superpositions of plane waves. This "plane wave spectrum" type of analysis can be viewed as a process of three-dimensional Fourier transformation from the space of a set of three position coordinates (x, y, z) to the space of a set of three components of a wave propagation vector $k_o \underset{\rightarrow}{\beta} = (k_o \beta_x, k_o \beta_y, k_o \beta_z)$. Since k_o, the propagation constant of free space, is a constant, we deal with the vector

space (β_x, β_y, β_z), subject to the constraint $\beta_x^2 + \beta_y^2 + \beta_z^2 = 1$. Because of that constraint, only two of the components β_x, β_y or β_z (say β_x, β_y) can be specified independently and the other (say β_z) can be calculated therefrom. Hence, the process degenerates to a <u>two-dimensional</u> Fourier transformation between two position coordinates (say x, y) and two components of $\underset{\sim}{\beta}$ (say β_x, β_y).

Section II of the report describes the general mathematical modelling of the problem. The plane-wave spectrum of the field at the antenna consists of four contributions, as follows:

(1) the direct wave from the slots in the cable [as if the ground and intruder (scatterer) were not present]

(2) the ground-reflected wave from the slots in the absence of an intruder (scatterer)

(3) the field scattered by the intruder directly into the antenna

(4) the ground-reflected field at the antenna resulting from scattering by the intruder.

The plane-wave spectrum type of modelling enables us to determine the contributions (2) and (4) using standard theory of reflection of a plane-wave from an infinite surface. Another very important reason for using that type of modelling is the fact that the scattering program we are using (the best available, in the writer's opinion, for the purpose at hand) assumes a plane-wave input. Thus, by considering the fields at every stage of the process as the fields of a plane-wave, we are enhancing the accuracy of the calculations (as compared with approximating fields of spherical waves or near-zone waves or other more complicated field patterns as plane-waves).

However, the negative feature of this kind of modelling is that it necessitates a process of inverse two-dimensional Fourier transformation at the last stage of the calculation in order to convert the field spectra,

functions of (β_x, β_y), into functions of the horizontal position coordinates (x, y). That process is computer-time intensive and, hence, the computations require more computer time than would simpler but more approximate modelling schemes we could have used.

Section 3 and Appendix I contain material on the method variously called the "Kirchhoff-Huyghens" or "Stratton-Chu" integral method of determination of the fields at an arbitrary point in space due to fields on a closed surface surrounding that point. This technique, widely used in antenna theory, is our method of calculating the fields from the slots along the cable. The method is presented in general in Appendix I. In Appendix II the general concept of the plane-wave spectral representation of fields is presented. Appendix III covers the spectral representation of the fields from an aperture as calculated using the Kirchhoff-Huyghens integral method. Section 3 of the main body of the report specializes the analysis in Appendix III to the case of the rectangular slot. The use of a rectangular slot shape for mathematical convenience is an approximation to the actual shape of slots on the cable of central interest. However, since slot dimensions are small compared with wavelength, the results are not significantly dependent on slot <u>shape</u> but only on slot <u>area</u> regardless of shape.

Section 4 specializes the analysis in Section 3 to the specific case of a slotted coaxial cable laid in a circular pattern, which is the actual case treated in our numerical work. The wave modes propagating in the cable are detailed in Appendix IV. The analysis in Section 4 is the basis of Subroutine SOURCE, which is our computer program to evaluate the fields from the cable as if the cable were in free space.

Section 5 treats the reflection of plane-wave fields from the ground surface. This analysis is the basis for a section in the main program which

is applied twice, first to the field from the cable, and secondly to the field from the scatterer.

Section 6 treats the coordinate transformations required to enter the scattering program. The latter is called "Subroutine BARBER", after Professor Peter Barber of the Bioengineering Department at the University of Utah, who developed the program and kindly gave us the program cards for use in Northeastern's VAX computer. Barber's program, discussed in Section 7, considers an incoming plane-wave specified by a magnitude and polarization in a "lab frame" (Barber's terminology) coordinate system. The basic coordinate system used in our problem, which we call the "ground frame", is the coordinate system in which our "Subroutine SOURCE" delivers the field components from the cable back into the main program. In the main program, the ground reflection operation is performed, and the superposition of plane-wave spectra of direct and ground-reflected source fields is then evaluated. The resultant field components are expressed in the ground frame. The analysis discussed in Section 6 describes the transformation of field components between Barber's lab frame and our ground frame, so that the input to Barber's scattering program can be expressed in his lab frame. The program to implement the analysis in Section 6 is called "Subroutine BIS" ("Barber Input Subroutine").

As indicated above, the Barber scattering program is discussed in Section 7. In Section 8, we present the coordinate transformation required to transform the output of the scattering program, i.e., the scattered field components, from Barber's lab frame, in which these components are expressed in his program, back to the ground frame. The program based on this analysis is called "Subroutine BOS" ("Barber Output Subroutine").

In Section 9 we describe the analysis of the effect of ground reflection on the scattered field. Computationally, the implementation of this analysis

is accomplished in the main program, which receives from Subroutine BARBER via Subroutine BOS the scattered waves in two directions, one being that directed from the center of the scatterer to the antenna position, the other being that directed from the center of the scatterer to a "ground reflection point", which, as dictated by the law of reflection, sends the ground-reflected wave toward the antenna. The first of these scattered fields is logged in the main program as that received by the antenna [Contribution (3)] and the second is driven through the ground-reflection process in the main program and the result becomes Contribution (4) at the antenna.

The justification for considering scattering in only these two directions as opposed to all directions (which would have required prohibitively large computer time and would have required still another double Fourier transformation), is the fact that the scatterer is in the far-zone of the antenna and subtends a very small angle at the antenna, so that the antenna sees it as very nearly a point source. Hence, it appears as a plane-wave at the antenna. Barber's scattering program produces a plane-wave in any given direction, which when multiplied by the Green's function $e^{jk_o r}/r$, can be viewed by an observer at the antenna as a spherical wave from that direction, the curvature of whose phase front is negligible, i.e., equivalent to a plane-wave weighted by $\frac{1}{r}$. The ground-reflected scattered wave, to be treated rigorously, would require that scattered plane-waves in all directions be reflected from the ground and that the wave seen at the antenna is the superposition of all of these waves. However, the theory of the plane-wave spectral representation of fields[A-1,A-2] shows that, if the receiving point is sufficiently far away, the only significant contribution is that which obeys the law of reflection. Hence, according to this approximation, in view of the large distance between the antenna and the scatterer, and the fact that they are each in the other's "far

zone", it is sufficient to consider only one ground-reflected plane-wave from a single ground-reflection point. Invoking this approximation saves an enormous amount of computer time since it saves us from another round of double Fourier transformations.

Section 10 contains the analytical basis for the way in which the overall computation must be done to provide for the inverse Fourier transformation of the composite fields. This is done in the main program, with the aid of two small subroutines labeled COMPUTECO and COMPUTEEF. The first of these subroutines performs a numerical integration of each component of the spectral field vector on the angle ϕ_β [= $\tan^{-1}(\beta_y/\beta_x)$] from 0 to 2π. The second performs another numerical integration on β_h (= $\sqrt{\beta_x^2 + \beta_y^2}$) from 0 to 1. This double integration procedure is done in computing the inverse Fourier transform of the field components at the antenna in the absence of the scatterer.

It was attempted to carry out this same procedure in the case where the scatterer is present. In this case, the inverse Fourier transform must be computed at the position of the center of the scatterer, rather than the antenna position. It was found that, with the scatterer present, computer time becomes prohibitively large when the above procedure is used. It was decided to make use of the stationary phase principle to evaluate (approximately) the integral on ϕ_β analytically. A justification for the use of this method is presented in Section 10.

Section 11 contains numerical results and conclusions therefrom.

2. MATHEMATICAL MODELLING OF RF INTRUSION SENSOR SYSTEM

The generic system that is the subject of this study is shown in Figure 2.1. The point 0 on the diagram is the origin of coordinates.

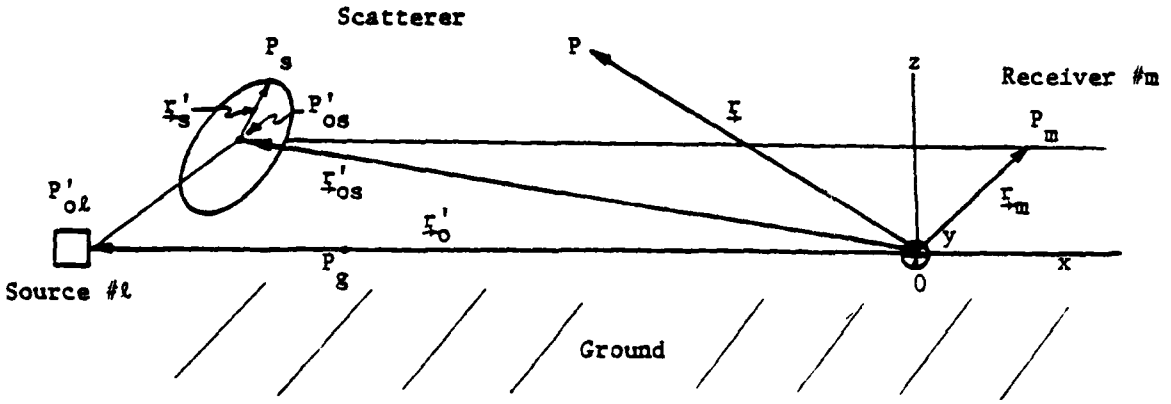

Figure 2-1. Generic Free-space System Geometry

Consider a collection of N sources numbered with an index ℓ ranging from 1 through N. The source numbered ℓ is centered at a position $P'_{o\ell}$ designated by a vector $\underline{r}'_{o\ell}$ originating at 0 and terminating on $P'_{o\ell}$. It occupies a small volume around the point $P'_{o\ell}$, but this volume is assumed to subtend a very small solid angle when viewed from the position of a receiving point and hence appears to be a point source at the receiving point. There may be a number of receiving points; hence they are numbered with an index m, ranging from 1 through M. The m^{th} receiving point P_m is designated by a vector $\underline{r}_m$, originating at 0 and terminating on P_m.

The scatterer is centered at a point P_{os}, designated by a vector $\underline{r}_{os}$

originating at 0 and terminating on P_{os}.

The point P is an arbitrary point in space, designated by a vector $\underset{\rightarrow}{r}$ emanating from 0 and terminating on P.

We denote the electric field vector at the point P due to excitation of the ℓ^{th} source by a three-element column vector $[\underset{\rightarrow}{E}_\ell(\underset{\rightarrow}{r}_m)]$ whose elements are the rectangular components of $\underset{\rightarrow}{E}$ in the basic (x,y,z) coordinate system. This system, as shown in Figure 2.1, has its z-axis in the vertical direction (upward) and its (x,y) plane along the ground surface. Thus, the electric field at the arbitrary point P due to excitation at source ℓ is:

$$[\underset{\rightarrow}{E}_\ell(\underset{\rightarrow}{r})] = \begin{bmatrix} E_{\ell x}(\underset{\rightarrow}{r}) \\ E_{\ell y}(\underset{\rightarrow}{r}) \\ E_{\ell z}(\underset{\rightarrow}{r}) \end{bmatrix} \tag{2.1}$$

Using the plane-wave spectral representation for the electric field[A-1,A-2] (Appendix II, Eq. II-3), we have

$$[\underset{\rightarrow}{E}_\ell(\underset{\rightarrow}{r})] = \iint_{-\infty}^{\infty} d^2\,\underset{\rightarrow}{\beta}_h\, e^{jk\underset{\rightarrow}{\beta}_h\cdot\underset{\rightarrow}{\rho}} \{e^{-jk|\beta_z|z}[\tilde{\underset{\rightarrow}{E}}_{\ell-}(\underset{\rightarrow}{\beta}_h) + e^{jk|\beta_z|z}[\tilde{\underset{\rightarrow}{E}}_{\ell+}(\underset{\rightarrow}{\beta}_h)]\} \tag{2.2}$$

where $\underset{\rightarrow}{r} = \underset{\rightarrow}{\rho} + \hat{\underset{\rightarrow}{z}}z$; $\underset{\rightarrow}{\rho} = x\hat{\underset{\rightarrow}{x}} + y\hat{\underset{\rightarrow}{y}}$

$$|\beta_z| = \sqrt{1 - \beta_h^2}\ ;\quad \beta_h = \hat{\underset{\rightarrow}{x}}\beta_x + \hat{\underset{\rightarrow}{y}}\beta_y\ ;$$

- and + refer to the cases $\beta_z = -|\beta_z|$ (downward propagation) and $\beta_z = +|\beta_z|$ (upward propagation), respectively.

where

$$[\tilde{\underset{\rightarrow}{E}}_{\ell\mp}(\underset{\rightarrow}{\beta}_h)] = \begin{bmatrix} \tilde{E}_{\underset{\rightarrow}{\ell}\mp,x}(\underset{\rightarrow}{\beta}_h) \\ \tilde{E}_{\underset{\rightarrow}{\ell}\mp,y}(\underset{\rightarrow}{\beta}_h) \\ \tilde{E}_{\underset{\rightarrow}{\ell}\mp,z}(\underset{\rightarrow}{\beta}_h) \end{bmatrix}$$

The magnetic field vector at P_m due to excitation at source ℓ is given by

$$[\underset{\rightarrow}{H}_\ell(r_m)] = \iint_{-\infty}^{\infty} d^2\,\underset{\rightarrow}{\beta}_h\, e^{jk\underset{\rightarrow}{\beta}_h\cdot\underset{\rightarrow}{\rho}_m} \{e^{-jk|\beta_z|z_m}[P_-(\underset{\rightarrow}{\beta}_h)][\tilde{E}_{\underset{\rightarrow}{\ell}-}(\underset{\rightarrow}{\beta}_h)]$$

$$+ e^{jk|\beta_z|z_m}[P_+(\underset{\rightarrow}{\beta}_h)][\tilde{E}_{\underset{\rightarrow}{\ell}+}(\underset{\rightarrow}{\beta}_h)]\} \qquad (2.3)$$

where (from the Maxwell equations $\underset{\rightarrow}{H} = \frac{1}{j\omega\mu_o}\nabla \times \underset{\rightarrow}{E}$)

$$P_{\mp}(\underset{\rightarrow}{\beta}_h) = \sqrt{\frac{\epsilon_o}{\mu_o}} \begin{bmatrix} 0 & \pm|\beta_z| & \beta_y \\ \mp|\beta_z| & 0 & -\beta_x \\ -\beta_y & \beta_x & 0 \end{bmatrix} \qquad (2.4)$$

The fields $\underset{\rightarrow}{E}_\ell$ and $\underset{\rightarrow}{H}_\ell$ have four contributions as follows:

$$[\underset{\rightarrow}{E}_\ell(\underset{\rightarrow}{r})] = [\underset{\rightarrow}{E}_\ell^{(a)}(\underset{\rightarrow}{r})] + [\underset{\rightarrow}{E}_\ell^{(b)}(\underset{\rightarrow}{r})] + [\underset{\rightarrow}{E}_\ell^{(c)}(\underset{\rightarrow}{r})] + [\underset{\rightarrow}{E}_\ell^{(d)}(\underset{\rightarrow}{r})] \qquad (2.5a)$$

$$[\underset{\rightarrow}{H}_\ell(\underset{\rightarrow}{r})] = [\underset{\rightarrow}{H}_\ell^{(a)}(\underset{\rightarrow}{r})] + [\underset{\rightarrow}{H}_\ell^{(b)}(\underset{\rightarrow}{r})] + [\underset{\rightarrow}{H}_\ell^{(c)}(\underset{\rightarrow}{r})] + [\underset{\rightarrow}{H}_\ell^{(d)}(\underset{\rightarrow}{r})] \qquad (2.5b)$$

where the superscripts a, b, c, d correspond to the following:

(a) Direct wave from source ℓ to point P in infinite free space (i.e., in absence of ground or scatterer)

(b) Reflected wave from ground due to excitation of source ℓ in absence of scatterer, as observed at point P

(c) Direct wave from scatterer (as if the scatterer were in infinite free space) where the fields incident on the scatterer consist of the superposition of the direct wave from $P'_{o\ell}$ to the scatterer and the ground-reflected wave at the scatterer resulting from excitation of source ℓ

(d) Ground-reflected wave at P in response to the scattered wave fields.

It will be shown in Section 5 (see 5.18a) that the plane wave spectrum of the reflected wave field (superscript (b)) is related to that of the incident wave field (superscript (a)) by the expression

$$[\tilde{\underset{\rightarrow}{E}}_{r+}(\underset{\rightarrow}{\beta}_h)] = [R_E(\underset{\rightarrow}{\beta}_h)][\tilde{\underset{\rightarrow}{E}}_{i-}(\underset{\rightarrow}{\beta}_h)] \tag{2.6}$$

where $[R_E(\underset{\rightarrow}{\beta}_h)]$ is given by Eq. (5.18a) and Eq. (5.19). The receiving point is always above ground-level; hence the subscripts and the incident wave at the ground reflecting point always propagate downward; + and - are used on the reflected and incident waves, respectively.

The plane-wave spectrum of the reflected wave as given by Eq. (2.6) corresponds to the wave with superscript (b) while the spectrum of the incident wave corresponds to that with superscript (a). Using these superscripts in their appropriate places in Eq. (2.2), with the aid of Eqs. (2.5a,b) and (2.6), we obtain the following results:

Case A: Presence of ground not accounted for; scatterer not present. Fields at point P are [see Eqs. (2.2) and (2.5a)]

$$[\underset{\rightarrow}{E}_{\ell}^{(a)}(\underset{\rightarrow}{r})]_{\text{case A}} \iint_{-\infty}^{\infty} d^2\,\underset{\rightarrow}{\beta}_h\, e^{jk\underset{\rightarrow}{\beta}_h\cdot\underset{\rightarrow}{\rho}}\, e^{-jk|\beta_z|z}\, \tilde{\underset{\rightarrow}{E}}_{\ell-}^{(a)}(\underset{\rightarrow}{\beta}_h) \qquad (2.7a)$$

if source is above P

$$\iint_{-\infty}^{\infty} d^2\,\underset{\rightarrow}{\beta}_h\, e^{jk\underset{\rightarrow}{\beta}_h\cdot\underset{\rightarrow}{\rho}}\, e^{jk|\beta_z|z}\, \tilde{\underset{\rightarrow}{E}}_{\ell+}^{(a)}(\underset{\rightarrow}{\beta}_h)$$

if source is below P.

where

$\tilde{\underset{\rightarrow}{E}}_{\ell\pm}^{(a)}(\underset{\rightarrow}{\beta}_h)$ = spectrum of electric field due to source ℓ in infinite free space,

and where

$\beta_z = +|\beta_z|$ for subscript +

$-|\beta_z|$ for subscript -

Also, from Eqs. (2.3), (2.4) and (2.5b)

$$[\underset{\rightarrow}{H}_{\ell}(\underset{\rightarrow}{r})]_{\text{case A}} = \iint_{-\infty}^{\infty} d^2\,\underset{\rightarrow}{\beta}_h\, e^{jk\underset{\rightarrow}{\beta}_h\cdot\underset{\rightarrow}{\rho}}\, e^{-jk|\beta_z|z}\, [P_-(\underset{\rightarrow}{\beta}_h)][\tilde{\underset{\rightarrow}{E}}_{\ell-}^{(a)}(\underset{\rightarrow}{\beta}_h)] \qquad (2.7b)$$

if source is above P

$$\iint_{-\infty}^{\infty} d^2\,\underset{\rightarrow}{\beta}_h\, e^{jk\underset{\rightarrow}{\beta}_h\cdot\underset{\rightarrow}{\rho}}\, e^{jk|\beta_z|z}\, [P_+(\underset{\rightarrow}{\beta}_h)][\tilde{\underset{\rightarrow}{E}}_{\ell+}^{(a)}(\underset{\rightarrow}{\beta}_h)]$$

if source is below P.

Case B: Presence of ground is accounted for; scatterer not present. The fields are (see Eqs. (2.2, (2.3), (2.4), (2.5a,b) and (2.6)).

$$[\underset{\rightarrow}{E}_{\ell}(r)]_{\text{case B}} = [\underset{\rightarrow}{E}_{\ell}^{(a)}(r)] + [\underset{\rightarrow}{E}_{\ell}^{(b)}(r)] \tag{2.8a}$$

$$[\underset{\rightarrow}{H}_{\ell}(r)]_{\text{case B}} = [\underset{\rightarrow}{H}_{\ell}^{(a)}(r)] + [\underset{\rightarrow}{H}_{\ell}^{(b)}(r)] \tag{2.8b}$$

where $[\underset{\rightarrow}{E}_{\ell}^{(a)}]$ and $[\underset{\rightarrow}{H}_{\ell}^{(a)}]$ are given in general by Eqs. (2.7a) and (2.7b), respectively, with the aid of Eq. (2.4), and where (from Eqs. (2.2), (2.3), (2.4), (2.5a,b) and (2.6)),

$$[\underset{\rightarrow}{E}_{\ell}^{(b)}(\underset{\rightarrow}{r})]_{\text{case B}} = \iint_{-\infty}^{\infty} d^2\,\underset{\rightarrow}{\beta}_h\, e^{jk\underset{\rightarrow}{\beta}_h\cdot\underset{\rightarrow}{\rho}} e^{jk|\beta_z|z}\,[R_E(\underset{\rightarrow}{\beta}_h)][\tilde{\underset{\rightarrow}{E}}_{\ell-}^{(a)}(\underset{\rightarrow}{\beta}_h)] \tag{2.9a}$$

$$[\underset{\rightarrow}{H}_{\ell}^{(b)}(\underset{\rightarrow}{r})]_{\text{case B}} = \iint_{-\infty}^{\infty} d^2\,\underset{\rightarrow}{\beta}_h\, e^{jk\underset{\rightarrow}{\beta}_h\cdot\underset{\rightarrow}{\rho}} e^{jk|\beta_z|z}\,[P_+(\underset{\rightarrow}{\beta}_h)][R_E(\underset{\rightarrow}{\beta}_h)][\tilde{\underset{\rightarrow}{E}}_{\ell-}^{(a)}(\underset{\rightarrow}{\beta}_h)] \tag{2.9b}$$

where $[P_+(\underset{\rightarrow}{\beta}_h)]$ is given by Eq. (2.4) and the matrix $[R_E(\underset{\rightarrow}{\beta}_h)]$ is given in Section 5 [Eqs. (5.18a) and (5.19)].

Case C: Presence of ground is accounted for in determination of the fields incident on the scatterer but not in evaluating the scattered field (i.e., ground-reflection of scattered wave is neglected). In this case, the fields at point P are: (see Eqs. (2.4 through 2.8b))

$$[\underset{\rightarrow}{E}_{\ell}(\underset{\rightarrow}{r})]_{\text{case C}} = [\underset{\rightarrow}{E}_{\ell}^{(a)}(\underset{\rightarrow}{r})] + [\underset{\rightarrow}{E}_{\ell}^{(b)}(\underset{\rightarrow}{r})] + [\underset{\rightarrow}{E}_{\ell}^{(c)}(\underset{\rightarrow}{r})] \tag{2.10a}$$

$$[H_\ell(\underset{\rightarrow}{r})]_{\text{case C}} = [H_{\underset{\rightarrow}{\ell}}^{(a)}(\underset{\rightarrow}{r})] + [H_{\underset{\rightarrow}{\ell}}^{(b)}(\underset{\rightarrow}{r})] + [H_{\underset{\rightarrow}{\ell}}^{(c)}(\underset{\rightarrow}{r})] \tag{2.10b}$$

where $[E_{\underset{\rightarrow}{\ell}}^{(a)}(\underset{\rightarrow}{r})]$, $[H_{\underset{\rightarrow}{\ell}}^{(a)}(\underset{\rightarrow}{r})]$, $[E_{\underset{\rightarrow}{\ell}}^{(b)}(\underset{\rightarrow}{r})]$ and $[H_{\underset{\rightarrow}{\ell}}^{(b)}(\underset{\rightarrow}{r})]$ are given by Eqs. (2.7a), (2.7b), (2.8a), (2.9a) and (2.8b), (2.9b), respectively, aided by Eqs. (2.2) through (2.6). The field vectors $[E_{\underset{\rightarrow}{\ell}}^{(c)}(\underset{\rightarrow}{r})]$ and $[H_{\underset{\rightarrow}{\ell}}^{(c)}(\underset{\rightarrow}{r})]$ will be discussed in what follows.

Referring to Figure 2.1, we can express the scattered field in the form

$$[E_{\underset{\rightarrow}{\ell}}^{(c)}(\underset{\rightarrow}{r})] = \iint_{-\infty}^{\infty} d^2\,\underset{\rightarrow}{\beta}_h\, e^{jk\underset{\rightarrow}{\beta}_h\cdot\underset{\rightarrow}{\rho}} \{\tilde{E}_{\underset{\rightarrow}{\ell}-}^{(c)}(\underset{\rightarrow}{\beta}_h)\, e^{-jk|\beta_z|z} + \tilde{E}_{\underset{\rightarrow}{\ell}+}^{(c)}(\underset{\rightarrow}{\beta}_h)\, e^{jk|\beta_z|z}\} \tag{2.11}$$

where

$$\tilde{E}_{\underset{\rightarrow}{\ell}-}^{(c)}(\ _h) = [\tilde{S}_-^{(-)}(\underset{\rightarrow}{\beta}_h)][\tilde{E}_{\underset{\rightarrow}{\ell}-}^{(a)+(b)}(\underset{\rightarrow}{\beta}_h)] + [\tilde{S}_+^{(-)}(\underset{\rightarrow}{\beta}_h)][\tilde{E}_{\underset{\rightarrow}{\ell}+}^{(a)+(b)}(\underset{\rightarrow}{\beta}_h)]$$

$$\tilde{E}_{\underset{\rightarrow}{+}}^{(c)}(\underset{\rightarrow}{\beta}_h) = [\tilde{S}_-^{(+)}(\underset{\rightarrow}{\beta}_h)][\tilde{E}_{\underset{\rightarrow}{\ell}-}^{(a)+(b)}(\underset{\rightarrow}{\beta}_h)] + [\tilde{S}_+^{(+)}(\underset{\rightarrow}{\beta}_h)][\tilde{E}_{\underset{\rightarrow}{\ell}+}^{(a)+(b)}(\underset{\rightarrow}{\beta}_h)]$$

and where

$$[\tilde{S}_-^{(-)}(\underset{\rightarrow}{\beta}_h)],\ [\tilde{S}_+^{(-)}(\underset{\rightarrow}{\beta}_h)],\ [\tilde{S}_-^{(+)}(\underset{\rightarrow}{\beta}_h)] \text{ and } [\tilde{S}_+^{(+)}(\underset{\rightarrow}{\beta}_h)]$$

are 3x3 matrices, and

$$[\tilde{E}^{(a)+(b)}_{\rightarrow\mp}(\beta_{\rightarrow h})] = [\tilde{E}^{(a)}_{\rightarrow\mp}(\beta_{\rightarrow h})] + [\tilde{E}^{(b)}_{\rightarrow\mp}(\beta_{\rightarrow h})]$$

We will not discuss the details of this constituent of the field at this point.

3. SPECTRAL FIELDS FROM A RECTANGULAR SLOT

We will approximate the slots in the cable as rectangular. Since the slots are always small relative to wavelength, the exact shape of the slot will not be critical. This supposition is borne out by the approximations that can be justified when actual parameter values are assigned, as will become evident later in this report.

Let us assign a set of coordinates $(x'_\ell, y'_\ell, z'_\ell)$ to the ℓ^{th} slot, together with a "length" L_ℓ in the x'_ℓ direction and a "width" W_ℓ in the y'_ℓ direction and a slot center located at a point $(x'_{\ell o}, y'_{\ell o}, z'_{\ell o})$. We note that the $(x'_\ell - y'_\ell)$ plane is in the plane of the slot and hence $z'_{\ell o} = 0$. We have not specified the origin of this coordinate system.

Referring to Appendix III, Eqs. (III.6a,b) and (III.7a,b), points on the slot are designated by a vector

$$\underset{\rightarrow}{r}' = \underset{\rightarrow}{r}'_\ell = \underset{\rightarrow}{r}'_{\ell o} + \Delta\underset{\rightarrow}{r}'_\ell \tag{3.1}$$

where $\underset{\rightarrow}{r}'_{\ell o}$ is the vector representing the center of the slots.

The vector referred to in Eqs. (III.6a,b) and (III.7a,b) emanates at the origin of the basic (x, y, z) coordinate system. Therefore, it would be correct to designate the vector $\underset{\rightarrow}{r}'_{\ell o}$ as follows:

$$\underset{\rightarrow}{r}'_{\ell o} = \hat{\underset{\rightarrow}{x}} x_{\ell o} + \hat{\underset{\rightarrow}{y}} y_{\ell o} + \hat{\underset{\rightarrow}{z}} z_{\ell o} \tag{3.2}$$

where $(x_{\ell o}, y_{\ell o}, z_{\ell o})$ are the slot center coordinates in the basic (x, y, z) system.

The vector $\Delta\underset{\rightarrow}{r}'_\ell$, on the other hand, which refers to the displacement of a

point on the slot surface from the slot center, should be expressed in the slot coordinates as

$$\Delta \underset{\rightarrow}{r}'_\ell = \hat{\underset{\rightarrow}{x}}'_\ell \, \Delta x'_\ell + \hat{\underset{\rightarrow}{y}}'_\ell \, \Delta y'_\ell \tag{3.3}$$

where $(\hat{\underset{\rightarrow}{x}}'_\ell, \hat{\underset{\rightarrow}{y}}'_\ell, \hat{\underset{\rightarrow}{z}}'_\ell)$ are the unit base vectors in the slot coordinate system and $\Delta x'_\ell$ and $\Delta y'_\ell$ are the displacements from the slot center in the x'_ℓ and y'_ℓ directions, respectively. There is no displacement in the z'_ℓ direction, so it is clear that $\Delta z'_\ell = 0$.

We will now make an additional assumption which will apply in every case considered, namely that the most general spatial dependence of key terms in the vector field components

$$\hat{\underset{\rightarrow}{n}}' \times \underset{\rightarrow}{E}, \; \hat{\underset{\rightarrow}{n}}' \cdot \underset{\rightarrow}{E}, \; \hat{\underset{\rightarrow}{n}}' \times \underset{\rightarrow}{H} \text{ and } \hat{\underset{\rightarrow}{n}}' \cdot \underset{\rightarrow}{H}$$

in Eqs. (III.6a,b) and (III.7a,b) is exponential in x'_ℓ and y'_ℓ. Moreover, the exponential dependence is the same for all four of these vectors. Mathematically, we can express this with the statements:

$$\hat{\underset{\rightarrow}{n}}' \times \underset{\rightarrow}{E} = \sum_n \underset{\rightarrow}{C}_{an\ell}(z'_\ell) \, e^{jk_o(\xi_n x'_\ell + \zeta_n y'_\ell)} \tag{3.4a}$$

$$\hat{\underset{\rightarrow}{n}}' \cdot \underset{\rightarrow}{E} = \sum_n C_{bn\ell}(z'_\ell) \, e^{jk_o(\xi_n x'_\ell + \zeta_n y'_\ell)} \tag{3.4b}$$

$$\hat{\underset{\rightarrow}{n}}' \times \underset{\rightarrow}{H} = \sum_n \underset{\rightarrow}{C}_{cn\ell}(z'_\ell) \, e^{jk_o(\xi_n x'_\ell + \zeta_n y'_\ell)} \tag{3.4c}$$

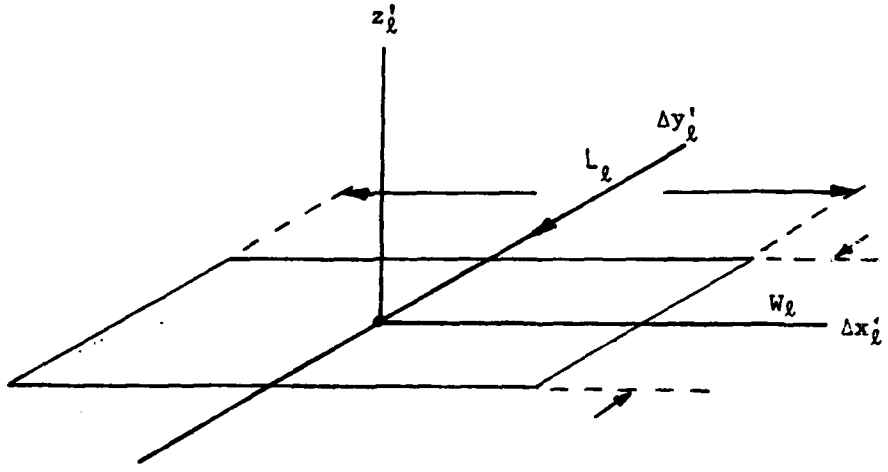

Figure 3-1. Slot Geometry

$$\hat{n}' \cdot \underset{\rightarrow}{H} = \sum_n C_{dn\ell}(z'_\ell)\, e^{jk_o(\xi_n x'_\ell + \zeta_n y'_\ell)} \tag{3.4d}$$

where it is indicated that the vectors $\underset{\rightarrow}{C}^{(\ell)}_{an\ell}$ and $\underset{\rightarrow}{C}_{cn\ell}$ and the scalars $C_{bn\ell}$ and $C_{dn\ell}$ are in general functions of z'_ℓ and ξ_n and ζ_n are in general complex.

We should carefully note here the fact that the coordinates $(x'_{\ell o}, y'_{\ell o}, z'_{\ell o})$ are the coordinates of the slot center in the $(x'_\ell, y'_\ell, z'_\ell)$ system. The origin of this system will generally be placed at the launching point for the energy that drives the source and this origin has no relationship to the origin of the basic (x, y, z) coordinate system. Failure to take note of this point could lead to confusion in the formulation of the equations to follow.

Substituting Eqs. (3.4a,b,c,d) into Eqs. (III.6a,b) and (III.7a,b), we would obtain [where $\underset{\rightarrow}{\beta}^{\pm} = \underset{\rightarrow}{\beta}_h \pm \hat{z}|\beta_z|$ and $\beta^{\pm}_{x'_\ell}$, $\beta^{\pm}_{y'_\ell}$, $\beta^{\pm}_{z'_\ell}$ are the $(x'_\ell, y'_\ell, z'_\ell)$ components of $\underset{\rightarrow}{\beta}^{\pm}$. Note that the components of $\underset{\rightarrow}{\beta}^{\pm}$ in the basic x, y, z system are β_x, β_y, $\pm|\beta_z|$ and the components of the slot center in that system are $x_{\ell o}$, $y_{\ell o}$, $z_{\ell o}$. [Also note that we have not indicated explicitly the spatial dependence of the modified spectral fields in what follows.]

$$[\underset{\rightarrow}{\tilde{E}}_{\pm}(\underset{\rightarrow}{\beta}_h)]_\ell = \frac{(j\,k_o)^2}{4\pi} \sum_n e^{-jk_o(\beta_x x_{\ell o} + \beta_y y_{\ell o} \pm |\beta_z| z_{\ell o})} \{[I^{\pm}_{\underset{\rightarrow}{E}}(\underset{\rightarrow}{\beta}_h)]_\ell\}_n \tag{3.5a}$$

$$---f^{\pm}$$

$$[\underset{\rightarrow}{\tilde{H}}_{\pm}(\underset{\rightarrow}{\beta}_h)]_\ell = \frac{(j\,k_o)^2}{4\pi} \sum_n e^{-jk_o(\beta_x x_{\ell o} + \beta_y y_{\ell o} \pm |\beta_z| z_{\ell o})} \{[I^{\pm}_{\underset{\rightarrow}{H}}(\underset{\rightarrow}{\beta}_h)]_\ell\}_n \tag{3.5b}$$

$$---f^{\pm}$$

where

$$\{[I^{\pm}_{\underset{\rightarrow}{E}}(\underset{\rightarrow}{\beta}_h)]_\ell\}_n = e^{jk_o(\xi_n x'_{\ell o} + \zeta_n y'_{\ell o})} \int_{-L_\ell/2}^{L_\ell/2} d(\Delta x'_\ell) e^{jk_o \Delta x'_\ell (\xi_n - \beta^{\pm}_{x',\ell})}$$

$$\cdot \int_{-W_\ell/2}^{W_\ell/2} d(\Delta y'_\ell)\, e^{jk_o \Delta y'_\ell (\zeta_n - \beta^{\pm}_{y',\ell})}$$

$$\cdot \{-Z_o \underset{\rightarrow}{C}_{cn\ell}(z'_{\ell o}) - [\underset{\rightarrow}{\beta}^{\pm} \times \underset{\rightarrow}{C}_{an\ell}(z'_{\ell o}) - \beta^{\pm} C_{bn\ell}(z'_{\ell o})]\} \tag{3.6a}$$

$$\{[I^{\pm}_{H}(\underset{\rightarrow}{\beta}_h)]_\ell\}_n = e^{jk_o(\xi_n x'_{\ell o} + \zeta_n y'_{\ell o})} \int_{-L_\ell/2}^{L_\ell/2} d(\Delta x'_\ell)\, e^{jk_o \Delta x'_\ell (\xi_n - \beta^{\pm}_{x'_\ell})}$$

$$\cdot \int_{-W_\ell/2}^{W_\ell/2} d(\Delta y'_\ell)\, e^{jk_o \Delta y'_\ell (\zeta_n - \beta^{\pm}_{y'_\ell})} \{Y_o \underset{\rightarrow}{C}_{an\ell}(z'_{\ell o})$$

$$- [\underset{\rightarrow}{\beta}^{\pm} \times \underset{\rightarrow}{C}_{cn\ell}(z'_{\ell o}) - \underset{\rightarrow}{\beta}^{\pm} C_{dn\ell}(z'_{\ell o})]\} \tag{3.6b}$$

The integrals in Eqs. (3.6a,b) are easily evaluated. They are "sinc" functions (i.e., $\frac{\sin x}{x}$) with complex arguments. Incorporating that fact into Eqs. (3.6a,b) with the aid of Eqs. (3.4a,b,c,d), we can summarize the results as follows:

$$[\underset{\rightarrow}{\tilde{E}}^{\pm}(\underset{\rightarrow}{\beta}_h)]_\ell = \frac{(j\,k_o)^2}{4\pi} \sum_n e^{-jk_o(\beta_x x_{\ell o} + \beta_y y_{\ell o} \pm |\beta_z| z_{\ell o})}\, e^{jk_o(\xi_n x'_{\ell o} + \zeta_n y'_{\ell o})}$$

$$\ldots \operatorname{sinc}\left[k_o(\beta^{\pm}_{x'_\ell} - \xi_n)\frac{L_\ell}{2}\right] \operatorname{sinc}\left[k_o(\beta^{\pm}_{y'_\ell} - \zeta_n)\frac{W_\ell}{2}\right]$$

$$\ldots \{-Z_o \underset{\rightarrow}{C}_{cn\ell}(z'_{\ell o}) + [\underset{\rightarrow}{\beta}^{\pm} C_{bn\ell}(z'_{\ell o}) - (\underset{\rightarrow}{\beta}^{\pm} \times \underset{\rightarrow}{C}_{an\ell}(z'_{\ell o}))]\}\, f^{\pm} \tag{3.7a}$$

$$[\underline{\tilde{H}}_{\pm}(\underline{\beta}_n)]_\ell = \frac{(j\,k_o)^2}{4\pi} \sum_n e^{-jk_o(\beta_x x_{\ell o} + \beta_y y_{\ell o} \pm |\beta_z| z_{\ell o})} e^{jk_o(\zeta_n x'_{\ell o} + \zeta_n y'_{\ell o})}$$

$$\ldots \operatorname{sinc}\left[k_o(\beta^{\pm}_{x'\ell} - \zeta_n)\frac{L_\ell}{2}\right] \operatorname{sinc}\left[k_o(\beta^{\pm}_{y'\ell} - \zeta_n)\frac{W_\ell}{2}\right]$$

$$\ldots \{Y_o \underline{C}_{an\ell}(z'_{\ell o}) + [\underline{\beta}^{\pm} C_{dn\ell}(z'_{\ell o}) - (\underline{\beta}^{\pm} \times \underline{C}_{cn\ell}(z'_{\ell o}))]\} f^{\pm} \tag{3.7b}$$

The forms (3.7a,b) will be used in Section 4 as the basis for development of the field expressions to be used in our final results.

4. SPECTRAL FIELDS FROM SLOTS IN A COAXIAL CABLE LAID CIRCULARLY

We consider the source configuration to consist of a leaky coaxial cable laid in a circular pattern, with the radius of curvature of the configuration sufficiently large to justify considering the propagation down the cable to be equivalent to that along a straight cable. The geometry is shown in Figure 4.1.

The local cylindrical coordinates used within the cable in the vicinity of the ℓ^{th} slot are designated as $(r''_\ell, \phi''_\ell, z''_\ell)$ with corresponding rectangular coordinates $(x''_\ell, y''_\ell, z''_\ell)$. The inner and outer conductor radii are denoted by a and b respectively. The finite thickness of the outer conductor is neglected in designating the radial coordinate of the slot; hence, $r''_\ell = b$ in all cases.

The radius of the cable configuration is denoted by R. In all cases to be considered, it will be true that

$$k_o a << 1 \tag{4.1a}$$

$$k_o b << 1 \tag{4.1b}$$

$$R >> a \tag{4.1c}$$

$$R >> b \tag{4.1d}$$

$$k_o R >> 1 \tag{4.1e}$$

To obtain needed relationships between coordinate systems, we consider Figure 4.2a,b,c,d.

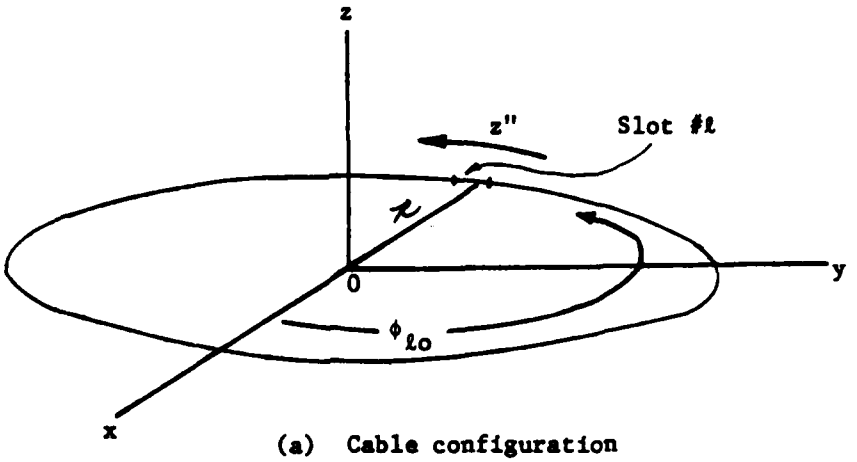

(a) Cable configuration

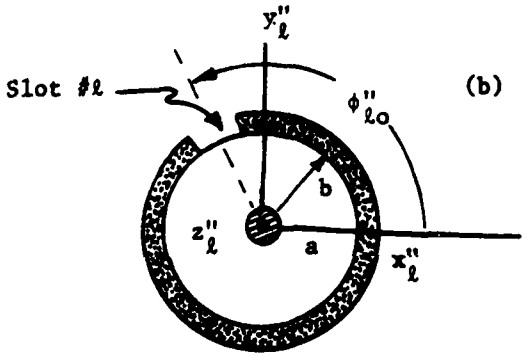

(b) Coaxial cable

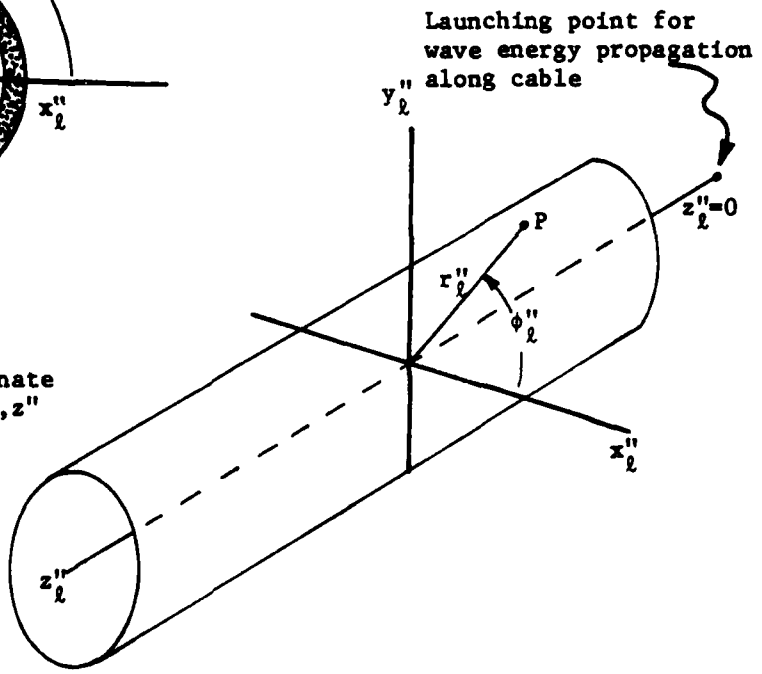

(c) Cable coordinate system r",ϕ",z"

Figure 4-1. Geometry of cable

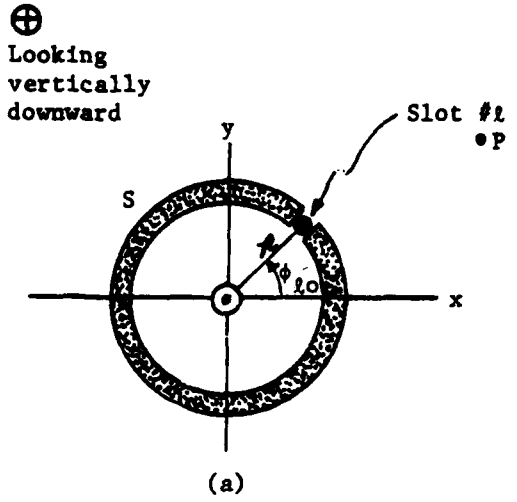

(a)

Coordinates of point P in system S = (x, y, z)

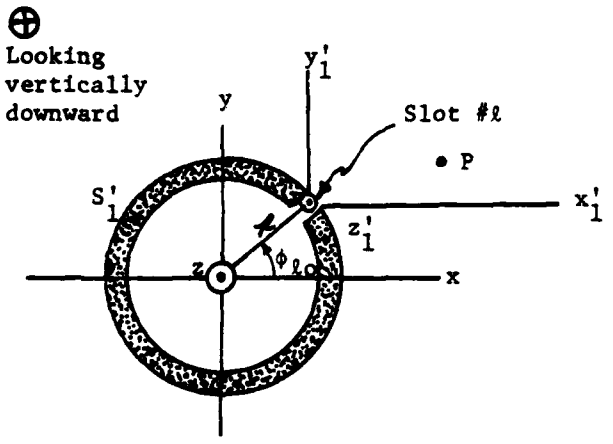

(b)

Coordinates of point P in system S_1' = (x_1', y_1', z_1')

$$x = R \cos \phi_{\ell o} + x_1' \quad (4.2a)$$

$$y = R \sin \phi_{\ell o} + y_1' \quad (4.2b)$$

$$z = b + z_1' \quad (4.2c)$$

$$x_1' = x - R \cos \phi_{\ell o} \quad (4.2d)$$

$$y_1' = y - R \sin \phi_{\ell o} \quad (4.2e)$$

$$z_1' = z - b \quad (4.2f)$$

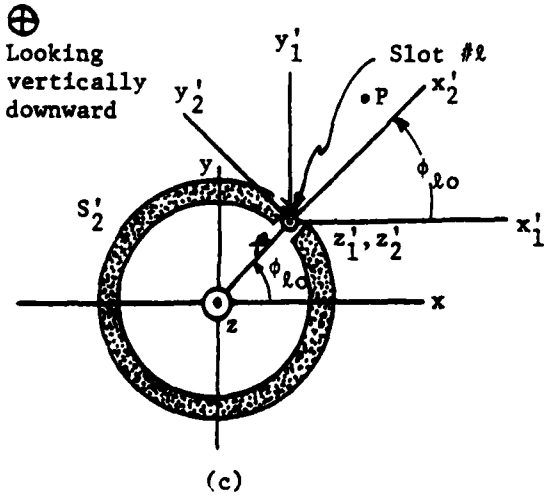

(c)

Coordinates of point P in system S_2' = (x_2', y_2', z_2')

$$x_1' = x_2' \cos \phi_{\ell o} - y_2' \sin \phi_{\ell o} \quad (4.3a)$$

$$y_1' = x_2' \sin \phi_{\ell o} + y_2' \cos \phi_{\ell o} \quad (4.3b)$$

$$z_1' = z_2' \quad (4.3c)$$

$$x_2' = x_1' \cos \phi_{\ell o} + y_1' \sin \phi_{\ell o} \quad (4.3d)$$

$$y_2' = -x_1' \sin \phi_{\ell o} + y_1' \cos \phi_{\ell o} \quad (4.3e)$$

$$z_2' = z_1' \quad (4.3f)$$

Figure 4-2. Coordinate Systems

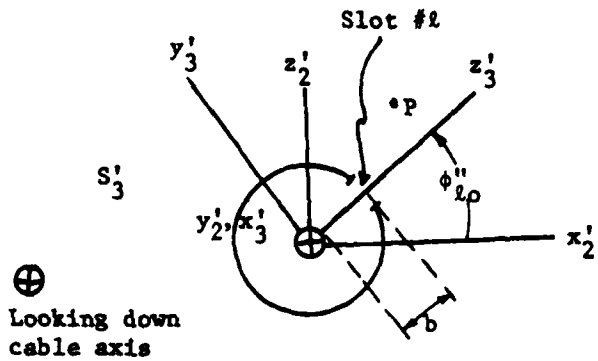

Looking down cable axis near Slot #ℓ

(d)

Coordinates of point P in system $S_3' = (x_3', y_3', z_3')$

$$x_2' = z_3' \cos \phi''_{\ell o} - y_3' \sin \phi''_{\ell o} \quad (4.4a)$$

$$y_2' = x_3' \quad (4.4b)$$

$$z_2' = z_3' \sin \phi''_{\ell o} + y_3' \cos \phi''_{\ell o} \quad (4.4c)$$

$$x_3' = y_2' \quad (4.4d)$$

$$y_3' = -x_2' \sin \phi''_{\ell o} + z_2' \cos \phi''_{\ell o} \quad (4.4e)$$

$$z_3' = x_2' \cos \phi''_{\ell o} + z_2' \sin \phi''_{\ell o} \quad (4.4f)$$

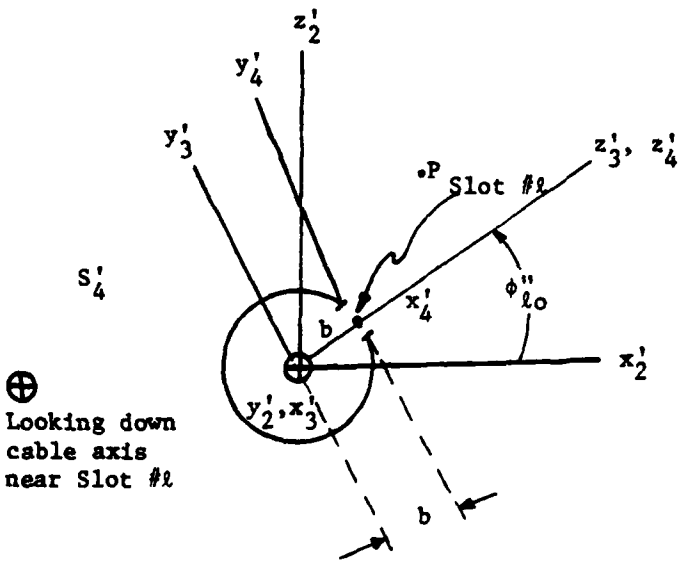

Looking down cable axis near Slot #ℓ

(e)

Coordinates of point P in System $S_4' = (x_4', y_4', z_4')$

$$x_3' = x_4' \quad (4.5a)$$

$$y_3' = y_4' \quad (4.5b)$$

$$z_3' = b + z_4' \quad (4.5c)$$

$$x_4' = x_3' \quad (4.5d)$$

$$y_4' = y_3' \quad (4.5e)$$

$$z_4' = z_3' - b \quad (4.5f)$$

Figure 4-2. Coordinate Systems (cont'd)

From the equations in Figure 4.2a,b,c,d the point P has (x, y, z) coordinates given by

$$x = R\cos\phi_{\ell o} + x_1' = R\cos\phi_{\ell o} + x_2'\cos\phi_{\ell o} - y_2'\sin\phi_{\ell o}$$

$$= R\cos\phi_{\ell o} + (z_3'\cos\phi_{\ell o}'' - y_3'\sin\phi_{\ell o}'')\cos\phi_{\ell o} - x_3'\sin\phi_{\ell o}$$

$$= R\cos\phi_{\ell o} + [(b + z_4')\cos\phi_{\ell o}'' - y_4'\sin\phi_{\ell o}'']\cos\phi_{\ell o} - x_4'\sin\phi_{\ell o} \qquad (4.6a)$$

$$y = R\sin\phi_{\ell o} + y_1' = R\sin\phi_{\ell o} + x_2'\sin\phi_{\ell o} + y_2'\cos\phi_{\ell o}$$

$$= R\sin\phi_{\ell o} + (z_3'\cos\phi_{\ell o}'' - y_3'\sin\phi_{\ell o}'')\sin\phi_{\ell o} + x_3'\cos\phi_{\ell o}$$

$$= R\sin\phi_{\ell o} + [(b + z_4')\cos\phi_{\ell o}'' - y_4'\sin\phi_{\ell o}'']\sin\phi_{\ell o} + x_4'\cos\phi_{\ell o} \qquad (4.6b)$$

$$z = b + z_1' = b + z_2' = b + (z_3'\sin\phi_{\ell o}'' + y_3'\cos\phi_{\ell o}'')$$

$$= b + [(b + z_4')\sin\phi_{\ell o}'' + y_4'\cos\phi_{\ell o}''] \qquad (4.6c)$$

If P is at the center of Slot #ℓ, then

$$x_4' = y_4' = z_4' = 0 \qquad (4.7)$$

Substituting Eq. (4.7) into Eqs. (4.6a,b,c), we have for the (x, y, z) coordinates at the ℓ^{th} slot center [with the aid of the condition (4.1d)]

$$x_{\ell o} = (R + b \cos \phi''_{\ell o}) \cos \phi_{\ell o} \simeq R \cos \phi_{\ell o} \tag{4.8a}$$

$$y_{\ell o} = (R + b \cos \phi''_{\ell o}) \sin \phi_{\ell o} \simeq R \sin \phi_{\ell o} \tag{4.8b}$$

$$z_{\ell o} = b(1 + \sin \phi''_{\ell o}) \tag{4.8c}$$

Note that [see Eqs. (3.1), (3.2), (3.3)], if $\Delta \underset{\rightarrow}{r}_\ell = \hat{\underset{\rightarrow}{x}}\, \Delta x_\ell + \hat{\underset{\rightarrow}{y}}\, \Delta y_\ell + \hat{\underset{\rightarrow}{z}}\, \Delta z_\ell$,

$$\begin{aligned} \underset{\rightarrow}{\beta}^{\pm} \cdot \Delta \underset{\rightarrow}{r}_\ell &= \beta_x \Delta x_\ell + \beta_y \Delta y_\ell \pm |\beta_z| \Delta z_\ell \\ &= \Delta x'_\ell(-\beta_x \sin \phi'_{\ell o} + \beta_y \cos \phi'_{\ell o}) \\ &\quad + \Delta y'_\ell[-(\beta_x \cos \phi_{\ell o} + \beta_y \sin \phi_{\ell o}) \sin \phi''_{\ell o} \pm |\beta_z| \cos \phi''_{\ell o}] \end{aligned} \tag{4.9}$$

where it follows from Eq. (4.8) that

$$\beta^{+}_{x',\ell} = \beta^{-}_{x',\ell} = -\beta_x \sin \phi_{\ell o} + \beta_y \cos \phi_{\ell o} \tag{4.10a}$$

$$\beta^{\pm}_{y',\ell} = -(\beta_x \cos \phi_{\ell o} + \beta_y \sin \phi_{\ell o}) \sin \phi''_{\ell o} \pm |\beta_z| \cos \phi''_{\ell o} \tag{4.10b}$$

$$\beta^{\pm}_{z',\ell} = \pm \sqrt{1 - (\beta^{\pm}_{x',\ell})^2 - (\beta^{\pm}_{y',\ell})^2} \tag{4.10c}$$

The exponential factors in Eqs. (3.5a,b) can be written [with the aid of Eqs. (4.8a,b,c)] in the form

$$e^{-jk_o(\beta_x x_{\ell o}+\beta_y y_{\ell o}\pm|\beta_z|z_{\ell o})}$$

$$= e^{-jk_o\beta_h(R+b\cos\phi''_{\ell o})\cos(\phi_{\ell o}-\phi_\beta)\mp jk_o|\beta_z|b(1+\sin\phi''_{\ell o})} \qquad (4.11)$$

where

$$\beta_h = \sqrt{\beta_x^2 + \beta_y^2}\ ;\ \phi_\beta = \tan^{-1}\left(\frac{\beta_y}{\beta_x}\right)$$

The slot center coordinate $x'_{\ell o}$ appearing in Eqs. (3.7a,b) is the displacement <u>along</u> the cable of the ℓ^{th} slot center from the launching point for wave energy propagating down the cable [as indicated earlier, this point will be designated as the origin of the coordinate system defined with respect to the cable itself, i.e., the (r", ϕ", z") system]. It is easy to deduce (see Figure 4.2) that (if subscript ℓo indicates ℓ^{th} slot center for all coordinates)

$$x'_{\ell o} = z''_{\ell o} = R\phi_{\ell o} \qquad (4.12)$$

The other slot center coordinate appearing in Eqs. (3.7a,b), denoted by $y'_{\ell o}$, is the linear coordinate corresponding to the angular position of the slot center <u>around</u> the preiphery of the cable. It is evident from Figure 4.2 that this coordinate is given by

$$y'_{\ell o} = b\phi''_{\ell o} \qquad (4.13)$$

The approximations used to justify the modelling of the slots as rectangular (ignoring the curvature of the slots both <u>along</u> the cable and <u>around</u> its periphery) and thereby justify the use of Eqs. (4.12) and (4.13) are:

(1) The radius R is so large and the slot length L_ℓ so small that in the vicinity of the ℓ^{th} slot we can ignore the curvature of the slot along the cable, i.e., in the direction of wave propagation.

(2) The slot width W_ℓ is small enough to neglect the curvature of the slot around the cable periphery.

*****

The forms (3.4a,b,c,d) used to represent fields are valid in the case of propagation along a coaxial cable, since fields can be represented as a series of propagating modes, where the n^{th} mode has a factor

$$F_n(z'', \phi'') = e^{-jk_{zn}z''} \cdot e^{jn\phi''} \tag{4.14}$$

where k_{zn} is the complex propagation constant of mode #n and n is the mode integer.

To relate Eq. (4.14) to the forms (3.4a,b,c,d) we set z" and ϕ" to $z''_{\ell o}$ and $\phi''_{\ell o}$ in Eq. (4.14) and then, with the aid of Eq. (4.12)

$$\xi_n = -\hat{k}_{zn} \tag{4.15}$$

where

$$\hat{k}_{zn} = \frac{k_{znR} - j\alpha_n}{k_o} = \hat{k}_{znR} + j\hat{k}_{znI} = \hat{k}_{znR} - j\hat{\alpha}_n$$

$$k_{znR} = \frac{\omega}{v_n}$$

v_n = phase velocity of n^{th} mode in meters/second

α_n = attenuation of n^{th} mode in nepers/meter

$$\hat{k}_{znR} = \frac{k_{znR}}{k_o}$$

$$\hat{k}_{znI} = -\hat{\alpha}_n = \frac{-\alpha_n}{k_o}$$

From Eqs. (4.13), (3.4a,b,c,d), and (4.14)

$$\zeta_n = \frac{n}{k_o b} \tag{4.16}$$

The variable z'_ℓ in Eqs. (3.4a,b,c,d) is the radial coordinate r"; hence, we can designate $\underset{\rightarrow}{C}_{an}$, $\underset{\rightarrow}{C}_{bn}$ ... etc. in Eqs. (3.4a,b,c,d) as functions of the value of r" at the slot, which is equal to b, the outer radius of the cable. Thus, the forms of Eqs. (3.7a,b) for the specialization in this section are [using Eqs. (4.11) through (4.16)]:

$$\begin{aligned}
[\underset{\rightarrow}{\tilde{E}}_{\pm}(\beta_{\rightarrow h})]_\ell = {} & \frac{(j\,k_o)^2}{4\pi} \cdot \sum_n e^{-jk_o\beta_h(R+b\cos\phi''_{\ell o})\cos(\phi_{\ell o}-\phi_\beta)} \\
& \cdots e^{\mp jk_o|\beta_z|b(1+\sin\phi''_{\ell o})}\; e^{-jk_o(\hat{k}_{zn}R)\varphi_{\ell o}} \cdot e^{jn\phi''_{\ell o}} \\
& \cdots \operatorname{sinc}\left[\frac{k_o L_\ell}{2}\left[\beta^{\pm}_{x',\ell} + \hat{k}_{zn}\right)\right] \operatorname{sinc}\left[\frac{k_o W_\ell}{2}\left(\beta^{\pm}_{y',\ell} - \frac{n}{k_o b}\right)\right] \\
& \cdots \{-Z_o\, \underset{\rightarrow}{C}^{(\ell)}_{cn\ell}(b) + [\underset{\rightarrow}{\beta}^{\pm}\, \underset{\rightarrow}{C}^{(\ell)}_{bn\ell}(b) - (\underset{\rightarrow}{\beta}^{\pm} \times \underset{\rightarrow}{C}^{(\ell)}_{an\ell}(b))]\} \qquad (4.17a) \\
& \cdots f^{\pm}
\end{aligned}$$

$$[\bar{H}_{\rightarrow}(\beta_{\ell}^{+})]_{\ell} = \frac{(j\,k_o)^2}{4\pi} \sum_{n} e^{-jk_o \rho_h (\sin\theta''_{\ell o}) \cos(\phi''_{\ell o} - \phi'_{\ell})}$$

$$\cdots e^{+jk_o |z'_{\ell}| (1+\sin\theta''_{\ell o})} e^{-jk_o (\hat{k}_{zn}) z'_{\ell}} \cdot e^{jn\phi''_{\ell o}}$$

$$\cdots \operatorname{sinc}\left[\frac{k_o L_x}{2} (\beta^{+}_{x',\ell} + \hat{k}_{zn})\right] \operatorname{sinc}\left[\frac{k_o W_y}{2} (\beta^{+}_{y',\ell} - k_o^{n} \bar{b})\right]$$

$$\cdots \{Y_o \underset{\rightarrow}{C}_{an\ell}(b) + [\underset{\rightarrow}{\beta}^{+} \underset{\rightarrow}{C}_{dn\ell}(b) - (\underset{\rightarrow}{\hat{\imath}}^{+} \times \underset{\rightarrow}{C}_{cn\ell}(b))]\} \qquad (4.17b)$$

$$\cdots f^{+}$$

where in Eqs. (4.17a,b) $\alpha^{+}_{x',\ell}$ and $\beta^{+}_{y',\ell}$ are given by Eqs. (4.10a,b).

From Appendix IV, we know that an arbitrary mode will have the generic forms [where subscripts (r", ϕ", z") denote components along the indicated directions and ($\hat{r}$", $\hat{\phi}$", $\hat{z}$") are the unit base vectors in the double-primed cable coordinate system)

$$\underset{\rightarrow}{C}_{an\ell} = \hat{z}''_{\ell} \bar{E}^{(n)}_{\phi''}(b) - \hat{\phi}''_{\ell} \bar{E}^{(n)}_{z''}(b) \qquad (4.18a)$$

$$C_{bn\ell} = \bar{E}^{(n)}_{r''}(b) \qquad (4.18b)$$

$$\underset{\rightarrow}{C}_{cn\ell} = \hat{z}''_{\ell} \bar{H}^{(n)}_{\phi''}(b) - \hat{\phi}''_{\ell} \bar{H}^{(n)}_{z''}(b) \qquad (4.18c)$$

$$C_{dn\ell} = \bar{H}^{(n)}_{r''}(b) \qquad (4.18d)$$

where, in general,

$$\underset{\rightarrow}{E}(b, \phi'', z'') = \bar{F}^{(n)}(b)\, e^{-jk_o \hat{k}_{zn} z''} \cdot e^{jn\phi''}$$

$$\underset{\rightarrow}{H}^{(n)}(b, \phi'', z'') = \bar{H}(b)\, e^{-jk_o \hat{k}_{zn} z''} \cdot e^{jn\phi''}$$

and where

$$\bar{E}_{z'}^{(n)} = 0 \text{ for a TE mode}$$

$$\bar{H}_{z'}^{(n)} = 0 \text{ for a TM mode}$$

and

$$\bar{E}_{z'}^{(n)} = \bar{H}_{z'}^{(n)} = 0 \text{ for a TEM mode}$$

It is easily deduced from the cable geometry that

$$\hat{r}''_{\ell} = \hat{x}(\cos\phi_{\ell o}\cos\phi''_{\ell o}) + \hat{y}(\sin\phi_{\ell o}\cos\phi''_{\ell o}) + \hat{z}(\sin\phi_{\ell o}) \quad (4.19a)$$

$$\hat{\phi}''_{\ell} = \hat{x}(-\cos\phi_{\ell o}\sin\phi''_{\ell o}) + \hat{y}(-\sin\phi_{\ell o}\sin\phi''_{\ell o}) + \hat{z}(\cos\phi''_{\ell o}) \quad (4.19b)$$

$$\hat{z}''_{\ell} = -\hat{x}\sin\phi_{\ell o} + \hat{y}\cos\phi_{\ell o} \quad (4.19c)$$

Substituting Eqs. (4.19a,b,c) into Eqs. (4.18a) and (4.18c), the x, y, z components of the vectors $\underset{\rightarrow}{C}_{an}$ and $\underset{\rightarrow}{C}_{cn}$ are:

$$C_{an\ell x} = -\sin\phi_{\ell o}\,\bar{E}_{\phi''}^{(n)}(b) + \cos\phi_{\ell o}\sin\phi''_{\ell o}\,\bar{E}_{z''}^{(n)}(b) \quad (4.20a)$$

$$C_{an\ell y} = \cos\phi_{\ell o}\,\bar{E}_{\phi''}^{(n)}(b) + \sin\phi_{\ell o}\sin\phi''_{\ell o}\,\bar{E}_{z''}^{(n)}(b) \quad (4.20b)$$

$$C_{an\ell z} = -\cos\phi''_{\ell o}\,\bar{E}_{z''}^{(n)}(b) \quad (4.20c)$$

$$C_{cn\ell x} = -\sin\phi_{\ell o}\,\bar{H}_{\phi''}^{(n)}(b) + \cos\phi_{\ell o}\sin\phi''_{\ell o}\,\bar{H}_{z''}^{(n)}(b) \quad (4.21a)$$

$$C_{cn\ell y} = \cos\phi_{\ell o}\,\bar{H}^{(n)}_{\phi''}(b) + \sin\phi_{\ell o}\sin\phi''_{\ell o}\,\bar{H}^{(n)}_{z''}(b) \tag{4.21b}$$

$$C_{cn\ell z} = -\cos\phi''_{\ell o}\,\bar{H}^{(n)}_{z''}(b) \tag{4.21c}$$

From Eqs. (4.20a,b,c) and (4.21a,b,c), the bracketed expressions in Eqs. (4.17a,b) are given by

$$\tilde{\vec{F}}^{\pm}_{E} = \left(-Z_c\,\vec{C}_{cn\ell}(b) + [\vec{\beta}^{\pm}\,C_{bn\ell}(b) - \{\vec{\beta}^{\pm}\times\vec{C}_{an\ell}(b)]\}\right)f^{\pm}$$

$$= \hat{x}\,\tilde{F}^{\pm}_{Ex} + \hat{y}\,\tilde{F}^{\pm}_{Ey} + \hat{z}\,\tilde{F}^{\pm}_{Ez} \tag{4.22a}$$

and

$$\tilde{F}^{\pm}_{H} = \left(Y_o\,\vec{C}_{an\ell}(b) + \{\vec{\beta}^{\pm}\,C_{dn\ell}(b) - [\vec{\beta}^{\pm}\times\vec{C}_{cn\ell}(b)]\}\right)f^{\pm}$$

$$= \hat{x}\,\tilde{F}^{\pm}_{Hx} + \hat{y}\,\tilde{F}^{\pm}_{Hy} + \hat{z}\,\tilde{F}^{\pm}_{Hz} \tag{4.22b}$$

where

$$\tilde{F}^{\pm}_{Ex} = \Big(Z_o[\sin\phi_{\ell o}\,\bar{H}^{(n)}_{\phi''}(b) - \cos\phi_{\ell o}\sin\phi''_{\ell o}\,\bar{H}^{(n)}_{z''}(b)]$$

$$+ \beta_x\,\bar{E}^{(n)}_{r''}(b) \pm |\beta_z|[\cos\phi_{\ell o}\,\bar{E}^{(n)}_{\phi''}(b) + \sin\phi_{\ell o}\sin\phi''_{\ell o}\,\bar{E}^{(n)}_{z''}(b)]$$

$$+ \beta_y[\cos\phi''_{\ell o}\,\bar{E}^{(n)}_{z''}(b)]\Big)f^{\pm} \tag{4.22ax)'}$$

$$\tilde{F}^{\pm}_{Ey} = \Big(-Z_o[\cos\phi_{\ell o}\,\bar{H}^{(n)}_{\phi''}(b) + \sin\phi_{\ell o}\sin\phi''_{\ell o}\,\bar{H}^{(n)}_{z''}(b)]$$

$$+ \beta_y\,\bar{E}^{(n)}_{r''}(b) - \beta_x[\cos\phi''_{\ell o}\,\bar{E}^{(n)}_{z''}(b)]$$

$$\mp |\beta_z|[\sin\phi_{\ell o}\,\bar{E}^{(n)}_{\phi''}(b) - \cos\phi_{\ell o}\sin\phi''_{\ell o}\,\bar{E}^{(n)}_{z''}(b)]\Big)\,f^{\pm} \qquad (4.22ay)'$$

$$\tilde{F}^{\pm}_{Ez} = \Big(Z_o[\cos\phi''_{\ell o}\,\bar{H}^{(n)}_{z''}(b)] \pm |\beta_z|\bar{E}^{(n)}_{r''}(b)$$

$$- \beta_y[\sin\phi_{\ell o}\,\bar{E}^{(n)}_{\phi''}(b) - \cos\phi_{\ell o}\sin\phi''_{\ell o}\,\bar{E}^{(n)}_{z''}(b)]$$

$$- \beta_x[\cos\phi_{\ell o}\,\bar{E}^{(n)}_{\phi''}(b) + \sin\phi_{\ell o}\sin\phi''_{\ell o}\,\bar{E}^{(n)}_{z''}(b)]\Big)\,f^{\pm} \qquad (4.22az)'$$

$$\tilde{F}^{\pm}_{Hx} = \Big(-Y_o[\sin\phi_{\ell o}\,\bar{E}^{(n)}_{\phi''}(b) - \cos\phi_{\ell o}\sin\phi''_{\ell o}\,\bar{E}^{(n)}_{z''}(b)]$$

$$+ \beta_x\,\bar{H}^{(n)}_{r''}(b)$$

$$\pm |\beta_z|[\cos\phi_{\ell o}\,\bar{H}^{(n)}_{\phi''}(b) + \sin\phi_{\ell o}\sin\phi''_{\ell o}\,\bar{H}^{(n)}_{z''}(b)]$$

$$+ \beta_y[\cos\phi''_{\ell o}\,\bar{H}^{(n)}_{z''}(b)]\Big)\,f^{\pm} \qquad (4.22bx)$$

$$\tilde{F}^{\pm}_{Hy} = \Big(Y_o[\cos\phi_{\ell o}\,\bar{E}^{(n)}_{\phi''}(b) + \sin\phi_{\ell o}\sin\phi''_{\ell o}\,\bar{E}^{(n)}_{z''}(b)]$$

$$+ \beta_y\,\bar{H}^{(n)}_{r''}(b) - \beta_x[\cos\phi''_{\ell o}\,\bar{H}^{(n)}_{z''}(b)]$$

$$\pm |\beta_z|[\sin\phi_{\ell o}\,\bar{H}^{(n)}_{\phi''} - \cos\phi_{\ell o}\sin\phi''_{\ell o}\,\bar{H}^{(n)}_{z''}(b)]\Big)\,f^{\pm} \qquad (4.22by)$$

$$\tilde{F}^{\pm}_{Hz} = \Big(-Y_o[\cos\phi''_{\ell o}\,\bar{E}^{(n)}_{z''}(b)] \pm |\beta_z|\bar{H}^{(n)}_{r''}(b)$$

$$- \beta_y[\sin\phi_{\ell o}\,\bar{H}^{(n)}_{\phi''}(b) - \cos\phi_{\ell o}\sin\phi''_{\ell o}\,\bar{H}^{(n)}_{z''}(b)]$$

$$- \beta_x[\cos\phi_{\ell o}\,\bar{H}^{(n)}_{\phi''}(b) + \sin\phi_{\ell o}\sin\phi''_{\ell o}\,\bar{H}^{(n)}_{z''}(b)]\Big)\,f^{\pm} \qquad (4.22bz)$$

From Eqs. (4.17a,b), (4.22a,x,y,z)' and (4.22bx,y,z)' we have the following expressions for the x, y, z components of the plane-wave spectra of the fields from Slot #ℓ with Mode #n propagating along the cable:

$$\begin{bmatrix} [\tilde{E}^{(n)}_{\pm}(\beta_h)]_{\ell x} \\ \qquad\quad y \\ \qquad\quad z \\ [\tilde{H}^{(n)}_{\pm}(\beta_h)]\ x \\ \qquad\quad y \\ \qquad\quad z \end{bmatrix} = \frac{(j\,k_o)^2}{2\beta} \sum_n e^{-jk_o\beta_h(\rho_{\ell o}\cos\phi''_{\ell o})\cos(\phi_{\ell o}-\phi_\beta)} e^{\mp}$$

$$\ldots e^{\mp jk_o|\beta_z|b(1+\sin\phi''_{\ell o})} \cdot e^{-jk_o(\hat{k}_{zn}\cdot\vec{\rho})\varphi_{\ell o}} \cdot e^{jn\phi''_{\ell o}}$$

$$\ldots \operatorname{sinc}\left[\frac{k_o L_\ell}{2}(\beta^{\pm}_{x'\ell} + \hat{k}_{zn})\right] \operatorname{sinc}\left[\frac{k_o W_\ell}{2}(\beta^{\pm}_{y'\ell} - \frac{n}{k_o b})\right]$$

$$\ldots \left\{ \begin{matrix} A^{(\ell)}_{11} F^{(n)}_{r''}(b) + A^{(\ell)}_{12} E^{(n)}_{\phi''}(b) + A^{(\ell)}_{13} E^{(n)}_{z''}(b) \\ 21 \qquad\qquad 22 \qquad\qquad 23 \\ 31 \qquad\qquad 32 \qquad\qquad 33 \\ 41 \qquad\qquad 42 \qquad\qquad 43 \\ 51 \qquad\qquad 52 \qquad\qquad 53 \\ 61 \qquad\qquad 62 \qquad\qquad 63 \end{matrix} \right.$$

$$\left. \begin{matrix} + B^{(\ell)}_{11} H^{(n)}_{r''}(b) + B^{(\ell)}_{12} H^{(n)}_{\phi''}(b) + B^{(\ell)}_{13} H^{(n)}_{z''}(b) \\ 21 \qquad\qquad 22 \qquad\qquad 23 \\ 31 \qquad\qquad 32 \qquad\qquad 33 \\ 41 \qquad\qquad 42 \qquad\qquad 43 \\ 51 \qquad\qquad 52 \qquad\qquad 53 \\ 61 \qquad\qquad 62 \qquad\qquad 63 \end{matrix} \right\} \qquad (4.23a,b)$$

$$A^{(\ell)}_{11} = B^{(\ell)}_{41} = \beta_x$$

$$A^{(\ell)}_{21} = B^{(\ell)}_{51} = \beta_y$$

$$A_{31}^{(\ell)} = B_{61}^{(\ell)} = \pm |\beta_z|$$

$$A_{41}^{(\ell)} = A_{51}^{(\ell)} = A_{61}^{(\ell)} = B_{11}^{(\ell)} = B_{21}^{(\ell)} = B_{31}^{(\ell)} = 0$$

$$A_{12}^{(\ell)} = B_{42}^{(\ell)} = \pm |\beta_z| \cos \phi_{\ell o}$$

$$A_{22}^{(\ell)} = B_{52}^{(\ell)} = \pm |\beta_z| \sin \phi_{\ell o}$$

$$A_{32}^{(\ell)} = B_{62}^{(\ell)} = -(\beta_x \cos \phi_{\ell o} + \beta_y \sin \phi_{\ell o})$$

$$A_{42}^{(\ell)} = -Y_o \sin \phi_{\ell o} = -\frac{Y_o}{Z_o} B_{12}^{(\ell)}$$

$$A_{52}^{(\ell)} = Y_o \cos \phi_{\ell o} = -\frac{Y_o}{Z_o} B_{22}^{(\ell)}$$

$$A_{62}^{(\ell)} = B_{32}^{(\ell)} = 0$$

$$A_{13}^{(\ell)} = B_{43}^{(\ell)} = \pm |\beta_z| \sin \phi_{\ell o} \sin \phi''_{\ell o} + \beta_y \cos \phi''_{\ell o}$$

$$A_{23}^{(\ell)} = B_{53}^{(\ell)} = \mp |\beta_z| \cos \phi_{\ell o} \sin \phi''_{\ell o} - \beta_x \cos \phi''_{\ell o}$$

$$A_{33}^{(\ell)} = B_{63}^{(\ell)} = (-\beta_x \sin \phi_{\ell o} + \beta_y \cos \phi_{\ell o}) \sin \phi''_{\ell o}$$

$$A_{43}^{(\ell)} = Y_o \cos \phi_{\ell o} \sin \phi''_{\ell o} = -\frac{Y_o}{Z_o} B_{13}^{(\ell)}$$

$$A_{53}^{(\ell)} = Y_o \sin \phi_{\ell o} \sin \phi''_{\ell o} = -\frac{Y_o}{Z_o} B_{23}^{(\ell)}$$

$$A_{63}^{(\ell)} = -Y_o \cos \phi''_{\ell o} = -\frac{Y_o}{Z_o} B_{33}^{(\ell)}$$

If $\phi''_{\ell o}$ is <u>not</u> the same for all slots and if the slots are <u>not</u> uniformly spaced along the cable, then the procedure for computation is the programming of Eqs. (4.23a,b) as given above for each value of the index ℓ, followed by accumulation of the sum over ℓ from $\ell = 1$ to $\ell = N_S$, where N_S is the total number of slots along the cable. If this technique is to be used, then taking advantage of various approximations that apply, such as Eqs. (4.1a,b,c,d,e), to simplify the expressions is not very productive, since the effect of these simplifications on computer time is negligible. A program has been written in accordance with the above procedure to allow for the possibility that we might wish to evaluate the general case where the slots are not all of the same dimensions and not all uniformly spaced both along and around the cable. In a practical sense, this computation might involve a prohibitve cost in computer time because N_S, the number of slots, might number in the thousands.

For those reasons, we find it necessary to search for justifiable simplifications in Eqs. (4.23a,b). Fortunately, in the problem of immediate interest, the cable's slots are all placed at the same angle <u>around</u> the cable and are uniformly spaced <u>along</u> the cable. Thus, for this case

$$\phi''_{\ell o} = \phi''_o \qquad \text{for all values of } \ell \tag{4.24}$$

$$\phi_{\ell o} = \phi_{1o} + (\ell - 1)\,\Delta\,\phi_o = \phi_{1o} + \frac{2\pi\,(\ell - 1)}{N_S} \tag{4.25}$$

where ϕ_{1o} is the position of the first slot center, $\Delta\,\phi_o$ is the angular spacing between slot centers, and since the N_S slots are distributed uniformly

along the entire cable, $N_S \Delta \phi_0 = 2\pi$.

$$L_\ell = L \text{ for all } \ell \tag{4.26}$$

$$W_\ell = W \text{ for all } \ell \tag{4.27}$$

It is shown in Appendix V that over the range of parameter values of direct interest in this study

$$\text{sinc}\left[\frac{k_o L_\ell}{2}\left(\beta^{\pm}_{x',\ell} + \hat{k}_{zn}\right)\right] \approx 1 \text{ for all } \ell,\ n \tag{4.28}$$

and

$$\text{sinc}\left[\frac{k_o W_\ell}{2}\left(\beta^{\pm}_{y',\ell} - \frac{n}{k_o b}\right)\right] \approx \text{sinc}\left(\frac{n W_\ell}{2b}\right) \tag{4.29}$$

for all ℓ, n

Using Eqs. (4.24) through (4.29) in Eqs. (4.23a,b) we obtain, after summing over all slots (i.e., $\ell = 1$ to N_S),

$$\begin{bmatrix} [\tilde{E}^{(n)}_{\pm}(\beta_{nh})]_x \\ \quad\ y \\ \quad\ z \\ [\tilde{H}^{(n)}_{\pm}(\beta_{nh})]_x \\ \quad\ y \\ \quad\ z \end{bmatrix} = \frac{(j k_o)^2}{4\pi} e^{\mp j k_o |\beta_z| b(1+\sin\phi''_o)} \cdot e^{jn\phi''_o} \text{sinc}\left(\frac{nW}{2b}\right) f^{\pm}$$

$$\cdots e^{-jk_o(\hat{k}_{zn}R)\phi_{1o}} \text{ -------}$$

$$--- \begin{bmatrix} [\bar{\tilde{E}}_{\pm}^{(n)}]_x \\ [\bar{\tilde{E}}_{\pm}^{(n)}]_y \\ [\bar{\tilde{E}}_{\pm}^{(n)}]_z \\ [\bar{\tilde{H}}_{\pm}^{(n)}]_x \\ [\bar{\tilde{H}}_{\pm}^{(n)}]_y \\ [\bar{\tilde{H}}_{\pm}^{(n)}]_z \end{bmatrix} \tag{4.30}$$

where (with explicit indication of argument $\underline{\beta}_{\pm h}$ deleted)

$$[\bar{\tilde{E}}_{\pm}^{(n)}]_x = [\beta_x \bar{E}_{r''}^{(n)} + \beta_y \cos\phi_o'' \bar{E}_{z''}^{(n)}] S_o^{(n)}$$

$$+ \frac{e^{j\phi_{1o}}}{2} [\pm|\beta_z| \bar{E}_{\phi''}^{(n)} \mp j|\beta_z| \sin\phi_o'' \bar{E}_{z''}^{(n)} - jZ_o \bar{H}_{\phi''}^{(n)}$$

$$- Z_o \sin\phi_o'' \bar{H}_{z''}^{(n)}] S_+^{(n)}$$

$$+ \frac{e^{-j\phi_{1o}}}{2} [\pm|\beta_z| \bar{E}_{\phi''}^{(n)} \pm |\beta_z| \sin\phi_o'' \bar{E}_{z''}^{(n)} + jZ_o \bar{H}_{\phi''}^{(n)}$$

$$- Z_o \sin\phi_o'' \bar{H}_{z''}^{(n)}] S_-^{(n)} \tag{4.30a}'$$

$$[\bar{\tilde{E}}^{(n)}]_y = [\beta_y \bar{E}_{r''}^{(n)} - \beta_x \cos\phi_o'' \bar{E}_{z''}^{(n)}] S_o^{(n)}$$

$$+ \frac{e^{j\phi_{1o}}}{2} [\mp j|\beta_z| \bar{E}_{\phi''}^{(n)} \mp |\beta_z| \sin\phi_o'' \bar{E}_{z''}^{(n)} - Z_o \bar{H}_{\phi''}^{(n)}$$

$$+ jZ_o \sin\phi_o'' \bar{H}_{z''}^{(n)}] S_+^{(n)}$$

$$+ jZ_o \sin\phi_o'' \bar{H}_{z''}^{(n)}] S_+^{(n)}$$

$$+ \frac{e^{-j\phi_{1o}}}{2} [\pm j|\beta_z| \bar{E}_{\phi''}^{(n)} \mp |\beta_z| \sin\phi_o'' \bar{E}_{z''}^{(n)} - Z_o \bar{H}_{\phi''}^{(n)}$$

$$- jZ_o \sin\phi_o'' \bar{H}_{z''}^{(n)}] S_-^{(n)} \qquad (4.30b)'$$

$$[\bar{\tilde{E}}^{(n)}]_z = [\pm|\beta_z| \bar{E}_{r''}^{(n)} + Z_o \cos\phi_o'' \bar{H}_{z''}^{(n)}] S_o^{(n)}$$

$$+ \frac{e^{j\phi_{1o}}}{2} [-(\beta_x - j\beta_y) \bar{E}_{\phi''}^{(n)} + j(\beta_x - j\beta_y) \bar{E}_{z''}^{(n)}] S_+^{(n)}$$

$$+ \frac{e^{-j\phi_{1o}}}{2} [-(\beta_x + j\beta_y) \bar{E}_{\phi''}^{(n)} - j(\beta_x + j\beta_y) \bar{E}_{z''}^{(n)}] S_-^{(n)} \qquad (4.30c)'$$

$$[\bar{\tilde{H}}_{\pm}^{(n)}]_x = [\beta_x \bar{H}_{r''}^{(n)} + \beta_y \cos\phi_o'' \bar{H}_{z''}^{(n)}] S_o^{(n)}$$

$$+ \frac{e^{j\phi_{1o}}}{2} [\pm|\beta_z| \bar{H}_{\phi''}^{(n)} \mp j|\beta_z| \sin\phi_o'' \bar{H}_{z''}^{(n)} + jY_o \bar{E}_{\phi''}^{(n)}$$

$$+ Y_o \sin\phi_o'' \bar{E}_{z''}^{(n)}] S_+^{(n)}$$

$$+ \frac{e^{-j\phi_{1o}}}{2} [\pm|\beta_z| \bar{H}_{\phi''}^{(n)} \pm j|\beta_z| \sin\phi_o'' \bar{H}_{z''}^{(n)} - jY_o \bar{E}_{\phi''}^{(n)}$$

$$+ Y_o \sin\phi_o'' \bar{E}_{z''}^{(n)}] S_-^{(n)} \qquad (4.30d)'$$

$$[\bar{\tilde{H}}_{\pm}^{(n)}]_y = [\beta_y \bar{H}_{r''}^{(n)} - \beta_x \cos\phi_o'' \bar{H}_{z''}^{(n)}] S_o^{(n)}$$

$$+ \frac{e^{j\phi_{1o}}}{2} \left[\mp j|\beta_z| \, \bar{H}_{\phi''}^{(n)} \mp |\beta_z| \sin\phi_o'' \, \bar{H}_{z''}^{(n)} + Y_o \, \bar{E}_{\phi''}^{(n)} \right.$$

$$\left. - jY_o \sin\phi_o'' \, \bar{E}_{z''}^{(n)} \right] S_+^{(n)}$$

$$+ \frac{e^{-j\phi_{1o}}}{2} \left[\mp j|\beta_z| \, \bar{H}_{\phi''}^{(n)} \mp |\beta_z| \sin\phi_o'' \, \bar{H}_{z''}^{(n)} + Y_o \, \bar{E}_{\phi''}^{(n)} \right.$$

$$\left. + jY_o \sin\phi_o'' \, \bar{E}_{z''}^{(n)} \right] S_-^{(n)} \qquad (4.30e)'$$

$$[\bar{\tilde{H}}_{\pm}^{(n)}]_z = \left[\pm|\beta_z| \, \bar{H}_{r''}^{(n)} - Y_o \cos\phi_o'' \, \bar{E}_{z''}^{(n)} \right] S_0^{(n)}$$

$$+ \frac{e^{j\phi_{1o}}}{2} \left[-(\beta_x - j\beta_y) \, \bar{H}_{\phi''}^{(n)} + j(\beta_x - j\beta_y) \, \bar{H}_{z''}^{(n)} \right] S_+^{(n)}$$

$$+ \frac{e^{-j\phi_{1o}}}{2} \left[-(\beta_x + j\beta_y) \, \bar{H}_{\phi''}^{(n)} - j(\beta_x + j\beta_y) \, \bar{H}_{z''}^{(n)} \right] S_-^{(n)} \qquad (4.30f)'$$

where

$$S_0^{(n)} = \sum_{\ell=1}^{N_S} e^{-jk_o\beta_h R\cos\left[\phi_{1o} + \frac{2\pi(\ell-1)}{N_S} - \phi_\beta\right]} e^{-jk_o(\hat{k}_{zn}R)[2\pi(\ell-1)/N_S]} \qquad (4.31a)$$

$$S_+^{(n)} = \sum_{\ell=1}^{N_S} e^{-jk_o\beta_h R\cos\left[\phi_{1o} + \frac{2\pi(\ell-1)}{N_S} - \phi_\beta\right]} e^{-jk_o(\hat{k}_{zn}R)[2\pi(\ell-1)/N_S]}$$

$$\cdots e^{j[2\pi(\ell-1)/N_S]} \qquad (4.31b)$$

$$S_-^{(n)} = \sum_{\ell=1}^{N_S} e^{-jk_o\beta_h R\cos[\phi_{1o} + \frac{2\pi(\ell-1)}{N_S} - \phi_\beta]} \cdot e^{-jk_o(\hat{k}_{zn}R)[2\pi(\ell-1)/N_S]}$$

$$\cdots e^{-j[2\pi(\ell-1)/N_S]} f^{\pm} \qquad (4.31c)$$

To evaluate Eqs. (4.31a,b,c) in cases where the effect of the factors $f^{\pm}$ can be approximated as unity, we can invoke the well known Bessel function relationships[A-4]

$$e^{jx\sin} = e^{jx\cos(\theta-\frac{\pi}{2})} = \sum_{p=-\infty}^{\infty} J_p(x)\, e^{jp} \qquad (4.32a)$$

and

$$J_p(-x) = (-1)^p J_p(x) \qquad (4.32b)$$

which, when substituted into Eqs. (4.31a,b,c) yields after interchanging the order of the summations,

$$\begin{bmatrix} S_o^{(n)} \\ S_+^{(n)} \\ S_-^{(n)} \end{bmatrix} = \sum_{p=-\infty}^{\infty} (-1)^p J_p(k_o \beta_h R)\, e^{jp(\phi_{1o}-\phi_\beta-\frac{\pi}{2})} \text{ ----- }$$

$$\text{--- } \sum_{\ell=1}^{N_S} e^{jp[2\pi(\ell-1)/N_S]-j[2\pi(\ell-1)/N_S]} \begin{matrix} [k_o(\hat{k}_{zn} R)] \\ [k_o(\hat{k}_{zn} R) + 1] \\ [k_o(\hat{k}_{zn} R) - 1] \end{matrix} \qquad (4.33)$$

We now invoke the well-known formula for the truncated geometric series

$$\sum_{\ell=1}^{N_S} z^{\ell-1} = \sum_{\nu=0}^{N_S-1} z^{\nu} = \frac{1 - z^{N_S}}{1 - z} \quad \text{if } z \neq 1$$

$$N_S \qquad \text{if } z = 1 \tag{4.34}$$

Applying Eq. (4.34) to Eq. (4.33) and noting that [as indicated below Eq. (4.15)]

$$\hat{k}_{zn} = \frac{k_{znR} - j\alpha_n}{k_o} = \hat{k}_{znR} - j\hat{\alpha}_n \tag{4.35}$$

we obtain

$$\begin{bmatrix} S_o^{(n)} \\ S_+^{(n)} \\ S_-^{(n)} \end{bmatrix} = \sum_{p=-\infty}^{\infty} (-1)^p J_p(k_o \beta_h R)\, e^{jp(\phi_{io} - \phi_\beta - \frac{\pi}{2})} \text{ ---}$$

$$\text{---} \begin{bmatrix} \bar{S}_o^{(np)} \\ \bar{S}_+^{(np)} \\ \bar{S}_-^{(np)} \end{bmatrix} \tag{4.36a}$$

where

$$\bar{S}_o^{(np)} = \left[\frac{1 - e^{j2\pi[p - k_o \hat{k}_{znR} R]} \cdot e^{-2\pi\alpha_n R}}{1 - e^{j(2\pi/N_S)[p - k_o \hat{k}_{znR} R]} \cdot e^{-(2\pi/N_S)(\alpha_n R/N_S)}} \right] \quad \text{if } \alpha_n \neq 0$$

$$= N_S \text{ if } p = k_o \hat{k}_{znR} R + 2\pi m, \text{ where } m \text{ is an integer and } \alpha_n = 0$$

$$S_+^{(np)} = \left[\frac{1 - e^{j2\pi[p+1-k_o \hat{k}_{znR} R]} \cdot e^{-2\pi\alpha_n R}}{1 - e^{j(2\pi/N_S)[p+1-k_o \hat{k}_{znR} R]} \cdot e^{-2\pi\alpha_n R/N_S}} \right] \text{ if } \alpha_n \neq 0$$

$$= N_S \text{ if } p = k_o \hat{k}_{znR} R - 1 + 2\pi m \text{ and } \alpha_n = 0$$

$$S_-^{(np)} = \left[\frac{1 - e^{j2\pi[p-1-k_o \hat{k}_{znR} R]} \cdot e^{-2\pi\alpha_n R}}{1 - e^{j(2\pi/N_S)[p-1-k_o \hat{k}_{znR} R]} \cdot e^{-2\pi\alpha_n R/N_S}} \right] \text{ if } \alpha_n \neq 0$$

$$= N_S \text{ if } p = k_o \hat{k}_{znR} R + 1 + 2\pi m \text{ and } \alpha_n = 0$$

Using as a basis the approximations justified in Appendix V we will assume that $k_o \hat{k}_{znR} R$, which is a very large positive number, can be approximated by an integer, i.e.,

$$k_o \hat{k}_{znR} R \simeq q, \text{ where } q \text{ is a positive integer greater than 20} \qquad (4.36b)$$

Also justified in Appendix V is the approximation

$$e^{-2\pi\alpha_n R/N_S} \simeq 1 \qquad (4.36c)$$

and the fact that

$$\alpha_n \neq 0 \quad \text{in all cases of interest} \qquad (4.36d)$$

At this point, we will test the equations (4.17a,b) from which Eqs. (4.30a,b,c,d,e,f) are derived, to determine whether they satisfy the Maxwell equations in their present forms. As noted in Appendix III, if Eqs. (4.16a,b) are consistent with Eq. (III.6a), that is sufficient to confirm this consistency. Performing the operation $(Y_o \underset{\rightarrow}{\beta}^{\pm} x)$ on $\underset{\rightarrow}{\tilde{F}}_E^{\pm}$ as given by Eq. (4.22a), we obtain (with the aid of the vector identity $\underset{\rightarrow}{a}x(\underset{\rightarrow}{b}x\underset{\rightarrow}{c}) = \underset{\rightarrow}{b}(\underset{\rightarrow}{a},\underset{\rightarrow}{c}) - \underset{\rightarrow}{c}(\underset{\rightarrow}{a},\underset{\rightarrow}{b})$, and the fact that by definition $Z_o Y_o = 1$ and of course $\underset{\rightarrow}{\beta}^{\pm} x \underset{\rightarrow}{\beta}^{\pm} = 0$, $\underset{\rightarrow}{\beta}^{\pm} \cdot \underset{\rightarrow}{\beta}^{\pm} = 1$):

$$Y_o \underset{\rightarrow}{\beta}^{\pm} x \underset{\rightarrow}{\tilde{F}}_E^{\pm} = \underset{\rightarrow}{\tilde{F}}_H^{\pm}$$

$$- \underset{\rightarrow}{\beta}^{\pm}[Y_o \underset{\rightarrow}{\beta}^{\pm} \cdot \underset{\rightarrow}{C}_{an\ell}(b) + C_{dn\ell}(b)] \qquad (4.37a)$$

Performing the operation $(-Z_o \underset{\rightarrow}{\beta}^{\pm} x \ldots)$ on $\underset{\rightarrow}{\tilde{F}}_H^{\pm}$ as given by Eq. (4.22b), we obtain

$$-Z_o \underset{\rightarrow}{\beta}^{\pm} x \underset{\rightarrow}{\tilde{F}}_H^{\pm} = \underset{\rightarrow}{\tilde{F}}_E^{\pm} + \underset{\rightarrow}{\beta}^{\pm}[Z_o(\underset{\rightarrow}{\beta}^{\pm} \cdot \underset{\rightarrow}{C}_{cn\ell}(b)) - C_{bn\ell}(b)] \qquad (4.37b)$$

Performing the operation $(\underset{\rightarrow}{\beta}^{\pm} \cdot \ldots)$ on $\underset{\rightarrow}{\tilde{F}}_E^{\pm}$ and $\underset{\rightarrow}{\tilde{F}}_H^{\pm}$, we obtain

$$\underset{\rightarrow}{\beta}^{\pm} \cdot \underset{\rightarrow}{\tilde{F}}_E^{\pm} = -Z_o[\underset{\rightarrow}{\beta}^{\pm} \cdot \underset{\rightarrow}{C}_{cn\ell}(b)] - C_{bn\ell}(b) \qquad (4.37c)$$

$$\underset{\rightarrow}{\beta}^{\pm} \cdot \underset{\rightarrow}{F}_H^{\pm} = Y_o[\underset{\rightarrow}{\beta}^{\pm} \cdot \underset{\rightarrow}{C}_{an\ell}(b)] + C_{dn\ell}(b) \qquad (4.37d)$$

It follows from Eqs. (4.17a,b), (III.6a,b,c,d) and (4.37a,b,c,d) that the conditions required for consistency with the Maxwell equations are

$$Z_o[\underset{\rightarrow}{\beta}^{\pm} \cdot \underset{\rightarrow}{C}_{cn\ell}(b)] - C_{bn\ell}(b) = 0 \qquad (4.38a)$$

and

$$Y_o[\underset{\rightarrow}{\beta}^{\pm} \cdot \underset{\rightarrow}{C}_{an\ell}(b)] + C_{dn\ell}(b) = 0 \qquad (4.38b)$$

For the particular case of interest, Eqs. (4.18a,b,c,d) translate Eqs. (4.38a,b) into the form

$$Z_o \bar{H}^{(n)}_{\phi''}(b)(\underset{\rightarrow}{\beta}^{\pm} \cdot \underset{\rightarrow}{\hat{z}}''_{\ell}) - Z_o \bar{H}^{(n)}_{z''}(b)(\underset{\rightarrow}{\beta}^{\pm} \cdot \underset{\rightarrow}{\hat{\phi}}''_{\ell}) - \bar{E}^{(n)}_{r''}(b) = 0 \qquad (4.39a)$$

$$Y_o \bar{E}^{(n)}_{\phi''}(b)(\underset{\rightarrow}{\beta}^{\pm} \cdot \underset{\rightarrow}{\hat{z}}''_{\ell}) - Y_o \bar{E}^{(n)}_{z''}(b)(\underset{\rightarrow}{\beta}^{\pm} \cdot \underset{\rightarrow}{\hat{\phi}}''_{\ell}) + \bar{H}^{(n)}_{r''}(b) = 0 \qquad (4.39b)$$

For TEM modes, where $\bar{E}^{(n)}_{\phi''}$, $\bar{E}^{(n)}_{z''}$, $\bar{H}^{(n)}_{r''}$, $\bar{H}^{(n)}_{z''}$ all vanish, Eq. (4.39a) becomes

$$[\bar{E}^{(n)}_{r''}(b)]^{(TEM)} = Z_o[\bar{H}^{(n)}_{\phi''}(b)]^{(TEM)}(\underset{\rightarrow}{\beta}^{\pm} \cdot \underset{\rightarrow}{\hat{z}}''_{\ell}) \qquad (4.40)$$

and Eq. (4.39b) is an identity

For TM modes in the special case where the boundary conditions require that $E^{(n)}_{z''}(b) = \bar{E}^{(n)}_{\phi''}(b) = \bar{H}^{(n)}_{r''}(b) = 0$ and the TM nature of the modes requires that $\bar{H}^{(n)}_{z''} = 0$, again Eq. (4.39a) becomes

$$[\bar{E}^{(n)}_{r''}(b)]^{(TM)} = Z_o[\bar{H}^{(n)}_{\phi''}(b)]^{(TM)}(\underset{\rightarrow}{\beta}^{\pm} \cdot \underset{\rightarrow}{\hat{z}}''_{\ell}) \qquad (4.41)$$

and Eq. (4.39b) is again an identity.

For TE modes, in the special case where the boundary conditions

require that

$$\bar{E}_{\phi''}^{(n)}(b) = H_{r''}^{(n)}(b) = 0$$

and the TE nature of the modes requires that $\bar{E}_{z''}^{(n)} = 0$, Eq. (4.39a) becomes

$$[\bar{E}_{r''}^{(n)}(b)]^{TE} = Z_o[\bar{H}_{\phi''}^{(n)}(b)]^{TE}(\underset{\rightarrow}{\beta}^{\pm} \cdot \hat{\underset{\rightarrow}{z}}'') - Z_o[\bar{H}_{z''}^{(n)}(b)]^{TE}(\underset{\rightarrow}{\beta}^{\pm} \cdot \hat{\underset{\rightarrow}{\phi}}'') \quad (4.42)$$

and Eq. (4.39b) is an identity.

If $\underset{\rightarrow}{\beta}^{\pm}$ were along $\hat{\underset{\rightarrow}{z}}''$, this would imply a plane-wave propagating along the cable.

At this point we will make an adjustment in the expressions (4.17a,b) and the subsequent relationships derived therefrom. In effect, we are forcing Eqs. (4.17a,b) into consistency with the Maxwell equations in $\underline{\beta}$-space (i.e., those of a plane-wave with propagation vector $\underline{\beta}$). Another way of looking at this is to consider it as a matching of the fields just inside the slots with the fields just outside the slots. The latter must obey the conditions (4.38a,b), which in turn must be equivalent to the vanishing of the last set of terms in Eq. (III.7), since both of these conditions imply consistency with the $\underline{\beta}$-space Maxwell equations. Such consistency is required of the plane-wave spectrum of a field. The original assumption that the fields on the slots can be approximated by those of the wave propagating along the cable as if the slots were not present is being replaced by the assumption that there is a small perturbation due to the slots. This perturbation changes the fields on the slots just enough to force the plane-wave spectrum of the fields at an arbitrary point in space to obey the Maxwell equations for a plane wave with propagation vector $\underset{\rightarrow}{\beta}$. The reason the original plane-wave spectra (4.17a,b) did not show

consistency with these equations was because of our insistence that the fields on the slot be exactly equal to those propagating down a slotless cable at the slot position. Both of these sets of plane-wave spectra (4.17a,b) and those to be given in what follows are rough approximations to the truth. It is asserted that the latter are better approximations than the former.

The indicated adjustment in the original forms (4.17a,b) consists of redefinition of $\tilde{\underset{\rightarrow}{F}}^{\pm}_{E}$ and $\tilde{\underset{\rightarrow}{F}}^{\pm}_{H}$ in Eqs. (4.22a) and (4.22b) respectively, as follows:

$$\tilde{\underset{\rightarrow}{F}}^{\pm}_{E} = \left(-Z_o \underset{\rightarrow}{C}_{cn\ell}(b) - \underset{\rightarrow}{\beta}^{\pm} \times \underset{\rightarrow}{C}_{an\ell}(b) + \underset{\rightarrow}{\beta}^{\pm} Z_o[\underset{\rightarrow}{\beta}^{\pm} \cdot \underset{\rightarrow}{C}_{cn\ell}(b)]\right) f^{\pm} \qquad (4.43a)$$

$$\tilde{\underset{\rightarrow}{F}}^{\pm}_{H} = \left(Y_o \underset{\rightarrow}{C}_{an\ell}(b) - \underset{\rightarrow}{\beta}^{\pm} \times \underset{\rightarrow}{C}_{cn\ell}(b) - \underset{\rightarrow}{\beta}^{\pm} Y_o[\underset{\rightarrow}{\beta}^{\pm} \cdot \underset{\rightarrow}{C}_{an\ell}(b)]\right) f^{\pm} \qquad (4.43b)$$

Applying $(Y_o \underset{\rightarrow}{\beta}^{\pm} \times \ldots)$ to $\tilde{\underset{\rightarrow}{F}}^{\pm}_{E}$ as given in Eq. (4.43a) yields

$$Y_o \underset{\rightarrow}{\beta}^{\pm} \times \tilde{\underset{\rightarrow}{F}}^{\pm}_{E} = \tilde{\underset{\rightarrow}{F}}^{\pm}_{H} \qquad (4.44a)$$

Applying $(-Z_o \underset{\rightarrow}{\beta}^{\pm} \times \ldots)$ to $\tilde{\underset{\rightarrow}{F}}^{\pm}_{H}$ as given in Eq. (4.43b) yields

$$-Z_o \underset{\rightarrow}{\beta}^{\pm} \times \tilde{\underset{\rightarrow}{F}}^{\pm}_{H} = \tilde{\underset{\rightarrow}{F}}^{\pm}_{E} \qquad (4.44b)$$

Applying $(\underset{\rightarrow}{\beta}^{\pm} \cdot \ldots)$ to $\tilde{\underset{\rightarrow}{F}}^{\pm}_{E}$ and $\tilde{\underset{\rightarrow}{F}}^{\pm}_{H}$ yields

$$\underset{\rightarrow}{\beta}^{\pm} \cdot \tilde{\underset{\rightarrow}{F}}^{\pm}_{E} = 0 \qquad (4.44c)$$

$$\underset{\rightarrow}{\beta}^{\pm} \cdot \tilde{\underset{\rightarrow}{F}}^{\pm}_{H} = 0 \qquad (4.44d)$$

The equations (4.44a,b,c,d) establish the consistency of the forms of $\tilde{\underset{\rightarrow}{E}}^{\pm}(\underset{\rightarrow}{\beta}_h)$

and $\vec{\tilde{H}}^{\pm}(\beta_h)$ implied by Eqs. (4.43a,b) with the Maxwell equations (III.6a,b,c,d). The quantities replacing $\tilde{F}_{Ex}, \ldots, \tilde{F}_{Hz}$ in Eqs. (4.22a,b,c,d,e,f)' are:

$$(\tilde{\bar{F}}^{\pm}_{Ex})^{\ell n} = \Big(\bar{E}^{(n)}_{r''}[0] + \bar{E}^{(n)}_{\phi''}[\pm|\beta_z| \cos\phi_{\ell o}]$$

$$+ \bar{E}^{(n)}_{z''}[\beta_y \cos\phi''_{\ell o} \pm |\beta_z| \sin\phi_{\ell o} \sin\phi''_{\ell o}] + \bar{H}^{(n)}_{r''}[0]$$

$$+ \bar{H}^{(n)}_{\phi''}[Z_o\{(1 - \beta_x^2) \sin\phi_{\ell o} + \beta_x \beta_y \cos\phi_{\ell o}\}]$$

$$+ \bar{H}^{(n)}_{z''}[Z_o\{-\sin\phi''_{\ell o}((1 - \beta_x^2) \cos\phi_{\ell o} - \beta_x \beta_y \sin\phi_{\ell o})$$

$$\mp \beta_x|\beta_z| \cos\phi''_{\ell o}\}]\Big) f^{\pm} \qquad (4.45a)$$

$$(\tilde{\bar{F}}^{\pm}_{Ey})^{\ell n} = \Big(\bar{E}^{(n)}_{r''}[0] + \bar{E}^{(n)}_{\phi''}[\pm|\beta_z| \sin\phi_{\ell o}]$$

$$+ \bar{E}^{(n)}_{z''}[-\beta_x \cos\phi''_{\ell o} \pm|\beta_z| \cos\phi_{\ell o} \sin\phi''_{\ell o}] + \bar{H}^{(n)}_{r''}[0]$$

$$+ \bar{H}^{(n)}_{\phi''}[-Z_o\{(1 - \beta_y^2) \cos\phi_{\ell o} + \beta_x \beta_y \sin\phi_{\ell o}\}]$$

$$+ \bar{H}^{(n)}_{z''}[-Z_o\{\sin\phi''_{\ell o}((1 - \beta_y^2) \sin\phi_{\ell o} - \beta_x \beta_y \cos\phi_{\ell o})$$

$$\pm |\beta_z|\beta_y \cos\phi''_{\ell o}\}]\Big) f^{\pm} \qquad (4.45b)$$

$$(\tilde{\bar{F}}^{\pm}_{Ez})^{\ell n} = \Big(\bar{E}^{(n)}_{r''}[0] + \bar{E}^{(n)}_{\phi''}[-(\beta_x \cos\phi_{\ell o} + \beta_y \sin\phi_{\ell o})]$$

$$+ \bar{E}^{(n)}_{z''}[\sin\phi''_{\ell o}(-\beta_x \sin\phi_{\ell o} + \beta_y \cos\phi_{\ell o})]$$

$$+ \bar{H}_{r''}^{(n)}[0] + \bar{H}_{\phi''}^{(n)}[\pm Z_0|\beta_z|(-\beta_x \sin\phi_{\ell o} + \beta_y \cos\phi_{\ell o})]$$

$$+ \bar{H}_{z''}^{(n)}[Z_0\{-|\beta_z|^2 \cos\phi''_{\ell o} \pm |\beta_z| \sin\phi''_{\ell o}(\beta_x \cos\phi_{\ell o}$$

$$+ \beta_y \sin\phi_{\ell o})\}]\Big) f^{\pm} \qquad (4.45c)$$

$$(\tilde{\bar{F}}^{\pm}_{Hx})^{\ell n} = \Big(\bar{E}_{r''}^{(n)}[0] + \bar{E}_{\phi''}^{(n)}[-Y_0\{(1-\beta_x^2)\sin\phi_{\ell o} + \beta_x \beta_y \cos\phi_{\ell o}\}]$$

$$+ \bar{E}_{z''}^{(n)}[Y_0\{\sin\phi''_{\ell o}((1-\beta_x^2)\cos\phi_{\ell o} - \beta_x \beta_y \sin\phi_{\ell o})$$

$$\mp \beta_x|\beta_z| \cos\phi''_{\ell o}\}] + \bar{H}_{r''}^{(n)}[0] + \bar{H}_{\phi''}^{(n)}[\pm|\beta_z| \cos\phi_{\ell o}]$$

$$+ \bar{H}_{z''}^{(n)}[\beta_y \cos\phi''_{\ell o} \pm |\beta_z| \sin\phi_{\ell o} \sin\phi''_{\ell o}]\Big) f^{\pm} \qquad (4.45d)$$

$$(\tilde{\bar{F}}^{\pm}_{Hy})^{\ell n} = \Big(\bar{E}_{r''}^{(n)}[0] + \bar{E}_{\phi''}^{(n)}[y_0\{(1-\beta_y^2)\cos\phi_{\ell o} + \beta_x \beta_y \sin\phi_{\ell o}\}]$$

$$+ \bar{E}_{z''}^{(n)}[Y_0\{\sin\phi''_{\ell o}((1-\beta_y^2)\sin\phi_{\ell o} - \beta_x \beta_y \cos\phi_{\ell o})$$

$$\mp \beta_y|\beta_z| \cos\phi''_{\ell o}\}] + \bar{H}_{r''}^{(n)}[0] + \bar{H}_{\phi''}^{(n)}[\pm|\beta_z| \sin\phi_{\ell o}]$$

$$+ \bar{H}_{z''}^{(n)}[-\beta_x \cos\phi''_{\ell o} \pm |\beta_z| \cos\phi_{\ell o} \sin\phi''_{\ell o}]\Big) f^{\pm} \qquad (4.45e)$$

$$(\tilde{\bar{F}}^{\pm}_{Hz})^{\ell n} = \Big(\bar{E}_{r''}^{(n)}[0] + \bar{E}_{\phi''}^{(n)}[\mp|\beta_z| Y_0(-\beta_x \sin\phi_{\ell o} + \beta_y \cos\phi_{\ell o})]$$

$$+ \bar{E}_{z''}^{(n)}[-Y_0\{-|\beta_z|^2 \cos\phi''_{\ell o} \pm |\beta_z| \sin\phi''_{\ell o}(\beta_x \cos\phi_{\ell o}$$

$$+ \beta_y \sin\phi_{\ell o})\}] + \bar{H}_{r''}^{(n)}[0] + \bar{H}_{\phi''}^{(n)}[-(\beta_x \cos\phi_{\ell o} + \beta_y \sin\phi_{\ell o})]$$

$$+ \bar{H}_{z''}^{(n)}[\sin\phi''_{\ell 0}(-\beta_x \sin\phi_{\ell 0} + \beta_y \cos\phi_{\ell 0})]\Big) f' \qquad (4.45f)$$

The case actually programmed for the computer was that wherein $\phi''_{\ell 0}$ is constant and the slots are spaced equally along the cable, resulting in the conditions (4.24) and (4.25). For this case, the expressions analogous to Eqs. (4.30a,b,c,d,e,f)' [obtained from Eqs. (4.45a,b,c,d,e,F)] are as follows (in abbreviated notation):

$$[\bar{\tilde{E}}_{\pm}^{(n)}]_{\substack{x\\y\\z}} = S_0^{(n)}[(\bar{\tilde{E}}_{\pm}^{(n)})_0]_{\substack{x\\y\\z}} + \frac{e^{j\phi_{10}}}{2} S_+^{(n)}[(\bar{\tilde{E}}_{\pm}^{(n)})_+]_{\substack{x\\y\\z}} + \frac{e^{-j\phi_{10}}}{2} S_-^{(n)}[(\bar{\tilde{E}}_{\pm}^{(n)})_-]_{\substack{x\\y\\z}} \qquad (4.46a)$$

$$[\bar{\tilde{H}}_{\pm}^{(n)}]_{\substack{x\\y\\z}} = S_0^{(n)}[(\bar{\tilde{H}}_{\pm}^{(n)})_0]_{\substack{x\\y\\z}} + \frac{e^{j\phi_{10}}}{2} S_+^{(n)}[(\bar{\tilde{H}}_{\pm}^{(n)})_+]_{\substack{x\\y\\z}} + \frac{e^{-j\phi_{10}}}{2} S_-^{(n)}[(\bar{\tilde{H}}_{\pm}^{(n)})_-]_{\substack{x\\y\\z}} \qquad (4.46b)$$

where

$$[(\bar{\tilde{E}}_{\pm}^{(n)})_0]_{\substack{x\\y\\z}} = \left\{ \bar{H}_{z''}^{(n)} Z_0 \begin{bmatrix} \mp\beta_x|\beta_z| \\ \mp\beta_y|\beta_z| \\ |\beta_z|^2 \end{bmatrix} + \bar{F}_{z''}^{(n)} \begin{bmatrix} \beta_y \\ -\beta_x \\ 0 \end{bmatrix} \right\} \cos\phi''_0 \qquad (4.47a)$$

$$[(\bar{\tilde{H}}_{\pm}^{(n)})_0]_{\substack{x\\y\\z}} = \left\{ \bar{E}_{z''}^{(n)} Y_0 \begin{bmatrix} \mp\beta_x|\beta_z| \\ \mp\beta_y|\beta_z| \\ |\beta_z|^2 \end{bmatrix} + \bar{H}_{z''}^{(n)} \begin{bmatrix} \beta_y \\ -\beta_x \\ 0 \end{bmatrix} \right\} \cos\phi''_0 \qquad (4.47b)$$

$$[(\bar{\tilde{E}}_{\pm}^{(n)})_{+}]_{\substack{x\\y\\z}} = \left\{ \bar{E}_{\phi''}^{(n)} \begin{bmatrix} \pm|\beta_z| \\ \mp j|\beta_z| \\ -(\beta_x - j\beta_y) \end{bmatrix} + \bar{E}_{z''}^{(n)} \begin{bmatrix} \mp j|\beta_z| \\ \mp|\beta_z| \\ j(\beta_x - j\beta_y) \end{bmatrix} \sin\phi_o'' \right.$$

$$\left. + \bar{H}_{\phi''}^{(n)} Z_o \begin{bmatrix} -jA_x \\ -A_y^* \\ \pm j|\beta_z|(\beta_x - j\beta_y) \end{bmatrix} + \bar{H}_{z''}^{(n)} Z_o \begin{bmatrix} -A_x \\ jA_y^* \\ \pm|\beta_z|(\beta_x - j\beta_y) \end{bmatrix} \sin\phi_o'' \right\} . \quad (4.47c)$$

where

$$A_x = (1 - \beta_x^2) + j\beta_x \beta_y$$

$$A_y = (1 - \beta_y^2) + j\beta_x \beta_y$$

$$[(\bar{\tilde{H}}_{\pm}^{(n)})_{+}]_{\substack{x\\y\\z}} = \left\{ \bar{H}_{\phi''}^{(n)} \begin{bmatrix} \pm|\beta_z| \\ \mp j|\beta_z| \\ -(\beta_x - j\beta_y) \end{bmatrix} + \bar{H}_{z''}^{(n)} \begin{bmatrix} \mp j|\beta_z| \\ \pm|\beta_z| \\ j(\beta_x - j\beta_y) \end{bmatrix} \sin\phi_o'' \right.$$

$$\left. + Y_o \bar{E}_{\phi''}^{(n)} \begin{bmatrix} jA_x \\ A_y^* \\ \mp j|\beta_z|(\beta_x - j\beta_y) \end{bmatrix} + Y_o \bar{E}_{z''}^{(n)} \begin{bmatrix} A_x \\ -jA_y^* \\ \mp|\beta_z|(\beta_x - j\beta_y) \end{bmatrix} \sin\phi_o'' \right\} . \quad (4.47d)$$

$$\left[\left(\bar{\tilde{E}}^{(n)}_{\pm}\right)_{-}\right]_{\substack{x\\y\\z}} = \left\{ \bar{E}^{(n)}_{\phi''} \begin{bmatrix} \pm|\beta_z| \\ \pm j|\beta_z| \\ -(\beta_x + j\beta_y) \end{bmatrix} + \bar{E}^{(n)}_{z''} \begin{bmatrix} \pm j|\beta_z| \\ \mp|\beta_z| \\ -j(\beta_x + j\beta_y) \end{bmatrix} \sin\phi''_o \right.$$

$$\left. + \bar{H}^{(n)}_{\phi''} Z_o \begin{bmatrix} jA^*_x \\ -A_y \\ \mp j|\beta_z|(\beta_x + j\beta_y) \end{bmatrix} + \bar{H}^{(n)}_{z''} Z_o \begin{bmatrix} -A^*_x \\ -jA_y \\ \pm|\beta_z|(\beta_x + j\beta_y) \end{bmatrix} \sin\phi''_o \right\}$$

(4.47e)

$$\left[\left(\bar{\tilde{H}}^{(n)}_{\pm}\right)_{-}\right]_{\substack{x\\y\\z}} = \left\{ \bar{H}^{(n)}_{\phi''} \begin{bmatrix} \pm|\beta_z| \\ \pm j|\beta_z| \\ -(\beta_x + j\beta_y) \end{bmatrix} + \bar{H}^{(n)}_{z''} \begin{bmatrix} \pm j|\beta_z| \\ \mp|\beta_z| \\ -j(\beta_x + j\beta_y) \end{bmatrix} \sin\phi''_o \right.$$

$$\left. + \bar{E}^{(n)}_{\phi''} Y_o \begin{bmatrix} -jA^*_x \\ A_y \\ \pm j|\beta_z|(\beta_x + j\beta_y) \end{bmatrix} + \bar{E}^{(n)}_{z''} Y_o \begin{bmatrix} A^*_x \\ jA_y \\ \mp|\beta_z|(\beta_x + j\beta_y) \end{bmatrix} \sin\phi''_o \right\}$$

(4.47f)

Specializations of Eqs. (4.46a,b,c,d,e,f) to the case of TEM, TE and TM modes are presented below. These are based on the forms of the fields for these modes developed in Appendix IV.

TEM, TM Modes

These fields are given by Eqs. (4.46a,b), where

$$\left[\left(\bar{\tilde{E}}_{\pm}^{(n)}\right)_o\right]_{\substack{x\\y\\z}}^{\substack{(TEM)\\(TM_n)}} = \left[\left(\bar{\tilde{H}}_{\pm}^{(n)}\right)_o\right]_{\substack{x\\y\\z}}^{\substack{(TEM)\\(TM_n)}} = 0 \tag{4.48a}$$

$$\left[\left(\bar{\tilde{E}}_{\pm}^{(n)}\right)_+\right]_{\substack{x\\y\\z}}^{\substack{(TEM)\\(TM_n)}} = Z_o\, Y_w\, \bar{E}_{r''}^{(n)}(b) \begin{bmatrix} -jA_x \\ -A_y^* \\ \pm j|\beta_z|(\beta_x - j\beta_y) \end{bmatrix} \tag{4.48b}$$

$$\left[\left(\bar{\tilde{E}}_{\pm}^{(n)}\right)_-\right]_{\substack{x\\y\\z}}^{\substack{(TEM)\\(TM_n)}} = Z_o\, Y_w\, \bar{E}_{r''}^{(n)}(b) \begin{bmatrix} jA_x^* \\ -A_y \\ \mp j|\beta_z|(\beta_x + j\beta_y) \end{bmatrix} \tag{4.48c}$$

$$\left[\left(\bar{\tilde{H}}_{\pm}^{(n)}\right)_+\right]_{\substack{x\\y\\z}}^{\substack{(TEM)\\(TM_n)}} = Y_w\, \bar{E}_{r''}^{(n)}(b) \begin{bmatrix} \pm|\beta_z| \\ \mp j|\beta_z| \\ -(\beta_x - j\beta_y) \end{bmatrix} \tag{4.48d}$$

$$\left[\left(\bar{\tilde{H}}_{\pm}^{(n)}\right)_-\right]_{\substack{x\\y\\z}}^{\substack{(TEM)\\(TM_n)}} = Y_w\, \bar{E}_{r''}^{(n)}(b) \begin{bmatrix} \pm|\beta_z| \\ \pm j|\beta_z| \\ -(\beta_x + j\beta_y) \end{bmatrix} \tag{4.48e}$$

$$\bar{E}^{(n)}_{r''}(b) = [\bar{E}^{(n)}_{r''}(b)]^{TEM} = \frac{V_o}{\ell n(b/a)b} \quad \text{for TEM mode} \tag{4.48f}$$

[from Eq. (IV.4a)], where V_o = voltage between inner boundary at r" = a and outer boundary at r" = b.

$$\bar{E}^{(n)}_{r''}(b) = [\bar{E}^{(n)}_{r''}(b)]^{TM_n} = - \frac{A^{TM_n}}{N_n(k_{cn}b)} \frac{j\hat{k}_{zn}}{\hat{k}_{cn}} L_n(k_{cn}\, b) \tag{4.48g}$$

for TE_n mode

[from Eq. (IV.11b)] where all quantities in Eq. (4.48g) are defined in Appendix IV.

$$A_x = (1 - \beta_x^2) + j\beta_x\, \beta_y \tag{4.48h}$$

$$A_y = (1 - \beta_y^2) + j\beta_x\, \beta_y \tag{4.48i}$$

$$Y_w = \text{wave admittance} \tag{4.48j}$$

For TEM mode

$$Y_w = \sqrt{\frac{\varepsilon_{ca}}{\mu_o}}\ ; \quad \varepsilon_{ca} = \text{complex dielectric constant of cable material} \tag{4.48k}$$

For TM_n mode

$$Y_w = Y_w^{TM_n} = \frac{\omega\, \varepsilon_{ca}}{k_{zn}} \tag{4.48ℓ}$$

For TE_n modes:

$$\left[\left(\underline{\tilde{E}}_{\pm}^{(n)}\right)_o\right]_{\substack{x\\y\\z}}^{(TE_n)} = \bar{H}_{z''}^{(n)}(b)\, Z_o \begin{bmatrix} \mp\beta_x|\beta_z| \\ \mp\beta_y|\beta_z| \\ |\beta_z|^2 \end{bmatrix} \tag{4.49a}$$

$$\left[\left(\underline{\tilde{H}}_{\pm}^{(n)}\right)_o\right]_{\substack{x\\y\\z}}^{(TE_n)} = \bar{H}_{z''}^{(n)}(b) \begin{bmatrix} \beta_y \\ -\beta_x \\ 0 \end{bmatrix} \tag{4.49b}$$

$$\left[\left(\underline{\tilde{E}}_{\pm}^{(n)}\right)_+\right]_{\substack{x\\y\\z}}^{(TE_n)} = Z_o \begin{bmatrix} -jA_x \\ -A_y^* \\ \pm j|\beta_z|(\beta_x - j\beta_y) \end{bmatrix} \left\{ Y_w^{TE_n} \bar{E}_{r''}^{(n)}(b) - j\bar{H}_{z''}^{(n)}(b) \sin\phi_o'' \right\} \tag{4.49c}$$

$$\left[\left(\underline{\tilde{E}}_{\pm}^{(n)}\right)_-\right]_{\substack{x\\y\\z}}^{(TE_n)} = Z_o \begin{bmatrix} jA_x \\ -A_y \\ \mp j|\beta_z|(\beta_x + j\beta_y) \end{bmatrix} \left\{ Y_w^{TE_n} \bar{E}_{r''}^{(n)}(b) + j\bar{H}_{z''}^{(n)}(b) \sin\phi_o'' \right\} \tag{4.49d}$$

$$\left[\left(\underline{\tilde{H}}_{\pm}^{(n)}\right)_+\right]_{\substack{x\\y\\z}}^{(TE_n)} = \begin{bmatrix} \pm|\beta_z| \\ \mp j|\beta_z| \\ -(\beta_x - j\beta_y) \end{bmatrix} \left\{ Y_w^{TE_n} \bar{E}_{r''}^{(n)}(b) - j\bar{H}_{z''}^{(n)}(b) \sin\phi_o'' \right\} \tag{4.49e}$$

$$[(\bar{\bar{H}}_{\pm}^{(n)})_{-}]_{x,y,z}^{(TE_n)} = \begin{bmatrix} \pm|\beta_z| \\ \pm j|\beta_z| \\ -(\beta_x + j\beta_y) \end{bmatrix} \left\{ Y_w^{TE_n} \bar{E}_{r''}^{(n)}(b) + jH_{z''}^{(n)}(b) \sin\phi_o'' \right\} \tag{4.49f}$$

$$\bar{E}_{r''}^{(n)}(b) = [\bar{E}_{r''}^{(n)}(b)]^{TE_n} = \frac{A^{TE_n} jn \hat{k}_{zn}}{Y_w^{TE_n} N_n'(k_{cn} b) \hat{k}_{cn}^2 b} \mathcal{L}_n(k_{cn} b) \tag{4.49g}$$

$$\bar{H}_{z''}^{(n)}(b) = [\bar{H}_{z''}^{(n)}(b)]^{TE_n} = \frac{A^{TE_n}}{N_n'(k_{cn} b)} \mathcal{L}_n(k_{cn} b) \tag{4.49h}$$

$$Y_w^{(TE_n)} = \frac{k_{zn}}{\omega \mu_o} \tag{4.49i}$$

Other quantities used in Eqs. (4.49a-i) are defined in Eq. (4.48h,i,j) or in Appendix IV.

The forms (4.48a-ℓ) and (4.49a-i) are those actually programmed and hence on which our numerical results are based. However, in the computations the sums over the cable slots, $S_{0,+,-}^{(n)}$ are not treated through Eqs. (4.33) through (4.36d). These expressions would be strictly valid only if $f^{\pm}$ were approximately unity. In the general case where $f^{\pm}$ is accounted for, the sums are replaced by integrals and a different technique is used for their approximate evaluation.

First, we take advantage of the fact that, in (4.31-a,b,c), parameter values in all cases of interest are such that [see (4.36b)]:

$$| k_o(\hat{k}_{znR}\mathcal{R}) | >> 1 \tag{4.50}$$

Equation (4.50) is used to justify the approximation

$$S_o^{(n)} \simeq S_+^{(n)} \simeq S_-^{(n)} \quad . \tag{4.51}$$

From (4.31-a,b,c) and (4.50), where

$$\phi' = \phi_{10} + \frac{2\pi(\ell-1)}{N_s} \tag{4.52}$$

we have

$$S_o^{(n)} \simeq S_+^{(n)} \simeq S_-^{(n)} \simeq \frac{1}{2\pi} \int_0^{2\pi} d\phi' f^{\pm}(\phi') e^{-jk_o\mathcal{R}[\rho_h \cos(\phi'-\phi_\beta) + \hat{k}_{zn}\phi']} \tag{4.53}$$

where the dependence of $f^{\pm}$ on ϕ' is explicitly indicated.

Noting that

$$\hat{k}_{zn} = \hat{k}_{znR} - j\frac{\alpha_n}{k_o} \tag{4.54}$$

where $\hat{k}_{znR}$ is the real part of $\hat{k}_{zn}$ and α_n is the attenuation along the cable, we can express (4.53) generically in the form

$$S = S_a + S_b$$

where

$$\begin{matrix} S_a \\ S_b \end{matrix} = \begin{bmatrix} 1 \\ -j \end{bmatrix} \int_{\phi'_L}^{\phi'_U} d\phi' g_{\begin{matrix} a \\ b \end{matrix}}(\phi') e^{j(k_o\mathcal{R})\psi(\phi')} \tag{4.55}$$

and where

$$\psi(\phi') = -[\hat{k}_{znR}\phi' + \beta_h \cos(\phi' - \phi_\beta)]$$

$$g_a(\phi') = e^{-\alpha_n \mathcal{R}\phi'} \left[1 + \frac{\underset{\rightarrow}{\beta}\cdot\underset{\rightarrow}{R}}{R}\right]$$

$$g_b(\phi') = e^{-\alpha_n \mathcal{R}\phi'} \left(\frac{1}{k_o R}\right)$$

$$\underset{\rightarrow}{R} = \hat{x}(\rho\cos\phi - \mathcal{R}\cos\phi') + \hat{y}(\rho\sin\phi - \mathcal{R}\sin\phi') + \hat{z}(z)$$

$$R = \sqrt{\mathcal{R}^2 + \rho^2 + z^2 - 2\mathcal{R}\rho\cos(\phi' - \phi)}$$

$$\frac{\underset{\rightarrow}{\beta} \pm \underset{\rightarrow}{R}}{R} = \frac{\beta_h[\rho\cos(\phi - \phi_\beta) - \mathcal{R}\cos(\phi' - \phi_\beta)] \pm |\beta_z| z}{\sqrt{\mathcal{R}^2 + \rho^2 + z^2 - 2\mathcal{R}\rho\cos(\phi' - \phi)}}$$

Since $g_a(\phi')$ and $g_b(\phi')$ are both real, and since

$$k_o\mathcal{R} >> 1 \tag{4.56}$$

for all cases of interest, the integrals S_a and S_b are both of a type that can be evaluated approximately by an asymptotic form given in Reference A.5, pages 276-278. The method is based on a form of the principal of stationary phase, but the case involved is that wherein there is no stationary point, i.e.,

$$\frac{d\psi}{d\phi}(\phi') \neq 0 \quad \text{at all points} \tag{4.57}$$

Since

$$\frac{d\psi(\phi')}{d\phi'} = \beta_h \sin(\phi' - \phi_\beta) - \hat{k}_{znR} \tag{4.58}$$

and since $\hat{k}_{znR} > 1$ in the cases under consideration, and $|\beta_h \sin(\phi' - \phi_\beta)| \leq 1$,

it follows that (4.57) must hold. Since (4.56) also holds in all cases of interest, the method is applicable.

The asymptotic solution is [Reference A.5, page 278, Eq. (6.57)]:

$$\begin{matrix} S_a \\ b \end{matrix} \simeq \frac{1}{jk_o \mathscr{R}} \left\{ \left. \frac{e^{jk_o \psi(\phi')}}{\left[\frac{d\psi(\phi')}{d\phi'}\right]} \right|_{\phi'=\phi'_U} \begin{matrix} g_a \\ b \end{matrix} (\phi'_U) - \left. \frac{e^{jk_o \psi(\phi')}}{\left[\frac{d\psi(\phi')}{d\phi'}\right]} \right|_{\phi'=\phi'_L} \begin{matrix} g_a(\phi'_L) \\ b \end{matrix} \right\} \tag{4.59}$$

where upper and lower limits ϕ'_U and ϕ'_L for S_a and S_b are dependent on the forms of $g_a(\phi')$ and $g_b(\phi')$ respectively.

Another term was included in the computations to account for the $\frac{R}{R^3}$ term present at points very close to the cable. This term was also evaluated by the above method.

5. PLANE-WAVE SPECTRAL REPRESENTATION OF GROUND-REFLECTED FIELDS

We can do the ground reflection problem for a particular spectral component (i.e., particular values of β_x and β_y) and having accounted for the boundary conditions for each such component, we can then integrate over all β_x, β_y. This, of course, reduces the problem to the classical case of plane-wave reflection from an infinite boundary between two media.[A-1]

We will now outline the method of analysis which was carried out to obtain the (x,y,z) components of the reflected wave fields and to construct a matrix relating the reflected fields to the incident fields. Since the literature is replete with solutions of this problem there is certainly nothing new or original about this portion of the analysis.

Consider incident and reflected wave electric and magnetic field components for a particular value of (β_x, β_y) where incident fields are denoted by $(\underset{\sim}{E}_{\pm i}, \underset{\sim}{H}_{\pm i})$ and reflected fields by $(\underset{\sim}{E}_{\pm r}, \underset{\sim}{H}_{\pm r})$. We must also include the fields of the wave transmitted into the ground, denoted by $(\underset{\sim}{E}_{\pm t}, \underset{\sim}{H}_{\pm t})$.

For fixed values of (β_x, β_y) (see Appendix II) the horizontal components of the electric field above ground (in free space) are:

$$\begin{matrix} E_{ix} \\ y \\ z \end{matrix} + \begin{matrix} E_{rx} \\ y \\ z \end{matrix} = e^{jk(\beta_x x+\beta_y y)} \left[\begin{matrix} \tilde{E}_{ix} \\ y \\ z \end{matrix} e^{-jk|\beta_z|z} + \begin{matrix} \tilde{E}_{rx} \\ y \\ z \end{matrix} e^{jk|\beta_z|z} \right] \qquad (5.1a)$$

(where it is noted that the incident and reflected waves propagate downward and upward respectively).

The horizontal components of the electric field in the ground ($z < 0$) is (note downward propagation only)

$$\begin{matrix} E_{tx} \\ y \\ z \end{matrix} = \begin{matrix} \tilde{E}_{tx} \\ y \\ z \end{matrix} e^{jk(\beta_x x+\beta_y y)} \; e^{-jk\gamma_z z} \qquad (5.1b)$$

where

$$\gamma_z = \sqrt{\nu^2 - (\beta_x^2 + \beta_y^2)}$$

and ν is the complex refractive index of the earth, given by

$$\nu = \nu_R + j\nu_I \tag{5.2}$$

where

$$\nu_R = \sqrt{\frac{\varepsilon_R}{2}} \sqrt{1 + \sqrt{1 + \left(\frac{\sigma}{\omega \varepsilon_o \varepsilon_R}\right)^2}}$$

$$\nu_I = \sqrt{\frac{\varepsilon_R}{2}} \sqrt{-1 + \sqrt{1 + \left(\frac{\sigma}{\omega \varepsilon_o \varepsilon_R}\right)^2}}$$

and where ε_R = relative permittivity of ground, ε_o = permittivity of free space = $8.854(10^{-12})$ farads/meter, μ_o = $4\ (10^{-7})$ henries/meter = Magnetic permeability of free space, assumed to be also that of the earth, σ = conductivity of ground in mhos/meter. The horizontal magnetic field components are:

<u>$z > 0$</u>

$$H_{ix} + H_{rx} = \sqrt{\frac{\varepsilon_o}{\mu_o}}\, e^{jk(\beta_x x + \beta_y y)} \left[e^{-jk|\beta_z|z} (\beta_y \tilde{E}_{iz} + |\beta_z| \tilde{E}_{iy}) \right.$$

$$\left. + e^{jk|\beta_z|z} (\beta_y \tilde{E}_{rz} - |\beta_z| \tilde{E}_{ry})\right] \tag{5.3a}$$

$$H_{iy} + H_{ry} = \sqrt{\frac{\varepsilon_0}{\mu_0}}\, e^{jk(\beta_x x+\beta_y y)}\left[-e^{-jk|\beta_z|z}(|\beta_z|\tilde{E}_{ix} + \beta_x \tilde{E}_{iz})\right.$$

$$\left. + e^{jk|\beta_z|z}(|\beta_z|\tilde{E}_{rx} - \beta_x \tilde{E}_{rz})\right] \qquad (5.3b)$$

$\underline{z < 0}$

$$H_{tx} = \sqrt{\frac{\varepsilon_0}{\mu_0}}\, e^{jk(\beta_x x+\beta_y y)-jk\gamma_z z}(\beta_y \tilde{E}_{tz} + \gamma_z \tilde{E}_{ty}) \qquad (5.3c)$$

$$H_{ty} = \sqrt{\frac{\varepsilon_0}{\mu_0}}\, e^{jk(\beta_x x+\beta_y y)-jk\gamma_z z}(-\gamma_z \tilde{E}_{tx} - \beta_x \tilde{E}_{tz}) \qquad (5.3d)$$

To determine the vertical components of the electric field, we invoke the equations

$$\nabla \cdot \underset{\substack{\rightarrow \\ r}}{E_i} \alpha\, jk(\beta_x \tilde{E}_{ix} + \beta_y \tilde{E}_{iy} \mp |\beta_z| \tilde{E}_{iz}) = 0 \qquad (5.4a)$$

$$\nabla \cdot \underset{\rightarrow}{E_t} \alpha\, jk(\beta_x \tilde{E}_{tx} + \beta_y \tilde{E}_{ty} - \gamma_z \tilde{E}_{tz}) = 0 \qquad (5.4b)$$

Solving Eqs. (5.4a,b) for $\tilde{E}_{iz}$, $\tilde{E}_{rz}$, $\tilde{E}_{tz}$ in terms of $\tilde{E}_{ix}$, $\tilde{E}_{rx}$, $\tilde{E}_{tx}$ and equating the tangential components of both electric and magnetic fields at $z = 0$, we arrive at the set of equations:

$$(|\beta_z|\gamma_z)\, \tilde{E}_{rx} - (|\beta_z|\gamma_z)\, \tilde{E}_{tx} = -(|\beta_z|\gamma_z)\, \tilde{E}_{ix}$$

$$(|\beta_z|\gamma_z)\, \tilde{E}_{ry} - (|\beta_z|\ _z)\, \tilde{E}_{ty} = -(|\beta_z|\gamma_z)\, \tilde{E}_{iy} \qquad (5.5b)$$

$$(\beta_x\beta_y\gamma_z)\,\tilde{E}_{rx} + ((1-\beta_x^2)\,\gamma_z)\,\tilde{E}_{ry} + (\beta_x\beta_y|\beta_z|)\tilde{E}_{tx} + ((\nu^2-\beta_x^2)|\beta_z|)\,\tilde{E}_{ty}$$

$$= (\beta_x\beta_y\gamma_z)\,\tilde{E}_{ix} + ((1-\beta_x^2)\,\gamma_z)\,\tilde{E}_{iy} \qquad (5.5c)$$

$$((1-\beta_y^2)\,\gamma_z)\,\tilde{E}_{rx} + (\beta_x\beta_y\gamma_z)\,\tilde{E}_{ry} + ((\nu^2-\beta_y^2)|\beta_z|)\,\tilde{E}_{tx} + (\beta_x\beta_y|\beta_z|)\,\tilde{E}_{ty}$$

$$= ((1-\beta_y^2)\gamma_z)\,\tilde{E}_{ix} + (\beta_x\beta_y\gamma_z)\,\tilde{E}_{iy} \qquad (5.5d)$$

Solving Eqs. (5.5a,b,c,d) by Kramer's rule yields the horizontal components of the incident wave, as follows:

$$\tilde{E}_{rx+} = 2\left(\frac{\gamma_z - |\beta_z|}{\gamma_z + |\beta_z|}\right)\frac{1}{(1-\beta_z^2+|\beta_z|\gamma_z)}\{[\beta_x^2 - \tfrac{1}{2}(1-\beta_z^2+|\beta_z|\gamma_z)]\,\tilde{E}_{ix}$$

$$+ [\beta_x\beta_y]\,\tilde{E}_{iy-}\} \qquad (5.6a)$$

$$\tilde{E}_{ry+} = 2\left(\frac{\gamma_z - |\beta_z|}{\gamma_z + |\beta_z|}\right)\frac{1}{(1-\beta_z^2+|\beta_z|\gamma_z)}\{[\beta_x\beta_y]\,\tilde{E}_{ix-}$$

$$+ [\beta_y^2 - \tfrac{1}{2}(1-\beta_z^2+|\beta_z|\gamma_z)]\,\tilde{E}_{iy-}\} \qquad (5.6b)$$

where the minus sign on $\tilde{E}_{ix-}$ indicates downward propagation of the incident wave and the plus sign on $\tilde{E}_{rx+}$ indicated upward propagation. Invoking Eq. (5.4a) for both incident and reflected wave fields we obtain the vertical component of $\tilde{E}_{r+}$ from Eq. (5.6a,b)

$$\tilde{E}_{rz+} = -\left(\frac{\gamma_z - |\beta_z|}{\gamma z + |\beta_z|}\right)\left(\frac{1 - \beta_z^2 - |\beta_z|\gamma_z}{1 - \beta_z^2 + |\beta_z|\gamma_z}\right)\tilde{E}_{iz-} \qquad (5.6c)$$

We can easily determine the magnetic field components from (5.6a,b,c):

$$\tilde{H}_{rx+} = \sqrt{\frac{\varepsilon_0}{\mu_0}}\,(\beta_y\,\tilde{E}_{rz+} - |\beta_z|\,\tilde{E}_{ry+})$$

$$= \sqrt{\frac{\varepsilon_0}{\mu_0}}\left(\frac{\gamma_z - |\beta_z|}{\gamma_z + |\beta_z|}\right)\frac{1}{(1 - \beta_z^2 + |\beta_z|\gamma_z)}\{(-2|\beta_z|\beta_x\beta_y)\,\tilde{E}_{ix-}$$

$$+ (-2|\beta_z|[\beta_y^2 - \tfrac{1}{2}(1 - \beta_z^2 + |\beta_z|\gamma_z)])\,\tilde{E}_{iy-}$$

$$+ (-\beta_y(1 - \beta_z^2 - |\beta_z|\gamma_z))\,\tilde{E}_{iz-}\} \qquad (5.7a)$$

$$\tilde{H}_{ry+} = \sqrt{\frac{\varepsilon_0}{\mu_0}}\,(|\beta_z|\tilde{E}_{rx+} - \beta_x\,\tilde{E}_{rz+}) = \sqrt{\frac{\varepsilon_0}{\mu_0}}\left(\frac{\gamma_z - |\beta_z|}{\gamma_z + |\beta_z|}\right)\frac{1}{(1 - \beta_z^2 + |\beta_z|\gamma_z)} \cdots$$

$$\cdot\{(2|\beta_z|[\beta_x^2 - \tfrac{1}{2}(1 - \beta_z^2 + |\beta_z|\gamma_z)])\,\tilde{E}_{ix} + (2|\beta_z|\beta_x\beta_y)\,\tilde{E}_{iy-}$$

$$+ (-\beta_x(1 - \beta_z^2 - |\beta_z|\gamma_z))\,\tilde{E}_{iz-}\} \qquad (5.7b)$$

$$\tilde{H}_{rz+} = \sqrt{\frac{\varepsilon_0}{\mu_0}}\,(\beta_x\,\tilde{E}_{ry+} - \beta_y\,\tilde{E}_{rx+}) = \sqrt{\frac{\varepsilon_0}{\mu_0}}\left(\frac{\gamma_z - |\beta_z|}{\gamma_z + |\beta_z|}\right)(\beta_y\,\tilde{E}_{ix-} - \beta_x\,\tilde{E}_{iy-}) \qquad (5.7c)$$

To compare Eqs. (5.6a,b,c) and (5.7a,b,c) with well-known results on the reflection coefficients of plane waves incident on an interface between

two uniform semi-infinite media, consider the propagation vector $\underset{+}{\beta}$ as in the x-z plane, i.e.,

$$\beta_y = 0 \tag{5.8a}$$

$$\beta_x = \sin \theta_\beta \tag{5.8b}$$

$$\beta_z = \cos \theta_\beta \tag{5.8c}$$

Consider first the case of horizontal polarization, implying that

$$\tilde{E}_{ix-} = 0 \tag{5.9a}$$

$$\tilde{E}_{iy-} = \tilde{E}_{i-} \tag{5.9b}$$

$$\tilde{E}_{iz-} = 0 \tag{5.9c}$$

where $\tilde{E}_i$ is the complex amplitude of the incident wave. It follows from Eqs. (5.8a,b,c) and (5.9a,b,c) that Eqs. (5.6a,b,c) take the form:

$$\frac{\tilde{E}_{rx+}}{\tilde{E}_{i-}} = 0 \tag{5.10a}$$

$$\frac{\tilde{E}_{ry+}}{\tilde{E}_{i-}} = -\left(\frac{\gamma_z - \cos|\theta_\beta|}{\gamma_z + \cos|\theta_\beta|} \right) \tag{5.10b}$$

$$\frac{\tilde{E}_{rz+}}{\tilde{E}_{i-}} = 0 \tag{5.10c}$$

where $\gamma_z = \sqrt{\nu^2 - \sin^2 \theta_\beta}$

The results (5.10a,b,c) are consistent with well-known results on reflection coefficients with horizontal polarization [e.g., Stratton, p. 493].

From Eqs. (5.9a,b,c) and the Maxwell equations, the incident wave magnetic field components are

$$\tilde{H}_{ix-} = \sqrt{\frac{\epsilon_o}{\mu_o}}\,|\beta_z|\,\tilde{E}_{iy-} = \tilde{H}_{i-}|\cos\theta_\beta| \tag{5.11a}$$

(implying that $\tilde{E}_{iy-} = \sqrt{\frac{\mu_o}{\epsilon_o}}\,\tilde{H}_{i-}$)

$$\tilde{H}_{iy-} = 0 \tag{5.11b}$$

$$\tilde{H}_{iz-} = \sqrt{\frac{\epsilon_o}{\mu_o}}\,\beta_x\,\tilde{E}_{iy-} = \tilde{H}_{i-}\sin\theta_\beta \tag{5.11c}$$

(implying, as does Eq. (5.11a), that $\tilde{E}_{iy-} = \sqrt{\frac{\mu_o}{\epsilon_o}}\,\tilde{H}_{i-}$) where $\tilde{H}_{i-}$ is the complex amplitude of the magnetic field vector of the incident plane wave.

From Eqs. (5.9a,b,c), (5.11a,b,c) and (5.7a,b,c)

$$\frac{\tilde{H}_{rx+}}{\tilde{H}_{i-}} = \left(\frac{\gamma_z - |\cos\theta_\beta|}{\gamma_z + |\cos\theta_\beta|}\right)|\cos\theta_\beta| \tag{5.12a}$$

$$\frac{\tilde{H}_{ry+}}{\tilde{H}_{i-}} = 0 \tag{5.12b}$$

$$\frac{\tilde{H}_{rz+}}{H_{i-}} = -\left(\frac{\gamma_z - |\cos\theta_\beta|}{\gamma_z + |\cos\theta_\beta|} \right) \sin\theta_\beta \tag{5.12c}$$

For vertical polarization

$$\tilde{E}_{iy-} = 0 \tag{5.13a}$$

$$\tilde{E}_{ix-} = \tilde{E}_{i-} |\cos\theta_\beta| \tag{5.13b}$$

$$\tilde{E}_{iz-} = \tilde{E}_{i-} \sin\theta_\beta \tag{5.13c}$$

where $\tilde{E}_{i-}$ represents the complex amplitude of the incident plane wave field. In this case, Eqs. (5.6a,b,c) are:

$$\frac{\tilde{E}_{rx+}}{\tilde{E}_{i-}} = \left(\frac{\gamma_z - |\cos\theta_\beta|}{\gamma_z + |\cos\theta_\beta|} \right) \frac{[\sin^2\theta_\beta - |\cos\theta_\beta|\gamma_z]}{[\sin^2\theta_\beta + |\cos\theta_\beta|\gamma_z]} |\cos\theta_\beta|$$

$$= -\left(\frac{\nu^2|\cos\theta_\beta| - \gamma_z}{\nu^2|\cos\theta_\beta| + \gamma_z} \right) |\cos\theta_\beta| \tag{5.14a}$$

$$\frac{\tilde{E}_{ry+}}{\tilde{E}_{i-}} = 0 \tag{5.14b}$$

$$\frac{\tilde{E}_{rz+}}{\tilde{E}_{i-}} = -\left(\frac{\gamma_z - |\cos\theta_\beta|}{\gamma_z + |\cos\theta_\beta|} \right) \frac{[\sin^2\theta_\beta - |\cos\theta_\beta|\gamma_z]}{[\sin^2\theta_\beta + |\cos\theta_\beta|\gamma_z]} \sin\theta_\beta$$

$$= \left(\frac{\nu^2|\cos\theta_\beta| - \gamma_z}{\nu^2|\cos\theta_\beta| + \gamma_z} \right) \sin\theta_\beta \tag{5.14c}$$

From Eqs. (5.9a,b) and the Maxwell equations

$$\tilde{H}_{ix-} = 0 \tag{5.15a}$$

$$\tilde{H}_{iy-} = \sqrt{\frac{\epsilon_o}{\mu_o}}\,(-|\beta_z|\tilde{E}_{ix-} - \beta_x \tilde{E}_{iz-}) = -\sqrt{\frac{\epsilon_o}{\mu_o}}\,\tilde{E}_{i-}(\cos^2\theta_\beta + \sin^2\theta_\beta)$$

$$= -\sqrt{\frac{\epsilon_o}{\mu_o}}\,\tilde{E}_{i-} = \tilde{H}_{i-} \tag{5.15b}$$

(implying that $\tilde{E}_{i-} = -\sqrt{\frac{\mu_o}{\epsilon_o}}\,\tilde{H}_{i-}$).

$$\tilde{H}_{iz-} = 0 \tag{5.15c}$$

Substitution of Eqs. (5.13a,b,c) and (5.15a,b,c) into Eqs. (5.7a,b,c) yields

$$\frac{\tilde{H}_{rx+}}{\tilde{H}_{i-}} = 0 \tag{5.16a}$$

$$\frac{\tilde{H}_{ry+}}{\tilde{H}_{i-}} = -\left(\frac{\gamma_z - |\cos\theta_\beta|}{\gamma_z + |\cos\theta_\beta|}\right)\left(\frac{\sin^2\theta_\beta - |\cos\theta_\beta|\gamma_z}{\sin^2\theta_\beta + |\cos\theta_\beta|\gamma_z}\right)$$

$$= \frac{\nu^2|\cos\theta_\beta| - \gamma_z}{\nu^2|\cos\theta_\beta| + \gamma_z} \tag{5.16b}$$

$$\frac{\tilde{H}_{rz+}}{\tilde{H}_{i-}} = 0 \tag{5.16c}$$

The results (5.16a,b,c) are consistent with well-known results on reflection coefficient with vertical polarization [e.g., Stratton, p. 494].

It is sometimes convenient to write the results (5.6a,b,c) and (5.7a,b,c) in terms of the angles $(\theta_\beta, \phi_\beta)$, i.e.,

$$\tilde{E}_{rx+} = \left(\frac{\gamma_z - |\cos\theta_\beta|}{\gamma_z + |\cos\theta_\beta|} \right) \frac{1}{[\sin^2\theta_\beta + |\cos\theta_\beta|\gamma_z]} \{\tilde{E}_{ix-}[\sin^2\theta_\beta(\cos 2\phi_\beta) - |\cos\theta_\beta|\gamma_z] + \tilde{E}_{iy-} - [\sin^2\theta_\beta \sin 2\phi_\beta] \quad (5.17a)$$

$$\tilde{E}_{ry+} = \left(\frac{\gamma_z - |\cos\theta_\beta|}{\gamma_z + |\cos\theta_\beta|} \right) \frac{1}{[\sin^2\theta_\beta + |\cos\theta_\beta|\gamma_z]} \{\tilde{E}_{ix-}[\sin^2\theta_\beta(\sin 2\phi_\beta)] + \tilde{E}_{iy-}[\sin^2\theta_\beta(-\cos 2\phi_\beta) - |\cos\theta_\beta|\gamma_z]\} \quad (5.17b)$$

where $\gamma_z = \sqrt{\nu^2 - \sin^2\theta_\beta}$

$$\tilde{E}_{rz+} = -\sin\theta_\beta \left(\frac{\gamma_z - |\cos\theta_\beta|}{\gamma_z + |\cos\theta_\beta|} \right) \left(\frac{\sin^2\theta_\beta - |\cos\theta_\beta|\gamma_z}{\sin^2\theta_\beta + |\cos\theta_\beta|\gamma_z} \right) \tilde{E}_{iz-} \quad (5.17c)$$

where $\gamma_z = \sqrt{\nu^2 - \sin^2\theta_\beta}$

$$\tilde{H}_{rx+} = \sqrt{\frac{\epsilon_o}{\mu_o}} \left(\frac{\gamma_z - |\cos\theta_\beta|}{\gamma_z + |\cos\theta_\beta|} \right) \frac{1}{(\sin^2\theta_\beta + |\cos\theta_\beta|\gamma_z)} \cdots$$

$$\cdot \{(-|\cos\theta_\beta| \sin^2\theta_\beta \sin 2\phi_\beta)\, \tilde{E}_{ix-} + (-|\cos\theta_\beta|[\sin^2\theta_\beta(-\cos 2\phi_\beta) - |\cos\theta_\beta|\gamma_z])\, \tilde{E}_{iy-} + (-\sin\theta_\beta \sin\phi_\beta[\sin^2\theta_\beta - |\cos\theta_\beta|\gamma_z])\, \tilde{E}_{iz-}\} \quad (5.17d)$$

$$\tilde{H}_{ry+} = \sqrt{\frac{\varepsilon_o}{\mu_o}} \left(\frac{\gamma_z - |\cos\theta_\beta|}{\gamma_z + |\cos\theta_\beta|} \right) \frac{1}{(\sin^2\theta_\beta + |\cos\theta_\beta|\gamma_z)} \cdots$$

$$\cdot \{(|\cos\theta_\beta|[\sin^2\theta_\beta(\cos 2\phi_\beta) - |\cos\theta_\beta|\gamma_z])\ \tilde{E}_{ix-}$$

$$+ (|\cos\theta_\beta|\ \sin^2\theta_\beta \sin 2\phi_\beta)\ \tilde{E}_{iy-}$$

$$+ (-\sin\theta_\beta \cos\phi_\beta[\sin^2\theta_\beta - |\cos\theta_\beta|\gamma_z])\ \tilde{E}_{iz-}\} \qquad (5.17e)$$

$$\tilde{H}_{rz+} = \sqrt{\frac{\varepsilon_o}{\mu_o}} \left(\frac{y_z - |\cos\theta_\beta|}{y_z + |\cos\theta_\beta|} \right) \sin\theta_\beta(\sin\phi_\beta\ \tilde{E}_{ix-} - \cos\phi_\beta\ \tilde{E}_{iy-}) \qquad (5.17f)$$

It is convenient to write Eqs. (5.17a-f) as a pair of matrix equations of the form

$$\underset{\rightarrow}{\tilde{E}}_{r+} = \begin{bmatrix} \tilde{E}_{rx+} \\ \tilde{E}_{ry+} \\ \tilde{E}_{rz+} \end{bmatrix} = \begin{bmatrix} R_{E11} & R_{E12} & R_{E13} \\ R_{E21} & R_{E22} & R_{E23} \\ R_{E31} & R_{E32} & R_{E33} \end{bmatrix} \begin{bmatrix} \tilde{E}_{ix-} \\ \tilde{E}_{iy-} \\ \tilde{E}_{iz-} \end{bmatrix} = [R_E]\ \underset{\rightarrow}{\tilde{E}}_{i-} \qquad (5.18a)$$

$$\underset{\rightarrow}{\tilde{H}}_{r+} = \begin{bmatrix} \tilde{H}_{rx+} \\ \tilde{H}_{ry+} \\ \tilde{H}_{rz+} \end{bmatrix} = \begin{bmatrix} R_{H11} & R_{H12} & R_{H13} \\ R_{H21} & R_{H22} & R_{H23} \\ R_{H31} & R_{H32} & R_{H33} \end{bmatrix} \begin{bmatrix} \tilde{E}_{ix-} \\ \tilde{E}_{iy-} \\ \tilde{E}_{iz-} \end{bmatrix} = [R_H] \underset{\rightarrow}{\tilde{E}}_{i-} \tag{5.18b}$$

$$R_{EJK} = C_o(\beta_x, \beta_y)\ \hat{R}_{EJK}(\beta_x, \beta_y)$$

$$R_{HJK} = \sqrt{\frac{\varepsilon_o}{\mu_o}}\ C_o(\beta_x, \beta_y)\ \hat{R}_{HJK}(\beta_x, \beta_y)$$

$$C_o(\beta_x, \beta_y) = \left(\frac{\gamma_z - |\beta_z|}{\gamma_z + |\beta_z|} \right) \frac{1}{[\beta_h^2 + |\beta_z|\gamma_z]} \tag{5.19}$$

$$\beta_h = \sqrt{\beta_x^2 + \beta_y^2}$$

$$\hat{R}_{E11} = \beta_x^2 - \beta_y^2 - |\beta_z|\gamma_z$$

$$\hat{R}_{E12} = \hat{R}_{E21} = 2\beta_x\beta_y$$

$$\hat{R}_{E22} = \beta_y^2 - \beta_x^2 - |\beta_z|\gamma_z$$

$$\hat{R}_{E33} = \beta_h^2 - |\beta_z|\gamma_z$$

$$\hat{R}_{E13} = \hat{R}_{E23} = \hat{R}_{E31} = \hat{R}_{E32} = 0$$

$$\hat{R}_{H11} = -2|\beta_z|\beta_x\beta_y = -|\beta_z|\ \hat{R}_{E12}$$

$$\hat{R}_{H12} = -|\beta_z|[\beta_y^2 - \beta_x^2 - |\beta_z|\gamma_z] = -|\beta_z|\hat{R}_{E22}$$

$$\hat{R}_{H13} = -\beta_y[\beta_h^2 - |\beta_z|\gamma_z] = -\beta_y \hat{R}_{E33}$$

$$\hat{R}_{H21} = |\beta_z|[\beta_x^2 - \beta_y^2 - |\beta_z|\gamma_z] = |\beta_z| \hat{R}_{E11}$$

$$\hat{R}_{H22} = 2|\beta_z|\beta_x\beta_y = |\beta_z|\hat{R}_{E12} \qquad (5.19)$$

(cont'd)

$$\hat{R}_{H23} = -\beta_x[\beta_h^2 - |\beta_z|\gamma_z] = -\beta_x \hat{R}_{E33}$$

$$\hat{R}_{H31} = \beta_y[\beta_h^2 + |\beta_z|\gamma_z]$$

$$\hat{R}_{H32} = -\beta_x[\beta_h^2 + |\beta_z|\gamma_z]$$

$$\hat{R}_{H33} = 0$$

6. FIELDS INCIDENT ON THE SCATTERER-COORDINATE TRANSFORMATION AT INPUT TO SCATTERING PROCESS

The scattering theory that we are using confines itself to the scattering of a plane-wave by a body. The spectral fields as given by the superposition of Eqs. (4.16a,b) (the fields associated with the direct wave from the cable slots) and Eqs. (5.18a,b) (the fields associated with the ground-reflected wave from the slots) are the fields of a plane-wave propagating in the direction of the wave vector $\underset{\rightarrow}{\beta}^+$. Denoting these plane-wave fields by $\underset{\rightarrow}{\tilde{E}}_i(\underset{\rightarrow}{\beta}^+)$ and $\underset{\rightarrow}{\tilde{H}}_i(\underset{\rightarrow}{\beta}^+)$, the next phase of the solution to our problem is to evaluate the scattered fields when the incident fields are $\underset{\rightarrow}{\tilde{E}}_i(\underset{\rightarrow}{\beta}^+)$ and $\underset{\rightarrow}{\tilde{H}}_i(\underset{\rightarrow}{\beta}^+)$.

Before we can do the scattering problem, we must perform certain coordinate transformations.

The Barber scattering program, which will be discussed in Section 7, contains two coordinate systems. One is the "lab frame" and the other is the "body frame." The diagram of Figure 6.1, due to Dr. Peter Barber, illustrates the two systems.

First, note that Figure 6.1(a) and (b) which illustrate the "lab frame" (whose coordinate axes are denoted by x_L, y_L, z_L) and the direction of the incident wave with respect to the lab frame. The incident wave travels in the $+z_L$ direction in the lab frame (hence, $\underset{\rightarrow}{\beta}^+$ is in the $+z_L$ direction). The electric field vector of the incident wave, denoted by $\underset{\rightarrow}{\tilde{E}}_i(\underset{\rightarrow}{\beta}^+)$, lies in the $(x_L - y_L)$ plane and is at an angle ϕ_i with respect to the x_L axis in a clockwise direction, looking along the $+z_L$ axis.

The "body frame" [Figure 6.1(c)] is characterized by a set of rectangular coordinates (x_B, y_B, z_B). The scatterer is pictured as a spheroid with its axis of symmetry along the $+z_B$ axis. (This is only for graphical convenience;

(a) Lab frame

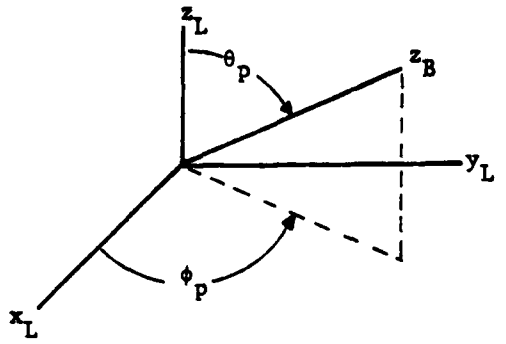

(b) Direction of incident wave with respect to lab frame coordinates

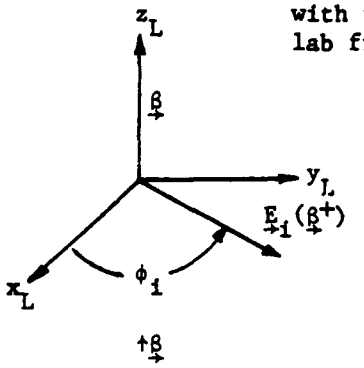

(c) Body frame

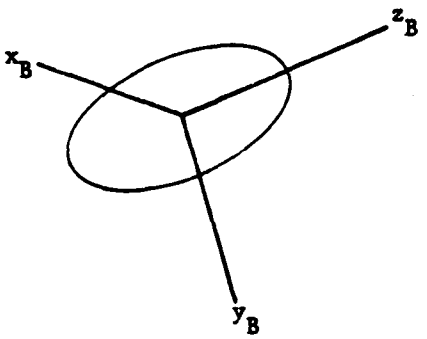

Figure 6-1. Coordinate systems for Barber Scattering Program

the theory does not require that the scatterer be a spheroid oriented as shown.) The direction of the $+z_B$ axis in the lab frame corresponds to two spherical coordinate angles, a polar angle Θ_p and an azimuthal angle ϕ_p, as shown in Figure 6.1(a).

Our first task is to develop a transformation between the body frame and lab frame coordinates.

A simple way to do this makes use of the diagrams of Figure 6.2(a), (b), (c), and the accompanying equations (6.1a,b,c), (6.2a,b,c) and (6.3a,b,c) appearing in the figure.

From Eqs. (6.1a,b,c), (6.2a,b,c) and (6.3a,b,c), the body frame coordinates of a point (x_B, y_B, z_B) in terms of the lab frame coordinates of that point (x_L, y_L, z_L), expressed in vector-matrix form, are:

$$[\underline{r}_B] = [M_{BL}][\underline{r}_L] \tag{6.4a}$$

and the inverse form

$$[\underline{r}_L] = [M_{LB}][\underline{r}_B] \tag{6.4b}$$

where

$$[\underline{r}_B] = \begin{bmatrix} x_B \\ y_B \\ z_B \end{bmatrix} \tag{6.4a}'$$

$$[\underline{r}_L] = \begin{bmatrix} x_L \\ y_L \\ z_L \end{bmatrix} \tag{6.4b}'$$

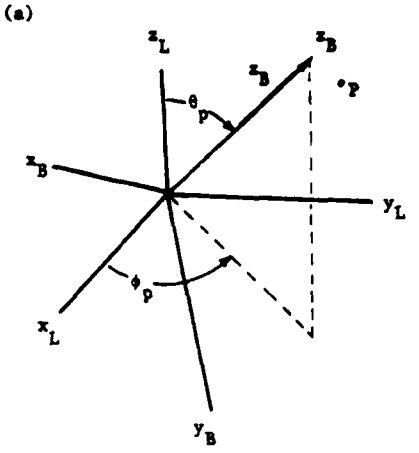

Coordinate system (x_L, y_L, z_L)

Point P. has coordinates (x_L, y_L, z_L)

$\hat{z}_B$ is unit vector in $+z_B$ direction

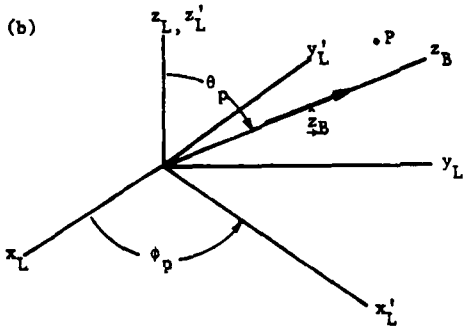

Point P has (x_L', y_L', z_L') coordinates

$$x_L' = x_L \cos\phi_p + y_L \sin\phi_p \qquad (6.1.a)$$

$$y_L' = -x_L \sin\phi_p + y_L \cos\phi_p \qquad (6.1.b)$$

$$z_L' = z_L \qquad (6.1.c)$$

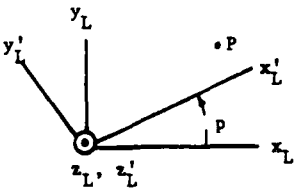

Rotate around z_L axis through angle ϕ_p, such that in new system (x_L', y_L', z_L'), $\hat{z}_B$ lies in $(x_L'\text{-}z_L')$ plane

Figure 6-2. Transformation between lab and body frame

(c)

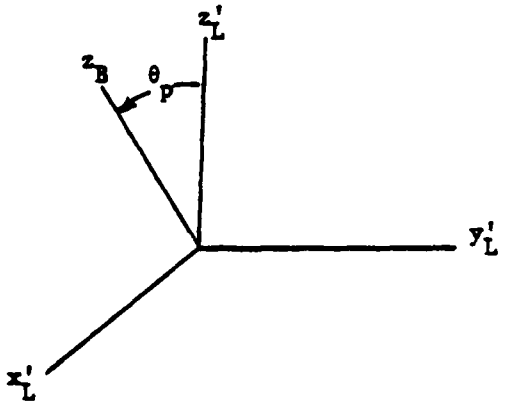

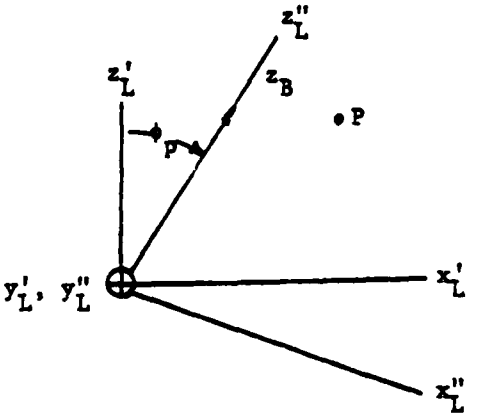

Point P has (x_L'', y_L'', z_L'') coordinates:

$$x_L'' = x_L' \cos\theta_p - z_L' \sin\theta_p \qquad (6.2.a)$$

$$y_L'' = y_L' \qquad (6.2.b)$$

$$z_L'' = x_L' \sin\theta_p + z_L' \cos\theta_p \qquad (6.2.c)$$

Rotate around y_L' axis through angle θ_p, such that $+z_L''$ and $+z_B$ directions are parallel.

(d)

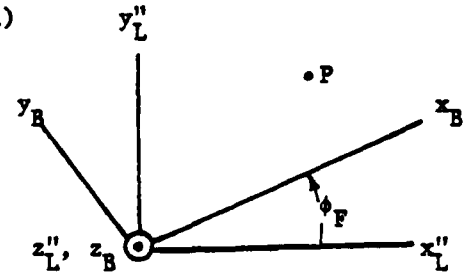

Rotate around z_L'' axis through angle ϕ_F counter clockwise looking $-z_B$ direction. Point P has x_B, y_B, z_B (body frame coordinates)

$$x_B = x_L'' \cos\phi_F + y_L'' \sin\phi_F \qquad (6.3.a)$$

$$y_B = x_L'' \sin\phi_F + y_L'' \cos\phi_F \qquad (6.3.b)$$

$$z_B = z_L'' \qquad (6.3.c)$$

Figure 6-2. Transformation between lab and body frame (cont'd.)

$$[M_{BL}] = \begin{bmatrix} (\cos\theta_p \cos\phi_p \cos\phi_F - \sin\phi_p \sin\phi_F) & (\cos\theta_p \sin\phi_p \cos\phi_F + \cos\phi_p \sin\phi_F) & (-\sin\theta_p \cos\phi_F) \\ (-\cos\theta_p \cos\phi_p \sin\phi_F - \sin\phi_p \cos\phi_F) & (-\cos\theta_p \sin\phi_p \sin\phi_F + \cos\phi_p \cos\phi_F) & (\sin\theta_p \sin\phi_F) \\ (\sin\theta_p \cos\phi_p) & (\sin\theta_p \sin\phi_p) & (\cos\theta_p) \end{bmatrix} \quad (6.4c)'$$

$$[M_{LB}] = \begin{bmatrix} (\cos\theta_p \cos\phi_p \cos\phi_F - \sin\phi_p \sin\phi_F) & (-\cos\theta_p \cos\phi_p \sin\phi_F - \sin\phi_p \cos\phi_F) & (\sin\theta_p \cos\phi_p) \\ (\cos\theta_p \sin\phi_p \cos\phi_F + \cos\phi_p \sin\phi_F) & (-\cos\theta_p \sin\phi_p \sin\phi_F + \cos\phi_p \cos\phi_F) & (\sin\theta_p \sin\phi_p) \\ (-\sin\theta_p \cos\phi_F) & (\sin\theta_p \sin\phi_F) & (\cos\theta_p) \end{bmatrix} \quad (6.4d)'$$

We can use Eqs. (6.4a,b) to obtain a vector-matrix relationship between the unit base vectors in the two coordinate systems. Note that the elements of $[\underset{\sim}{r}_B]$ and $[\underset{\sim}{r}_L]$ are coordinates of an arbitrary point in the body and lab coordinate systems respectively. The unit base vector along the x_B direction (for example), denoted by $\hat{\underset{\sim}{x}}_B$, terminates at a point P which has coordinates (1, 0, 0) in the body frame. In this case, Eq. (6.46) would read

$$\begin{bmatrix} x_L \\ y_L \\ z_L \end{bmatrix} = \begin{bmatrix} (M_{LB})_{11} & (M_{LB})_{12} & (M_{LB})_{13} \\ (M_{LB})_{21} & (M_{LB})_{22} & (M_{LB})_{23} \\ (M_{LB})_{31} & (M_{LB})_{32} & (M_{LB})_{33} \end{bmatrix} \begin{bmatrix} 1 \\ 0 \\ 0 \end{bmatrix} = \begin{bmatrix} (M_{LB})_{11} \\ (M_{LB})_{21} \\ (M_{LB})_{31} \end{bmatrix} \tag{6.5a}$$

By the same reasoning (for another example) the unit vector in the $\hat{\underset{\sim}{y}}_L$ direction, denoted by $\hat{\underset{\sim}{y}}_L$, terminates at a point P with coordinates (0, 1, 0) in the lab frame. Thus, Eq. (6.4a) in this case would read

$$\begin{bmatrix} x_B \\ y_B \\ z_B \end{bmatrix} = \begin{bmatrix} (M_{BL})_{11} & (M_{BL})_{12} & (M_{BL})_{13} \\ (M_{BL})_{21} & (M_{BL})_{22} & (M_{BL})_{23} \\ (M_{BL})_{31} & (M_{BL})_{33} & (M_{BL})_{33} \end{bmatrix} \begin{bmatrix} 0 \\ 1 \\ 0 \end{bmatrix} = \begin{bmatrix} (M_{BL})_{12} \\ (M_{BL})_{22} \\ (M_{BL})_{32} \end{bmatrix} \tag{6.5b}$$

From Eqs. (6.5a,b) and the fact [evident from Eqs. (6.4c,d)'] that $(M_{BL})_{jk} = (M_{LB})_{kj}$, it follows that

$$\hat{\underset{\sim}{x}}_B = (x_L \hat{\underset{\sim}{x}}_L + y_L \hat{\underset{\sim}{y}}_L + z_L \hat{\underset{\sim}{z}}_L)_{\substack{x_B=1 \\ y_B=z_B=0}} = (M_{LB})_{11} \hat{\underset{\sim}{x}}_L + (M_{LB})_{21} \hat{\underset{\sim}{y}}_L + (M_{LB})_{31} \hat{\underset{\sim}{z}}_L$$

$$= [(M_{BL})_{11}(M_{BL})_{12}(M_{BL})_{13}] \begin{bmatrix} \hat{x}_L \\ \hat{y}_L \\ \hat{z}_L \end{bmatrix} \tag{6.6a}$$

and

$$\hat{y}_L = (x_B \hat{x}_B + y_B \hat{y}_B + z_B \hat{z}_B)_{\substack{x_L=z_L=0 \\ y_L=1}} = (M_{BL})_{12} \hat{x}_B + (M_{BL})_{22} \hat{y}_B$$

$$+ (M_{BL})_{32} \hat{z}_B = [(M_{LB})_{21}(M_{LB})_{22}(M_{LB})_{23}] \begin{bmatrix} \hat{x}_B \\ \hat{y}_B \\ \hat{z}_B \end{bmatrix} \tag{6.6b}$$

Arguments like those leading to Eqs. (6.5a,b) and (6.6a,b) applied to all the unit vectors in both systems yield the following two vector-matrix equations:

$$[\hat{u}_B] = [M_{BL}][\hat{u}_L] \tag{6.7a}$$

and its inverse form

$$[\hat{u}_L] = [M_{LB}][\hat{u}_B] \tag{6.7b}$$

where $[\hat{u}_L]$ and $[\hat{u}_B]$ are "vectors of unit vectors" of the form

$$[\hat{u}_{\underset{\sim}{L}}] = \begin{bmatrix} \hat{x}_{\underset{\sim}{L}} \\ \hat{y}_{\underset{\sim}{L}} \\ \hat{z}_{\underset{\sim}{L}} \end{bmatrix} \qquad (6.7a)' \qquad [\hat{u}_{\underset{\sim}{B}}] = \begin{bmatrix} \hat{x}_{\underset{\sim}{B}} \\ \hat{y}_{\underset{\sim}{B}} \\ \hat{z}_{\underset{\sim}{B}} \end{bmatrix} \qquad (6.7b)'$$

We now wish to obtain (1) a transformation between the lab frame (x_L, y_L, z_L) and a coordinate system to be called the "ground frame" (x_o, y_o, z_o), obtained from the basic (x, y, z) coordinate system by a translation such that the origin of the ground frame is at the center of the scatterer; and (2) a transformation between the ground frame and the body frame (x_B, y_B, z_B). To accomplish this, we first note that Figures 6.3 and 6.4 contain diagrams which are both the equivalent of those in Figure 6.2 except for changes in coordinate names.

From Figures 6.3 and 6.4 and accompanying sets of equations (6.6a,b,c) through (6.13a,b,c), by analogy with Eqs. (6.4(a,b) and (6.5a,b), we obtain the following sets of vector-matrix transformation equations, analogous to Eqs. (6.4a,b) and (6.5a,b):

$$[\underset{\sim}{r}_B] = [M_{Bo}][\underset{\sim}{r}_o] \qquad (6.14a)$$

$$[\underset{\sim}{r}_o] = [M_{oB}][\underset{\sim}{r}_B] \qquad (6.14b)$$

$$[\hat{u}_{\underset{\sim}{B}}] = [M_{Bo}][\hat{u}_{\underset{\sim}{o}}] \qquad (6.15a)$$

$$[\hat{u}_{\underset{\sim}{o}}] = [M_{oB}][\hat{u}_{\underset{\sim}{B}}] \qquad (6.15b)$$

(a)

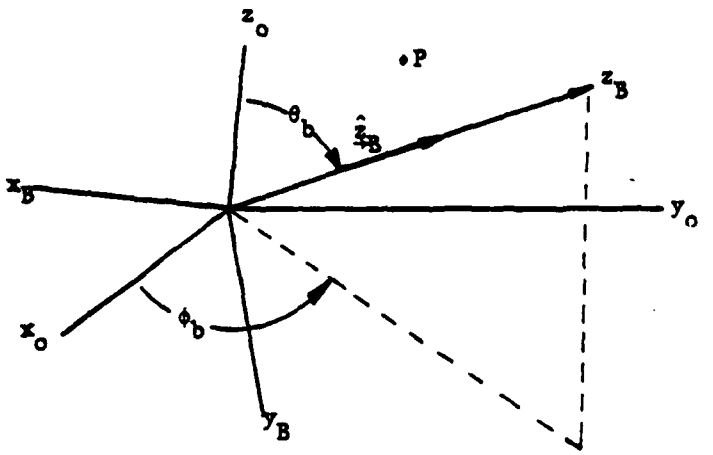

Analogous to Fig. 6.2.a, $x_L \rightarrow x_0$

$y_L \rightarrow y_0$

$z_L \rightarrow z_0$

$\phi_p \rightarrow \phi_b$

$\Theta_p \rightarrow \Theta_b$

(b)

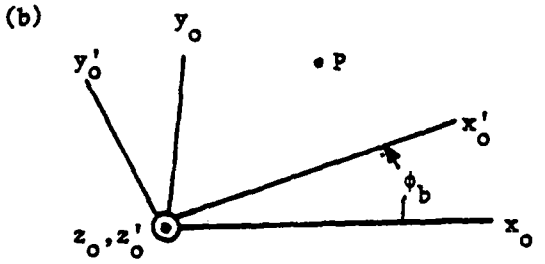

Rotate around z_0 axis through angle ϕ_b so $\hat{z}_B$ lies in $(x_0' - y_0')$ plane:

$$x_0' = x_0\cos\phi_b + y_0\sin\phi_b \qquad (6.8.a)$$

$$y_0' = -x_0\sin\phi_b + y_0\cos\phi_b \qquad (6.8.b)$$

$$z_0' = z_0 \qquad (6.8.c)$$

Analogous to Figure 6.2.b and Eqs. (6.1.a,b,c)

(c.1)

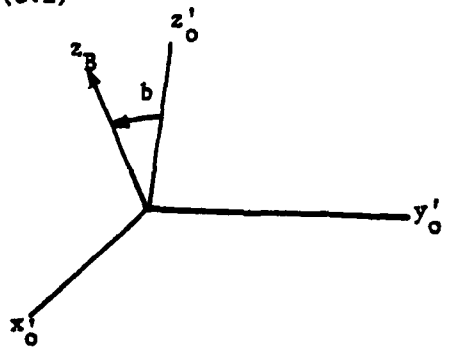

Rotate around y' axis through angle Θ_b so $z_0'' \parallel z_B$

Figure 6-3. Transformations between ground frame and body frame

(c.2)

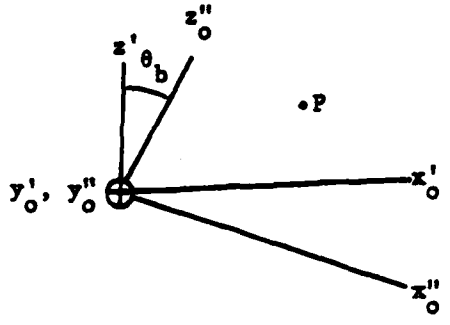

$$x_0'' = x_0' \cos\theta_b - z_0' \sin\theta_b \qquad (6.9.a)$$

$$y_0'' = y_0' \qquad (6.9.b)$$

$$z_0'' = x_0' \sin\theta_b + z_0' \cos\theta_b \qquad (6.9.c)$$

Analogous to Fig. (6.2.c)
and Eqs. (6.2.a,b,c)

(d)

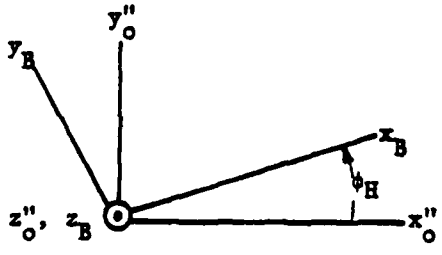

Rotate around z_0'' axis through angle ϕ_H CCW looking in $-z_B$ direction.

$$x_B = x_0'' \cos\phi_H + y_0'' \sin\phi_H \qquad (6.10.a)$$

$$y_B = -x_0'' \sin\phi_H + y_0'' \cos\phi_H \qquad (6.10.b)$$

$$z_B = z_0'' \qquad (6.10.c)$$

Analogous to Fig. (6.2.d)
and Eqs. (6.3.a,b,c)

Figure 6-3. Transformations between ground frame and body frame (cont'd.)

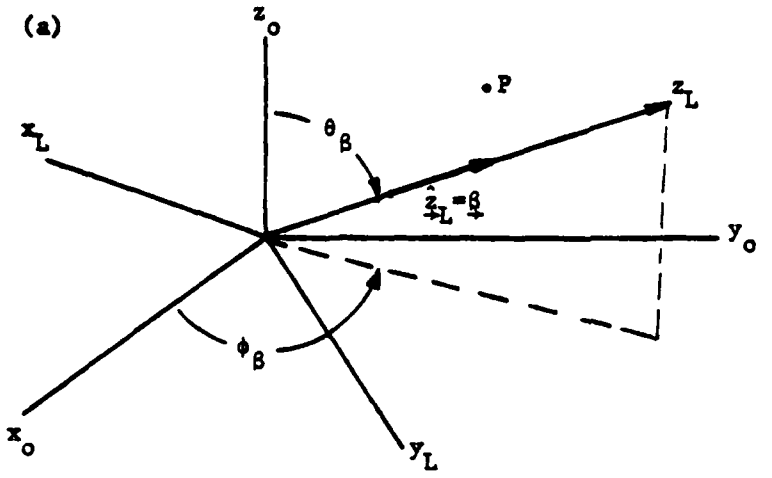

Analogous to Figure 6.2.a

$x_L \rightarrow x_0$ $\quad x_B \rightarrow x_L$

$y_L \rightarrow y_0$ $\quad y_B \rightarrow y_L$

$z_L \rightarrow z_0$ $\quad z_B \rightarrow z_L$

$\Theta_p \rightarrow \Theta_\beta$

$\phi_p \rightarrow \phi_\beta$

(Note: $\underset{\sim}{\beta}$ is along + z_L direction)

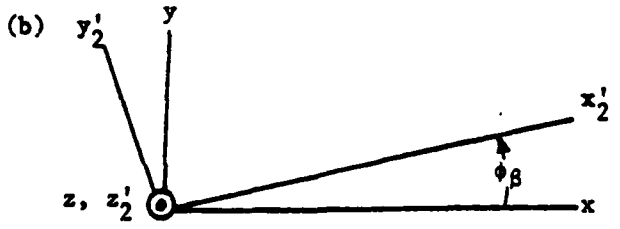

Rotate around z axis through angle ϕ_β so $\hat{z}_L$ lies in $(x_2' - z_2')$ plane

$$x_2' = x_0 \cos\phi_\beta + y_0 \sin\phi_\beta \qquad (6.11.a)$$

$$y_2' = -x_0 \sin\phi_\beta + y_0 \cos\phi_\beta \qquad (6.11.b)$$

$$z_2' = z_0 \qquad (6.11.c)$$

Analogous to Fig. (6.2.b) and Eqs. (6.1.a,b,c)

Figure 6-4. Transformation between ground frame and lab frame

(c.1)

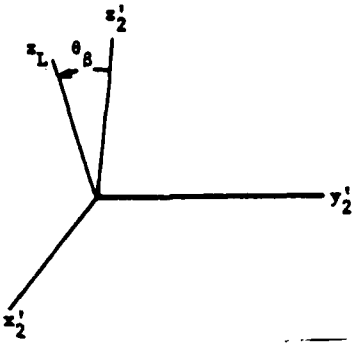

(c.2)

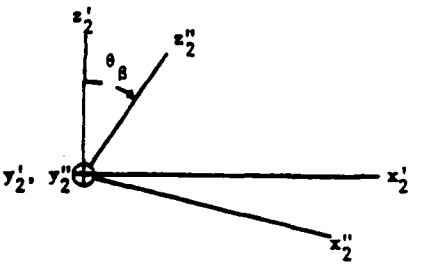

$$x_2'' = x_2' \cos\theta_\beta - z_2' \sin\theta_\beta \qquad (6.12.a)$$

$$y_2'' = y_2' \qquad (6.12.b)$$

$$z_2'' = x_2' \sin\theta_\beta + z_2' \cos\theta_\beta \qquad (6.12.c)$$

Rotate around y_2' axis through angle θ_β so $z_2'' \| z_B$

Analogous to Fig. (6.2.c) and Eqs. (6.2.a,b,c)

(d)

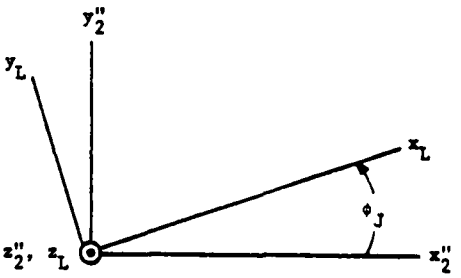

Rotate around z_2'' axis through angle ϕ_J, CCW looking in $-z_L$ direction.

$$x_L = x_2'' \cos\phi_J + y_2'' \sin\phi_J \qquad (6.13.a)$$

$$y_L = x_2'' \sin_J + y_2'' \cos_J \qquad (6.13.b)$$

$$z_L = z_2'' \qquad (6.13.c)$$

Analogous to Fig. (6.2.d) and Eqs. (6.3.a,b,c)

Figure 6-4. Transformation between ground frame and lab frame (cont'd.)

$$[\underset{\rightarrow}{r}_L] = [M_{Lo}][\underset{\rightarrow}{r}_o] \tag{6.16a}$$

$$[\underset{\rightarrow}{r}_o] = [M_{oL}][\underset{\rightarrow}{r}_L] \tag{6.16b}$$

$$[\hat{\underset{\rightarrow}{u}}_L] = [M_{Lo}][\hat{\underset{\rightarrow}{u}}_o] \tag{6.17a}$$

$$[\hat{\underset{\rightarrow}{u}}_o] = [M_{oL}][\hat{\underset{\rightarrow}{u}}_L] \tag{6.17b}$$

where

$$[\underset{\rightarrow}{r}_o] = \begin{bmatrix} x_o \\ y_o \\ z_o \end{bmatrix} = \begin{bmatrix} x - x_s \\ y - y_s \\ z - z_s \end{bmatrix} \tag{6.17c)'}$$

where x_s, y_s, z_s are the basic (x, y, z) coordinates of the scatterer center,

$$\hat{\underset{\rightarrow}{u}}_o = \begin{bmatrix} \hat{\underset{\rightarrow}{x}} \\ \hat{\underset{\rightarrow}{y}} \\ \hat{\underset{\rightarrow}{z}} \end{bmatrix} \tag{6.17d)'}$$

AD-A111 590 CLARKSON COLL OF TECHNOLOGY POTSDAM NY F/G 17/9
ANALYSIS OF THE POLARIZATION DEPENDENCE OF THE INTERACTION BETW--ETC(U)
NOV 81 H R RAEMER F30602-78-C-0102
UNCLASSIFIED RADC-TR-81-244 NL

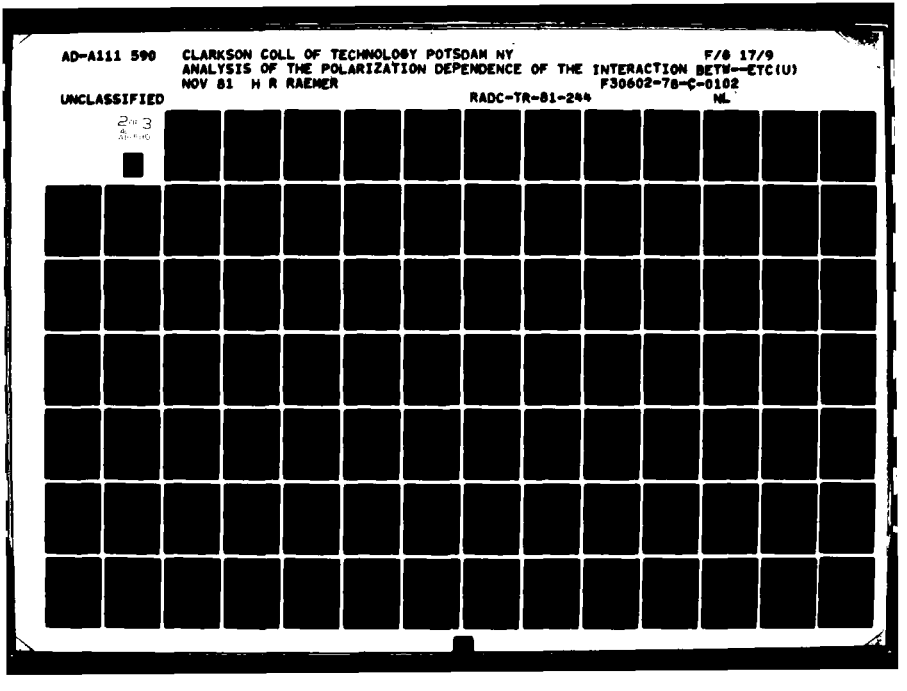

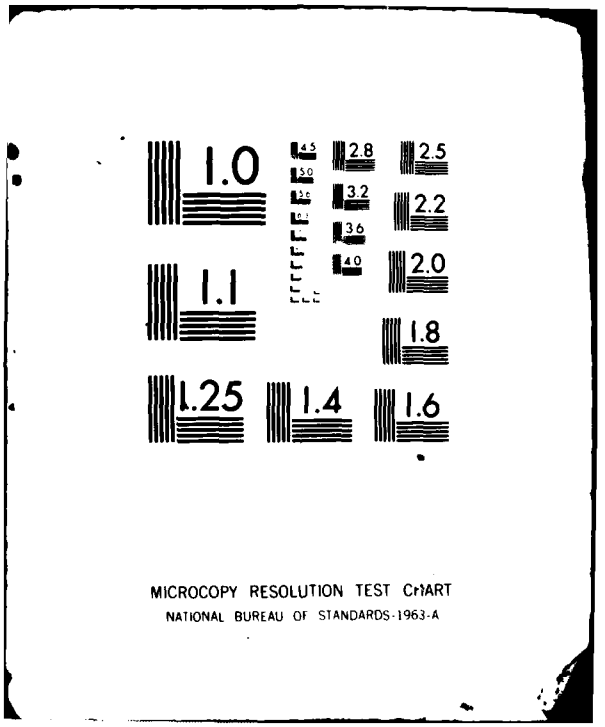
1.0
1.1
1.25
1.4
1.6
1.8
2.0
2.2
2.5
2.8
3.2
3.6
4.0
4.5
5.0
MICROCOPY RESOLUTION TEST CHART
NATIONAL BUREAU OF STANDARDS-1963-A

$$[M_{Bo}] = \begin{bmatrix} (\cos\theta_b \cos\phi_b \cos\phi_H - \sin\phi_b \sin\phi_H) & (\cos\theta_b \sin\phi_b \cos\phi_H + \cos\phi_b \sin\phi_H) & (-\sin\theta_b \cos\phi_H) \\ (-\cos\theta_b \cos\phi_b \sin\phi_H - \sin\phi_b \cos\phi_H) & (-\cos\theta_b \sin\phi_b \sin\phi_H + \cos\phi_b \cos\phi_H) & (\sin\theta_b \sin\phi_H) \\ (\sin\theta_b \cos\phi_b) & (\sin\theta_b \sin\phi_b) & (\cos\theta_b) \end{bmatrix}$$

(6.15a)'

$$[M_{Lo}] = \begin{bmatrix} (\cos\theta_b \cos\phi_b \cos\phi_H - \sin\phi_b \sin\phi_H) & (-\cos\theta_b \cos\phi_b \sin\phi_H - \sin\phi_b \cos\phi_H) & (\sin\theta_b \cos\phi_b) \\ (\cos\theta_b \sin\phi_b \cos\phi_H + \cos\phi_b \sin\phi_H) & (-\cos\theta_b \sin\phi_b \sin\phi_H + \cos\phi_b \cos\phi_H) & (\sin\theta_b \sin\phi_b) \\ (-\sin\theta_b \cos\phi_H) & (\sin\theta_b \sin\phi_H) & (\cos\theta_b) \end{bmatrix}$$

(6.15b)'

$$[M_{Lo}] = \begin{bmatrix} (\cos\theta_\beta \cos\phi_\beta \cos\phi_J - \sin\phi_\beta \sin\phi_J) & (\cos\theta_\beta \sin\phi_\beta \cos\phi_J + \cos\phi_\beta \sin\phi_J) & (-\sin\theta_\beta \cos\phi_J) \\ (-\cos\theta_\beta \cos\phi_\beta \sin\phi_J - \sin\phi_\beta \cos\phi_J) & (-\cos\theta_\beta \sin\phi_\beta \sin\phi_J + \cos\phi_\beta \cos\phi_J) & (\sin\theta_\beta \sin\phi_J) \\ (\sin\theta_\beta \cos\phi_\beta) & (\sin\theta_\beta \sin\phi_\beta) & (\cos\theta_b) \end{bmatrix} \quad (6.17a)'$$

$$[M_{oL}] = \begin{bmatrix} (\cos\theta_\beta \cos\phi_\beta \cos\phi_J - \sin\phi_\beta \sin\phi_J) & (-\cos\theta_\beta \cos\phi_B \sin\phi_J - \sin\phi_\beta \cos\phi_J) & (\sin\theta_\beta \cos\phi_\beta \\ (\cos\theta_\beta \sin\phi_\beta \cos\phi_J + \cos\phi_\beta \sin\phi_J) & (-\cos\theta_\beta \sin\phi_\beta \sin\phi_J + \cos\phi_\beta \cos\phi_J) & (\sin\theta_\beta \sin\phi_\beta) \\ (-\sin\theta_\beta \cos\phi_J) & (\sin\theta_\beta \sin\phi_J) & (\cos\theta_\beta) \end{bmatrix} \quad (6.17b)'$$

From the viewpoint of programming these calculations, we must distinguish between the variables that are specified at the beginning of the program ("given" variables) and those that are calculated from the given variables ("derived" variables). Of those variables appearing in $[M_{Bo}]$ or $(M_{oB}]$, θ_b and ϕ_b (the angles specifying the orientation of the scattering body) are given, while ϕ_H is derived. Of the variables appearing in $[M_{Lo}]$ or $[M_{oL}]$. θ_β and ϕ_β (direction angles of $\underset{\rightarrow}{\beta}$) are given, while ϕ_J is derived. Finally, of the variables in $[M_{BL}]$ or $[M_{LB}]$, θ_p, ϕ_p and ϕ_F are all derived.

To relate the matrixes $[M_{Bo}]$ (or $[M_{oB}]$), and $[M_{oL}]$ (or $[M_{Lo}]$), we form the matrix equations [from Eqs. (6.7a,b), (6.15a,b) and (6.17a,b)]:

$$[\hat{u}_{\underset{\rightarrow}{B}}] = [M_{Bo}][\hat{u}_{\underset{\rightarrow}{o}}] = [M_{Bo}][M_{oL}][\hat{u}_{\underset{\rightarrow}{L}}] = [M_{BL}][\hat{u}_{\underset{\rightarrow}{L}}] \tag{6.18a}$$

or

$$[\hat{u}_{\underset{\rightarrow}{L}}] = [M_{Lo}][\hat{u}_{\underset{\rightarrow}{o}}] = [M_{Lo}][M_{oB}][\hat{u}_{\underset{\rightarrow}{B}}] = [M_{LB}][\hat{u}_{\underset{\rightarrow}{B}}] \tag{6.18b}$$

Either of the matrix equations

$$[M_{BL}] = [M_{Bo}][M_{oL}] \tag{6.19a}$$

[derived from Eq. (6.18a)], or

$$[M_{LB}] = [M_{Lo}][M_{oB}] \tag{6.19b}$$

[derived from Eq. (6.18b)] constitutes a set of nine algebraic equations (not all independent) which contains the variables θ_p, ϕ_p, ϕ_F, θ_b, ϕ_b, θ_β, ϕ_β, ϕ_H and ϕ_J.

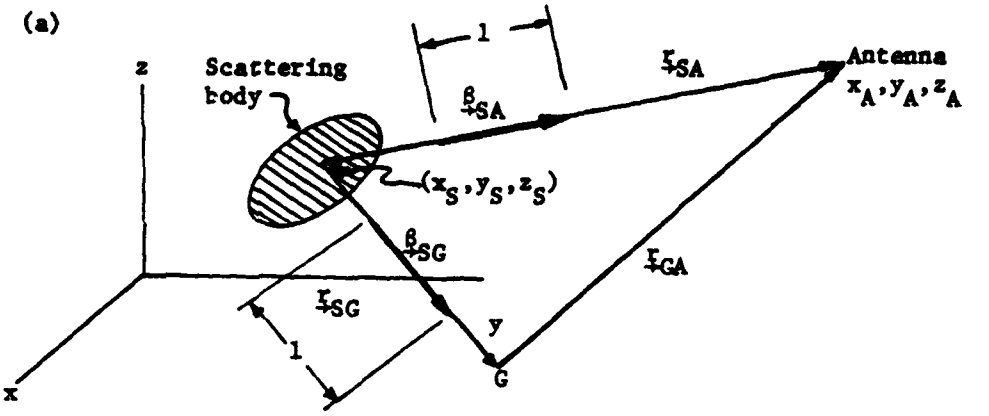

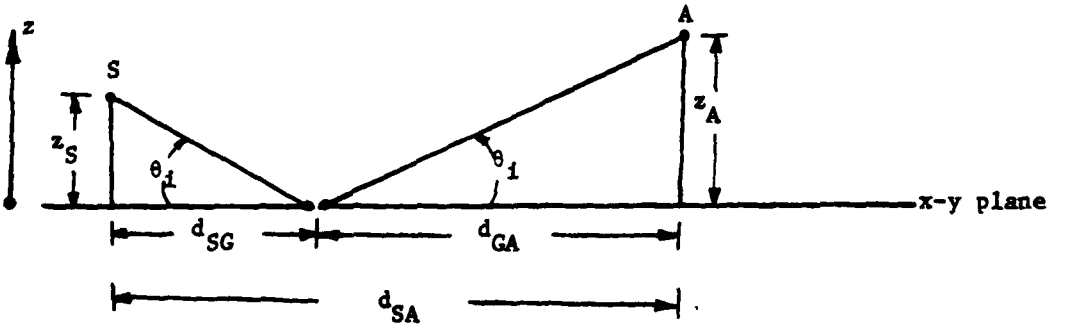

(c) Downward view

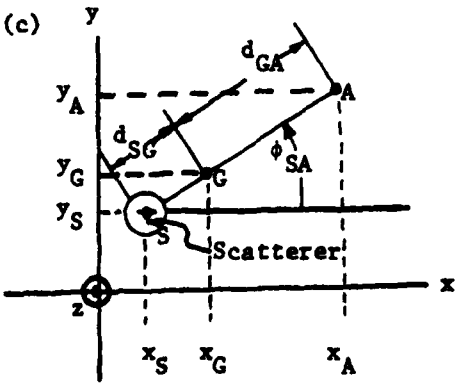

Figure 6-5. Scattering processes A and G

All of the machinery for performing the coordinate transformations needed to implement the scattering program is contained in the matrices $[M_{Bo}]$ (or $[M_{oB}]$), $[M_{Lo}]$ (or $[M_{oL}]$), and the matrix equations (6.19a,b). Fortunately, we only require limited knowledge of the variables contained in those equations. First, we must solve (in terms of known variables) for the variable ϕ_J contained in $[M_{Lo}]$ or $[M_{oL}]$, since the other variables in those matrices, θ_β and ϕ_β, are known. This is the purpose of the development to follow.

The Barber scattering program is constructed in such a way that the scattered wave is evaluated in the $(x_L, -z_L)$ plane. There are two plane-wave scattering processes to be considered (see Figure 6.5). We will call these processes A and G.

Process G is direct scattering from the body to the antenna. The wave propagation vector, for this process, denoted by $\underset{\rightarrow}{\beta}_{sA}$ and totally independent of $\underset{\rightarrow}{\beta}^{\pm}$, is along the vector $\underset{\rightarrow}{r}_{sA}$ (Figure 6.5a) from the center of the scatterer to the antenna.

Process G is the scattering from the body to a point G on the ground surface followed by ground reflection toward the antenna in accordance with the law of reflection. The wave vector for this process, denoted by $\underset{\rightarrow}{\beta}_{sG}$ and again independent of $\underset{\rightarrow}{\beta}^{\pm}$, is parallel to the vector $\underset{\rightarrow}{r}_{sG}$ shown in Figure 6.5a.

For the computation of the scattered fields using the Barber scattering program, both $\underset{\rightarrow}{r}_{sA}$ and $\underset{\rightarrow}{r}_{sG}$ must lie in the $(x_L - z_L)$ plane. Hence, these vectors must be perpendicular to the y_L coordinate direction. The conditions to be met are [with the aid of the second equation in the matrix relationship (6.17b)]

$$\underset{\rightarrow}{r}_{sA} \cdot \underset{\rightarrow}{\hat{y}}_L = (x_A - x_S)[-\cos\theta_\beta \cos\phi_\beta \sin(\phi_J)_A - \sin\phi_\beta \cos(\phi_J)_A]$$

$$+ (y_A - y_S)[-\cos\theta_\beta \sin\phi_\beta \sin(\phi_J)_A + \cos\phi_\beta \cos(\phi_J)_A]$$

$$+ (z_A - z_S)[\sin\theta_\beta \sin(\phi_J)_A] = 0 \qquad (6.21a)$$

$$\underset{\rightarrow}{r}_{sG} \cdot \hat{\underset{\rightarrow}{y}}_L = (x_G - x_S)[-\cos\theta_\beta \cos\phi_\beta \sin(\phi_J)_G - \sin\phi_\beta \cos(\phi_J)_G]$$

$$+ (y_G - y_S)[-\cos\theta_\beta \sin\phi_\beta \sin(\phi_J)_G + \cos\phi_\beta \cos(\phi_J)_G]$$

$$+ (z_G - z_S)[\sin\theta_\beta \sin(\phi_J)_G] = 0 \qquad (6.21b)$$

where $(\phi_J)_A$ and $(\phi_J)_G$ are values of ϕ_J for processes A and G, respectively, and where, from Eqs. (6.20e,g,f)

$$x_G = \frac{x_A z_S + x_S z_A}{z_A + z_S}$$

$$y_G = \frac{y_A z_S + y_S z_A}{z_A + z_S}$$

$$z_G = 0$$

$$\underset{\rightarrow}{r}_{sA} = \hat{\underset{\rightarrow}{x}}(x_A - x_S) + \hat{\underset{\rightarrow}{y}}(y_A - y_S) + \hat{\underset{\rightarrow}{z}}(z_A - z_S)$$

$$\underset{\rightarrow}{r}_{sG} = \hat{\underset{\rightarrow}{x}}(x_G - x_S) + \hat{\underset{\rightarrow}{y}}(y_G - y_S) + \hat{\underset{\rightarrow}{z}}(z_G - z_S)$$

Solution of Eq. (6.21a) for $\cos(\phi_J)_A$ and $\sin(\phi_J)_A$ or that of Eq. (6.21b)

for $\cos(\phi_J)_A$ and $\sin(\phi_J)_G$ (exactly the same form in both cases) yields

$$\cos(\phi_J)_A = \frac{\rho_{SA} \cos\theta_\beta \cos(\phi_\beta - \phi_{AS}) - (z_A - z_S) \sin\theta_\beta}{\sqrt{[\rho_{SA} \cos\theta_\beta \cos(\phi_\beta - \phi_{AS}) - (z_A - z_S) \sin\theta_\beta]^2 + [\rho_{SA} \sin(\phi_\beta - \phi_{AS})]^2}} \tag{6.22a}$$

$$\sin(\phi_J)_A = \frac{-\rho_{SA} \sin(\phi_\beta - \phi_{AS})}{\sqrt{[\rho_{SA} \cos\theta_\beta \cos(\phi_\beta - \phi_{AS}) - (z_A - z_S) \sin\theta_\beta]^2 + [\rho_{SA} \sin(\phi_\beta - \phi_{AS})]^2}} \tag{6.22b}$$

$$\cos(\phi_J)_G = \frac{\rho_{SG} \cos\theta_\beta \cos(\phi_\beta - \phi_{GS}) + z_S \sin\theta_\beta}{\sqrt{[\rho_{SG} \cos\theta_\beta \cos(\phi_\beta - \phi_{GS}) + z_s \sin\theta_\beta]^2 + [\rho_{SG} \sin(\phi_\beta - \phi_{GS})]^2}} \tag{6.22c}$$

$$\sin(\phi_J)_G = \frac{-\rho_{SG} \sin(\phi_\beta - \phi_{GS})}{\sqrt{[\rho_{SG} \cos\theta_\beta \cos(\phi_\beta - \phi_{GS}) + z_S \sin\theta_\beta]^2 + [\rho_{SG} \sin(\phi_\beta - \phi_{GS})]^2}} \tag{6.22d}$$

where

$$\rho_{SA} = \sqrt{(x_A - x_S)^2 + (y_A - y_S)^2}$$

$$\phi_{SA} = \tan^{-1}\left(\frac{y_A - y_S}{x_A - x_S}\right)$$

$$\rho_{SG} = \sqrt{(x_G - x_S)^2 + (y_G - y_S)^2}$$

$$\phi_{SG} = \tan^{-1}\left(\frac{y_G - y_S}{x_G - x_S}\right)$$

$$x_G = \frac{x_A z_S + x_S z_A}{z_A + z_S}$$

$$y_G = \frac{y_A z_S + y_S z_A}{z_A + z_S}$$

At this point we will invoke three of the equations in the matrix equation system (6.19a), as follows:

$$([M_{Bo}][M_{oL}])_{jk} = [M_{BL}]_{jk} \qquad (6.23)$$

$(j = 3, k = 1)$

$$\cos\phi_J(-[\cos\theta_b \sin\theta_\beta - \sin\theta_b \cos\theta_\beta \cos(\phi_b - \phi_\beta)])$$

$$+ \sin\phi_J(\sin\theta_b \sin(\phi_b - \phi_\beta)) = \sin\theta_p \cos\phi_p \qquad (6.23a)'$$

$(j = 3, k = 2)$

$$\cos\phi_J(\sin\theta_b \sin(\phi_b - \phi_\beta)$$

$$+ \sin\phi_J(-[\sin\theta_b \cos\theta_\beta \cos(\phi_b - \phi_\beta) - \cos\theta_b \sin\theta_\beta])$$

$$= \sin\theta_p \sin\phi_p \qquad (6.23b)'$$

$(j = 3, k = 3)$

$$\sin\theta_b \sin\theta_\beta \cos(\phi_b - \phi_\beta) + \cos\theta_b \cos\theta_\beta = \cos\theta_p \qquad (6.23c)'$$

Note that the left hand side of Eq. (6.23c)' consists entirely of given (and therefore <u>known</u>) variables. This equation can be used to evaluate θ_p, thus from Eq. (6.23c)',

$$\theta_p = \cos^{-1}[\sin\theta_b \sin\theta_\beta \cos(\phi_b - \phi_\beta) + \cos\theta_b \cos\theta_\beta] \qquad (6.24)$$

From Eqs. (6.23a)' or (6.23b)' we can solve for $(\phi_p)_A$ and $(\phi_p)_G$ (the azimuthal angle of the body axis in the lab frame for scattering processes A and G, respectively) in terms of known variables, as follows (if $\theta_p \neq 0$; otherwise $(\phi_p)_A$ and $(\phi_p)_G$ are arbitrary):

$$(\phi_p)_A = \cos^{-1}\left(\frac{1}{\sin\theta_p}\{-\cos(\phi_J)_A[\cos\theta_b \sin\theta_\beta - \sin\theta_b \cos\theta_\beta \cos(\phi_b - \phi_\beta)] + \sin(\phi_J)_A(\sin\theta_b \sin(\phi_b - \phi_\beta))\}\right)$$

$$= \text{(equivalently) } \sin^{-1}\left(\frac{1}{\sin\theta_p}\{\cos(\phi_J)_A(\sin\theta_b \sin(\phi_b - \phi_\beta)) + \sin(\phi_J)_A[\cos\theta_b \sin\theta_\beta - \sin\theta_b \cos\theta_\beta \cos(\phi_b - \phi_\beta)]\}\right) \qquad (6.25a)$$

where $\cos(\phi_J)_A$ and $\sin(\phi_J)_A$ are given by Eqs. (6.22a) and (6.22b), respectively,

and $\sin \theta_p$ is obtained from Eq. (6.23c)'.

$$(\phi_p)_G = \cos^{-1} \left(\frac{1}{\sin \theta_p} \{-\cos (\phi_J)_G [\cos \theta_b \sin \theta_\beta \right.$$

$$- \sin \theta_b \cos \theta_\beta \cos (\phi_b - \phi_\beta)]$$

$$\left. + \sin (\phi_J)_G (\sin \theta_b \sin (\phi_b - \phi_\beta)\}\right)$$

$$= \text{(equivalently) } \sin^{-1} \left(\frac{1}{\sin \theta_p} \{\cos (\phi_J)_G (\sin \theta_b \sin (\phi_b - \phi_\beta)) \right.$$

$$\left. + \sin (\phi_J)_G [\cos \theta_b \sin \theta_\beta - \sin \theta_b \cos \theta_\beta \cos (\phi_b - \phi_\beta)]\}\right) \tag{6.25b}$$

where $\cos (\phi_J)_G$ and $\sin (\phi_J)_G$ are given by Eqs. (6.22c) and (6.22d), respectively, and $\sin \theta_p$ is obtainable from Eq. (6.23c)'.

We must now obtain a transformation between the ground-frame coordinates of the electric field plane-wave spectrum incident on the scatterer (i.e., the field spectrum directly from the cable superposed on the ground-reflected field spectrum from the cable. Both of these are expressed in ground-frame coordinates (x_o, y_o, z_o) and the lab frame coordinates of these same field spectra (i.e., the x_L and y_L components, since the z_L component must be zero for a plane-wave propagating in the z_L direction). To this end, we write, where $\tilde{\underset{\rightarrow}{E}}_i$ is the incident field (spectrum) vector

$$\tilde{\underset{\rightarrow}{E}}_i = \hat{\underset{\rightarrow}{x}}_L \tilde{E}_{ix_L} + \hat{\underset{\rightarrow}{y}}_L \tilde{E}_{iy_L} + \hat{\underset{\rightarrow}{z}}_L(0) = [\tilde{\underset{\rightarrow}{E}}_i^{(L)}]^T [\hat{\underset{\rightarrow}{u}}_L]$$

$$= \hat{\underset{\rightarrow}{x}} \tilde{E}_{ix} + \hat{\underset{\rightarrow}{y}} \tilde{E}_{iy} + \hat{\underset{\rightarrow}{z}} \tilde{E}_{iz} = [\tilde{\underset{\rightarrow}{E}}_i^{(0)}]^T [\hat{\underset{\rightarrow}{u}}_o] \tag{6.26}$$

where

$$\tilde{\underset{\rightarrow}{E}}_i^{(L)} = \begin{bmatrix} \tilde{E}_{ix_L} \\ \tilde{E}_{iy_L} \\ \tilde{E}_{iz_L} \end{bmatrix} = \begin{bmatrix} \tilde{E}_{ix_L} \\ \tilde{E}_{iy_L} \\ 0 \end{bmatrix}$$

$$\begin{pmatrix} \tilde{E}_{ix_L} = x_L \text{ component of } \underset{\rightarrow}{E}_i \\ \tilde{E}_{iy_L} = y_L \text{ component of } \underset{\rightarrow}{E}_i \end{pmatrix}$$

$$[\tilde{\underset{\rightarrow}{E}}_i^{(0)}] = \begin{bmatrix} \tilde{E}_{ix} \\ \tilde{E}_{iy} \\ \tilde{E}_{iz} \end{bmatrix} \qquad \begin{pmatrix} \tilde{E}_{ix} = x \text{ component of } \tilde{\underset{\rightarrow}{E}}_i \\ \tilde{E}_{iy} = y \text{ component of } \tilde{\underset{\rightarrow}{E}}_i \\ \tilde{E}_{iz} = z \text{ component of } \tilde{\underset{\rightarrow}{E}}_i \end{pmatrix}$$

and where $[\hat{\underset{\rightarrow}{u}}_L]$ and $[\hat{\underset{\rightarrow}{u}}_o]$ are defined in Eqs. (6.7a)' and (6.17d)' respectively.

From Eqs. (6.26) and (6.18a,b),

$$[\tilde{\underset{\rightarrow}{E}}_i^{(0)}]^T[M_{oL}][\hat{\underset{\rightarrow}{u}}_L] = [\tilde{\underset{\rightarrow}{E}}_i^{(L)}]^T[\hat{\underset{\rightarrow}{u}}_L] \tag{6.27}$$

which implies [using the fact that $[M_{oL}]^T = [M_{Lo}]$ evident from the definitions below Eq. (6.17b)] after taking the transpose of both sides of Eq. (6.26), that

$$[\tilde{\underset{\rightarrow}{E}}_i^{(L)}] = [M_{oL}]^T[\tilde{\underset{\rightarrow}{E}}_i^{(0)}] = [M_{Lo}][\tilde{\underset{\rightarrow}{E}}_i^{(0)}] \tag{6.28}$$

in longhand notation Eq. (6.28) takes the form

$$\tilde{E}_{ix_L} = (\cos\theta_\beta \cos\phi_\beta \cos\phi_J - \sin\phi_\beta \sin\phi_J)\,\tilde{E}_{ix}$$

$$+ (\cos\theta_\beta \sin\phi_\beta \cos\phi_J + \cos\phi_\beta \sin\phi_J)\,\tilde{E}_{iy} \qquad (6.28a)'$$

$$- (\sin\theta_\beta \cos\phi_J)\,\tilde{E}_{iz} \qquad (6.28a)'$$

$$\tilde{E}_{iy_L} = -(\cos\theta_\beta \cos\phi_\beta \sin\phi_J + \sin\phi_\beta \cos\phi_J)\,\tilde{E}_{ix}$$

$$- (\cos\theta_\beta \sin\phi_\beta \sin\phi_J - \cos\phi_\beta \cos\phi_J)\,\tilde{E}_{iy}$$

$$+ (\sin\theta_\beta \sin\phi_J)\,\tilde{E}_{iz} \qquad (6.28b)'$$

$$\tilde{E}_{iz_L} = 0 = (\sin\theta_\beta \cos\phi_\beta)\,\tilde{E}_{ix} + (\sin\theta_\beta \sin\phi_\beta)\,\tilde{E}_{iy} + (\cos\theta_\beta)\,\tilde{E}_{iz} \qquad (6.28c)'$$

where $\phi_J = (\phi_J)_A$ and $(\phi_J)_G$ for A and G scattering processes respectively. Since we know from the Maxwell equation $\nabla \cdot \underset{\rightarrow}{E} = 0$ that

$$\tilde{E}_{iz} = -\frac{1}{\beta_z}\left[\beta_x \tilde{E}_{ix} + \beta_y \tilde{E}_{iy}\right]$$

$$= -\frac{1}{\cos\theta_\beta}\left[\sin\theta_\beta\,(\tilde{E}_{ix}\cos\phi_\beta + \tilde{E}_{iy}\sin\phi_\beta)\right] \qquad (6.29)$$

it follows that Eq. (6.28c)' is valid, since Eqs. (6.29) and (6.28c)' are identical. It also follows from Eqs. (6.28a,b,c)', with a little manipulation, that

$$\tilde{E}_{ix_L} = \tilde{E}_{ix}\{\frac{1}{\cos\theta_\beta}[\cos\phi_\beta\cos\phi_J - \cos\theta_\beta\sin\phi_\beta\sin\phi_J]\}$$

$$+ \tilde{E}_{iy}\{\frac{1}{\cos\theta_\beta}[\sin\phi_\beta\cos\phi_J + \cos\theta_\beta\cos\phi_\beta\sin\phi_J]\} \quad (6.30a)$$

if $\theta_\beta \neq \frac{\pi}{2}$.

$$\tilde{E}_{iy_L} = \tilde{E}_{ix}\{-\frac{1}{\cos\theta_\beta}[\cos\phi_\beta\sin\phi_J + \cos\theta_\beta\sin\phi_\beta\cos\phi_J]\}$$

$$+ \tilde{E}_{iy}\{-\frac{1}{\cos\theta_\beta}[\sin\phi_\beta\sin\phi_J - \cos\theta_\beta\cos\phi_\beta\cos\phi_J]\} \quad (6.30b)$$

if $\theta_\beta \neq \frac{\pi}{2}$.

If $\theta_\beta = \frac{\pi}{2}$, then Eq. (6.28c) implies that (where subscripts R and I indicate real and imaginary parts respectively)

$$\frac{(\tilde{E}_{ix})_R}{(\tilde{E}_{iy})_R} = \frac{(\tilde{E}_{ix})_I}{(\tilde{E}_{iy})_I} = -\tan\phi_\beta \quad (6.31)$$

From Eqs. (6.28a,b)' and (6.31), if $\theta_\beta = \frac{\pi}{2}$, we can infer the following relationships for real and imaginary parts of $\tilde{E}_{ix_L}$ and $\tilde{E}_{iy_L}$:

$$(\tilde{E}_{ix_L})_{\substack{R\\I}} = \tilde{E}_{ix_{\substack{R\\I}}}[-\frac{\sin\phi_J}{\sin\phi_\beta}] - \tilde{E}_{iz_{\substack{R\\I}}}\cos\phi_J \quad (6.32a)$$

if $\phi_\beta \neq 0, \pi$, $\theta_\beta = \frac{\pi}{2}$.

$$(\tilde{E}_{iy_L})_{\substack{R \\ I}} = \tilde{E}_{ix_{\substack{R \\ I}}} \left[\frac{\cos \phi_J}{\sin \phi_\beta} \right] + \tilde{E}_{iz_{\substack{R \\ I}}} \sin \phi_J \qquad (6.32b)$$

if $\phi_\beta \neq 0, \pi$, $\theta_\beta = \frac{\pi}{2}$.

$$(\tilde{E}_{ix_L})_{\substack{R \\ I}} = \tilde{E}_{iy_{\substack{R \\ I}}} \left[\frac{\sin \phi_J}{\cos \phi_\beta} \right] - \tilde{E}_{iz_{\substack{R \\ I}}} \cos \phi_J \qquad (6.32c)$$

if $\phi_\beta \neq \frac{\pi}{2}, \frac{3\pi}{2}$, $\theta_\beta = \frac{\pi}{2}$.

$$(\tilde{E}_{iy_L})_{\substack{R \\ I}} = \tilde{E}_{iy_{\substack{R \\ I}}} \left[- \frac{\cos \phi_J}{\cos \phi_\beta} \right] + \tilde{E}_{iz_{\substack{R \\ I}}} \sin \phi_J \qquad (6.32d)$$

if $\phi_\beta \neq \frac{\pi}{2}, \frac{3\pi}{2}$, $\theta_\beta = \frac{\pi}{2}$.

A further step is required to construct the inputs to the Barber scattering program.

The amplitude $\tilde{E}_i$ and the angle ϕ_i, the polarization angle of the incident field in the lab frame, are required as inputs to the scattering program. The amplitude, independent of polarization, is easily obtained without any coordinate transformations, i.e. [with the aid of Eqs. (6.29 and (6.32)],

$$\tilde{E}_i = \sqrt{\tilde{E}_i \cdot \tilde{E}_i^*} = \sqrt{|\tilde{E}_{ix}|^2 + |\tilde{E}_{iy}|^2 + |\tilde{E}_{iz}|^2}$$

$$= \sqrt{\{|\tilde{E}_{ix}|^2(1 + \tan^2 \theta_\beta \cos^2 \phi_\beta) + |\tilde{E}_{iy}|^2(1 + \tan^2 \theta_\beta \sin^2 \phi_\beta) \ldots}$$

$$\overline{\ldots + 2\mathrm{Re}(\tilde{E}_{ix} \tilde{E}_{iy} \cos \phi_\beta \sin \phi_\beta \tan^2 \theta_\beta)\}} \qquad (\text{if } \theta_\beta \neq \tfrac{\pi}{2})$$

$$= \sqrt{\frac{|\tilde{E}_{ix}|^2}{\sin^2 \phi_\beta} + |\tilde{E}_{iz}|^2} \qquad \text{if } \theta_\beta = \frac{\pi}{2}\ ,\ \phi_\beta \neq 0,\pi$$

$$+ \sqrt{\frac{|\tilde{E}_{iy}|^2}{\cos^2 \phi_\beta} + |\tilde{E}_{iz}|^2} \qquad \text{if } \theta_\beta = \frac{\pi}{2}\ ,\ \phi_\beta \neq \frac{\pi}{2}\ ,\ \frac{3\pi}{2} \qquad (6.33)$$

The polarization angle ϕ_i, assuming that the phase angles of $\tilde{E}_{ix_L}$ and $\tilde{E}_{iy_L}$ are the same (linear polarization) is given by

$$\phi_i = \tan^{-1} \left(\frac{\pm |\tilde{E}_{iy_L}|}{|\tilde{E}_{ix_L}|} \right) \qquad (6.34)$$

where $\tilde{E}_{ix_L}$ and $\tilde{E}_{iy_L}$ are given by Eqs. (6.28a,b,c)' or alternatively by Eqs. (6.30a,b) if $\theta_\beta \neq \pi/2$ or by Eqs. (6.32a,b) if $\theta_\beta = \pi/2$, $\phi_\beta \neq 0,\pi$ or by Eqs. (6.32c,d) if $\theta_\beta = \pi/2$, $\phi_\beta \neq \pi/2,\ 3\pi/2$.

If the phase angles of $\tilde{E}_{ix_L}$ and $\tilde{E}_{iy_L}$ are not the same, that fact would imply that the wave incident on the scatterer is elliptically polarized. We could exclude that possibility by assuming that, if a particular source should generate a superposition of elliptically polarized plane waves, then for each such wave the rate of rotation of the plane of polarization is sufficiently slow that, throughout the scatterer region, where the incident wave can have an influence on the scattered wave, the rotation of the plane of polarization can be considered approximately constant.

Once the fields from the source have been found, we can determine to what extent the relative phase angles between x, y and z components constitute a problem. Since free space is a reciprocal medium, it would seem that it

should not be a problem at all. Any plane waves propagating from the slots should be linearly polarized.

To ascertain that this is indeed the case, we can examine the expressions for x, y and z components of fields in Eqs. (4.46a,b), (4.47c,d,e,f) or the specialized forms of these equations (4.48b,c,d,e) or (4.49a,b,c,d,e,f).

To obtain the field components we must add the quantities with subscript + to those with subscript - [i.e., Eqs. (4.47c) + (4.47e), (4.47d) + (4.47f), (4.48b) + (4.48c), (4.48d) + (4.48e)]. The results of the first set of these summations are as follows [where we note that $S_-^{(n)} = (S_+^{(n)})^*$]:

Eqs. (4.47c) and (4.47e):

	x	y	z
Factors in $\bar{E}_{\phi''}^{(n)}$ term	$\pm\lvert\beta_z\rvert \mathrm{Re}[S_+^{(n)} e^{j\phi}10]$	$\pm\lvert\beta_z\rvert \mathrm{Im}[S_+^{(n)} e^{j\phi}10]$	$-\beta_x \mathrm{Re}[S_+^{(n)} e^{j\phi}10]$
Factors in $\bar{E}_{z''}^{(n)}$ term	$\pm\lvert\beta_z\rvert \mathrm{Im}[S_+^{(n)} e^{j\phi}10]$	$\mp\lvert\beta_z\rvert \mathrm{Re}[S_+^{(n)} e^{j\phi}10]$	$\beta_y \mathrm{Re}[S_+^{(n)} e^{j\phi}10]$
Factors in $\bar{H}_{\phi''}^{(n)}$ term	$\mathrm{Im}[A_x S_+^{(n)} e^{j\phi}10]$	$-\mathrm{Re}[A_y S_+^{(n)} e^{j\phi}10]$	$\pm\lvert\beta_z\rvert\beta_y \mathrm{Re}[S_+^{(n)} e^{j\phi}10]$
Factors in $\bar{H}_{z''}^{(n)}$ term	$-\mathrm{Re}[A_x S_+^{(n)} e^{j\phi}10]$	$\mathrm{Im}[A_y S_+^{(n)} e^{j\phi}10]$	$\pm\lvert\beta_z\rvert\beta_x \mathrm{Re}[S_+^{(n)} e^{j\phi}10]$
	(All real numbers)	(All real numbers)	(All real numbers)

Eqs. (4.47d) and (4.47f):

	x	y	z
Factors in $\bar{H}_{\phi''}^{(n)}$ term	$\pm\lvert\beta_z\rvert \mathrm{Re}[S_+^{(n)} e^{j\phi}10]$	$\pm\lvert\beta_z\rvert \mathrm{Im}[S_+^{(n)} e^{j\phi}10]$	$-\beta_x \mathrm{Re}[S_+^{(n)} e^{j\phi}10]$
Factors in $\bar{H}_{z''}^{(n)}$ term	$\pm\lvert\beta_z\rvert \mathrm{Im}[S_+^{(n)} e^{j\phi}10]$	$\pm\lvert\beta_z\rvert \mathrm{Re}[S_+^{(n)} e^{j\phi}10]$	$\beta_y \mathrm{Re}[S_+^{(n)} e^{j\phi}10]$
Factors in $\bar{E}_{\phi''}^{(n)}$ term	$-\mathrm{Im}[A_x S_+^{(n)} e^{j\phi}10]$	$\mathrm{Re}[A_y S_+^{(n)} e^{j\phi}10]$	$\mp\lvert\beta_z\rvert\beta_y \mathrm{Re}[S_+^{(n)} e^{j\phi}10]$
Factors in $\bar{E}_{z''}^{(n)}$ term	$\mathrm{Re}[A_x S_+^{(n)} e^{j\phi}10]$	$-\mathrm{Im}[A_y S_+^{(n)} e^{j\phi}10]$	$\mp\lvert\beta_z\rvert\beta_x \mathrm{Re}[S_+^{(n)} e^{j\phi}10]$
	(All real numbers)	(All real numbers)	(All real numbers)

From the chart above, it is clear that all three components, x, y, and z, have the same phase. Each component associated with one of the slot fields, e.g., $\bar{H}_{\phi''}^{(n)}$ or $\bar{E}_{z''}^{(n)}$, has a complex factor common to all three components and another complex factor that is different for the three components. It is the latter set of factors that the chart refers to, and when the plus and minus terms are added, the sums of those factors are all real numbers. Hence, the plane-wave fields from the slots are all plane-polarized. The ground-reflection will not change this, since the ground is also a reciprocal medium.

The same arguments apply to the summations [(4.48b) + (4.48c)], [(4.48d) + (4.48e)], [(4.49c) + (4.49d)] and [(4.49e) + (4.49f)], since these are only special cases of those summations discussed above.

Note that the corresponding factors in the field components with subscript o [as evidenced by Eqs. (4.47a,b), (4.48a) and (4.49a,b)] are all real numbers.

We will now summarize the steps required to implement the calculations described in this section on the computer.

A. Feed in the variables x_A, y_A, z_A, x_S, y_S, z_S, θ_β, ϕ_β, θ_b, ϕ_b and $(\tilde{E}_{ix}, \tilde{E}_{iy}, \tilde{E}_{iz})$, the components of the spectral field of the plane wave incident on the scatterer, from the main program to a subprogram to be called Subroutine BIS ("Barber Input Subroutine").

B. Compute x_G and y_G from Eqs. (6.20e,f) (repeated and renumbered for convenience):

$$x_G = \frac{x_A z_S + x_S z_A}{z_A + z_S} \tag{6.35a}$$

$$y_G = \frac{y_A z_S + y_S z_A}{z_A + z_S} \tag{6.35b}$$

C. Using x_G and y_G from Step B, compute the following quantities [see the definitions below Eq. (6.22d)]:

$$\rho_{SA} = \sqrt{(x_A - x_S)^2 + (y_A - y_S)^2} \tag{6.36a}$$

$$\phi_{SA} = \tan^{-1}\left(\frac{y_A - y_S}{x_A - x_S}\right) \tag{6.36b}$$

$$\rho_{SG} = \sqrt{(x_G - x_S)^2 + (y_G - y_S)^2} \tag{6.36c}$$

$$\phi_{SG} = \tan^{-1}\left(\frac{y_G - y_S}{x_G - x_S}\right) \tag{6.36d}$$

D. Using the results of A, B, and C, compute $\cos\ (\phi_J)_{\substack{A\\G}}$ and $\sin\ (\phi_J)_{\substack{A\\G}}$ from Eqs. (6.22a,b,c,d) (repeated and renumbered):

$$\cos\ (\phi_J)_A = \frac{\rho_{SA} \cos\theta_\beta \cos\ (\phi_\beta - \phi_{AS}) - (z_A - z_S) \sin\theta_\beta}{\sqrt{[\rho_{SA} \cos\theta_\beta \cos\ (\phi_\beta - \phi_{AS}) - (z_A - z_S) \sin\theta_\beta]^2 + [\rho_{SA} \sin\ (\phi_\beta - \phi_{AS})]^2}} \tag{6.37a}$$

$$\sin\ (\phi_J)_A = \frac{-\rho_{SA} \sin\ (\phi_\beta - \phi_{AS})}{\sqrt{[\rho_{SA} \cos\theta_\beta \cos\ (\phi_\beta - \phi_{AS}) - (z_A - z_S) \sin\theta_\beta]^2 + [\rho_{SA} \sin\ (\phi_\beta - \phi_{AS})]^2}} \tag{6.37b}$$

$$\cos (\phi_J)_G = \frac{\rho_{SG} \cos \theta_\beta \cos (\phi_\beta - \phi_{GS}) + z_S \sin \theta_\beta}{\sqrt{[\rho_{SG} \cos \theta_\beta \cos (\phi - \phi_{GS}) + z_s \sin \theta_\beta]^2 + [\rho_{SG} \sin (\phi_\beta - \phi_{GS})]^2}} \quad (6.37c)$$

$$\sin (\phi_J)_G = \frac{-\rho_{SG} \sin (\phi_\beta - \phi_{GS})}{\sqrt{[\rho_{SG} \cos \theta_\beta \cos (\phi_\beta - \phi_{GS}) + z_S \sin \theta_\beta]^2 + [\rho_{SG} \sin (\phi_\beta - \phi_{GS})]^2}} \quad (6.37d)$$

where

$$\rho_{SA} = \sqrt{(x_A - x_S)^2 + (y_A - y_S)^2}$$

$$\phi_{SA} = \tan^{-1} \left(\frac{y_A - y_S}{x_A - x_S} \right)$$

E. From the results of A, B, C, and D, compute $(\phi_p)^A_G$ from Eqs. (6.25a,b) repeated and renumbered):

$$(\phi_p)_A = \cos^{-1} \left(\frac{1}{\sin \theta_p} \{-\cos (\phi_J)_A [\cos \theta_b \sin \theta_\beta - \sin \theta_b \cos \theta_\beta \cos (\phi_b - \phi_\beta)] \right.$$

$$\left. + \sin (\phi_J)_A (\sin \theta_b \sin (\phi_b - \phi_\beta))\} \right)$$

$$= \text{(equivalently) } \sin^{-1} \left(\frac{1}{\sin \theta_p} \{\cos (\phi_J)_A (\sin \theta_b \sin (\phi_b - \phi)) \right.$$

$$\left. + \sin (\phi_J)_A [\cos \theta_b \sin \theta_\beta - \sin \theta_b \cos \theta_\beta \cos (\phi_b - \phi_\beta)]\} \right) \quad (6.38a)$$

where $\cos(\phi_J)_A$ and $\sin(\phi_J)_A$ are given by Eqs. (6.22a) and (6.22b) respectively, and $\sin\theta_p$ is obtainable from Eq. (6.23c)'.

$$(\phi_p)_G = \cos^{-1}\left(\frac{1}{\sin\theta_p}\{-\cos(\phi_J)_G[\cos\theta_b \sin\theta_\beta - \sin\theta_b \cos\theta_\beta \cos(\phi_b - \phi_\beta)]\right.$$

$$\left. + \sin(\phi_J)_G (\sin\theta_b \sin(\phi_b - \phi_\beta))\}\right)$$

$$= \text{(equivalently) } \sin^{-1}\left(\frac{1}{\sin\theta_p}\{\cos(\phi_J)_G(\sin\theta_b \sin(\phi_b - \phi_\beta))\right.$$

$$\left. + \sin(\phi_J)_G[\cos\theta_b \sin\theta_\beta - \sin\theta_b \cos\theta_\beta \cos(\phi_b - \phi_\beta)]\}\right) \qquad (6.38b)$$

where $\cos(\phi_J)_G$ and $\sin(\phi_J)_G$ are given by Eqs. (6.22c) and (6.22d) respectively, and $\sin\theta_p$ is obtainable from Eq. (6.23c)'.

F. Compute [from Eq. (6.33), repeated and renumbered] the amplitude of the plane-wave incident on the scatterer:

$$\tilde{E}_i = \sqrt{|\tilde{E}_{ix}|^2 + |\tilde{E}_{iy}|^2 + |\tilde{E}_{iz}|^2} \qquad (6.39)$$

G. Compute [from Eq. (6.34, repeated and renumbered] the phase of the incident wave for both scattering process (antenna-directed and ground-directed):

$$\phi_i^{(A),(G)} = \left[\tan^{-1}\left(\frac{\pm|\tilde{E}_{iy_L}|}{|\tilde{E}_{ix_L}|}\right)\right]^{(A),(G)} \tag{6.40}$$

where the arguments are chosen in accordance with the "lab system" defined for each scattering process.

H. Transfer the results θ_p, $(\phi_p)_A$, $(\phi_p)_G$, $\tilde{E}_i$, $(\phi_i)_A$ and $(\phi_i)_G$ into the Barber scattering program.

7. THE BARBER SCATTERING PROGRAM

It was decided early in this project to use, if possible, a scattering program that was already developed as opposed to generating a new one. This seemed sensible in view of the time limitations of this project and the extensive research that has been done on electromagnetic scattering during the past 30 years. It might have required virtually all the project time and effort available to develop a suitable computer program to treat electromagnetic scattering from an object designed to simulate a human frame target. If such a program had already been developed and was available, it would seem that we should use it.

Hence, early in the project an extensive literature search was done on electromagnetic scattering at radio frequencies. The bibliography resulting from that search is included in the list of references at the end of this report.[D-1 through D-35]

In the process of conducting the literature search, it was found that virtually all the scattering theory done by previous workers had severe limitations when one considers scattering from a live human body. The theory can only be done rigorously for uniform or layered spheres, uniform or layered <u>infinite</u> circular cylinders (not finite cylinders), and with considerably more difficulty for uniform or layered ellipsoids or uniform or layered cylinders with elliptical cross-section. When scatterer dimensions are very small compared with wavelength (or more precisely, when $\frac{2\pi d}{\lambda} << 1$, where d is the largest scatterer dimension and λ is the wavelength in the scatterer material) whatever series of special functions are to be used (e.g., spherical or cylindrical vector wave functions in the cases of spheres and cylinders, respectively)[A-1] require fewer terms for a given level of accuracy. In implementing scattering

problems on a computer, even for these simple tractable shapes, it is highly desirable that the scatterers be (a) of uniform constitutive parameters, as opposed to being layered, which although theoretically tractable always involves more computer time; (b) either perfectly conducting (complex dielectric constant a pure imaginary) or perfectly dielectric (complex dielectric constant purely real), also resulting in a smaller expenditure of computing time; (c) very small or very large dimension compared with wavelength, allowing the use of fewer terms in the appropriate series in the former case (as remarked above) or the use of physical optics approximations in the latter case. Either of these two extremes simplifies the computations and thereby saves computer time.

Unfortunately, none of the simplifications above are necessarily applicable to human frame targets within the frequency range of interest. Wavelength in free space (λ_o) for our frequency range of 50 to 500MHz ranges from 0.6 to 6 meters. Considering 2 meters as d, the largest dimension of a human frame target, the parameter ($\frac{2\pi d}{\lambda_o}$) ranges from about 2 at 50MHz to about 20 at 500MHz. If we consider $\frac{2\pi d}{\lambda}$, where λ is the wavelength in the medium of which the scatterer is composed, we must correct these numbers by a multiplicative factor of

$$\sqrt{\left|\hat{\varepsilon}_{cs} + \frac{j\,\sigma_s}{\omega\,\varepsilon_o}\right|} \quad , \text{ where } \hat{\varepsilon}_{cs} = \frac{\varepsilon_{cs}}{\varepsilon_o} \quad ,$$

ε_{cs} being the permittivity of the scatterer, and σ_s is the conductivity of the scatterer. Suppose we use values $\hat{\varepsilon}_{cs} = 20$ and $\sigma_s = 1$ mho/meter, which were close to the values used in our computer program, based on Reference D-34.

The correction factor would range from about 5 at 500MHz to about 20 at 50MHz. Thus the parameter $\frac{2\pi d}{\lambda}$, referred to the scatterer material rather

than free space, is somewhere between roughly 40 at 50MHz and roughly 100 at 500MHz. These numbers are well above unity but not necessarily large enough to allow the use of physical optics approximations. They are certainly not small enough to allow the use of highly truncated series of harmonic functions and, in fact, require large numbers of terms for convergence of these series. Also, human targets cannot be modelled as perfect conductors or perfect dielectrics at these frequencies, which again brings the problem into the domain of more computer-intensive scattering problems. A sphere or circular cylinder is an extremely crude model of a human body. An ellipsoid would be a much better model, but again it would be desirable from a computer-time viewpoint to have some symmetry in the scatterer; nence, a good compromise between analytical simplicity and realism is a spheroid, particularly a prolate spheroid.

As a part of the literature search, the bioengineering literature on absorption and scattering of electromagnetic waves by biological objects was perused.[D-1 through D-35] Bioengineers are primarily interested in absorption rather than scattering, but the boundary value problem they must attack to determine the absorption also contains the mathematical machinery to determine the scattering from the body. Hence, a particular piece of work done by Professor Peter Barber of the Bioengineering Department at the University of Utah in Salt Lake City appeared to be highly applicable to the problem of interest on this project.[D-29]

Barber had authored or co-authored a number of papers on this work and had developed a very extensive computer program to implement the analytical solutions.[D-13,D-17,D-19,D-22,D-24,D-29,D-30,D-32,D-34] The program had been used on a number of problems of interest to bioengineers over a period of about five years and had been thoroughly "debugged." It had been used by others on different computer facilities and had produced reliable results. It seemed

that the best procedure for us would be to ask Barber for his program cards and adapt the program to Northeastern's VAX. All of this was done, as indicated in the quarterly status reports on this project, and Professor Barber's scattering program was adapted to the VAX and implemented as a subroutine in our overall program. It is called "Subroutine BARBER."

The details of the theory behind this scattering program are given in Barber's papers, particularly References D-13, D-17, D-19, D-22, D-29. It is based on an integral equation technique called the "Extended Boundary Condition Method" (EBCM).

Following a development due to Waterman,[D-4] the incident and scattered electric fields at position $\underset{\rightarrow}{r} = (r, \theta, \phi)$ are expanded in a series of spherical vector wave functions as follows (using some of Barber's notation):

$$\underset{\rightarrow}{E}^{i}(\underset{\rightarrow}{r}) = \sum_{\nu=1}^{\infty} D_{\nu}[a_{\nu} \overline{M}_{\nu}^{1}(k\underset{\rightarrow}{r}) + b_{\nu} \overline{N}_{\nu}^{1}(k\underset{\rightarrow}{r})] \tag{7.1a}$$

$$\underset{\rightarrow}{E}^{s}(\underset{\rightarrow}{r}) = \sum_{\nu=1}^{\infty} 4D_{\nu}(f_{\nu} \overline{M}_{\nu}^{3}(k\underset{\rightarrow}{r}) + g_{\nu} \overline{N}_{\nu}^{3}(k\underset{\rightarrow}{r})] \tag{7.1b}$$

where superscripts i and s refer to "incident" and "reflected", respectively, where $\overline{M}_{\nu}^{1}$, $\overline{N}_{\nu}^{1}$, $\overline{M}_{\nu}^{3}$, $\overline{N}_{\nu}^{3}$ are vector wave functions, superscripts 1 and 3 referring to particular classifications of these wave functions (e.g., 3 refers to radiation fields, i.e., Hankel function expansions), k being the propagation constant in the ambient medium, ν being a combined index incorporating spherical harmonic indices, and D_{ν} being a normalization constant. The constants a_{ν} and b_{ν} are assumed known for a specified incident wave. The task of solving for the scattered wave field is that of evaluating the unknown constants f_{ν} and g_{ν}.

The method is valid for any homogeneous, linear, isotropic scatterer, and has also been extended to include layered scatterers each of whose layers is homogeneous, linear and isotropic. The technique lends itself most readily to scattering from spherical objects but can be used to treat objects of arbitrary shape.

The scattering object is completely surrounded by a sphere whose diameter is the largest dimension of the object itself. If the fields on the surface of the sphere are known, then the Kirchhoff-Huyghens integral equation [see Appendix I, Eqs. (I.3a,b) or (I.6a,b)] can be used to determine the fields outside the sphere. To relate the fields on that sphere (a knowledge of which is tantamount to solution of the scattering problem) to the boundary conditions on the bounding surface of the nonspherical scattering object itself, an analytic continuation process is used. Through the Kirchhoff-Huyghens integral equation, the expansions in Eqs. (7.1a,b) and the application of the boundary conditions on the scatterer's surface, a set of matrix equations are developed from which the coefficients f_ν and g_ν, and hence the scattered fields, may be determined.

Further details on the basic theory behind the EBCM is explained quite thoroughly in Waterman's 1971 paper,[D-4] in which he also references a great deal of previous work on this and related techniques for solving scattering problems. Barber's principle contribution was to apply that theory to the development of computer programs that can handle a wide range of difficult scattering problems and the application of the theory, via those programs, to problems involving biological scatterers. The particular scatterer to which we have applied his program is a homogeneous, linear, isotropic prolate spheroid designed to simulate a human being.

It should be mentioned that another analytical method of treating scattering

from a human frame target, together with a computer program to implement the method, was developed by Barber and one of his Ph.D. students, Mark Hagmann. This work is presented in Hagmann's Ph.D. thesis, Reference D-31 on our reference list.

Professor Barber gave the writer a copy of this dissertation for possible use on the project. The method treats a human body as an electromagnetic scatterer in a much more accurate way than does the theory that we actually used. Head, torso and limbs are each modelled and scattering processes from all of these parts and interactions between them are considered. The unfortunate aspect of this work from our point of view is that it is an almost completely numerical technique and is much more computer-intensive than the method we have actually used. An attempt to use this technique would probably have exhausted our computation resources before we could have obtained any significant results. For this reason, we decided upon the simpler, more analytical method, wherein the "human" scatterer is modelled in a somewhat crude manner, but the amount of computer time required to determine a point is large but still reasonable.

8. SCATTERED FIELDS-COORDINATE TRANSFORMATION AT OUTPUT OF SCATTERING PROCESS

The scattered field, as produced by the Barber scattering program, is measured along the $(x_L - y_L)$ plane in the lab frame. This is illustrated in Figure 8.1. The scattering angle θ_{SL} is the polar angle of $\underset{\rightarrow}{\beta}_S$, the wave propagation vector for the scattered wave, measured in the lab frame. (Note again that $\underset{\rightarrow}{\beta}_S$ is entirely unrelated to $\underset{\rightarrow}{\beta}^{\pm}$).

The Barber scattering program yields as its output the "vertically polarized" and "horizontally polarized" components of the plane-wave field scattered in the θ_S direction. The former, denoted by $\tilde{E}_{SV}$, is the component normal to the $(x_L - z_L)$ plane, and the latter, denoted by $\tilde{E}_{SH}$, is the component parallel to the $(x_L - y_L)$ plane. From $\tilde{E}_{SV}$ and $\tilde{E}_{SH}$, we can determine the lab frame components of the scattered field. We must then find the ground frame components of the field. The procedure for accomplishing this will be described below.

From Eqs. (6.26) and (6.18a,b) applied to $\underset{\rightarrow}{\tilde{E}}_S$ in lieu of $\underset{\rightarrow}{\tilde{E}}_i$,

$$[\underset{\rightarrow}{\tilde{E}}_S^{(o)}]^T[\underset{\rightarrow}{\hat{u}}_o] = [\underset{\rightarrow}{\tilde{E}}_S^{(L)}]^T[M_{Lo}][\underset{\rightarrow}{\hat{u}}_o] \tag{8.1}$$

where

$$[\underset{\rightarrow}{\tilde{E}}_S^{(o)}] = \begin{bmatrix} \tilde{E}_{Sx} \\ \tilde{E}_{Sy} \\ \tilde{E}_{Sz} \end{bmatrix}, \quad [\underset{\rightarrow}{\tilde{E}}_S^{(L)}] = \begin{bmatrix} \tilde{E}_{Sx_L} \\ \tilde{E}_{Sy_L} \\ \tilde{E}_{Sz_L} \end{bmatrix}$$

Taking the transpose of both sides of Eq. (8.1) and noting again that $[M_{oL}]^T = [M_{Lo}]$, we obtain

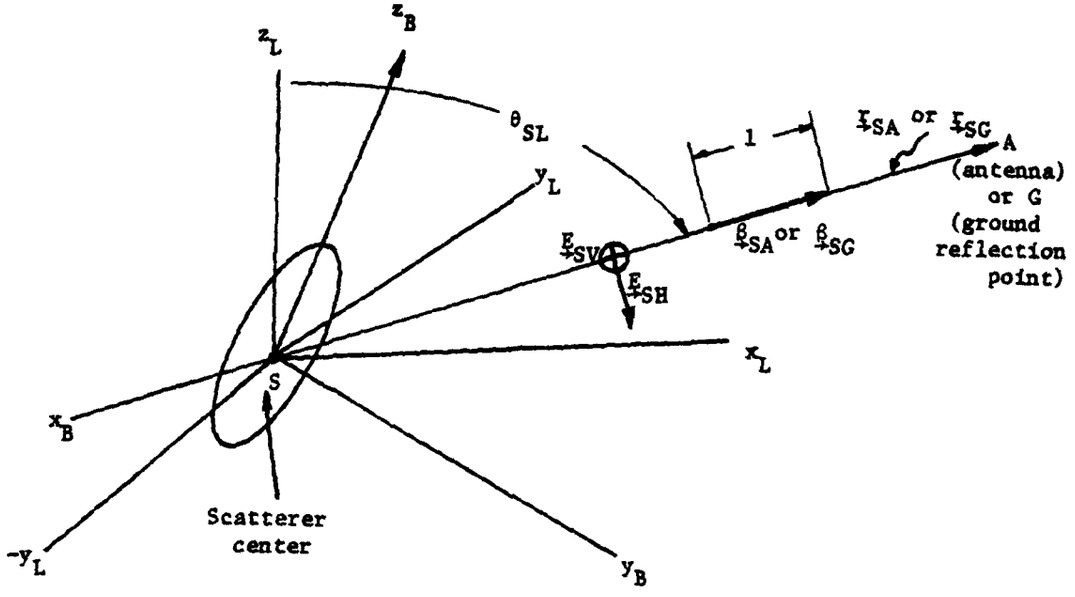

Figure 8-1. Scattered field

$$[\tilde{E}_{\underset{\rightarrow}{S}}^{(o)}] = [M_{oL}][\tilde{E}_{\underset{\rightarrow}{S}}^{(L)}] \tag{8.2}$$

In longhand [from the matrix definitions (6.17a,b)']

$$\tilde{E}_{Sx} = (\cos\theta_\beta \cos\phi_\beta \cos\phi_J - \sin\theta_\beta \sin\phi_J)\,\tilde{E}_{Sx_L}$$

$$- (\cos\theta_\beta \cos\phi_\beta \sin\phi_J + \sin\phi_\beta \cos\phi_J)\,\hat{E}_{Sy_L} + (\sin\theta_\beta \cos\phi_\beta)\,\tilde{E}_{Sz_L} \tag{8.2a)'}$$

$$\tilde{E}_{Sy} = (\cos\theta_\beta \sin\phi_\beta \cos\phi_J + \cos\phi_\beta \sin\phi_J)\,\hat{E}_{Sx_L}$$

$$- (\cos\theta_\beta \sin\phi_\beta \sin\phi_J - \cos\phi_\beta \cos\phi_J)\,\tilde{E}_{Sy_L} + (\sin\theta_\beta \sin\phi_\beta)\,\tilde{E}_{Sz_L} \tag{8.2b)'}$$

$$\tilde{E}_{Sz} = -(\sin\theta_\beta \cos\phi_J)\,\tilde{E}_{Sx_L} + (\sin\theta_\beta \sin\phi_J)\,\tilde{E}_{Sy_L} + (\cos\theta_\beta)\,\tilde{E}_{Sz_L} \tag{8.2c)'}$$

The angle θ_{SL} (see Figure 8.1) is the polar angle of the vector $\underset{\rightarrow}{\beta}_S$ as measured in the lab frame. It is evident from Figure (8.1) that

$$\tilde{E}_{Sx_L} = E_{SH} \cos\theta_{SL} \tag{8.3a}$$

$$\tilde{E}_{Sy_L} = E_{SV} \tag{8.3b}$$

$$\tilde{E}_{Sz} = -E_{SG} \sin\theta_{SL} \tag{8.3c}$$

and hence, from Eqs. (8.2a,b,c)' and (8.3a,b,c)

$$\tilde{E}_{Sx}^{(A)(G)} = [(\cos\theta_\beta \cos\phi_\beta \cos(\phi_J)_{\substack{A\\G}} - \sin\phi_\beta \sin(\phi_J)_{\substack{A\\G}}) \cos\theta_{SL}^{(A)(o)}$$

$$- (\sin\theta_\beta \cos\phi_\beta) \sin\theta_{SL}^{(A)(G)}] \tilde{E}_{SH}^{(A)(G)}$$

$$- -[\cos\theta_\beta \cos\phi_\beta \sin(\phi_J)_{\substack{A\\G}} + \sin\phi_\beta \cos(\phi_J)_{\substack{A\\G}}] \tilde{E}_{Sv}^{(A)(G)} \qquad (8.4a)$$

$$\tilde{E}_{Sy}^{(A)(G)} = [(\cos\theta_\beta \sin\phi_\beta \cos(\phi_J)_{\substack{A\\G}} + \cos\phi_\beta \sin(\phi_J)_{\substack{A\\G}}) \cos\theta_{SL}^{(A)(G)}$$

$$- (\sin\theta_\beta \sin\phi_\beta) \sin\theta_{SL}^{(A)(G)}] \tilde{E}_{SH}^{(A)(G)}$$

$$- [\cos\theta_\beta \sin\phi_\beta \sin(\phi_J)_{\substack{A\\G}} - \cos\phi_\beta \cos(\phi_J)_{\substack{A\\G}}] \tilde{E}_{Sv}^{(A)(G)} \qquad (8.4b)$$

$$\tilde{E}_{Sz}^{(A)(G)} = [-(\sin\theta_\beta \cos(\phi_J)_{\substack{A\\G}}) \cos\theta_{SL}^{(A)(G)} - (\cos\theta_\beta) \sin\theta_{SL}^{(A)(G)}] \tilde{E}_{SH}^{(A)(G)}$$

$$+ [\sin\theta_\beta \sin(\phi_J)_{\substack{A\\G}}] \tilde{E}_{Sv}^{(A)(G)} \qquad (8.4c)$$

where subscripts and superscripts (A) and (G) in Eq. (8.4a,b,c) correspond to A and G scattering processes, respectively, and where $\cos(\phi_J)_A$, $\sin(\phi_J)_A$,

cos $(\phi_J)_G$ and sin $(\phi_J)_G$ are obtained from Eqs. (6.22a,b,c and d) respectively.

Confining attention in what follows to the A scattering process, it remains to evaluate cos $\theta_{SL}^{(A)}$ and sin $\theta_{SL}^{(A)}$. Since $\underset{\rightarrow}{\beta}_{SA}$ (parallel to $\underset{\rightarrow}{r}_{SA}$) is in the $(x_L - z_L)$ plane, the lab-frame azimuthal angle $\phi_{SL} = 0$ or π. It follows from the transformation between spherical and rectangular coordinates that (since the antenna lives in the $x_L - z_L$) plane)

$$\cos \theta_{SL}^{(A)} = \frac{z_{LA}}{r_{SA}} \tag{8.5a}$$

$$\sin \theta_{SL}^{(A)} = \frac{|x_{LA}|}{r_{SA}} \tag{8.5b}$$

where

$$r_{SA} = \sqrt{(x_A - x_S)^2 + (y_A - y_S)^2 + (z_A - z_S)^2}$$

and where x_{LA}, y_{LA}, z_{LA} are the lab-frame coordinates of the antenna. (Noting that the lab frame has its origin at the scatterer center, it follows that $x_{LS} = y_{LS} = z_{LS} = 0$. Also, since the antenna is in the $(x_L - z_L)$ plane, we know that $y_{LA} = 0$.)

From Eq. (6.16a) applied at the antenna position

$$\begin{aligned} x_{LA} = {} & [\cos \theta_\beta \cos \phi_\beta \cos (\phi_J)_A - \sin \phi_\beta \sin (\phi_J)_A](x_A - x_S) \\ & + [\cos \theta_\beta \sin \phi_\beta \cos (\phi_J)_A + \cos \phi_\beta \sin (\phi_J)_A](y_A - y_S) \\ & - [\sin \theta_\beta \cos (\phi_J)_A](z_A - z_S) \end{aligned} \tag{8.6a}$$

$$y_{LA} = -[\cos\theta_\beta \cos\phi_\beta \sin(\phi_J)_A + \sin\phi_\beta \cos(\phi_J)_A](x_A - x_S)$$

$$- [\cos\theta_\beta \sin\phi_\beta \sin(\phi_J)_A - \cos\phi_\beta \cos(\phi_J)_A](y_A - y_S)$$

$$+ [\sin\theta_\beta \sin(\phi_J)_A](z_A - z_S) = 0 \qquad (8.6b)$$

$$z_{LA} = (\sin\theta_\beta \cos\phi_\beta)(x_A - x_S) + (\sin\theta_\beta \sin\phi_\beta)(y_A - y_S)$$

$$+ (\cos\theta_\beta)(z_Z - z_S) \qquad (8.6c)$$

We will now summarize the procedures required to transform the output of the Barber scattering program into the basic (x, y, z) coordinate system.

(A) The complex field components $\tilde{E}_{SH}^{(A)}$ and $\tilde{E}_{SV}^{(A)}$ are extracted from the output of the Barber program. These are respectively the "horizontally" and "vertically" polarized scattered fields in the direction of the antenna in response to the incident plane-wave with propagation vector $k_0\beta^{\pm}$. These field components are fed from the Barber program into a subprogram which we call Subroutine BOS ("Barber Output Subprogram"). The variables x_A, y_A, z_A, x_S, y_S, z_S, ϕ_β and θ_β are read into the BOS from the main program

(B) The following computations are made [introduced below Eq. (6.22d)]:

$$\rho_{SA} = \sqrt{(x_A - x_S)^2 + (y_A - y_S)^2} \qquad (8.7a)$$

$$\phi_{SA} = \tan^{-1}\left(\frac{y_A - y_S}{x_A - x_S}\right) \qquad (8.7b)$$

$$r_{SA} = \sqrt{(x_A - x_S)^2 + (y_A - y_S)^2 + (z_A - z_S)^2} \qquad (8.7c)$$

(C) Using the results of (B), $\cos(\phi_J)_A$ and $\sin(\phi_J)_A$ are computed from Eqs. (6.22a,b) (repeated and renumbered below for convenience):

$$\cos(\phi_J)_A = \frac{\rho_{SA} \cos\theta_\beta \cos(\phi_\beta - \phi_{AS}) - (z_A - z_S)\sin\theta_\beta}{\sqrt{[\rho_{SA} \cos\theta_\beta \cos(\phi_\beta - \phi_{AS}) - (z_A - z_S)\sin\theta_\beta]^2 + [\rho_{SA} \sin(\phi_\beta - \phi_{AS})]^2}} \qquad (8.8a)$$

$$\sin(\phi_J)_A = \frac{-\rho_{SA} \sin(\phi_\beta - \phi_{AS})}{\sqrt{[\rho_{SA} \cos\theta_\beta \cos(\phi_\beta - \phi_{AS}) - (z_A - z_S)\sin\theta_\beta]^2 + [\rho_{SA} \sin(\phi_\beta - \phi_{AS})]^2}} \qquad (8.8b)$$

(D) Using the results of (B) and (C), x_{LA}, y_{LA} and z_{LA} are computed from Eqs. (8.6a,b,c) (repeated and renumbered below). Note that Eq. (8.6b) is not needed in the computation, since y_{LA} is known to be zero.

$$\begin{aligned} x_{LA} = {} & [\cos\theta_\beta \cos\phi_\beta \cos(\phi_J)_A - \sin\phi_\beta \sin(\phi_J)_A](x_A - x_S) \\ & + [\cos\theta_\beta \sin\phi_\beta \cos(\phi_J)_A + \cos\phi_\beta \sin(\phi_J)_A](y_A - y_S) \\ & - [\sin\theta_\beta \cos(\phi_J)_A](z_A - z_S) \end{aligned} \qquad (8.9a)$$

$$y_{LA} = -[\cos\theta_\beta \cos\phi_\beta \sin(\phi_J)_A + \sin\phi_\beta \cos(\phi_J)_A](x_A - x_S)$$

$$- [\cos\theta_\beta \sin\phi_\beta \sin(\phi_J)_A - \cos\phi_\beta \cos(\phi_J)_A](y_A - y_S)$$

$$+ [\sin\theta_\beta \sin(\phi_J)_A](z_A - z_S) = 0 \qquad (8.9b)$$

$$z_{LA} = (\sin\theta_\beta \cos\phi_\beta)(x_A - x_S) + (\sin\theta_\beta \sin\phi_\beta)(y_A - y_S)$$

$$+ (\cos\theta_\beta)(z_A - z_S) \qquad (8.9c)$$

(E) From the results of (A), (B), (C), and (D), $\cos\theta_{SL}^{(A)}$ and $\sin\theta_{SL}^{(A)}$ are computed from Eqs. (8.5a,b) (repeated and renumbered here):

$$\cos\theta_{SL}^{(A)} = \frac{z_{LA}}{r_{SA}} \qquad (8.10a)$$

$$\sin\theta_{SL}^{(A)} = \frac{|x_{LA}|}{r_{SA}} \qquad (8.10b)$$

(F) From the results of (A), (B), (C), (D) and (E), compute $\tilde{E}_{Sx}^{(A)}$, $\tilde{E}_{Sy}^{(A)}$ and $\tilde{E}_{Sz}^{(A)}$ from Eqs. (8.4a,b,c) (repeated and renumbered here):

$$\tilde{E}_{Sx}^{(A)} = [(\cos\theta_\beta \cos\phi_\beta \cos(\phi_J)_A - \sin\phi_\beta \sin(\phi_J)_A) \cos\theta_{SL}^{(A)}$$

$$- (\sin\theta_\beta \cos\phi_\beta) \sin\theta_{SL}^{(A)}] \tilde{E}_{SH}^{(A)}$$

$$- [\cos\theta_\beta \cos\phi_\beta \sin(\phi_J)_A + \sin\phi_\beta \cos(\phi_J)_A] \tilde{E}_{Sv}^{(A)} \qquad (8.11a)$$

$$\tilde{E}_{Sy}^{(A)} = [(\cos\theta_\beta \sin\phi_\beta \cos(\phi_J)_A + \cos\phi_\beta \sin(\phi_J)_A) \cos\theta_{SL}^{(A)}$$

$$- (\sin\theta_\beta \sin\phi_\beta) \sin\theta_{SL}^{(A)}{}_{(G)}] \tilde{E}_{SH}^{(A)}$$

$$- [\cos\theta_\beta \sin\phi_\beta \sin(\phi_J)_A - \cos\phi_\beta \cos(\phi_J)_A] \tilde{E}_{Sv}^{(A)} \qquad (8.11b)$$

$$\tilde{E}_{Sz}^{(A)} = [-(\sin\theta_\beta \cos(\phi_J)_{A\atop G}) \cos\theta_{SL}^{(A)} - (\cos\theta_\beta) \sin\theta_{SL}^{(A)}] \tilde{E}_{SH}^{(A)}$$

$$+ [\sin\theta_\beta \sin(\phi_J)_A] \tilde{E}_{Sv}^{(A)} \qquad (8.11c)$$

(G) Return the results of (F) to the main program.

9. EFFECT OF GROUND REFLECTIONS ON THE SCATTERED FIELD

In this section, we will evaluate the effect of ground reflections on the scattered field at the antenna. We will also discuss the procedures for implementing these calculations on the computer.

The calculations to be performed to obtain this term in the total field can be divided into two phases, as follows:

Phase 1: Calculation of the field of the plane-wave scattered from the body toward the ground reflection point G.

Phase 2: Calculation of the plane-wave reflected from G and propagating toward the antenna A.

Phase 1 of these procedures begins with Eqs. (8.4a,b,c) with superscripts and subscripts G rather than A. This step is followed by the equivalent of Eqs. (8.5a,b) with G substituted for A, i.e.,

$$\cos \theta_{SL}^{(G)} = \frac{z_{LG}}{r_{SG}} \tag{9.1a}$$

$$\sin \theta_{SL}^{(G)} = \frac{|x_{LG}|}{r_{SG}} \tag{9.1b}$$

We note that, in this case

$$r_{SG} = \sqrt{(x_G - x_S)^2 + (y_G - y_S)^2 + (z_G - z_S)^2} \tag{9.2}$$

and [from Eqs. (6.20e,f,g)]

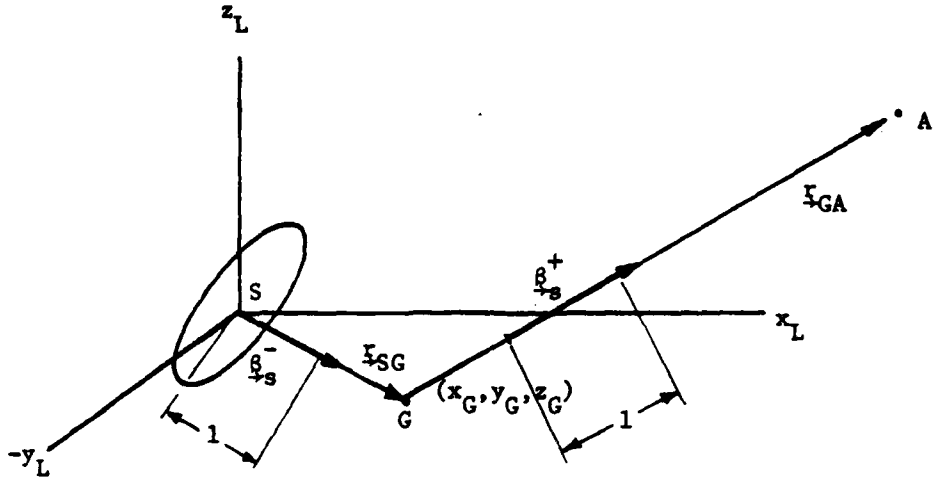

S = Scatterer center

G = Ground reflection point

A = Antenna

Figure 9-1. Ground-reflected Scattered Field

$$x_G - x_S = \frac{z_S}{z_S + z_A}(x_A - x_S) \qquad (9.2a)'$$

$$y_G - y_S = \frac{z_S}{z_S + z_A}(y_A - y_S) \qquad (9.2b)'$$

$$z_G - z_S = -z_S \qquad (9.2c)'$$

From Eqs. (9.2a,b,c)'

$$r_{SG} = \left(\frac{z_S}{z_S + z_A}\right)\sqrt{(x_A - x_S)^2 + (y_A - y_S)^2 + (z_A + z_S)^2} \qquad (9.3)$$

It will be recognized that r_{SG} as given by Eq. (9.3) is, except for the factor $z_S/(z_S + z_A)$, the distance from the "image" of the scatterer center, located at $(x_S, y_S, -z_S)$, to the antenna. The factor $z_S/(z_S + z_A)$ implies, as supported by our intuition, that if $z_S = z_A$, then r_{SG} is one-half of the image-to-antenna separation distance. If $z_S >> z_A$, then r_{SG} is the image-to-antenna separation distance, and if $z_S << z_A$, then r_{SG} is the separation distance multiplied by the ratio of scatterer center height to antenna height.

The lab frame coordinates of the ground-reflection point G, (x_{LG}, y_{LG}, z_{LG}), are calculated from equations analogous to Eqs. (8.6a,b,c), where $(\phi_J)_G$ replaces $(\phi_J)_A$ and coordinates (x_G, y_G, z_G) replace (x_A, y_A, z_A).

We will now summarize the steps required to implement these calculations on the computer. The steps A through G below are analogous to signs A through G in Section 8.

A. The complex field components $\tilde{E}_{SH}^{(G)}$ and $\tilde{E}_{SV}^{(G)}$ are extracted from the output of the Barber program. These components are analogous to $\tilde{E}_{SH}^{(A)}$

and $\tilde{E}_{SV}^{(A)}$, where the scattering process G (scatterer to ground reflection point) replaces the process A (scatterer to antenna). These components are fed from the Barber program into subroutine BOS (see Step A in the summary in Section 8). It was indicated in Section 8 that variables x_A, y_A, z_A, x_S, y_S, z_S, ϕ_β and θ_β are read into BOS form the main program. Also ν, the complex refractive index of the ground, is read into BOS from the main program.

B. The following computations are made: [analogous to Eqs. (8.7a,b,c) where x_G, y_G, z_G replace x_A, y_A, z_A], [with the aid of Eqs. (9.2a,b,c)']

$$\rho_{SG} = \sqrt{(x_G - x_S)^2 + (y_G - y_S)^2} = \left(\frac{z_S}{z_S + z_A} \right) \rho_{SA} \qquad (9.4a)$$

$$\phi_{SG} = \tan^{-1} \left(\frac{y_G - y_S}{x_G - x_S} \right) = \phi_{SA} \qquad (9.4b)$$

[Eq. (9.3) repeated and renumbered]

$$r_{SG} = \left(\frac{z_S}{z_S + z_A} \right) \sqrt{(x_A - x_S)^2 + (y_A - y_S)^2 + (z_A + z_S)^2} \qquad (9.4c)$$

C. Using the results of B, $\cos (\phi_J)_G$ and $\sin (\phi_J)_G$ are computed from Eqs. (6.22c,d) (repeated and renumbered below):

$$\cos (\phi_J)_G = \frac{\rho_{SG} \cos \theta_\beta \cos (\phi_\beta - \phi_{GS}) + z_S \sin \theta_\beta}{\sqrt{[\rho_{SG} \cos \theta_\beta \cos (\phi_\beta - \phi_{GS}) + z_S \sin \theta_\beta]^2 + [\rho_{SG} \sin (\phi_\beta - \phi_{GS})]^2}} \qquad (9.5a)$$

$$\sin (\phi_J)_G = \frac{-\rho_{SG} \sin (\phi_\beta - \phi_{GS})}{\sqrt{[\rho_{SG} \cos \theta_\beta \cos (\phi_\beta - \phi_{GS}) + z_S \sin \theta_\beta]^2 + [\rho_{SG} \sin (\phi_\beta - \phi_{GS})]^2}} \tag{9.5b}$$

where

$$\rho_{SG} = \sqrt{(x_G - x_S)^2 + (y_G - y_S)^2}$$

$$\phi_{SG} = \tan^{-1} \left(\frac{y_G - y_S}{x_G - x_S} \right) = \tan^{-1} \left(\frac{y_A - y_S}{x_A - x_S} \right)$$

D. Using the results of B and C, x_{LG}, y_{LG} and z_{LG} are computed from equations equivalent to Eqs. (8.6a,b,c) where x_G, y_G, z_G and $(\phi_J)_G$ replace x_A, y_A, z_A and $(\phi_J)_A$, respectively (As is the case with the antenna, the ground-reflection point G is in the $(x_L - z_L)$ plane; hence, we know that $y_{LG} = 0$ and we don't need Eq. (9.6b) in the computations).

$$\begin{aligned} x_{LG} = {} & [\cos \theta_\beta \cos \phi_\beta \cos (\phi_J)_G - \sin \phi_\beta \sin (\phi_J)_G](x_G - x_S) \\ & + [\cos \theta_\beta \sin \phi_\beta \cos (\phi_J)_G + \cos \phi_\beta \sin (\phi_J)_G](y_G - y_S) \\ & + [\sin \theta_\beta \cos (\phi_J)_G] z_S \end{aligned} \tag{9.6a}$$

$$\begin{aligned} y_{LG} = {} & -[\cos \theta_\beta \cos \phi_\beta \sin (\phi_J)_G + \sin \phi_\beta \cos (\phi_J)_G](x_G - x_S) \\ & - [\cos \theta_\beta \sin \phi_\beta \sin (\phi_J)_G - \cos \phi_\beta \cos (\phi_J)_G](y_G - y_S) \end{aligned}$$

$$- [\sin \theta_\beta \sin (\phi_J)_G] z_S = 0 \qquad (9.6b)$$

$$z_{LG} = (\sin \theta_\beta \cos \phi_\beta)(x_G - x_S) + (\sin \theta_\beta \sin \phi_\beta)(y_G - y_S)$$

$$- (\cos \theta_\beta) z_S \qquad (9.6c)$$

E. From the results of A, B, C, and D, $\cos \theta_{SL}^{(G)}$ and $\theta_{SL}^{(G)}$ are computed from Eqs. (9.1a,b) (repeated and renumbered below):

$$\cos \theta_{SL}^{(G)} = \frac{z_{LG}}{r_{SG}} \qquad (9.7a)$$

$$\sin \theta_{SL}^{(G)} = \frac{|x_{LG}|}{r_{SG}} \qquad (9.7b)$$

F. From the results of A, B, C, D, and E, compute $\tilde{E}_{Sx}^{(G)}$, $\tilde{E}_{Sy}^{(G)}$, and $\tilde{E}_{Sz}^{(G)}$ from Eqs. (8.4a,b,c) (repeated and renumbered below):

$$\tilde{E}_{Sx}^{(G)} = [(\cos \theta_\beta \cos \phi_\beta \cos (\phi_J)_G - \sin \phi_\beta \sin (\phi_J)_G) \cos \theta_{SL}^{(G)}$$

$$- (\sin \theta_\beta \cos \phi_\beta) \sin \theta_{SL}^{(G)}] \tilde{E}_{SH}^{(G)}$$

$$- [\cos \theta_\beta \cos \phi_\beta \sin (\phi_J)_G + \sin \phi_\beta \cos (\phi_J)_G] \tilde{E}_{SV}^{(G)} \qquad (9.8a)$$

$$\tilde{E}_{Sy}^{(G)} = [(\cos \theta_\beta \sin \phi_\beta \cos (\phi_J)_G + \cos \phi_\beta \sin (\phi_J)_G) \cos \theta_{SL}^{(G)}$$

$$- (\sin \theta_\beta \sin \phi_\beta) \sin \theta_{SL}^{(G)}] \tilde{E}_{SH}^{(G)}$$

$$- [\cos\theta_\beta \sin\phi_\beta \sin(\phi_J)_G - \cos\phi_\beta \cos(\phi_J)_G]\, \tilde{E}_{SV}^{(G)} \qquad (9.8b)$$

$$\tilde{E}_{Sz}^{(G)} = [-(\sin\theta_\beta \cos(\phi_J)_G) \cos\theta_{SL}^{(G)} - (\cos\theta_\beta) \sin\theta_{SL}^{(G)}]\, \tilde{E}_{SH}^{(G)}$$

$$+ [\sin\theta_\beta \sin(\phi_J)_G]\, \tilde{E}_{SV}^{(G)} \qquad (9.8c)$$

G. Return the results of F to the main program, in which the remaining part of the computation, Phase 2, is performed.

*****

To continue with Phase 2, we must calculate the fields of the ground-reflected plane-wave due to the scattering process. To this end, we invoke equations analogous to Eqs. (5.18a) and (5.19), but in a different context.

Equations (5.18a) and (5.19) contain the (x, y, z) components of the vectors $\underset{\rightarrow}{\beta}^+$ and $\underset{\rightarrow}{\beta}^-$. The analog of $\underset{\rightarrow}{\beta}^-$ in the present development is a vector $\underset{\rightarrow}{\beta}_S$, which we will rename $\underset{\rightarrow}{\beta}_S^-$, and which is the unit vector parallel to a vector originating at the scatterer center and terminating at the ground-reflection point G. The analog of $\underset{\rightarrow}{\beta}^+$, which will be called $\underset{\rightarrow}{\beta}_S^+$, is the unit vector parallel to a vector originating at G and terminating at the antenna A. It is easily deduced from these definitions that (where vectors $\underset{\rightarrow}{r}_{SG}$ and $\underset{\rightarrow}{r}_{GA}$) $\underset{\rightarrow}{\beta}_S^-$ and $\underset{\rightarrow}{\beta}_S^+$ are illustrated in Figure 9.1.

$$\underset{\rightarrow}{\beta}_S^- = \hat{\underset{\rightarrow}{x}}\, \beta_{Sx}^- + \hat{\underset{\rightarrow}{y}}\, \beta_{Sy}^- + \hat{\underset{\rightarrow}{z}}\, \beta_{Sz}^- = \frac{\underset{\rightarrow}{r}_{SG}}{r_{SG}} = \frac{\hat{\underset{\rightarrow}{x}}(x_G - x_S) + \hat{\underset{\rightarrow}{y}}(y_G - y_S) - \hat{\underset{\rightarrow}{z}}(z_S)}{\sqrt{(x_G - x_S)^2 + (y_G - y_S)^2 + z_S^2}} \qquad (9.9a)$$

and

$$\underset{\rightarrow}{\beta}_S^+ = \hat{\underset{\rightarrow}{x}}\,\beta_{Sx}^+ + \hat{\underset{\rightarrow}{y}}\,\beta_{Sy}^+ + \hat{\underset{\rightarrow}{z}}\,\beta_{Sz}^+ = \frac{\underset{\rightarrow}{r}_{GA}}{r_{GA}} = \frac{\hat{\underset{\rightarrow}{x}}(x_A - x_G) + \hat{\underset{\rightarrow}{y}}(y_A - y_G) + \hat{\underset{\rightarrow}{z}}(z_A)}{\sqrt{(x_A - x_G)^2 + (y_A - y_G)^2 + z_A^2}} \tag{9.9b}$$

We invoke Eqs. (9.2a,b,c)' and (9.4c), and recognize that [using Eq. (6.20e,f)], similar relationships can be derived for $x_A - x_G$ and $y_A - y_G$

$$x_A - x_G = \frac{z_A}{z_A + z_S}(x_A - x_S) \tag{9.10a}$$

$$y_A - y_G = \frac{z_A}{z_A + z_S}(y_A - y_S) \tag{9.10b}$$

$$r_{GA} = \frac{z_A}{z_A + z_S}\sqrt{(x_A - x_S)^2 + (y_A - y_S)^2 + (z_A + z_S)^2} \tag{9.10c}$$

We now invoke the analog of Eq. (5.18a) in a form suitable for the present discussion:

$$\left[\tilde{\underset{\rightarrow}{E}}_S^{(GA)}\right] = \begin{bmatrix}\tilde{E}_{Sx}^{(GA)}\\ \tilde{E}_{Sy}^{(GA)}\\ \tilde{E}_{Sz}^{(GA)}\end{bmatrix} = \begin{bmatrix}R_{E11}^{(GA)} & R_{E12}^{(GA)} & R_{E13}^{(GA)}\\ R_{E21}^{(GA)} & R_{E22}^{(GA)} & R_{E23}^{(GA)}\\ R_{E31}^{(GA)} & R_{E32}^{(GA)} & R_{E33}^{(GA)}\end{bmatrix}\begin{bmatrix}\tilde{E}_{Sx}^{(G)}\\ \tilde{E}_{Sy}^{(G)}\\ \tilde{E}_{Sz}^{(G)}\end{bmatrix} = \left[R_E^{(GA)}\right]\left[\tilde{\underset{\rightarrow}{E}}_S^{(G)}\right] \tag{9.11}$$

where the elements of $[\tilde{\underset{\rightarrow}{E}}_S^{(G)}]$ (whose propagation vector is $k_o\,\underset{\rightarrow}{\beta}_S^-$) are given by Eqs. (9.8a,b,c), where $[\tilde{\underset{\rightarrow}{E}}_S^{(GA)}]$ (whose propagation vector is $k_o\,\underset{\rightarrow}{\beta}_S^+$) is the field of the plane-wave due to the scattering process propagating toward the antenna after ground-reflection and where the elements of $[R_E^{(GA)}]$ are the same as those in Eq. (5.19) except that β_x, β_y, β_z, β_h and γ_z are replaced by β_{Sx}, β_{Sy}, β_{Sz},

β_{Sh} and γ_{Sz}, respectively.

We can now return to the summary of steps in programming of the calculations. The steps in implementation of Phase 2, continuing after Step G, are as follows:

H. Compute the following variables which will be needed in subsequent computations [from Eqs. (9.9a,b) and (9.10a,b,c)]

$$r_{GA} = \frac{z_A}{z_A + z_S}\sqrt{(x_A - x_S)^2 + (y_A - y_S)^2 + (z_A + z_S)^2} \qquad (9.12a)$$

$$\beta_{Sx}^{-} = \left(\frac{z_S}{z_S + z_A}\right)\frac{(x_A - x_S)}{r_{SG}} \qquad (9.12b)$$

$$\beta_{Sy}^{-} = \left(\frac{z_S}{z_S + z_A}\right)\frac{(y_A - y_S)}{r_{SG}} \qquad (9.12c)$$

$$\beta_{Sh}^{-} = \sqrt{(\beta_{Sx}^{-})^2 + (\beta_{Sy}^{-})^2} \qquad (9.12d)$$

$$\beta_{Sz}^{-} = \frac{-z_S}{r_{SG}} = -\sqrt{1 - (\beta_{Sh}^{-})^2} \qquad (9.12e)$$

$$\beta_{Sx}^{+} = \left(\frac{z_A}{z_S + z_A}\right)\frac{(x_A - x_S)}{r_{GA}} \qquad (9.12f)$$

$$\beta_{Sy}^{+} = \left(\frac{z_A}{z_S + z_A}\right)\frac{(y_A - y_S)}{r_{GA}} \qquad (9.12g)$$

$$\beta_{Sh}^{+} = \sqrt{(\beta_{Sx}^{+})^2 + (\beta_{Sy}^{+})^2} \tag{9.12h}$$

$$\beta_{Sz}^{+} = \frac{z_A}{r_{GA}} = + \sqrt{1 - (\beta_{Sh}^{+})^2} \tag{9.12i}$$

$$\gamma_{Sz}^{-} = \sqrt{\nu^2 - (\beta_{Sh}^{-})^2} \tag{9.12j}$$

$$\gamma_{Sz}^{+} = \sqrt{\nu^2 - (\beta_{Sh}^{+})^2} \tag{9.12k}$$

I. Using the computations of $\tilde{E}_{Sx}^{(G)}$, $\tilde{E}_{Sy}^{(G)}$, and $\tilde{E}_{Sz}^{(G)}$ performed in F and the variables computed in H as inputs to this step, compute $[\tilde{\underset{\rightarrow}{E}}_{S}^{(GA)}]$ through the matrix equation in Eq. (9.11) (repeated and renumbered)

$$[\tilde{\underset{\rightarrow}{E}}_{S}^{(GA)}] = [R_E^{(GA)}][\tilde{\underset{\rightarrow}{E}}_{S}^{(G)}] \tag{9.13}$$

where

$$R_{EJK}^{(GA)} = C_o(\beta_{Sx}, \beta_{Sy})\, \hat{R}_{EJK}^{(GA)}$$

$$C_o(\beta_{Sx}, \beta_{Sy}) = \left(\frac{\gamma_{Sz}^{+} - |\beta_z^{+}|}{\gamma_{Sz}^{+} + |\beta_z^{+}|} \right) \frac{1}{[(\beta_{Sh}^{+})^2 + |\beta_{Sz}^{+}|\, \gamma_{Sz}^{+}]}$$

$$\hat{R}_{E11}^{(GA)} = (\beta_{Sx}^{+})^2 - (\beta_{Sy}^{+})^2 - |\beta_{Sz}^{+}|\, \gamma_{Sz}^{+}$$

$$\hat{R}_{E12}^{(GA)} = \hat{R}_{E21}^{(GA)} = 2\beta_{Sx}^{+}\ \beta_{Sy}^{+}$$

$$\hat{R}_{E22}^{(GA)} = (\beta_{Sy}^{+})^2 - (\beta_{Sx}^{+})^2 - |\beta_{Sz}^{+}|\ \gamma_{Sz}^{+}$$

$$\hat{R}_{E33}^{(GA)} = (\beta_{Sh}^{+})^2 - |\beta_{Zs}^{+}|\ \gamma_{Sz}^{+}$$

$$\hat{R}_{E13}^{(GA)} = \hat{R}_{E23}^{(GA)} = \hat{R}_{E31}^{(GA)} = \hat{R}_{E32}^{(GA)} = 0$$

10. TOTAL SPECTRAL FIELD AT THE OBSERVATION POINT AND ITS INVERSE FOURIER TRANSFORM

The plane-wave spectrum of the x, y, and z components of the total electric field at the observation point (receiving antenna position) is the end result of the calculations described in the previous sections.

Referring back to Section 2, the plane-wave spectrum of the electric field is the superposition of those of four fields, as follows:

(1) The contribution from the cable slots as if the cable were in free space (the sum of the fields from all the slots, neglecting the effect of the ground). The individual slot fields are denoted by $\tilde{\underset{\rightarrow}{E}}^{(a)}_{\ell}(\underset{\rightarrow}{\beta}_h)$ in Section 2. The calculation of these fields is described in Section 4.

(2) The contribution resulting from ground reflection of the plane-wave spectrum of the field resulting from excitation of the slots, which is denoted by $\tilde{\underset{\rightarrow}{E}}^{(b)}_{\ell}(\underset{\rightarrow}{\beta}_h)$ in Section 2 and whose calculation is described in Section 2.

(3) The contribution due to scattering from the target directly toward the antenna of the superposition of direct and ground-reflected plane-wave fields [i.e., $\tilde{\underset{\rightarrow}{E}}^{(a)}(\underset{\rightarrow}{\beta}_h) + \tilde{\underset{\rightarrow}{E}}^{(b)}(\underset{\rightarrow}{\beta}_h)$], which is denoted by $\tilde{\underset{\rightarrow}{E}}^{(c)}(\underset{\rightarrow}{\beta}_h)$ in Section 2 and whose calculation is described in Sections 6, 7, and 8.

(4) The contribution due to ground reflection of the scattered field, which is denoted by $\tilde{\underset{\rightarrow}{E}}^{(d)}(\underset{\rightarrow}{\beta}_h)$ in Section 2 and whose calculation is is described in Section 9.

The final step in the analysis is a two-dimensional Fourier transformation which transforms the spectral field components, which are functions of $\underset{\rightarrow}{\beta}_h$, into

actual field components which are functions of position.

In what follows we will consider this problem in a generic sense. Consider a spectral field component denoted by $\tilde{E}(\underset{\rightarrow}{\beta}_h)$. We would like to perform a double Fourier transform to convert this into a field component $E(\underset{\rightarrow}{r})$, where $\underset{\rightarrow}{r} = (x,y,z)$ = arbitrary point in space.

The transformation equation is (see Appendix III)

$$E(\underset{\rightarrow}{r}) = \left(\frac{j\,k_o}{2\pi}\right)^2 \iint_{-\infty}^{\infty} d^2\,\underset{\rightarrow}{\beta}_h\, e^{jk_o \underset{\rightarrow}{\beta}\cdot\underset{\rightarrow}{r}}\, \tilde{E}(\underset{\rightarrow}{\beta}_h) \tag{10.1}$$

We now convert both $\underset{\rightarrow}{r}$ and $\underset{\rightarrow}{\beta}$ to polar coordinates, i.e.,

$$\underset{\rightarrow}{r} = \rho(\hat{\underset{\rightarrow}{x}} \cos\phi + \hat{\underset{\rightarrow}{y}} \sin\phi) + \hat{\underset{\rightarrow}{z}} z \tag{10.2}$$

where

$$\rho = \sqrt{x^2 + y^2}\,, \quad \phi = \tan^{-1}\left(\frac{y}{x}\right)$$

Also:

$$\underset{\rightarrow}{\beta} = \beta_h(\hat{\underset{\rightarrow}{x}} \cos\phi_\beta + \hat{\underset{\rightarrow}{y}} \sin\phi_\beta) + \hat{\underset{\rightarrow}{z}}\,\beta_z \tag{10.3}$$

where

$$\beta_h = \sqrt{\beta_x^2 + \beta_y^2}\,; \quad \phi = \tan^{-1}\left(\frac{\beta_y}{\beta_x}\right);\ \beta_z = \pm|\beta_z|,\ |\beta_z| = \sqrt{1 - \beta_h^2}$$

We express $\tilde{E}(\underset{\rightarrow}{\beta}_h)$ as a function of ϕ_β and β_h, i.e., we rename the function arguments as follows:

$$\tilde{E}(\underset{\rightarrow}{\beta}_h) = \tilde{E}(\beta_h, \phi_\beta) \tag{10.4}$$

From Eqs. (10.1), (10.2), (10.3), and (10.4), we can write

$$E(\underset{\rightarrow}{r}) = \left(\frac{j\, k_o}{2\pi} \right)^2 \int_0^1 d\, \beta_h\, \beta_h \int_0^{2\pi} d\, \phi_\beta\, \tilde{E}(\beta_h, \phi_\beta) \text{ -----}$$

$$\text{--- } e^{jk_o \rho \beta_h \cos(\phi_\beta - \phi)} \cdot e^{jk_o z\sqrt{1-\beta_h^2}} \tag{10.5}$$

which reflects the fact that $\beta_h \leq 1$.

We could now invoke the well-known Bessel function relationship

$$e^{jx\sin\theta} = \sum_{n=-8}^{\infty} J_n(x)\, e^{jn\theta} \tag{10.6}$$

which, when applied to Eq. (10.5), would result in the expression

$$E(\underset{\rightarrow}{r}) = \left(\frac{j\, k_o}{2\pi} \right)^2 \sum_{n=-8}^{\infty} e^{-j[n\phi - (\pi/2)]} \int_0^1 d\, \beta_h\, \beta_h\, J_n(k_o\, \rho\, \beta_h) \text{ -----}$$

$$- \int_0^{2\pi} d\, \phi_\beta\, \tilde{E}(\beta_h, \phi_\beta)\, e^{jk_o z\sqrt{1-\beta_h^2}}\, e^{jn\phi_\beta} \tag{10.7}$$

Equation (10.7) is perfectly satisfactory from an analytical viewpoint, but preliminary investigation shows that it would be prohibitively time-consuming to implement on the computer. As an alternative technique, we write the ϕ_β integral as:

$$I_{\phi_\beta} = \int_0^{2\pi} d\,\phi'_\beta\, F(\beta_h,\, \phi'_\beta + \phi)\, e^{jk_o\rho\beta_h\cos\phi'_\beta} \tag{10.8}$$

where $\phi'_\beta = \phi_\beta - \phi$

Recognizing that the function

$$F(\phi'_\beta;\, \rho,\, \phi,\, \beta_h) = \tilde{E}(\beta_h,\, \phi'_\beta + \phi)\, e^{jk_o\rho\beta_h\cos\phi'_\beta} \tag{10.9}$$

can be expanded in an exponential Fourier series in ϕ'_β, we write

$$F(\phi'_\beta;\, \rho,\, \phi,\, \beta_h) = \sum_{n=-\infty}^{\infty} c_n(\rho,\, \phi;\, \beta_h)\, e^{jn\phi'_\beta} \tag{10.10}$$

It follows from Eqs. (10.8), (10.9), and (10.10) that

$$I_{\phi_\beta} = \sum_{n=-\infty}^{\infty} c_n(\rho,\, \phi;\, \beta_h) \int_0^{2\pi} d\,\phi'_\beta\, e^{jn\phi'_\beta} = 2\pi\, c_o(\rho,\, \phi;\, \beta_h) \tag{10.11}$$

where we note that

$$c_o(\rho,\, \phi;\, \beta_h) = \frac{1}{2\pi} \int_0^{2\pi} d\,\phi'_\beta\, \tilde{E}(\beta_h,\, \phi'_\beta + \phi)\, e^{jk_o\rho\beta_h\cos\phi'_\beta} \tag{10.12}$$

It follows in turn from Eq. (10.11) that Eq. (10.5) can be expressed in the form

$$\vec{E}(r) = \frac{(j\,k_o)^2}{2\pi} \int_0^1 d\,\beta_h\, \beta_h\, e^{jk_o z\sqrt{1-\beta_h^2}}\, c_o(\rho,\, \phi;\, \beta_h) \tag{10.13}$$

The evaluation of $c_o(\rho,\, \phi;\, \beta_h)$ through Eq. (10.12) and the subsequent

evaluation of $E(\underset{\rightarrow}{r})$ through Eq. (10.13) are accomplished numerically. Unfortunately, for high accuracy these computations require a very large amount of computer time, particularly that of Eq. (10.12).

In the inverse Fourier transformation of the spectral fields $[\tilde{\underset{\rightarrow}{E}}^{(a)}(\underset{\rightarrow}{\beta}_h) + \tilde{\underset{\rightarrow}{E}}^{(b)}(\underset{\rightarrow}{\beta}_h)]$ of Section 2, i.e., those that exist in the absence of the scatterer, the point in space at which the fields are to be evaluated is the antenna location. In the coordinate system used in our problem, the antenna (coordinates x_A, y_A, z_A, such that $\rho = \rho_A = \sqrt{x_A^2 + y_A^2}$, $z = z_A$) is located near the point $x = 0$, $y = 0$. For that reason, the exponent in $e^{jk_o\beta_h\rho\cos(\phi_\beta - \phi)}$ is not necessarily large in those calculations. In fact, it is zero if the antenna is placed exactly at the origin. Even if it were assumed that the factor $\tilde{E}(\beta_h, \phi_\beta' + \phi)$ on the RHS of Eq. (10.9) is "slowly varying" in the angle ϕ_β' (which would seem to be a justifiable assumption because of the near-symmetry of the circular cable ("near" because of the cable attenuation; without that attenuation the same amount of energy would be leaking out of all the slots in the cable. The attenuation around the cable is sufficiently small so that the distribution of energy from different slots is quite close to uniform) the stationary phase method or some variation thereof would not be easy to justify. Hence, the full numerical integration technique is used in the evaluation of the field components in the absence of the scatterer.

In the case of the superposition of the direct scattered field and the ground-reflected scattered field, $[(\tilde{\underset{\rightarrow}{E}}^{(c)}(\underset{\rightarrow}{\beta}_h) + \tilde{\underset{\rightarrow}{E}}^{(d)}(\underset{\rightarrow}{\beta}_h)]$ in Section 2, the Fourier transformation is taken at the center of the scatterer, which is located near the cable. Hence, in this case

$$\rho = \rho_s = \sqrt{x_s^2 + y_s^2} \simeq R + \delta R \quad , \quad \text{where } |\delta R| << R \qquad (10.14)$$

The factor $(k_o \rho_s \beta_h)$ in the exponent in Eq. (10.12) is large enough to justify a stationary phase approximation provided β_h is at least as large as 0.01 and provided we can assume that $\tilde{E}(\beta_h, \phi'_\beta + \phi)$ is "slowly varying" in ϕ'_β. There is marginal justification for this assumption in this case, since the scattered field may be significantly variable with ϕ'_β. However, it is still likely that it does not vary in a highly oscillatory fashion with ϕ'_β and that the factor multiplying $e^{jk_o\rho_s\beta_h\cos\phi'_\beta}$ is still "slowly varying" compared with that exponential factor. Hence, the stationary phase method, based on the assumption that the integrand consists of a slowly varying factor and a highly oscillatory exponential factor will be invoked to approximate the ϕ'_β integral. The major contribution, in this case, comes from the stationary phase points.

Because of time and financial limitations in the execution of this project, it is not possible to carry out an extensive study to determine the validity of the stationary phase approximation for this problem. Further studies might dictate a full-scale numerical integration over ϕ'_β, which was originally planned. Such an integration is feasible, but preliminary studies indicate that it would require a very large expenditure of computer time to accomplish. Estimates indicate that this would exceed the project's resources, both temporal and financial. As a compromise, one might consider a numerical integration over a small range of angles near $\phi'_\beta = 0$ and π (which are the stationary phase points) which seem intuitively to be the directions in which most of the incident wave's energy would propagate. Even this approach would be much more computer-time intensive than stationary phase.

Originally, we considered a FFT algorithm. After a careful perusal of the problem, it was decided that this would not be much help because its primary utility is in reducing the number of computation points from N^2 to N log N in computations of the discrete Fourier transform at N points. In the present

computation, the Fourier transform is evaluated at only one point (the scatterer center position). A two-dimensional Fourier transformation on β_x and β_y is performed at that point, but because $\beta_h = \sqrt{\beta_x^2 + \beta_y^2}$ is between 0 and 1, the polar coordinate form (rather than the rectangular coordinate form) is the natural one, and when cast in this form, the problem reduces essentially to a single Fourier transform-type integral, that over the angle ϕ_β, and a subsequent integration over β_h. The latter is not necessarily a Fourier transform-type integration, because z_s is so small and might even vanish, in which case this last step reduces to an ordinary integration problem which has nothing whatsoever to do with Fourier transformation.

The stationary phase technique in this case involves the differentiation of the phase $k_o \rho \beta_h \cos \phi'_\beta$ in Eq. (10.12) with respect to ϕ'_β and the setting of this derivative to zero in order to find the stationary phase points.

$$\frac{\partial}{\partial \phi_\beta} (\cos \phi'_\beta) = -\sin \phi'_\beta = 0 \quad , \quad \phi'_\beta = 0 \text{ or } \pi \tag{10.15}$$

For ϕ'_β near zero and $\beta_h \neq 0$

$$e^{jk_o \rho \beta_h \cos \phi'_\beta} \simeq e^{jk_o \rho \beta_h \{1 - [(\phi'_\beta)/2]^2\}} \tag{10.16a}$$

For ϕ'_β near π and $\beta_h \neq 0$

$$(\phi'_\beta = \pi + \Delta\phi'_\beta, \ |\Delta\phi'_\beta| << \pi)$$

$$e^{jk_o \rho \beta_h \cos \phi'_\beta} \simeq e^{-jk_o \rho \beta_h \{1 - [(\Delta\phi'_\beta)/2]^2\}} \tag{10.16b}$$

From Eqs. (10.16a,b) and (10.12),

$$c_o(\rho, \phi, \beta_h) \simeq \frac{1}{2\pi} \tilde{E}(\beta_h, \phi)\, e^{jk_o\rho\beta_h} \int_{-\infty}^{\infty} d\,\phi'_\beta\, e^{-jk_o\rho\beta_h(\phi'_\beta/2)^2}$$

$$+ \frac{1}{2\pi} \tilde{E}(\beta_h, \pi + \phi)\, e^{-jk_o\rho\beta_h} \int_{-\infty}^{\infty} d(\Delta\phi'_\beta)\, e^{jk_o\rho\beta_h(\Delta\phi'_\beta/2)^2}$$

$$= \sqrt{\frac{2}{k_o\,\rho\,\beta_h}}\, \frac{1}{2\pi} \{\tilde{E}(\beta_h, \phi)\, e^{jk_o\rho\beta_h} \int_{-\infty}^{\infty} dx\, e^{-jx^2}$$

$$+ \tilde{E}(\beta_h, \pi + \phi)\, e^{-jk_o\rho\beta_h} \int_{-\infty}^{\infty} dx\, e^{jx^2}\} \qquad (10.17)$$

But

$$\int_{-\infty}^{\infty} dx\, e^{\mp jx^2} = 2\{\int_0^{\infty} dx\, \cos(x^2) \mp \int_0^{\infty} dx\, \sin(x^2)\} = \sqrt{\frac{\pi}{2}}\,(1 \mp j)$$

$$= \sqrt{\pi}\, e^{\mp j\frac{\pi}{4}} \qquad (10.18)$$

Substitution of Eq. (10.18) into Eq. (10.17) results in

$$c_o(\rho, \phi; \beta_h) \simeq \frac{1}{\sqrt{2\pi\, k_o\, \rho\, \beta_h}} \{\tilde{E}(\beta_h, \phi)\, e^{j(k_o\rho\beta_h - \frac{\pi}{4})}$$

$$+ \tilde{E}(\beta_h, \pi + \phi)\, e^{-j(k_o\rho\beta_h - \frac{\pi}{4})}\} \text{ if } \beta_h \neq 0 \qquad (10.19a)$$

If $\beta_h = 0$, then ϕ'_β is arbitrary. Setting ϕ'_β equal to zero in Eq. (10.12), we have

$$c_o(\rho, \phi; 0) = \tilde{E}(0, \phi) \quad \text{if } \beta_h = 0 \qquad (10.19b)$$

The numerical integration process is now reduced to a single rather than a double integration. In practical computation, we must choose a small value of β_h, which we may call β_{ho}, below which β_h may be approximated as zero, (this may be, for example, at $\beta_h = 0.01$), i.e., Eqs. (10.19a,b) may be re-written as

$$c_o(\rho, \phi; \beta_h) \simeq \frac{1}{\sqrt{2\pi\, k_o\, \rho\, \beta_h}} \{\tilde{E}(\beta_h, \phi)\, e^{j(k_o\rho\beta_h - \frac{\pi}{4})}$$

$$+ \tilde{E}(\beta_h, \phi + \pi)\, e^{-j(k_o\rho\beta_h - \frac{\pi}{4})}\} \quad \text{if } \beta_h \geq \beta_{ho}$$

$$\simeq \tilde{E}(0, \phi) \quad \text{if } \beta_h < \beta_{ho} \tag{10.20}$$

Using Eq. (10.20) in Eq. (10.13), we obtain

$$\underset{\rightarrow}{E}(\underset{\rightarrow}{r}) \simeq \frac{(j\, k_o)^2}{2\pi} \{\tilde{E}(0, \phi) \int_0^{\beta_{ho}} d\, \beta_h\, \beta_h\, e^{jk_o z\sqrt{1-\beta_h^2}}$$

$$+ \frac{1}{\sqrt{2\pi\, k_o\, \rho}} \int_{\beta_{ho}}^{1} d\, \beta_h \sqrt{\beta_h}\, [\tilde{E}(\beta_h, \phi)\, e^{j(k_o\rho\beta_h - \frac{\pi}{4})}$$

$$+ \tilde{E}(\beta_h, \phi + \pi)\, e^{-j(k_o\rho\beta_h - \frac{\pi}{4})}]\, e^{jk_o z\sqrt{1-\beta_h^2}}\} \tag{10.21}$$

But (since $\beta_{ho} << 1$)

$$\int_0^{\beta_{ho}} d\beta_h\, \beta_h\, e^{jk_o z\sqrt{1-\beta_h^2}} = \frac{-1}{j k_o z}\left(e^{jk_o z\sqrt{1-\beta_{ho}^2}}\sqrt{1-\beta_{ho}^2} - e^{jk_o z}\right)$$

$$+ \frac{1}{(j k_o z)^2}\left[e^{jk_o z\sqrt{1-\beta_{ho}^2}} - e^{jk_o z}\right] \approx \frac{\beta_{ho}^2}{2} e^{jk_o z} \qquad (10.22)$$

Substituting Eq. (10.22) into Eq. (10.21), we obtain the final approximate form of $\underset{\rightarrow}{E}(\underset{\rightarrow}{r})$,* i.e.,

$$\underset{\rightarrow}{E}(\underset{\rightarrow}{r}) \approx \frac{(j k_o)^2}{2\pi}\left\{\left(\frac{\beta_{ho}}{2}\right)^2 \tilde{E}(0, \phi)\, e^{jk_o z}\right.$$

$$+ \frac{1}{\sqrt{2\pi}\sqrt{k_o \rho}} \int_{\beta_{ho}}^{1} d\beta_h \sqrt{\beta_h}\left[\tilde{E}(\beta_h, \phi)\, e^{j(k_o \rho \beta_h - \frac{\pi}{4})}\right.$$

$$\left.\left. + \tilde{E}(\beta_h, \phi + \pi)\, e^{-j(k_o \rho \beta_h - \frac{\pi}{4})}\right] e^{jk_o z\sqrt{1-\beta_h^2}}\right\} \qquad (10.23)$$

The integration on β_h indicated in Eq. (10.23) is carried out on the computer using a Simpson's rule algorithm. In the case of the scattered fields, the parameters ρ and ϕ are those of the scatterer center

$$\rho = \rho_s = \sqrt{x_s^2 + y_s^2} \quad ; \quad \phi = \phi_s = \tan^{-1}\left(\frac{y_s}{x_s}\right) \qquad (10.24)$$

---

* In the numerical computations, only one of the two terms in (10.23) is used in any single computation. The first term wherein $\phi_\beta = \phi_s$, is used for scatterer positions outside the cable and the second term wherein $\phi_\beta = \phi_s + \pi$, is used for positions inside the cable. This choice is based on intuition and the knowledge that the predominant contributions come from the portion of the cable near the scatterer, and from values of the propagation vector $\underset{\rightarrow}{\beta}$ nearly parallel with the line-of-sight from the source.

11. NUMERICAL RESULTS AND CONCLUSIONS

11.1 Computer Problems

The numerical results for a number of cases that were run on the Northeastern University Faculty VAX are shown in Subsection 11.4. There have been extensive computation problems due to the transition from the CDC Cyber 70 to the VAX. Among these were: overflow problems due to the reduced range of the VAX; reprogramming required to adapt programs already running on the Cyber 70 to the new machine, thus requiring extensive debugging time; hardware errors on the VAX which have resulted in considerable down-time; and the necessity to use a batch processing system which severely limits the number of cases that can be run per day.

Because of these computer transition problems, which were beyond the control of the technical staff working on this project, there has been a delay of several weeks in the execution of production runs on the computer.

The computations performed on this problem are quite extensive and require considerable running time. For this reason, only a limited number of cases were computed for presentation in this report. The computer program is available and could be used to study many more parameter regimes that might be of practical interest.

11.2 Program Variables

For the results presented in this report, the following variables had fixed value ranges based on use of a specific cable configuration and some empirically determined values of certain parameters given to us by the Contract Monitor.

Parameters associated with the cable:

Fortran Name	Algebraic Symbol	Definition	Value
R	R	Radius of cable configuration in meters	24 (approximation based on circumference of 151 meters)
A	a	Inner radius of coaxial cable-meters	.00476
B	b	Outer radius of coaxial cable-meters	.0127
Length	L_ℓ	Slot length (along cable); same for all slots-meters	.003
Width	W_ℓ	Slot width (around cable); same for all slots-meters	.0155
EPSILONCA	ε_{ca}	Permittivity of cable material-farads/meter	$15.05(10^{-12}) = 1.7\varepsilon_o$
SIGMACA	σ_{ca}	conductivity of cable material - mhos/meter	0
NSLOTS	N_s	Number of slots on cable	31,723
PHIBAR	ϕ_{10}	Azimuthal angle along the cable of Slot #1. (The slot nearest the power source) in ground frame	0
PHI	$\phi_{\ell o}'' = \phi_o''$	Angle of slot center around periphery of cable	$\frac{\pi}{4} = 45^o$

Fortran Name	Algebraic Symbol	Definition	Value
NMODES	----	Number of modes of each category	1 TEM mode (quasi-TEM or coaxial mode observed to propagate in this cable as the principal mode)
ALTEM	$\alpha_n^{(TEM)}$	Attenuation of TEM mode-nepers/ meter	.002
ALTEN	$\alpha_n^{(TE)}$	Attenuation of TE mode- nepers/ meters	---
ALTMN	$\alpha_n(TM)$	Attenuation of TM_n mode-nepers/ meter	---
F	f	Radio frequency in Hertz	$57(10^6)$= 57 MHz
ATEN	$A^{(TE_n)}$	Amplitude of TE_n mode-units not indicated here, because this is treated as a scale factor and its units are not important	---
ATMN	$A^{(TM_n)}$	Amplitude of TM_n mode-same remarks as above concerning units	---

Fortran Name	Algebraic Symbol	Definition	Value
VO	V_o	Voltage between inner and outer convectors of coaxial cable-used in amplitude of TEM mode-volts	1
E	ε	Permittivity of ground-farads/meter	$35.416(10^{-12}) = 4\varepsilon_o$
SIGMA	σ	Ground conductivity -mhos/meter	0.002
XAP	x_A	x-coordinate of antenna-meters	0 (antenna at center of circular cable configuration)
YAP	y_A	y-coordinate of antenna-meters	0 (same remarks as above)
ZAP	z_A	z-coordinate of antenna-meters	0.5
BH	β_h	Magnitude of (x-y) plane projection of $\underset{\rightarrow}{\beta}$, i.e. $\sqrt{\beta_x^2 + \beta_y^2}$	Varied from 0 to 1
PHIB	ϕ_β	Azimuthal angle of (x-y) plane projection of $\underset{\rightarrow}{\beta}$, i.e. $\tan^{-1}\left(\frac{\beta_y}{\beta_x}\right)$	Varied from 0^o to 360^o

Parameters Associated with the Scatterer

Fortran Name	Algebraic Symbol	Definition	Values
XSP	x_s	x-coordinate of scatterer center-meters	Varied from case to case
YSP	y_s	y-coordinate of scatterer center-meters	Varied
ZSP	z_s	z-coordinate of scatterer center-meters	Varied
THB	Θ_b	Spherical polar angle of long axis of prolate spheroidal scatterer (in ground-frame)	Varied: 0 for "upright man" cases; $\frac{\pi}{2}$ for "crawling man" cases
PHB	ϕ_b	Azimuthal angle of long axis of scatterer (in ground-frame)	Varied
ES	ε_s	Permittivity of scatterer material-farads/meter	$408.992(10^{-11})$ = $46.2\varepsilon_o$ = $^2/_3\,(60\varepsilon_o)$, based on Reference D.19
SIGMAS	σ_s	Conductivity of scatterer material-mhos/meter	0.592 based on Reference D.19
RS (computed variable)	r_s	$\sqrt{x_s^2+y_s^2}$ = radial coordinate of scatterer center in ground frame	Varied
PHIS (computed variable)	ϕ_s	$\tan^{-1}\left(\frac{y_s}{x_s}\right)$ = azimuthal angle of scatterer center in ground frame	Varied

Fortran name	Algebraic Symbol	Definition	Values
RS	R_s	Radius of prolate spheroidal scatterer-meters	0.25
LS	L_s	Length of prolate spheroidal scatterer-meters	Varied

11.3 Delineation of Cases Studied

The outputs of the computations are:

$|E_x^{(q)}|$ = amplitude of x-component of the electric field of the signal at the antenna where q = o for the field in the absence of the scatterer, q = s for the scattered wave field and a = (0+s) for the superposition of the field without the scatterer and that due to the scatterer.

$|E_y^{(q)}|$ = amplitude of y component of field at antenna

$|E_z^{(q)}|$ = amplitude of z component of field at antenna

$$|E^{(q)}| = \sqrt{|E_x^{(q)}|^2 + |E_y^{(q)}|^2 + |E_z^{(q)}|^2}$$

The parameters to be varied in these computations are:

x_s = x component of scatterer center-meters

y_s = y component of scatterer center-meters

z_s = z component of scatterer center-meters

L_s = Long dimension of scatterer = Height of "man"-meters

ℓ_s = Height of "stilts" in cases where the intruder is assumed to be elevated-meters

$\phi_s = \tan^{-1}\left(\frac{y_s}{x_s}\right)$ = Azimuthal angle of scatterer center

$\Delta x_s = x_s - x_c$, where x_c = x coordinate of cable-meters

$\Delta y_s = y_s - y_c$, where y_c = y coordinate of cable-meters

$\Delta r_s = r_s - R$, where r_s = r coordinate of scatterer center-meters

The first set of results which are of course the same for all scatterer positions and orientations, are the field amplitudes of the antenna in the absence of the scatterer. These are as follows:*

$$|E_x^{(o)}| = 4.8166(10^{-4})$$
$$|E_y^{(o)}| = 2.3858(10^{-2})$$
$$|E_z^{(o)}| = 5.0226(10^{-4})$$

The computed field in the absence of a scatterer is predominantly in the y-direction. The interpretation of the result will be discussed in Subsection 11.4.6.

The cases involving an intruder are delineated below.

Cases I : "Upright Man" Model

These cases involve a model of an intruder walking in upright position across the cable. The intruder starts at a point outside the cable and walks radially inward, crosses the cable and continues to walk toward the center of the configuration.

Because of time limitations computations were made for only a few positions on either side of the cable. Since the effects should not be entirely circularly symmetric, due to cable attenuation and other effects, these computations were made at four different azimuthal angles.

Case I-A

"Upright man", walking radially inward across cable; $\Theta_b = 0^o$, $\phi_b = 0^o$, r_s varied from 28 to 17.5 meters in steps of 1.5 meters, $z_s = L_s/2$ (see diagram below); $\phi_s = 0°$ (i.e., path along x axis in -x direction).

* These "field amplitudes" are actually relative quantities and are not intended to represent the actual field amplitudes. If the true values of the power generated by the source in the cable were used here, these numbers would be true field amplitudes in volts per meter.

Case 1-A (continued)

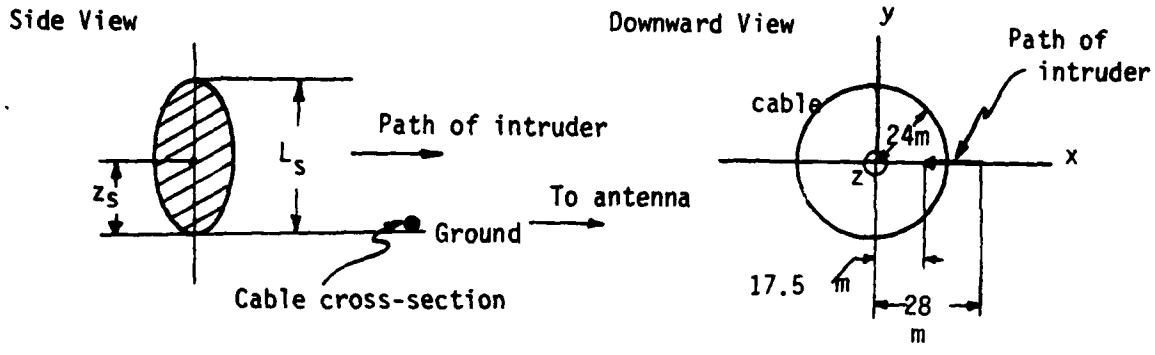

Case I-B; same as I-A, but $\phi_s = \frac{\pi}{2}$; path along y axis in -y direction

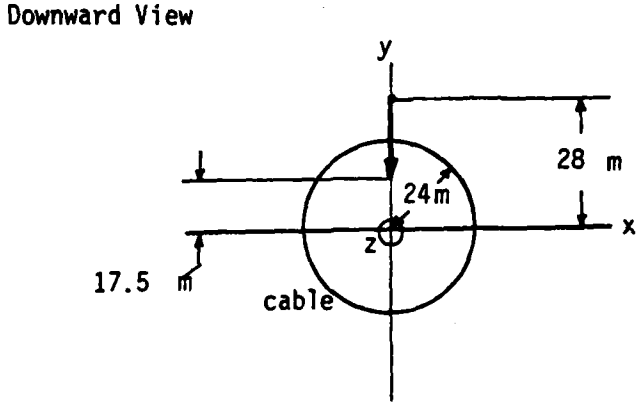

Case I-C, same as I-A and I-B but $\phi_s = \pi$; path along x axis in +x direction

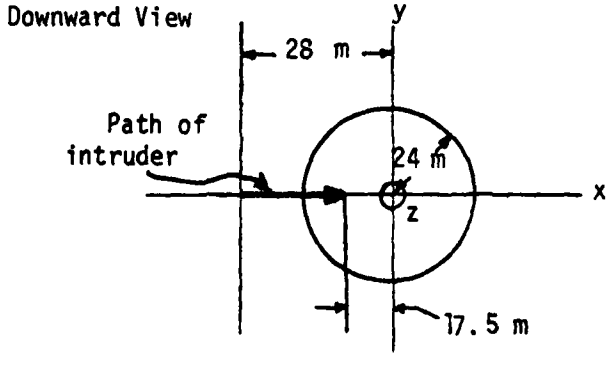

Downward View

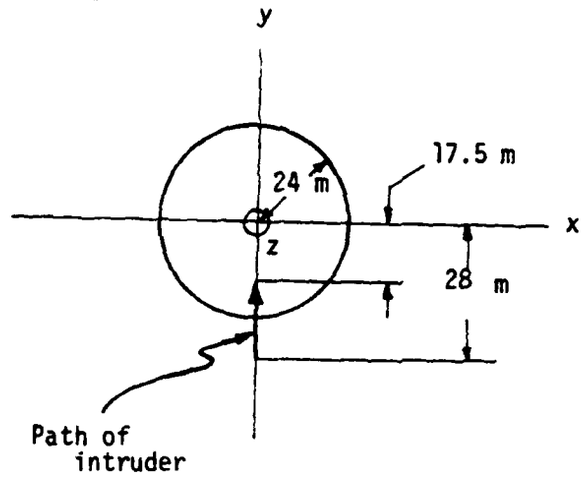

Case I-D: same as I-A, I-B and I-C, but $\phi_s = \frac{3\pi}{4}$; path along y axis in +y direction.

Cases II: "Elevated Upright Man" Model

In these cases the intruder is again upright, but elevated, i.e., on stilts. The stilts are assumed to scatter no energy; hence the only change in the mathematical model is that the scatterer center is raised (relative to Cases I) by an amount ℓ_s, the height of the stilts.

These cases are evaluated with the intruder at a few fixed positions, to determine at those positions the effect of various elevations on the field components seen at the antenna.

Case II-A Upright man on stilts; $\theta_b = 0^o$, $\phi_b = 0^o$; ℓ_s = Height of stilts; $z_s = \ell_s + \frac{L_s}{2}$; ℓ_s varied from 0.4 to 2.0 meters; $x_s = 22$, $y_s = 0$.

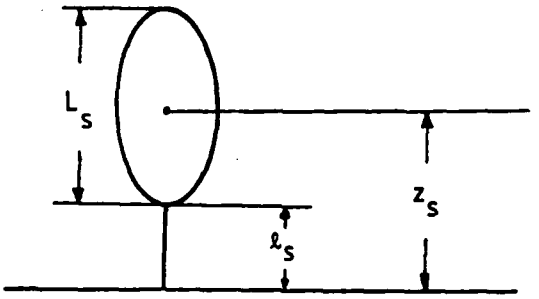

Case II-B. Same as Case II-A but $x_s = 23.5$

Case II-C. Same as Cases II-A and II-B but $x_s = 25$

Case III: "Upright Man", standing at ground level; $\Theta_b = 0^o$, $\phi_b = 0^o$, $z_s = \frac{L_s}{2}$, $y_s = 0$; L_s varied from 1.6 to 2.08. This case is for the purpose of examining the variation of the field components seen at the antenna with the height of the intruder. Case III-A, $x_s = 22$; Case III-B, $x_s = 23.5$; Case III-C, $x_s = 25$.

Case IV: "Crawling man" Models

In these cases the intruder is "crawling" radially inward from a position outside the cable to a position inside the cable. The spheroid in the model is lying on the ground surface with the long axis pointed in the radial direction.

Case IV-A: "Crawling man", $\Theta_b = \frac{\pi}{2}$, $\phi_b = 0^o$, $z_s = R_s/2$, $\phi_s = 0$, r_s varied from 28 to 17.5 meters in steps of 1 meter; path same as in Case IA.

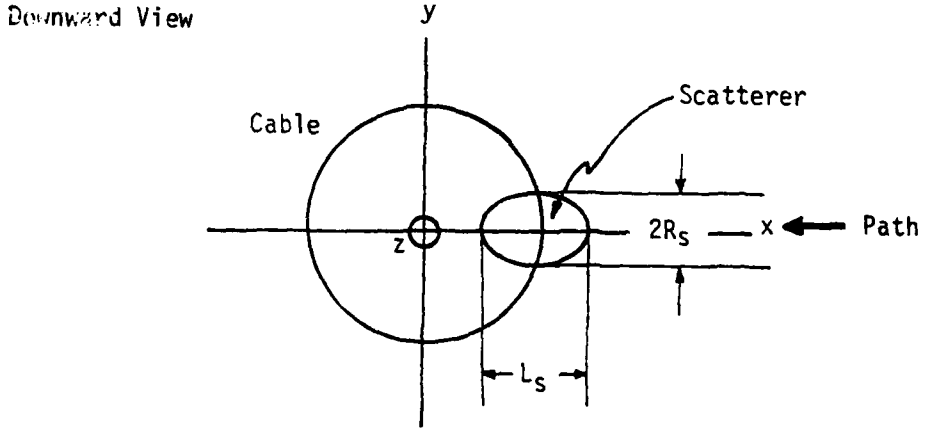

CASE IV-B Same as Case IV-A except that $\phi_b = \frac{\pi}{2}$, path same as in Case I-B.

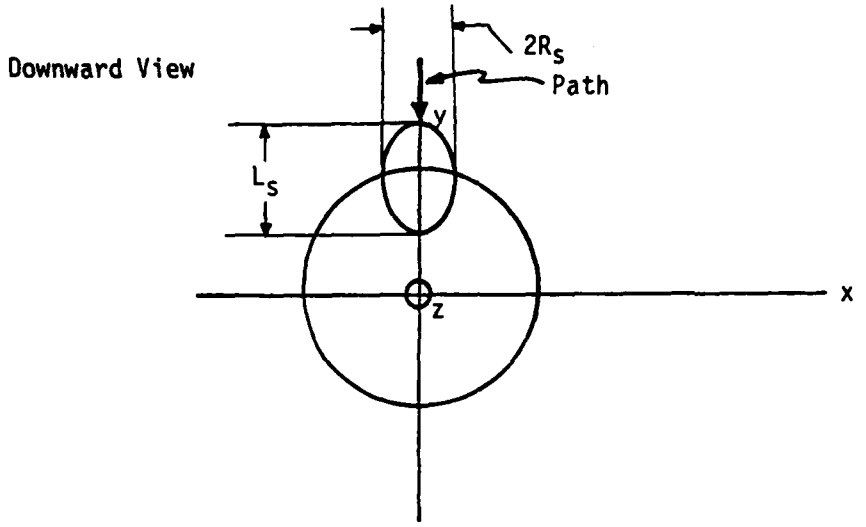

Case IV-C: same as Cases IV-A and IV-B except that $\phi_b = \pi$; path same as Case I-C.

Case IV-D: same as Cases IV-A,B,C except that $\phi_b = \frac{3\pi}{2}$, path same as Case I-D.

Case V: Prone Position Transverse to Radial Direction

In these cases, the intruder is in a prone position, but the long axis is transverse to the radial direction. Otherwise, same as "crawling man" cases. In cases V-A, V-B, V-C and V-D, ϕ_b = 0, $\pi/2$, π and $3\pi/2$, respectively.

In addition to Cases I through V above, two other sets of auxiliary computations were made. Their purpose was to determine the magnitude and polarization of the fields illuminating the scatterer at the positions assigned to its center in Cases I through V.

The first set of computations were of the field components due to the cable without ground reflections at the values of ρ and ϕ corresponding to the scatterer center values ρ_s = 17.5, 19, 20.5, 22, 23.5, 25, 26.5 and 28 meters. Four sets of these runs were made, at $\phi = 0^o$, 90^o, 180^o and 270^o. These values of ρ and ϕ correspond to the scatterer positions in Cases I-A, B, C, D, IV-A, B, C, D and V-A, B, C, D.

The second set of these illuminating field computations were identical with the first but with the inclusion of ground reflections, i.e., in the first set of computations the ground permittivity is that of free space and the ground conductivity is zero, those assignments being equivalent to the removal of the effect of the ground. In the second set the values of ground permittivity and conductivity were those indicated in the table in Section 11.2 above. Comparison of the first and second sets of results should allow a determination of the effect of ground reflections on the fields illuminating the scatterer.

11.4 Presentation and Discussion of Numerical Results

The available numerical results will be presented in this section, beginning with the results of the study of the fields illuminating the scatterer (Subsection 11.4-1), followed by: (Sec. 11.4-2) the "upright man" (or equivalently "radial walk") cases (Cases I-A, B, C, D); the "elevated upright man" or "man on stilts" cases (Cases II-A, B, C; Subsection 11.4-3); the "height variation" cases (Cases III-A, B, C; Subsection 11.4-4) and the "crawling man" cases (Cases IV-A, B, C, D and V-A, B, C, D; Subsection 11.4-5).

In discussing the results we have tried to take cognizance of available experimental results whenever they exist. Those experimental results mentioned in what follows are:

Reference B.2, Figure 5, Page 10 (circumferential walk)
Figure 8, Page 13 (" ")

Reference B.3, Figure 9, Page 15 (circumferential walk)
Figure 10, Page 16 (radial walk)
Figures 13, 15, 16, 17, Pages 18, 20, 21, 22 (circumferential walk)

Reference B.6, Figure 7, Page 12 (circumferential walk)
Figures 4, 5, 6, Pages 1, 12 (circumferential walk; analytical results based on L. Poirier's simplified analysis neglecting field polarization)

In all of the circumferential walk cases studied experimentally, a very substantial oscillation is observed in the results as the intruder walks around the periphery of the cable. This is also exhibited by L. Poirier's analysis reported in Reference B.6. Roughly speaking the oscillatory behavior is due to alternations between constructive and destructive interference as the scattering object changes azimuthal angle.

The experimental curves plotted in the above references are of the total signal voltage received at the antenna vs. ϕ_s, the scatterer's azimuthal angle. These are compared with the signal voltage in the absence of the scatterer (quiescent level). The signal voltage (assuming, of course, that the antenna is linear) is

proportional to the field strength of the component polarized in the direction to which the antenna is receptive. In the case of the monopole antenna used in making the measurements, that direction is the vertical. Hence, only our results on $|E_z|$, the amplitude of the vertical component of the field at the antenna, could be compared with those results. The horizontal components $|E_x|$ and $|E_y|$ cannot be so compared, since the antenna is not responsive to horizontal fields.

Two points must be made before proceeding with the numerical results. First, it was impractical under our time limitations to plot circumferential walks; consequently all results where the scatterer moves and also those results for the fields illuminating the scatterer at various positions are presented as "radial walks", i.e., the field components are presented for various radial positions ρ_s at a fixed azimuthal position ϕ_s. Moreover, the angles ϕ_s are confined to 0^0, 90^0, 180^0, and 270^0. It would be highly desirable to have results for many intermediate angles. There was insufficient time to compute enough points around the cable to obtain meaningful "circumferential walk" results. To do so would require computations for every few degrees(e.g. 2^0 spacing would require 180 computations for each fixed value of ρ_s). For this reason it was decided to confine attention to the radial varation at fixed azimuth angle.

A second point is that there is some question in our minds (and no remaining time to study the question and try to improve the model to rectify the problem if it exists) on the accuracy of the ratio of the computed scattered fields at the antenna (i.e., direct-plus-ground-reflected scattered fields) to the computed fields at the antenna in the absence of the scatterer (direct-plus-ground-reflected). According to our results the fields at the antenna (at the center of the configuration; $x_A = y_A = 0$, $z_A = 0.5$) in the absence of the scatterer are (in dB relative to an arbitrary reference level; the same reference level used in all of the results with and without scatterers presented in this report):

$$|E_x| = -66.3 \text{ dB}$$

$$|E_y| = -32.4 \text{ dB}$$

$$|E_z| = -65.9 \text{ dB}$$

These results will be discussed in Subsection 11.4-6.

Certain approximations used in our analysis if not as accurate as we originally believed, might have a different effect on the antenna fields in the absence of the scatterer than they do on the scattered fields. If indeed that is the case, then at the very least there might be a scale factor error in the results without the scatterer present or alternatively a scale factor error in the scattered fields, or possibly in both sets of fields. If that were the case, then coherent addition of the fields with the scatterer present to the fields without the scatterer present could produce totally meaningless results. The two important constituents of the analysis are the fields generated by the cable and the perturbation of the field by the scatterer. Rather than present large numbers of results on the composite fields (all of which have been computed for each case studied) which may be greatly in error because of an erroneous scale factor, it was decided to concentrate on the direct-plus-ground-reflected scattered field components and show their behavior as a function of various parameters.

11.4.1 Numerical Results on Illuminating Fields

The first results presented are those of the field components illuminating the scatterer. These appear in tabular form in Tables 11.1, 11.2 and 11.3, Columns 1 through 8. Some of the results are shown graphically in the curves of Figures 11.1 through 11.16.

Results are shown both with and without the effects of ground reflections. The format for each of the curves shown is a plot of a field component in dB relative to an arbitrary reference level against ρ, the radial coordinate, from $\rho = 17.5$ to $\rho = 28$ meters. The reference level has no significance because there are arbitrary factors which cause the computed field component magnitude to differ from the actual field magnitude in volts per meter. All plots in these figures and also those in subsequent figures are in dB relative to the same reference level, hence, it is the relative magnitudes of field strength rather than their absolute magnitudes on which attention should be focussed. Since the cable is at a radial distance of 24 meters, the plots may be considered to be from a distance of 6.5 meters inside the cable to a distance of 4 meters outside the cable.

From very simple reasoning based on a single plane wave propagating from the nearest cable slot to the observation point, we would expect something close to a decay in amplitude proportional to the inverse distance from the nearest cable slot. The coherent addition of contributions from different parts of the cable, with the attendant variability in the relative phase between contributions from different cable slots, would preclude exact inverse distance behavior. However, we look for some suggestion of such a variation with distance. Unfortunately we do not always attain behavior close to the above.

Focussing for the monent on the "best" results in terms of correlation with expectations based on simple reasoning, we examine the results in Table 11.3 and in

Figures 11.2, 11.4, 11.7 showing the z-components of the field as a function of radial distance without ground reflection.

At $\phi = 0^0$, the field amplitude decays from a value of -5.31dB at a radial distance of 0.5 meters from the cable to a value -39dB lower at 6.5 meters inside the cable and to a value -12dB lower at 4 meters outside the cable. The inverse distance behavior would give us a decay of roughly -22dB at 6.5 meters inside and -18dB at 4 meters outside. Thus the rate of decay is considerably larger than would be dictated by an inverse distance law. This could be at least partially due to the importance of the approximately inverse squared contribution at a distance very close to the scatterer.

The z-field amplitudes are not changed appreciably when ground reflections are added at $\phi = 0^0$. The z-field amplitudes are slightly smaller but within about 2 or 3dB of their corresponding values without ground reflections and the trends are qualitatively and quantitatively the same. Since interference between direct and reflected waves can be either constructive or destructive, there is no certainty that the ground reflection contribution will increase or decrease the field magnitude. In this case, at the reflection angles at which these effects occur, the interference appears to be mostly destructive.

At $\phi = 90^0$ (Table 11.3 and Figures 11.9, 11.11, 11.14) the trends in the z-field are qualitatively similar but the rates of decay with radial distance from the cable are not as pronounced. The decay between 0.5 and 6.5 meters inside the cable and that between 0.5 and 4 meters outside the cable are respectively 19.6dB and 16.9dB <u>without</u> ground reflections and 24.1dB and 22.1dB respectively <u>with</u> ground reflections. These values are much closer to the respective 22dB and 18dB that would prevail for an inverse distance decay law.

At $\phi = 180^0$ (Table 11.3 and Figure 11.14) the decay levels corresponding to the above comparisions are 17.3dB and 17.5dB respectively without ground reflections and 21.9dB and 19.6dB respectively with ground reflections. Again these values are within a few dB of what would be expected for an inverse distance dependence. Again, as at $\phi = 0^0$ and $\phi = 90^0$, the z-field magnitudes with ground reflection tend to be slightly lower, usually by less than 2dB, than their counterpart values without ground reflection, indicating mostly destructive interference between direct and ground reflected waves.

The z-field results for $\phi = 270^0$ (Table 11.3) appear anomalous with respect to the above considerations. The same comparison exists between results with and without ground reflections (nearly the same in both cases), but there is no obvious explanation for the strange behavior of the z-field magnitude outside the cable and its erratic behavior inside the cable.

The variation in the average z-field amplitudes as the angle ϕ changes through 90^0 increments is substantial, being nearly 30dB in some cases. This is not anomalous, since experimentally observed scattered field magnitudes (See e.g. circumferential walk results in Ref. B.2; Fig. 5, Pg. 10; Fig. 8, Pg. 13, Ref. B.3; Figs. 9, 13, 15, 16, 17, Pgs. 15, 18, 20, 21, 22; Ref. B.6; Fig. 7, Pg. 12) exhibit a highly oscillatory azimuthal variation. Since nulls exist at some angles no variation in dB would be anomalous. This can be explained at least partially by the highly complicated nature of the superposition of contributions with widely differing phases from various portions of the cable. More will be said of this in later discussions of the azimuthal variation of our numerical results on scattered field amplitudes.

The horizontal components of the computed illuminating fields are not generally as well-behaved as the vertical components with respect to any resemblance

to inverse distance behavior. This is possibly due to the fact that the waves from different slots along the cable not only add coherently with complicated relative phases, but also add vectorially. In all cases, the y-component seems to predominate.

11.4.2 Results for the "Upright Man" Cases

In Tables 11.4, 11.5 and 11.6, Column 1 through 4 and in Figures 11.17 - 11.23 some scattering results for a man 1.78 meters tall (about 5'10") and about 0.5 meters wide in upright position proceeding from (or to) a point 17.5 meters inside the cable to (or from) a point 28 meters outside the cable. These are the cases I-A, B, C, D delineated in Section 11.3, where A, B, C and D refer to scatterer center azimuthal angles $\phi_s = 0^o$, 90^o, 180^o and 270^o respectively.

The first point to be made is that all of the field component amplitudes exhibit a very large decrease (from 40 to 70dB) at $\phi_s = 90^o$ and 270^o relative to their values at $\phi_s = 0^o$ and 180^o. Magnitudes at 180^o are generally between 20 and 30dB below those at 0^o, while those at 270^o and those at 90^o are comparable at some positions and separated by 10 to 20dB at other positions. None of these variations appear to come directly from attenuation along the cable, which is a maximum of 2.62dB around the entire circumference of the cable. As was discussed in Section 11.4.1 in connection with illuminating fields, the circumferential variations in fields illuminating the cable are probably at least partially due to the wide variations in phase of the contributions from different portions of the cable. If one adds to that the phase variations in the scattering process itself, one cannot expect the scattered fields from various azimuthal angles to follow a smooth variation or to be comparable in magnitude, in spite of superficial indications of symmetry. If all cable field contributions were added noncoherently, i.e., if their amplitudes or squared amplitudes were added rather than their complex fields, the results would undoubtedly show much greater azimuthal symmetry. Experimental results for the vertical field components (Ref. B.3, Pg. 10; Ref. B.3, Pp. 15, 18, 20, 21, 22; Ref. B.6, Pg. 12) show substantial azimuthal fluctuations.

Turning our attention now to the radial variation in field amplitude at a fixed azimuthal angle most of the results in Tables 11.4, 11.5 and 11.6 and Figures 11.17 through 11.23 show a substantial decay as the scatterer recedes from the cable outside the cable but a flat or sometimes slightly increasing response as it recedes from the cable inside the cable. Also the peak doesn't always occur at 23.5, the closest radial distance to the cable for which a computation was made, but sometimes at 25 or at 22 or even further away in a few cases. Since computations were made at intervals of 1.5 meters, the actual peaks might occur between the computed points. But in general the occurrence of the peak at a point other than the point directly above the cable is consistent with the same observation made experimentally and discussed on Page 16 of Reference B.3. Figure 10 on Page 16 of that reference (radial walk) illustrates the point, wherein peak responses sometimes occur a meter or more away from the cable radius.

Based on the simple reasoning of Section 11.4.1 we should look for two contributions to variation of field amplitudes with radial distance in the present case. First, this simple reasoning would predict a variation as the reciprocal of the separation distance between the nearest cable slot and the scatterer position due to the expected variation in the illuminating field. Also there should be an inverse radial distance dependence due to the $\frac{1}{r^2}$ factor appearing in the scattered field component. For example,(Subsection 11.4.1) we should expect from the first of these mechanisms about 22dB of decrease in amplitude between 23.5 and 17.5 meters and about 18dB between 23.5 and 28 meters. From the second effect we should expect a 2.56dB increase as we go from 23.5 to 17.5 and a 1.52dB further decrease as we proceed from 23.5 to 28 meters. This means that the net decay should be about 19.5dB from 23.5 to 28 meters and about 20.5dB from 23.5 to 17.5 meters. If we were to base our interpretation of the results on these mechanisms alone, we would conclude that

the decay of between about 20 and 25dB that we observe on most of the field components between scatterer positions at 23.5 and 28 meters is quite reasonable, but that the flat or even increasing response we see as we proceed from 23.5 to 17.5 meters inside the cable cannot be explained by these mechanisms.

There is another feature of the geometry which could help to explain the great asymmetry between departures from the cable radius inside and outside the cable. Outside the cable, as we recede further from the cable radius, the cable appears convex from the observation point and the distances to the cable slots other than the nearest one become progressively greater as we move out. As we move inward inside the cable, however, the cable appears concave and the distances from the various parts of the cable nearest the observer become more nearly comparable, leading to a greater tendency toward constructive interference between contributions from various slots.

Some of the results shown in Tables 11.4, 11.5 and 11.6 appear anomalous, and there is no obvious explanation for them based on any of the mechanisms discussed above. More will be said of this in Subsection 11.5.

11.4.3 Results for the "Elevated Upright Man" Cases

These results correspond to cases II-A, B, C in Section 11.3. The "man" is placed on stilts in three different fixed positions ($\phi_s = 0^0$, ρ_s = 22, 23.5 and 25, those radial positions nearest the cable at which fields were computed). The results showing field component amplitude vs height of stilts at each position are presented in Tables 11.7, 11.8 and 11.9. Selected results are also shown in Figures (ρ_s = 22), Figure 11.26 (ρ_s = 23.5) and Figures 11.27, 11.28 (ρ_s = 25). In all three cases, the variation with stilt height is from 0 to 2.0 meters.

The field component amplitudes in all three coordinate directions (except for the vertical field component at ρ_s = 25m, which exhibits anomalous behavior) there is a decrease of between 2dB and 6dB between the case of zero stilt height and the case of 2 meter stilt height. This variation is in the proper direction, obviously, since the expectation is for a reduction in field strength as the scatterer is further elevated and therefore moves further away from the cable slots generating the fields. To examine the issue of how close the variation is to the inverse distance variation, we note that the difference between the "no stilts" case and 2 meter stilts (since the "man" is 1.78 meters tall) is a change in the z-coordinate of the scatterer center from 0.890 to 1.890. With a pure inverse distance law, this would result in roughly a 6dB decay between these two cases. This is not very far from the amount of decrease observed in most of the computed results.

11.4.4 Height Variation

A set of results showing field component amplitude variation versus intruder height at $\phi_s = 0^o$ and at ρ_s = 22, 23.5 and 25 meters (Cases III-A, III-B and III-C respectively in Section 11.3) are shown in Tables 11.10, 11.11 and 11.12. Selected results also appear in Figs. 11.29, 11.30, Figs. 11.31, 11.32 and Figs. 11.33 - 11.35 respectively. In each case the height is varied from 1.60 to 2.08 meters (about 5'3" to nearly 6'10", a more-than-reasonable range of heights for an adult male). In all of these cases, an increase in field amplitude of about 6dB is observed as the height increases over the indicated range.

This variation is certainly in the proper direction. The height range represents an increase of about 30%, if we want to consider the field amplitude as proportional to the length of the scatterer, this would imply an increase of about 2.27dB between the response of the short fellow of 5'3" and the basketball player of 6'10". The 6dB difference we actually observe would be more nearly consistent with a proportionality to the square of the scatterer length, implying a 4.56dB increase.

In fact, the scatterer long dimension is about a third of the wavelength at the frequency used in these computations and the parameter $\frac{2\pi L_s}{\lambda}$ is about 2 in free space. Hence no simple proportionality between the field strength and the scatterer length can be predicted, such relationships being usually applicable only to Rayleigh scatterers, very small compared to wavelength. However, for the cases computed, we do see a positive variation with intruder height L_s corresponding roughly to somewhere between L_s^2 and L_s^3.

11.4.5 Results for the "Crawling Man" Cases

Unfortunately, not all of the crawling man cases (Cases IV-A, B, C, D and V-A, B, C, D of Section 11.3) were run successfully. Attempts were made to run these cases immediately before the contract deadline. Some of the cases were aborted due to computer difficulties and there was no time left to correct these difficulties.

Most of the intended results were obtained and these are presented in Tables 11.4, 11.5, and 11.6, Columns 5 through 12. A subset of these results are shown graphically in Figures 11.36 through 11.39.

Comparisons of the "radially crawling man" (RCM), the "transverse crawling man" (TCM) and the "upright man" (UM) cases are best made from Tables 11.4, 11.5 and 11.6, where for each field component, the amplitudes for $\phi_s = 0^0$ are shown in Columns 1, 5 and 9 for UM, RCM and TCM respectively. At $\phi_s = 90^0$, the corresponding columns are 2 (UM), 6 (RCM) and 10 (TCM). At $\phi_s = 180^0$, we have 3 (UM), 7 (RCM) and 11 (TCM) and at $\phi_s = 270^0$, 4 (UM), 8 (RCM) and 12 (TCM). We now focus attention on the variation of the scattered field components at the antenna with distance of the scatterer from the cable. This was discussed for the UM cases in Section 11.4.2. Certain RCM and TCM cases have the expected behavior, beginning with low values at $\rho_s = 17.5$, peaking at or near 23.5 and decaying to low values at 28. At $\phi_s = 0^0$ this behavior is exhibited by $|E_x|$ and $|E_y|$ for RCM, but not by $|E_z|$, which shows a more nearly flat response as distance changes inside the cable, but a substantial decay as the scatterer recedes from the cable radius outside the cable. The available results for TCM at $\phi_s = 0^0$ (not all of these are available, as indicated in Column 9 of Table 11.4) do not seem to indicate that kind of behavior, in fact they depart from it very substantially. At $\phi_s = 90^0$, there is a small decay in all the components of both RCM and TCM between 17.5 and 23.5, opposite to the

desired trend, but again a substantial decay from 23.5 to 28.0. The rates of decay outside the cable for both $\phi_s = 0^0$ and $\phi_s = 90^0$ are comparable to those observed with UM, which have already been discussed in Subsection 11.4.2.

The RCM and TCM amplitudes for $\phi_s = 180^0$ and $\phi_s = 270^0$ are in general more erratic than their counterparts for $\phi_s = 0^0$ and $\phi_s = 90^0$. Some of these runs were aborted due to a difficulty in one of the subroutines in the Barber scattering program. This problem had not been encountered before. Since it occurred very near the end of the contract period, there was no time to correct the difficulty. Some very small changes in angle assignments were made to overcome the difficulty in doing re-runs of these cases. Some of the cases then ran successfully but produced very strange results which we believed to be unreliable. Consequently, some of the points are not presented in the tables. In one case (TCM, $\phi_s = 270^0$) the entire run was aborted and we have no results on this case.

Comparison of the overall order of magnitude differences between UM, RCM and TCM cases at a given value of ρ_s and ϕ_s can be made from the tables. At $\phi_s = 180^0$ and $\phi_s = 270^0$, too few computed points are available for meaningful comparisons. It is observed that for $\phi_s = 0^0$ and $\phi_s = 90^0$ (comparing column 1, 5 and 9 results) the values of $|E_x|$ and $|E_y|$ for RCM cases, through the range of values of ρ_s covered tend to be roughly comparable (on the average) to the corresponding UM cases, but the corresponding $|E_x|$ values in the TCM case (those available) are higher by between 10 and 20dB. The $|E_z|$ values exhibit somewhat different trends at $\phi_s = 0^0$. The TCM values are nearly comparable to the UM values but the RCM values tend to be higher, by as much as 20dB in some cases. At $\phi_s = 90^0$, the $|E_z|$ values for TCM are as much as 70 or 80dB. This would imply that at $\phi_s = 90^0$, the scattering is negligibly small for the RCM case relative to the TCM case.

The difference in orientation between the UM, RCM and TCM cases would not alter expectations for inverse distance behavior, which are based on the naive thought that the intruder has the properties of a point scatterer, i.e., subtends a small angle at both the source and the receiving antenna. That is certainly the case at the antenna, reasonably well into the scatterer's far zone, but not so at the nearest illuminating slot, which sees the scatterer as an extended object subtending a large angle and lying in its near-zone, particularly at radial positions near 24 meters.

The differences in orientation do produce substantial differences in the way the scatterer is illuminated and the angular position of the antenna in the object's scattering pattern. For the UM cases, the illumination and scattering are both predominantly broadside. For the RCM cases, both illumination and scattering are primarily "nose-on". For the TCM cases, illumination and scattering are again largely broadside, but with a much smaller illunimation coverage in the vertical direction than in the UM cases. All that can be said is that these differences in geometry should result in some differences in order-of-magnitude, as is observed in our results. But these observed differences are not always in the same direction. That might be considered anomalous if we were dealing with a Rayleigh scatterer illuminated by a single plane wave. In our model, however, we have a scatterer (free space wavelength - 5.26 meters) whose parameters $\frac{2\pi L_s}{\lambda}$ and $\frac{2\pi(2R_s)}{\lambda}$ in free space are respectively about 2.125 and 0.596. With the assumed scatterer permittivity ($\varepsilon_s = 46.2\varepsilon_o$), neglecting its conductivity, the wavelength in the scatterer medium is reduced to about .774 meters. Hence the parameters $\frac{2\pi L_s}{\lambda}$ and $\frac{2\pi(2R_s)}{\lambda}$ referred to the scatterer medium are now about 14.4 and 4.06 respectively. These numbers indicate that the scatterer is large enough compared with wavelength to produce scattered fields that may be highly oscillatory and highly directive.

Changes in orientation such as those between UM, RCM and TCM cases may well produce very pronounced differences in both the orders of magnitude of the scattered fields and their sensitivity to scatterer positions.

Another effect which complicates attempts at interpretation of these differences is that of ground reflection. The assumed ground parameters ($\varepsilon_g = 4\varepsilon_0$, $\sigma_g = .002$, $\frac{\sigma_g}{\omega\varepsilon_g} = 0.158$) are sufficiently large to produce very significant ground reflection terms. Coupled with the highly angle-dependent scattered fields, the ground reflections of both illuminating and scattered fields should further increase the sensitivity of the results to small changes in the geometry.

11.4.6 Relative Magnitudes of Components

The first result that warrants discussion in correction with this topic is that near the beginning of Subsection 11.4 giving the amplitudes of the x, y and z components of the electric field at the antenna in the absence of a scatterer. In summary, this result says that the y-component predominates, the x-component is between one and two orders of magnitude below the y-component and the z-component is comparable in magnitude to the x-component. To attempt to explain this, we first examine Eq. (I-3a) in Appendix I. We also observe that we have assumed that the TEM mode is the only propagating mode in the cable. For the TEM mode, the electric field is entirely radial and the magnetic field is entirely azimuthal. That implies that the $(\underset{\rightarrow}{n} \times \underset{\rightarrow}{E})$ component in (I-3a) vanishes, the $(\underset{\rightarrow}{n} \times \underset{\rightarrow}{H})$ component is entirely in the direction of the cable axis and the $(\underset{\rightarrow}{n} \cdot \underset{\rightarrow}{E})$ term is in the direction of $\nabla' \left(\frac{e^{jkR}}{R}\right)$. For any given value of $\underset{\rightarrow}{\beta}$, the latter is in the direction of $\underset{\rightarrow}{\beta}$.

If all slot contributions were in phase and if there were no attenuation along the cable, then circular symmetry would prevail. Since the antenna is at the center of the configuration, one would expect a cancellation of the horizontal electric field contributions from the cable slots and a summation of the vertical contributions, based on the observations made above. The assumed attenuation of the TEM mode is about .000728dB per degree of angle along the cable. This implies the following: (a) if the field strength of the TEM mode were unity at $\phi = 0^{o}$, it would decay to a value of about .927 at 90^{o}, .860 at 180^{o}, .798 at 270^{o} and .739 at 360^{o}. These values would not explain entirely the x-y asymmetry that is observed in the results.

In order that the y-directed field at the antenna will greatly exceed the x-directed field, the $(\underset{\rightarrow}{n} \times \underset{\rightarrow}{H})$ contribution, which is the predominant one for the TEM mode, must be primarily from the portion of the cable near $\phi = 0^{o}$, i.e., the contributions from that region must be more heavily weighted than those from other angular

regions. Although attenuation could play some role in that predominance, it is unlikely, as indicated above, to play a major role. The relative phases of the contributions from the other portions of the cable might cancel out the contributions from these regions in such a way as to leave the predominant contribution from the region near $\phi = 0^{o}$. If that occurs, then that would explain the observed predominance of the y-field.

In preliminary results presented a few months ago, this same asymmetry was observed, except that the z-component was even smaller relative to other components than in the present results and the y-component was larger compared with the x-component than in the present results. It was suggested at the time that the presence of an additional mode, subsequently removed, could be partially responsible for the asymmetry. If that was true, then the removal of that mode did not completely remove the asymmetry. Moreover, the method of summation of the contributions around the cable slots was changed since those results were obtained and the asymmetry still persists. Hence, barring an error in the computations, it must be due to some features of the source model itself.

In the numerical results for the illuminating fields with ground reflections (Subsection 11.4.1; Tables 11.1, 11.2, 11.3 and Figures 11.9-11.16)the same relative orders of magnitude between components is usually observed qualitatively i.e., the x and z components are of comparable magnitudes and the y-component is about one order of magnitude (about 20dB) above the x or z component. Without ground reflections (Figures11.2,11.4,11.7), the z component tends to be about 10 to 20dB below the x-component and the y-component is again larger than the x-component, but usually not as much larger. This indicates that ground reflections seem to enhance the x-y asymmetry.

Evidently, the same mechanism is producing these asymmetries in the results for the illuminating fields near the cable as is producing them at the antenna location far from the cable. Hence, it cannot be explained by the differences between the fields at the antenna, which are entirely far zone fields, and those at the potential scatterer locations, which are near zone fields.

The"Upright Man" cases (Subsection 11.4.2; Tables 11.4, 11.5 and 11.6 and Figures 11.17 - 11.23) and most of the "Crawling Man" cases (Subsection 11.4.5; Tables 11.13, 11.14 and 11.15 and Figures 11.36 - 11.39) do not exhibit the x-y asymmetry observed in the illuminating fields except in the anomalous case $\phi_s = 270^0$; where some of the y-components are lower than their corresponding x-components by as much as 20dB. Otherwise, x and y components tend to be of comparable magnitude and z-components tend to be below the x-components by between 10 and 20dB.

It would seem from the geometry that the horizontal field contributions from the scatterer at $\phi_s = 0^0$ and 180^0 should be predominantly y-directed and that those from $\phi_s = 90^0$ and 270^0 should be predominantly x-directed (since the scattered wave appears as a spherical wave emanating from the scatterer center). Considering the case of a scatterer at $\phi_s = 0^0$ or 180^0, the x-contribution comes from the fact that the scatterer center and antenna are at different elevations and hence the wave propagation vector for the scattered wave has a vertical component. This produces an x-component of the free-space scattered wave field.

Without ground reflections, this x-component might not be as large as the y-component. There would be only a y-component and a z-component if the antenna and scatterer center were at the same height and only a small x-component if the height discrepancy were small. The ground reflections should favor vertical over horizontal polarization, since the effective ground conductivity is reasonably high at 57MHz. The antenna and scatterer center heights are large enough to produce a

significant vertical component of the wave propagation vector for the ground-reflected scattered wave which is vertically polarized on ground reflection. The ground reflection of the y-component of the scattered wave is smaller because it is horizontally polarized. The vertically polarized ground reflected wave contains an x-component which is added to the x-component already present in the free-space scattered wave, whereas the ground reflected contribution to the y-component is smaller because it was horizontally polarized on ground reflection. All of these effects are in the direction of reducing the predominance of the y-component in the wave from a scatterer at $\phi_s = 0^o$ and 180^o. The same arguments can be applied to a scatterer at $\phi_s = 90^o$ and 270^o except that x and y are interchanged.

11.5 Conclusions and Suggestions for Future Research

The range of parameter values for which results have been obtained is extremely limited. It is not possible to draw sweeping conclusions about the generic class of RF intrusion-sensing systems exemplified by the system we have attempted to analyze on this project (or even about this specific configuration). Because of time and cost limitations, it was necessary to confine ourselves to a very specific configuration with tightly specified parameter values.

The electromagnetic effects we have investigated here are extremely complicated, involving near-zone effects and a scatterer with dimensions comparable to wavelength. There are a number of parameters to which the results might be quite sensitive. Among these are: constitutive parameters of the ground, which are highly sensitive to the chemical and physical composition and moisture content of soil; the constitutive parameters and dimensions of the "intruder" (the spheroidal model of which is an extremely crude approximation to a human body) and the geometric parameters of the cable, small changes in which might have a significant effect on the fields illuminating the scatterer.

The decision was made early in the project to construct an analytical model based on the concept of the plane-wave spectrum of an electromagnetic wave. This was based partially on the fact that the scattering program we planned to use, and did use, presupposed plane-wave illumination. The decision to use that particular scattering program, in turn was based on the following reasons. First, the Barber scattering program appeared to be the best one available for the purpose at hand, i.e., the best compromise between extremely accurate modelling of a human frame, requiring absolutely prohibitive computer time, and an extremely crude but highly inaccurate model requiring very little computer time. Secondly, the program had been used successfully many times and appeared to have been thoroughly checked

out. Thirdly, we had insufficient time and resources to devise a different program which would have allowed an illuminating field other than a plane wave.

Another reason for using the plane-wave spectrum concept was the desire to include ground reflection effects. For each plane wave in the spectrum, the simple theory of reflection of a plane wave by an infinite boundary can be used.

For the above reasons, no apology is made for using this form of analytical modelling. However, the negative aspect of this choice is the necessity for performing two-dimensional Fourier transformation as the final stage of the process. At the initial stage of the analysis, there was no way of knowing how computer-time intensive that process would be. After it was too late to turn back, it was found that (1) performance of the two dimensional inverse F.T. on the scattered field spectra with enough points for high accuracy and with no approximations reducing the number of points needed required a prohibitive amount of computer time, (2) conventional F.F.T. algorithims available as packaged programs would not be of much help and there was not time to devise an F.F.T. program that would fit our needs. For these reasons the stationary phase method was used as a crude approximation. It probably reduces accuracy somewhat but also reduces the required computer time very substantially and brings it within reasonable range. However, it is still too high to allow enough computations for the very extensive parametric study that we believe is needed to develop a really solid analytical understanding of the behavior of RF intrusion sensor systems of this class.

A set of preliminary results were presented several months ago, together with suggestions for ways to improve those results. Nearly all of the suggestions were carried out in the extension of the contract that followed (and some other

improvements not suggested were also made)* except for the suggestion that the use of stationary phase might not be a sufficiently good approximation and hence should be replaced by a more rigorous method of performing the inverse Fourier transformation. An attempt was made to follow that suggestion, but again there was insufficient time to develop a new and possibly more accurate approximation and attempts to use the rigorous F.T. method used to get fields in the absence of the scatterer required prohibitive computer time. Hence we reverted back to the use of the stationary phase method with only a minor modification just prior to the contract deadline, in order to allow sufficient time to produce the planned numerical results. These results were improved relative to the preliminary results, but we are still not satisfied with their accuracy.

A recommendation for future research, which we plan to carry out in continuing work on this problem, is to devise an approximate method of inverse Fourier transformation which will produce hopefully more accurate results in a much shorter running time per point. Once that is accomplished, we will re-run all of the results in this report and also study a great many more parameter variations. Separation of the various constituents of the field((1) source field in free space; (2) ground-reflected source field; (3) scattered field in free space; (4) ground-reflected scattered field) in order to assess the effects of each part of the process will be one aspect of a future study. Another aspect will be an improvement in the accuracy of the method of summing over the cable slots, which should in turn improve the accuracy of the ratio of the fields at the antenna with and without

* A "field mapping" to determine the spatial variation of illuminating fields; removal of a second propagation mode in the cable which was used in the earlier computations; reassessment of the use of the stationary phase method; correction of an erroneous value of scatterer radius; removal of all phase ambiguities in the program; improvement of the accuracy of the analytical model of the field from the source.

the scatterer. This problem was discussed in Section 11.4.6. It was the reason we did not directly address the issue of target detectability in this report. That is another task that is planned for the continuing work. As a final step, we will present those results for which experimental comparisons are possible in a form amenable to direct graphical comparison with these experimental results.

Table 11.1

x-component of Field Amplitude (-dB) (negative decibels)

$-\lvert E_x \rvert$ dB	1	2	3	4	5	6	7	8
	Illuminating Field No Ground Reflection				Illuminating Field With Ground Reflection			
ρ_s-meters	$\phi=0^o$	$\phi=90^o$	$\phi=180^o$	$\phi=270^o$	$\phi=0^o$	$\phi=90^o$	$\phi=180^o$	$\phi=270^o$
17.5	33.9	42.2	36.6	21.3	48.1	58.0	53.2	34.0
19.0	26.7	40.0	-	18.8	35.9	56.6	52.9	32.0
20.5	16.5	37.9	35.6	17.4	26.1	54.2	52.1	32.1
22.0	13.7	38.7	34.2	14.7	22.2	54.3	50.4	26.7
23.5	17.6	38.3	30.3	11.2	23.3	58.0	44.1	23.7
25.0	15.4	42.7	33.8	11.8	23.0	69.2	48.2	25.9
26.5	11.8	38.6	35.0	12.9	20.5	55.7	53.0	26.7
28.0	12.3	38.5	34.9	8.15	22.9	55.4	51.8	20.4

AD-A111 590 CLARKSON COLL OF TECHNOLOGY POTSDAM NY F/G 17/9
ANALYSIS OF THE POLARIZATION DEPENDENCE OF THE INTERACTION BETW--ETC(U)
NOV 81 H R RAEMER F30602-78-C-0102
UNCLASSIFIED RADC-TR-81-244 NL

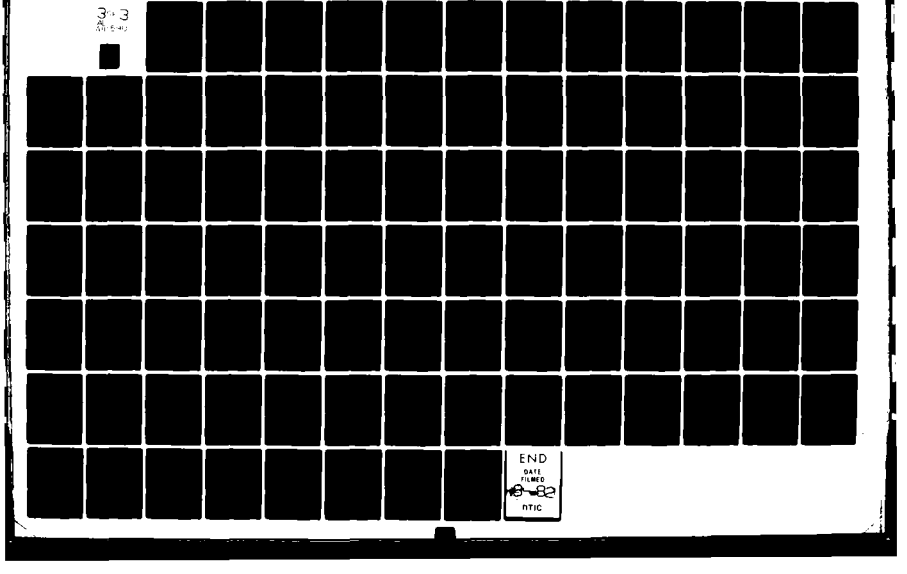

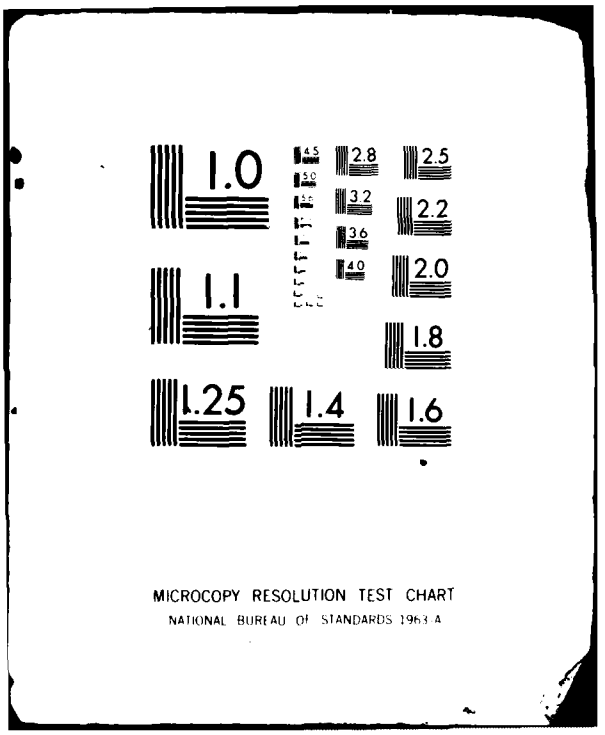
1.0
1.1
1.25
1.4
1.6
1.8
2.0
2.2
2.5
2.8
3.2
3.6
4.0
4.5
5.0
MICROCOPY RESOLUTION TEST CHART
NATIONAL BUREAU OF STANDARDS 1963-A

Table 11.2

y-component of Field Amplitude (-dB) (negative decibels)

$-\lvert E_y \rvert$ dB	1	2	3	4	5	6	7	8
	Illuminating Field No Ground Reflection				Illuminating Field With Ground Reflection			
ρ_s-meters	$\phi=0^o$	$\phi=90^o$	$\phi=180^o$	$\phi=270^o$	$\phi=0^o$	$\phi=90^o$	$\phi=180^o$	$\phi=270^o$
17.5	14.2	31.7	25.0	13.5	21.1	44.7	40.0	23.6
19.0	6.86	31.0	-	16.8	13.9	43.9	39.3	22.3
20.5	5.37	31.8	24.9	9.27	10.1	46.5	38.5	16.7
22.0	4.51	29.5	25.5	8.92	1.94	40.9	41.7	19.8
23.5	1.13	26.8	23.9	13.4	10.0	30.1	29.8	14.0
25.0	9.42	35.2	27.4	3.54	7.17	39.1	33.7	7.68
26.5	16.5	34.3	27.6	1.21	1.97	41.1	43.1	6.59
28.0	23.1	33.3	30.3	3.76	8.96	49.1	44.2	9.75

Table 11.3

z-component of Field Amplitude (-dB) (negative decibels)

$-\lvert E_z \rvert$ dB	1	2	3	4	5	6	7	8
	Illuminating Field No Ground Reflection				Illuminating Field With Ground Reflection			
ρ_s-meters	$\phi=0^o$	$\phi=90^o$	$\phi=180^o$	$\phi 270^o$	$\phi=0^o$	$\phi=90^o$	$\phi=180^o$	$\phi=270^o$
17.5	44.2	54.9	51.0	30.1	43.4	57.3	54.2	30.2
19.0	30.1	52.3	-	25.8	28.5	55.4	54.1	24.9
20.5	17.3	52.1	50.3	22.0	16.5	55.2	52.6	23.0
22.0	10.0	47.2	47.3	27.2	9.51	47.9	48.1	29.4
23.5	5.31	35.3	33.7	20.0	5.17	33.2	32.3	18.0
25.0	5.63	39.3	38.2	12.5	5.22	36.7	37.8	12.0
26.5	9.88	49.8	50.7	11.6	8.97	50.6	53.6	11.7
28.0	17.4	52.2	51.2	15.4	15.9	55.3	51.9	16.7

Table 11.4

x-component of Field Amplitude in (-dB) (negative decibels)

$-\lvert E_x \rvert$dB	1	2	3	4	5	6	7	8	9	10	11	12
	Upright Man				Radially Crawling Man				Transverse Crawling Man			
ρ_s-meters	$\phi_s=0^o$	$\phi_s=90^o$	$\phi_s=180^o$	$\phi_s=270^o$	$\phi_s=0^o$	$\phi_s=90^o$	$\phi_s=180^o$	$\phi_s=270^o$	$\phi_s=0^o$	$\phi_s=90^o$	$\phi_s=180^o$	$\phi_s=270^o$
17.5	64.7	120.0	92.6	126.0	70.5	120	92.2	92.6	43.7	54.7	110.7	-
19.0	64.7	119.0	89.8	128.0	67.3	131	91.5	95.4	45.6	56.1	110.5	-
20.5	66.2	120.0	89.3	130.0	59.6	130	89.7	97.4	47.5	57.5	110.2	-
22.0	68.2	121.0	90.3	138.0	64.4	124	89.9	98.3	49.2	58.9	110.2	-
23.5	69.3	123.0	92.3	138.0	65.0	123	91.5	98.5	50.8	60.1	110.7	-
25.0	91.8	140.0	62.6	126.0	92.8	128	57.1	90.8	-	83.3	54.1	-
26.5	93.7	141.0	63.4	127.0	95.7	131	59.7	92.3	-	80.9	108.6	-
28.0	96.2	144.0	64.4	128.0	97.8	133	62.7	93.9	-	79.9	107.7	-

Table 11.5

y-component of Field Amplitude in (-dB) (negative decibels)

$-\lvert E_y \rvert$ dB	1	2	3	4	5	6	7	8	9	10	11	12
	Upright Man				Radially Crawling Man				Transverse Crawling Man			
ρ_s-meters	$\phi_s=0^o$	$\phi_s=90^o$	$\phi_s=180^o$	$\phi_s=270^o$	$\phi_s=0^o$	$\phi_s=90^o$	$\phi_s=180^o$	$\phi_s=270^o$	$\phi_s=0^o$	$\phi_s=90^o$	$\phi_s=180^o$	$\phi_s=270^o$
17.5	67.8	123.0	91.7	143.0	72.6	124	89.7	95.7	195.0	57.8	106.2	-
19.0	68.7	123.0	89.0	144.0	68.9	126	85.1	97.8	197.0	59.1	108.3	-
20.5	68.3	124.0	89.6	147.0	66.1	128	83.1	99.5	199.	60.3	111.6	-
22.0	67.1	125.0	92.5	159.0	64.0	130	83.3	100.7	-	61.5	115.4	-
23.5	67.0	126.0	96.4	159.0	64.2	133	85.0	101.7	-	62.7	116.7	-
25.0	92.7	137.0	67.7	124.0	85.7	141	64.8	83.8	-	86.3	198.8	-
26.5	93.6	140.0	69.7	126.0	88.4	140	67.2	85.3	-	86.1	112.5	-
28.0	95.4	143.0	72.1	128.0	93.3	141	69.6	86.9	-	86.8	114.7	-

Table 11.6

z-component of Field Amplitude in (-dB) (negative decibels)

$-\|E_z\|$dB	1	2	3	4	5	6	7	8	9	10	11	12
	Upright Man				Radially Crawling Man				Transverse Crawling Man			
ρ_s-meters	$\phi_s=0^o$	$\phi_s=90^o$	$\phi_s=180^o$	$\phi_s=270^o$	$\phi_s=0^o$	$\phi_s=90^o$	$\phi_s=180^o$	$\phi_s=270^o$	$\phi_s=0^o$	$\phi_s=90^o$	$\phi_s=180^o$	$\phi_s=270^o$
17.5	75.6	148.0	99.4	132.0	55.3	126	88.5	93.1	68.1	54.0	113.1	-
19.0	76.9	155.0	102.0	138.0	56.5	129	91.2	94.6	72.9	55.4	118.1	-
20.5	77.5	153.0	101.0	141.0	70.5	131	94.5	96.2	82.7	56.7	123.6	-
22.0	77.1	156.0	100.0	146.0	58.4	132	96.0	97.8	82.2	57.9	119.8	-
23.5	75.9	161.0	100.0	145.0	60.0	133	95.2	99.3	73.2	59.2	116.5	-
25.0	110.0	156.0	69.7	156.0	97.5	135	65.7	84.6	-	82.7	68.3	-
26.5	109.0	158.0	69.3	158.0	96.4	137	66.9	86.2	-	81.3	109.9	-
28.0	104.0	159.0	68.9	160.0	98.0	139	66.8	87.8	-	81.2	116.8	-

Table 11.7 - Elevated Upright Man

x-component of Electric Field Amplitude (-dB) (negative decibels)

$-|E_x|$ dB

ℓ_s-meters	ρ_s=22.0	ρ_s=23.5	ρ_s=25.0
0.4	70.0	70.8	91.7
0.8	71.2	71.9	92.0
1.2	72.2	72.8	92.7
1.6	72.9	73.2	93.7
2.0	73.1	72.9	95.0

Table 11.8 - Elevated Upright Man

y-component of Electric Field Amplitude (-dB) (negative decibels)

$-|E_y|$ dB

ℓ_s-meters	ρ_s=22.0	ρ_s=23.5	ρ_s=25.0
0.4	67.2	68.1	94.5
0.8	67.5	69.7	95.0
1.2	68.4	72.4	96.5
1.6	70.1	76.4	96.6
2.0	72.8	77.2	96.0

Table 11.9 - Elevated Upright Man

z-component of Electric Field Amplitude (-dB) (negative decibels)

$-|E_z|$ dB

ℓ_s-meters	ρ_s=22.0	ρ_s=23.5	ρ_s=25.0
0.4	76.8	75.8	105.
0.8	76.7	76.0	100.
1.2	76.8	76.5	98.1
1.6	77.3	77.2	96.5
2.0	78.0	78.3	95.4

Table 11.10- Height Variation

x-component of Electric Field Amplitude (-dB) (negative decibels)

$-\|E_x\|$ dB L_s-meters	ρ_s=22.0	ρ_s=23.5	ρ_s= 25.0
1.60	94.9	72.0	71.0
1.70	93.1	70.6	69.4
1.78	91.7	69.3	68.2
1.88	90.2	67.7	66.8
1.98	89.1	66.5	65.7
2.08	88.1	76.7	75.6

Table 11.11- Height Variation

y-component of Electric Field Amplitude (-dB) (negative decibels)

$-|E_y|$dB

L_s-meters	ρ_s=22.0	ρ_s=23.5	ρ_s=25.0
1.60	95.2	70.0	70.3
1.70	93.7	68.3	68.5
1.78	92.7	67.0	67.1
1.88	91.8	65.5	65.5
1.98	91.3	64.3	64.2
2.08	90.9	63.8	62.7

Table 11.12- Height Variation

z-component Of Electric Field Amplitude (-dB) (negative decibels)

$-|E_z|$ dB

L_s-meters	ρ_s=22.0	ρ_s=23.5	ρ_s=25.0
1.60	117.0	78.8	80.1
1.70	113.0	77.1	78.4
1.78	110.0	75.8	77.1
1.88	107.0	74.7	75.8
1.98	104.0	73.9	74.8
2.08	102.0	72.0	69.0

Figure 11.1

$|E_x|$ dB vs. ρ

$\phi = 0^o$

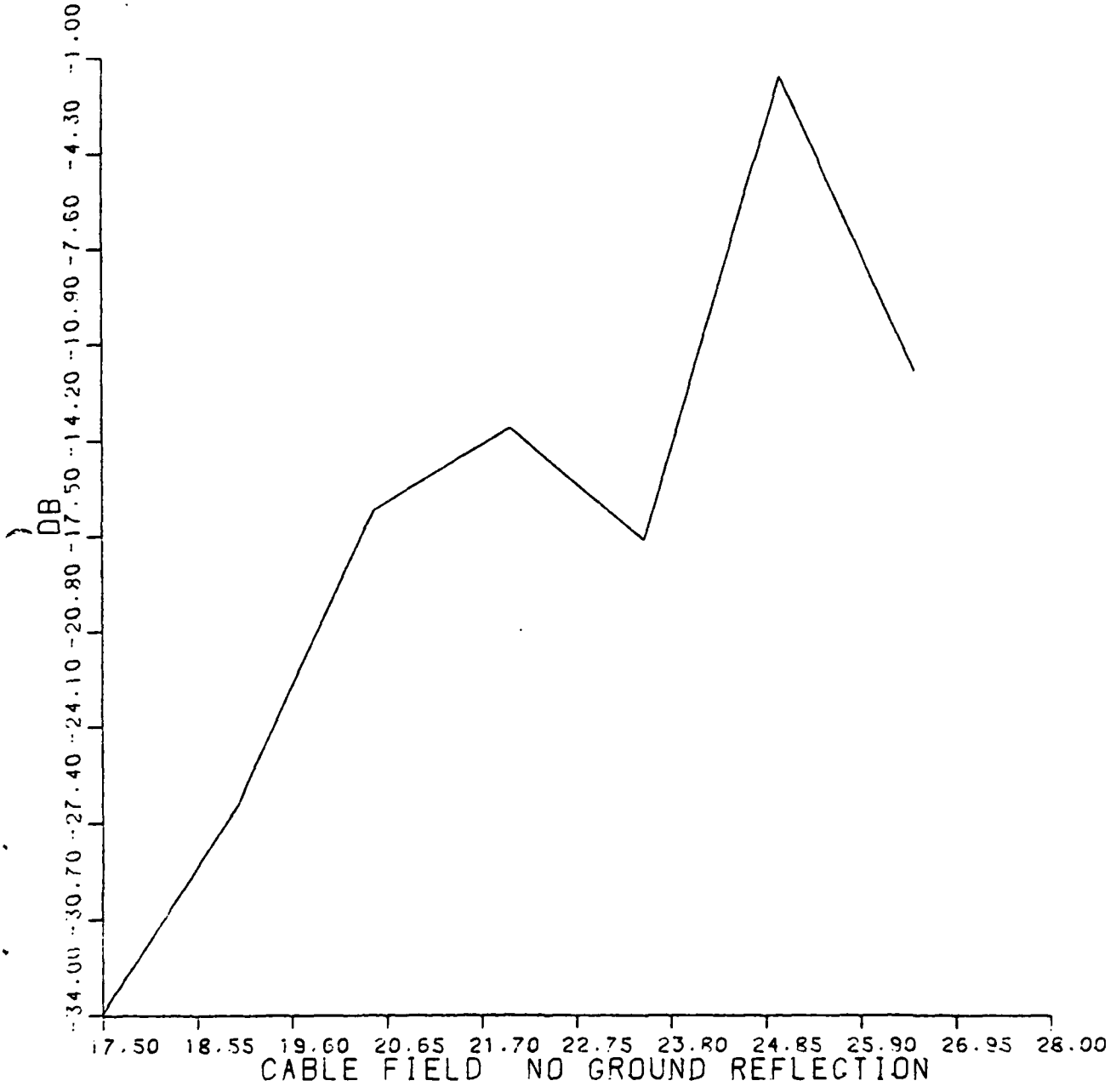

Figure 11.2

$|E_z|$dB vs. ρ

$\phi = 0^0$

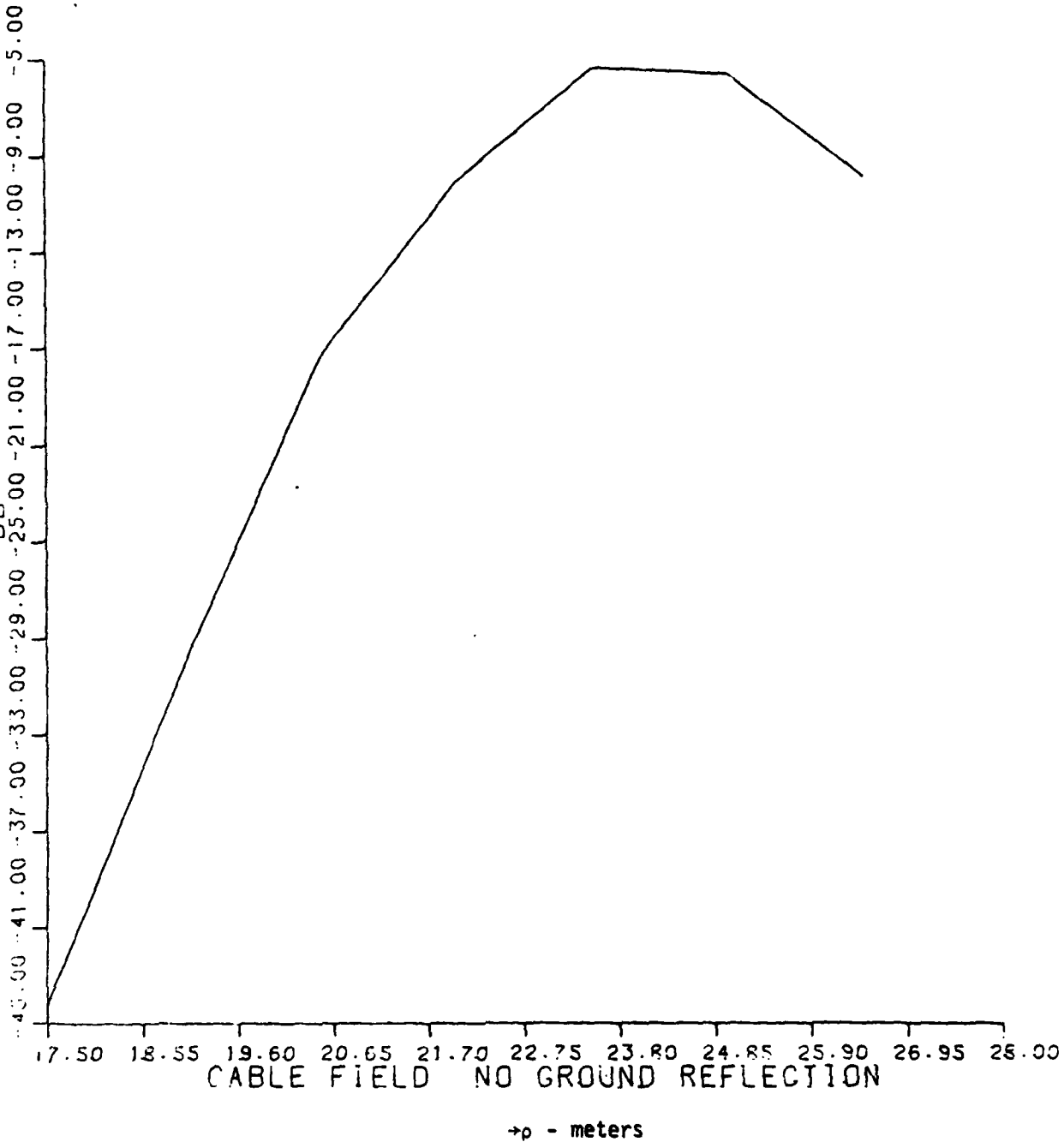

Figure 11.3

$|E_y|$ dB vs. ρ

$\phi = 90^{o}$

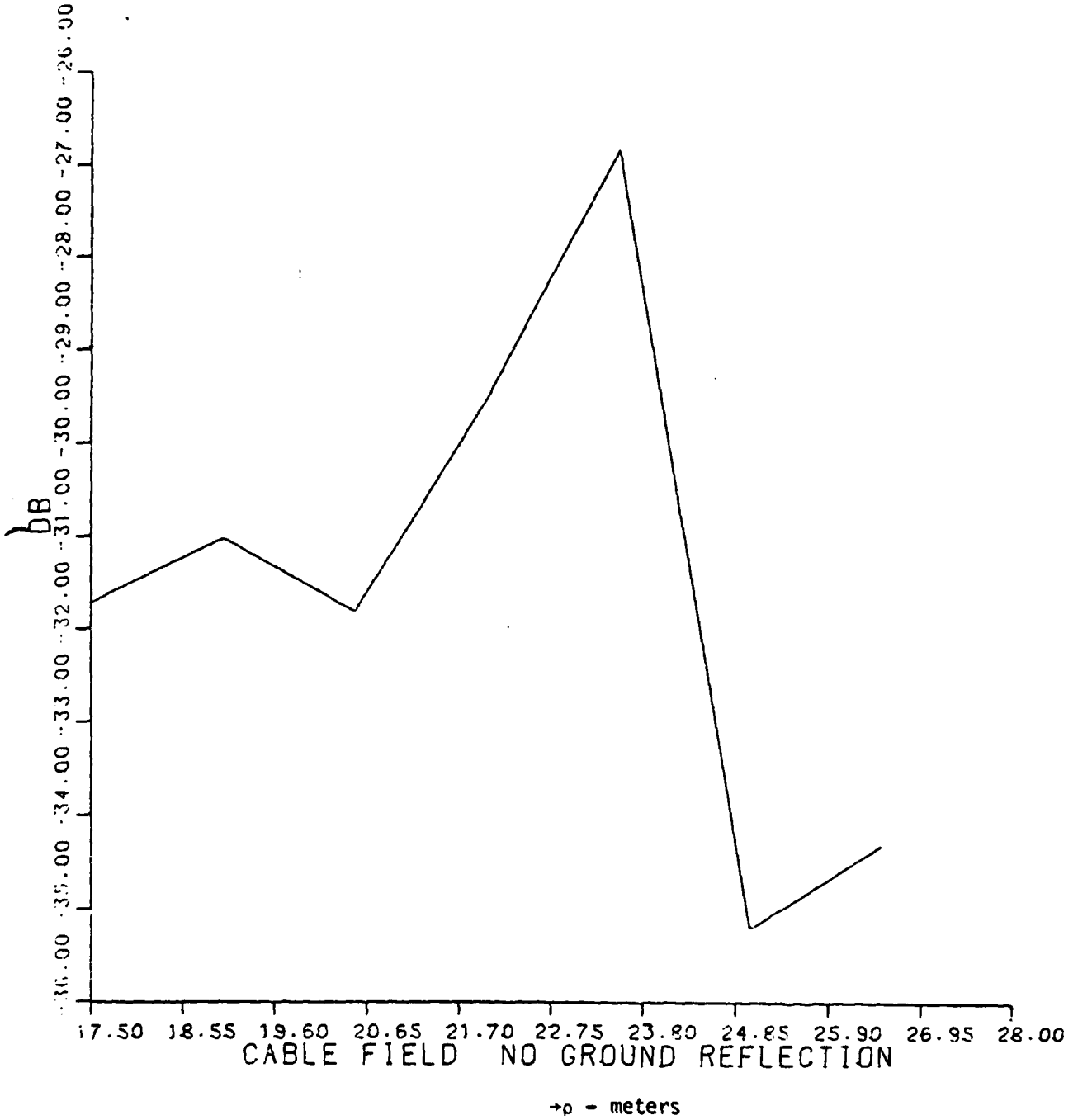

Figure 11.4

$|E_z|$dB vs. ρ

$\phi = 90^{o}$

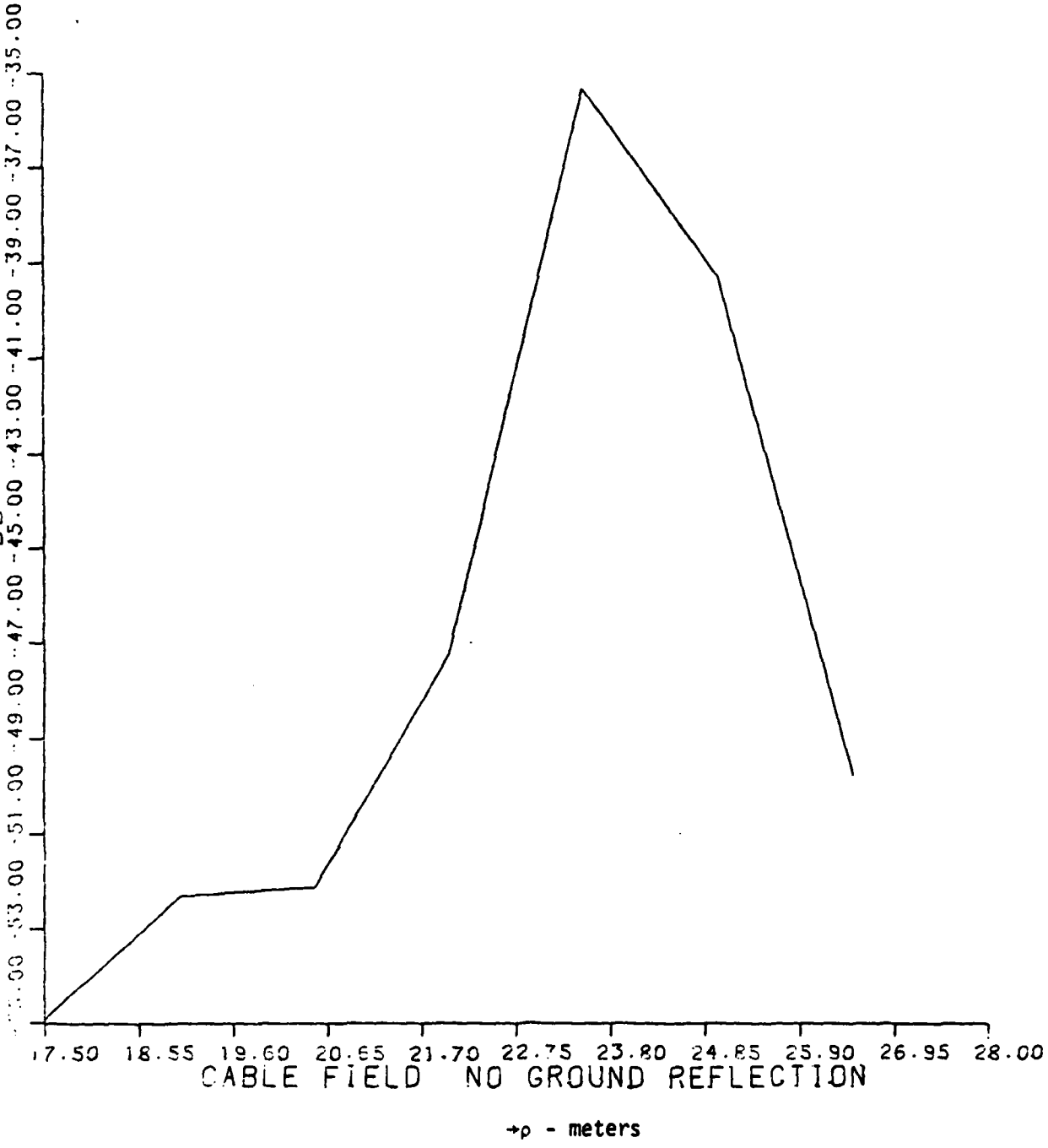

Figure 11.5

$|E_x|$ dB vs. ρ

$\phi = 180^0$

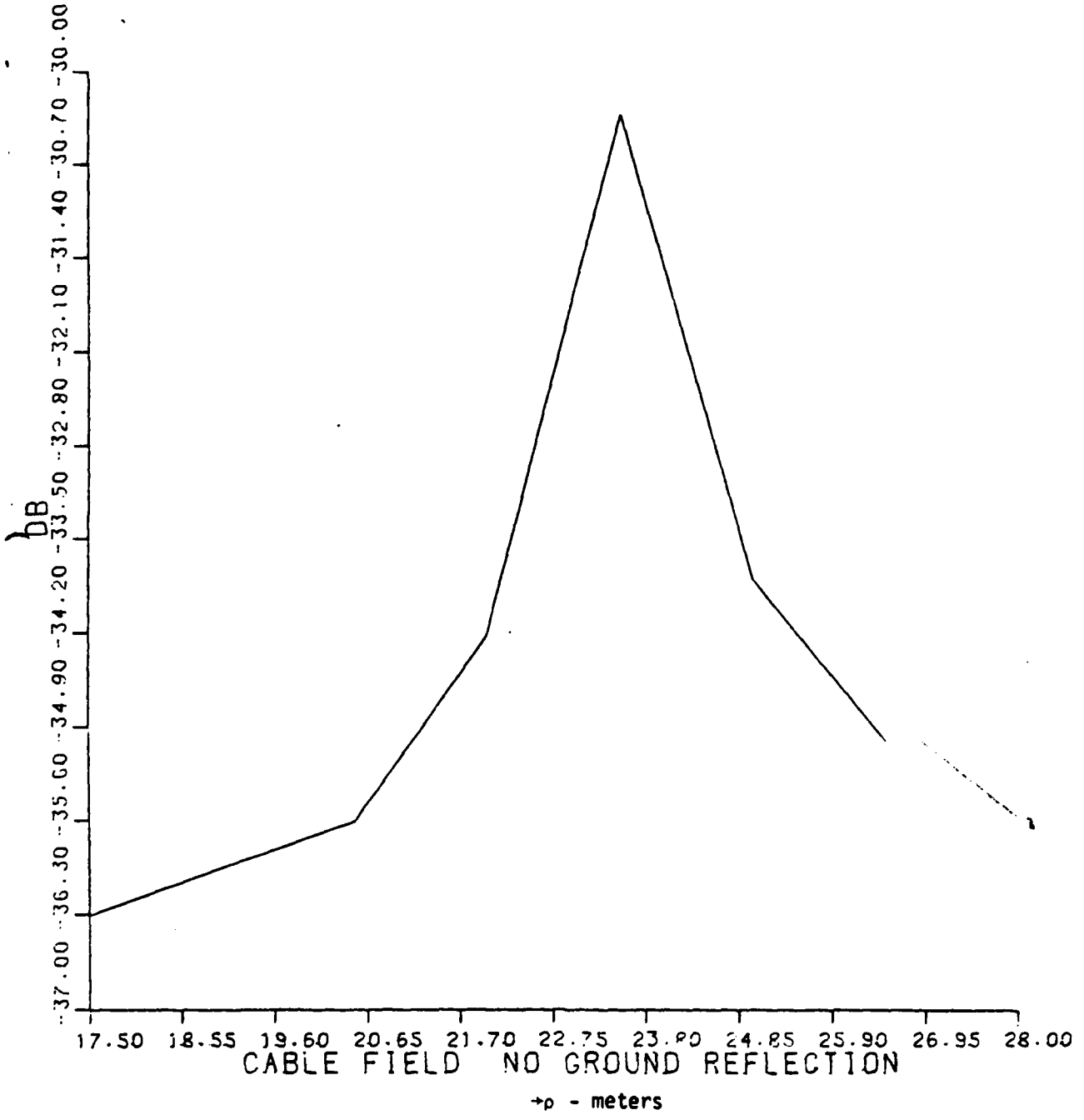

Figure 11.6

$|E_y|$dB vs. ρ

$\phi = 180^{o}$

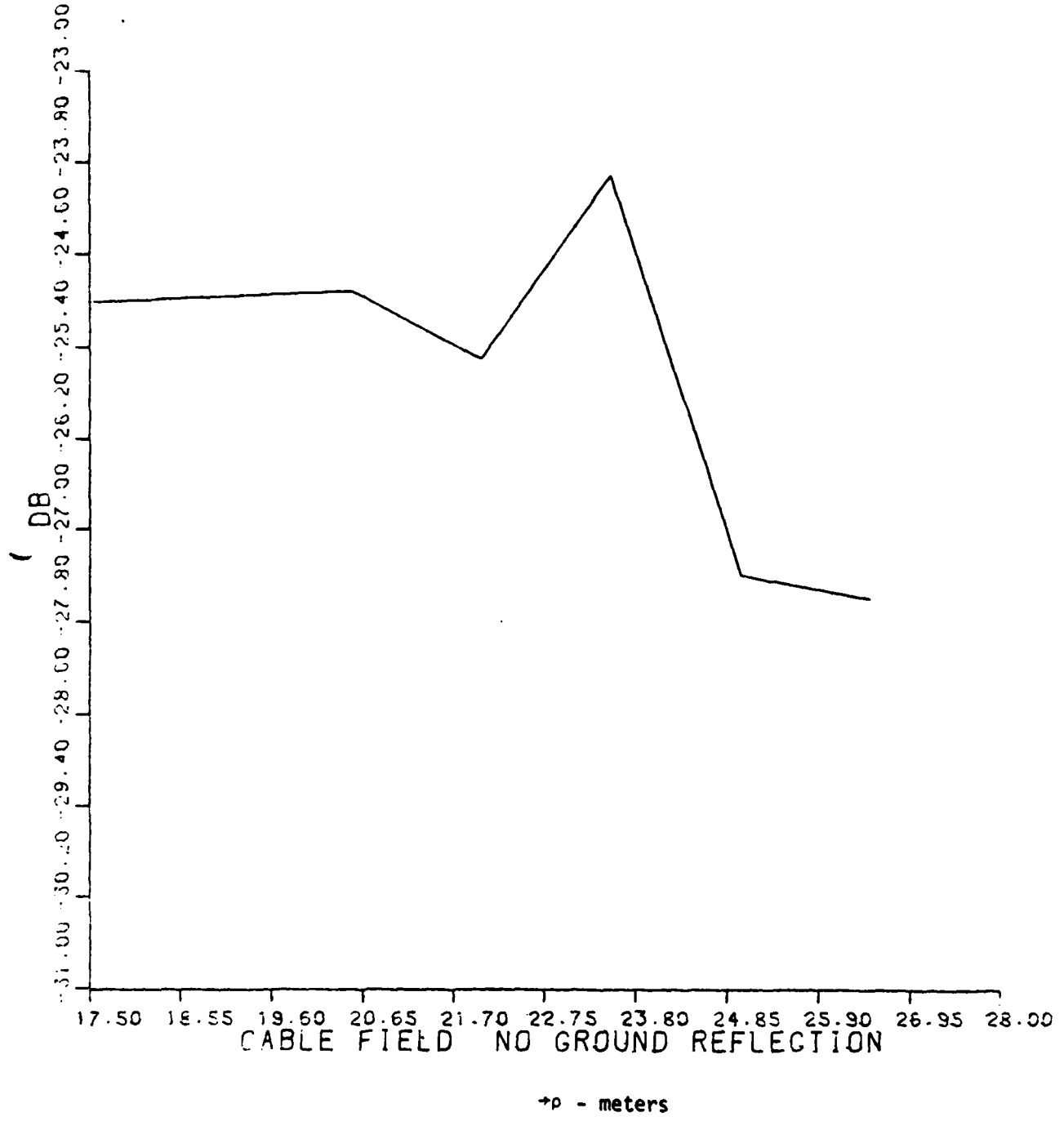

Figure 11.7

$|E_z|$ dB vs. ρ

$\phi = 180^0$

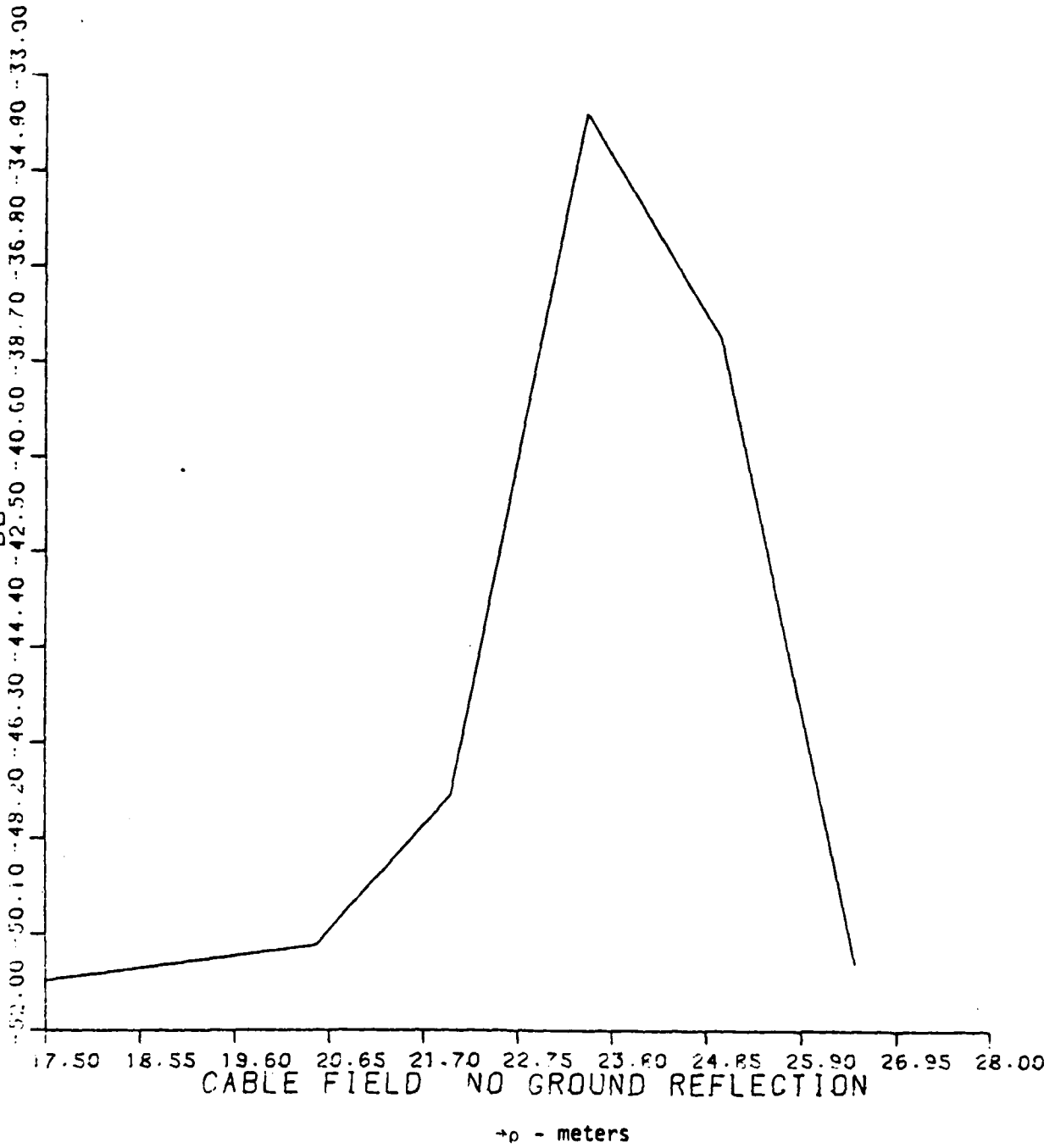

Figure 11.8

$|E_x|$dB vs. ρ

$\phi = 270^{o}$

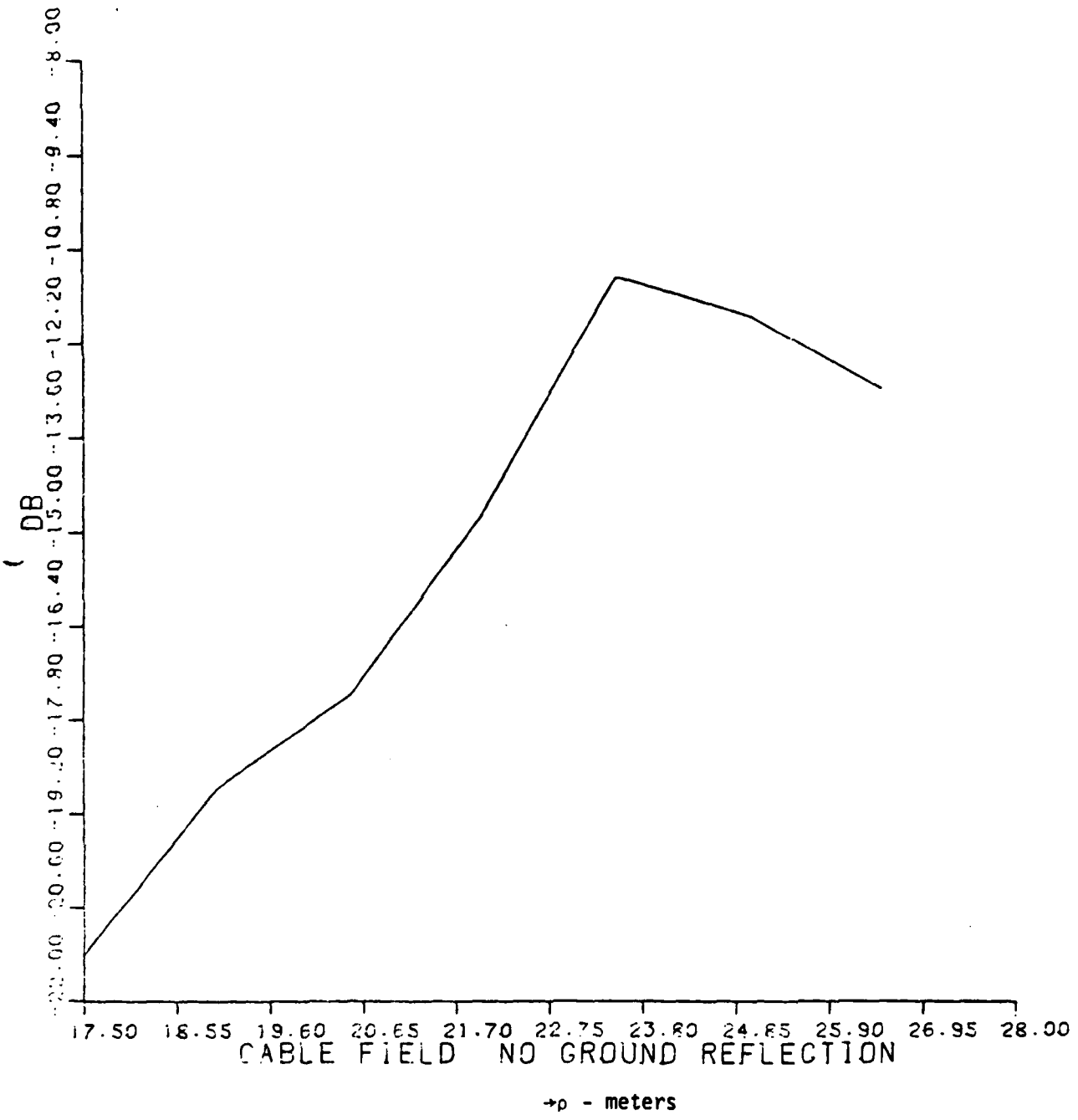

Figure 11.9

$|E_z|$ dB vs. ρ

$\phi = 0^0$

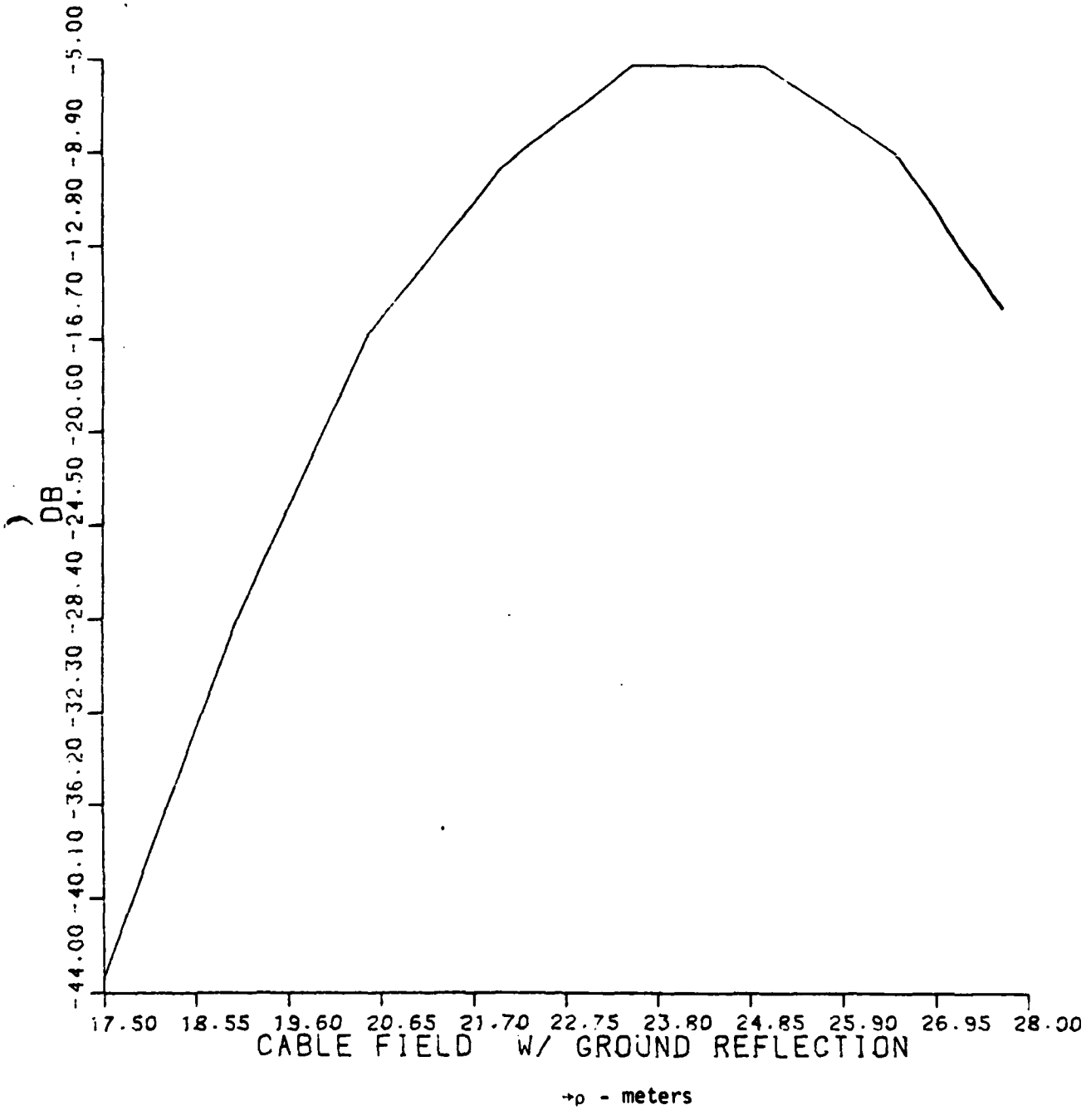

Figure 11.10

$|E_y|$dB vs. ρ

$\phi = 90^0$

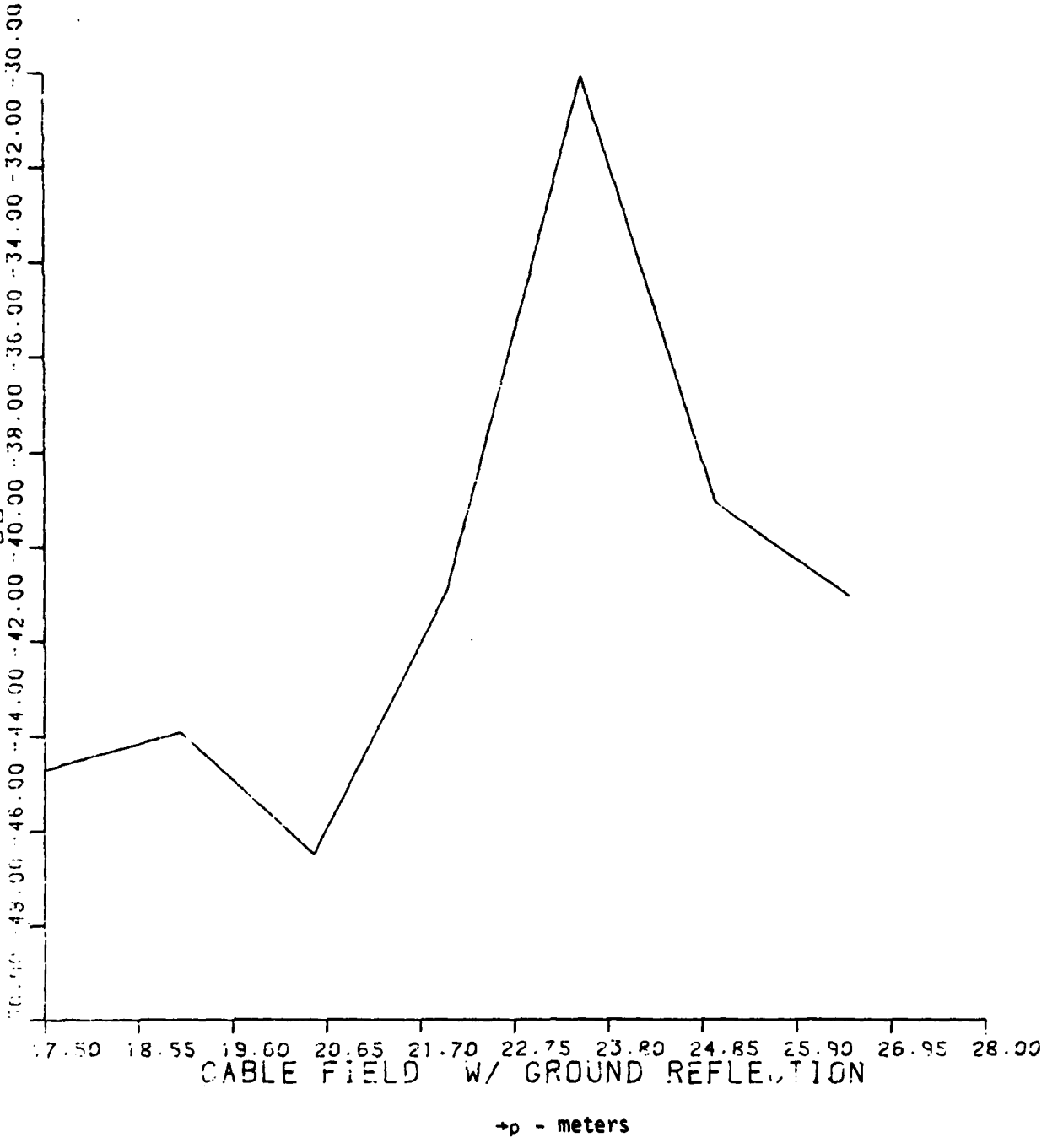

Figure 11.11

$|E_z|$dB vs. ρ

$\phi = 90^0$

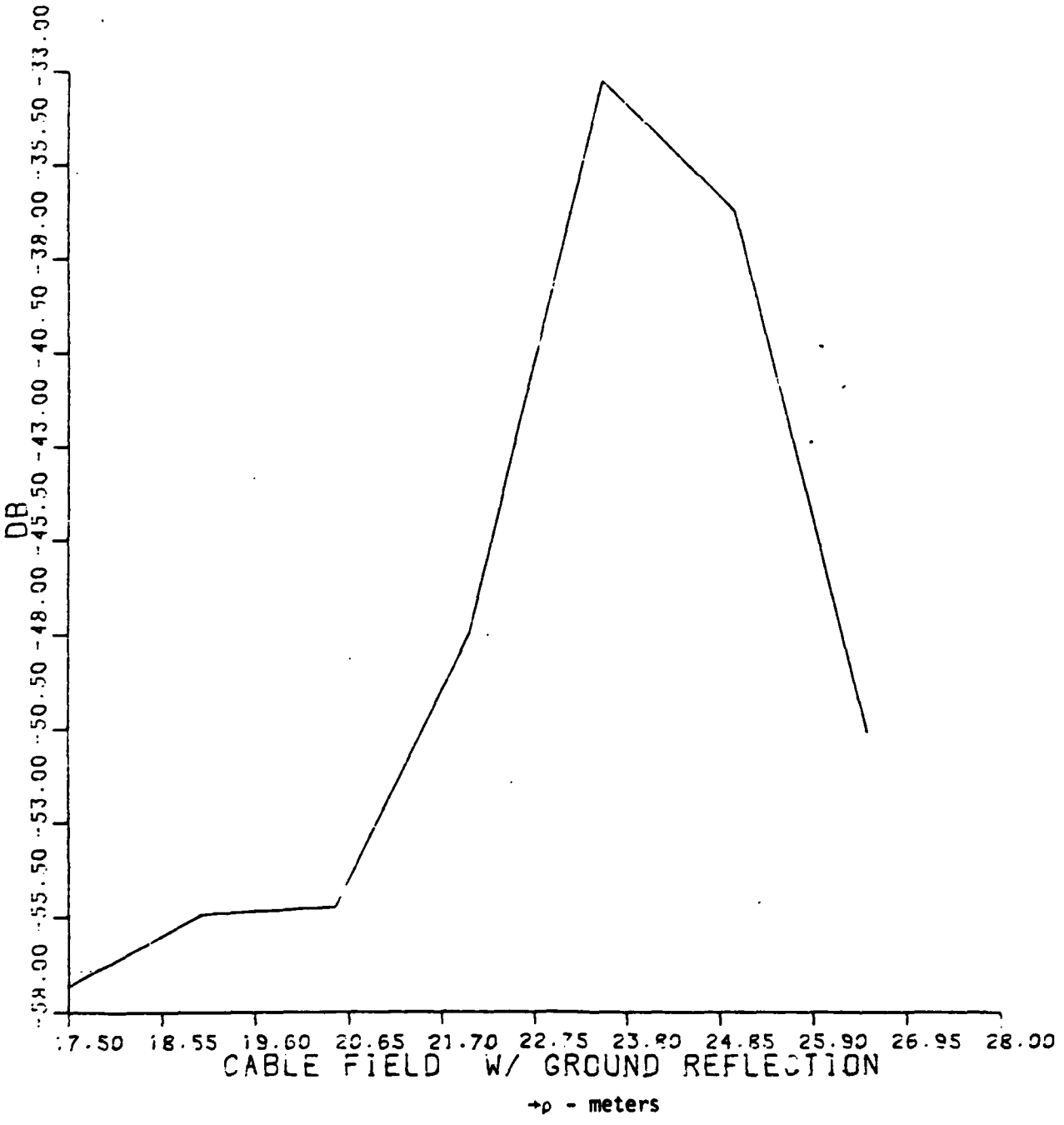

Figure 11.12

$|E_x|$dB vs. ρ

$\phi = 180^{\circ}$

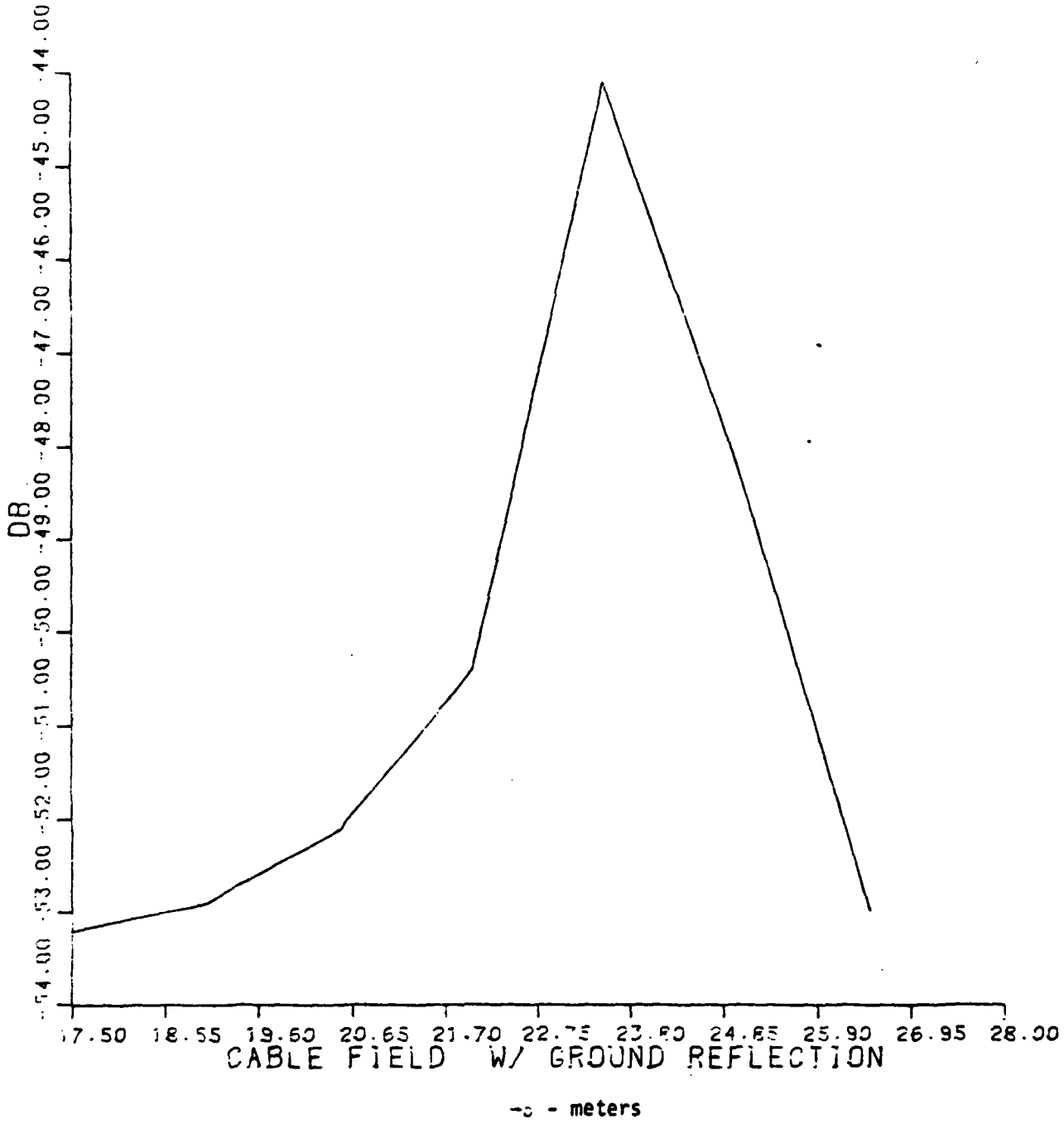

Figure 11.13

$|E_y|$ dB vs. ρ

$\phi = 180^{o}$

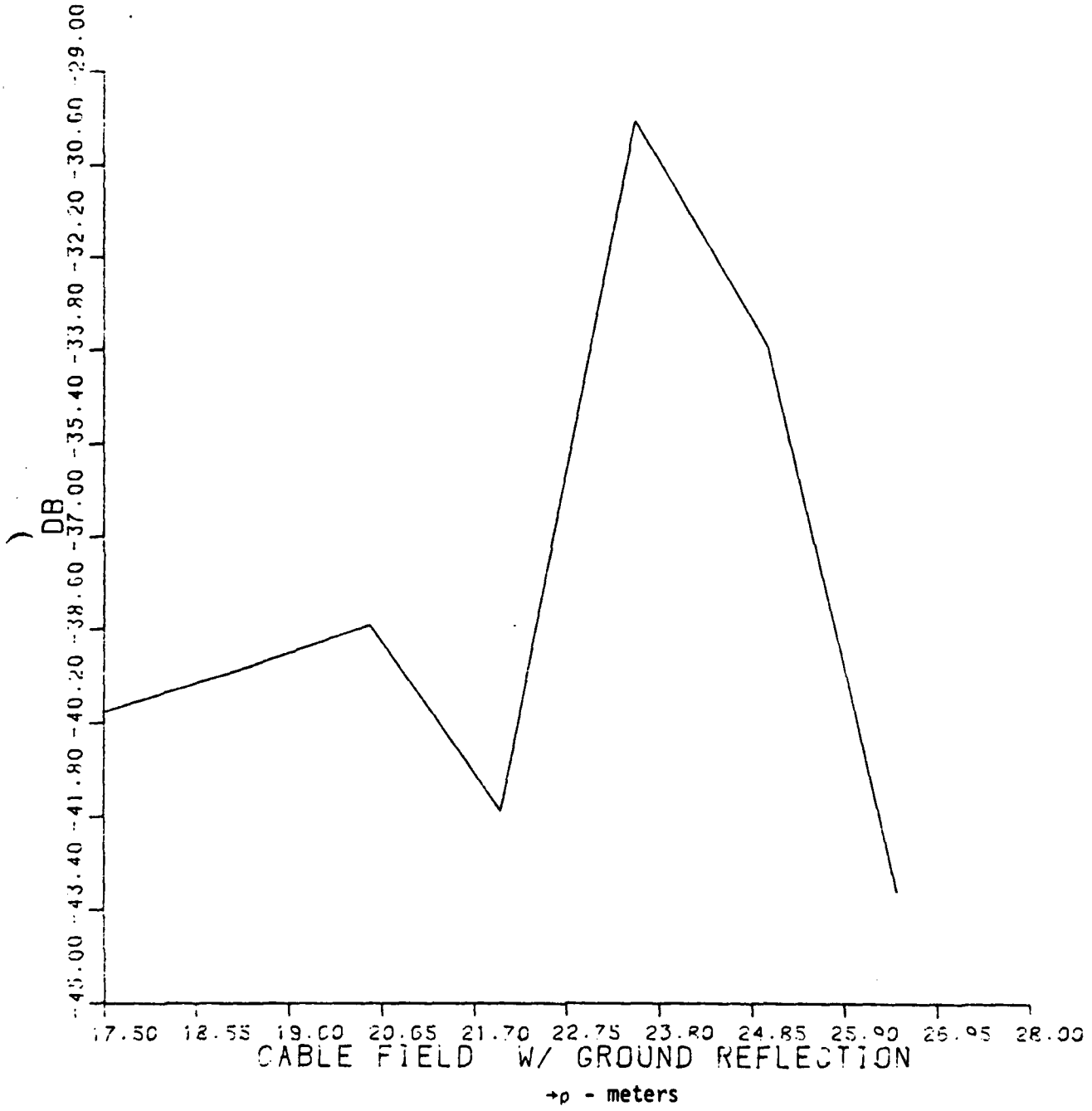

Figure 11.14

$|E_z|$ dB vs. ρ

$\phi = 180^0$

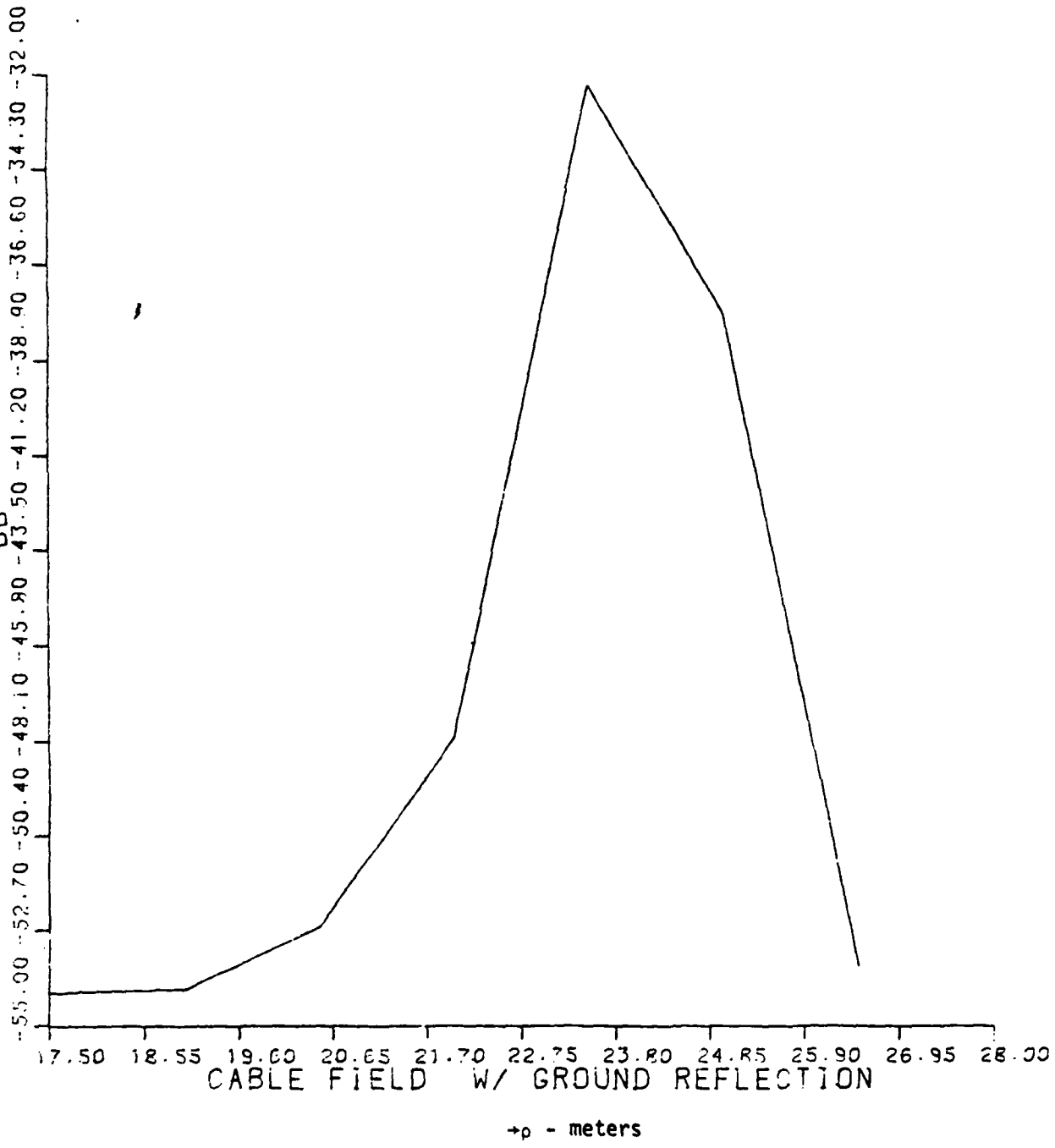

Figure 11.15

$|E_x|$ dB vs. ρ

$\phi = 270^0$

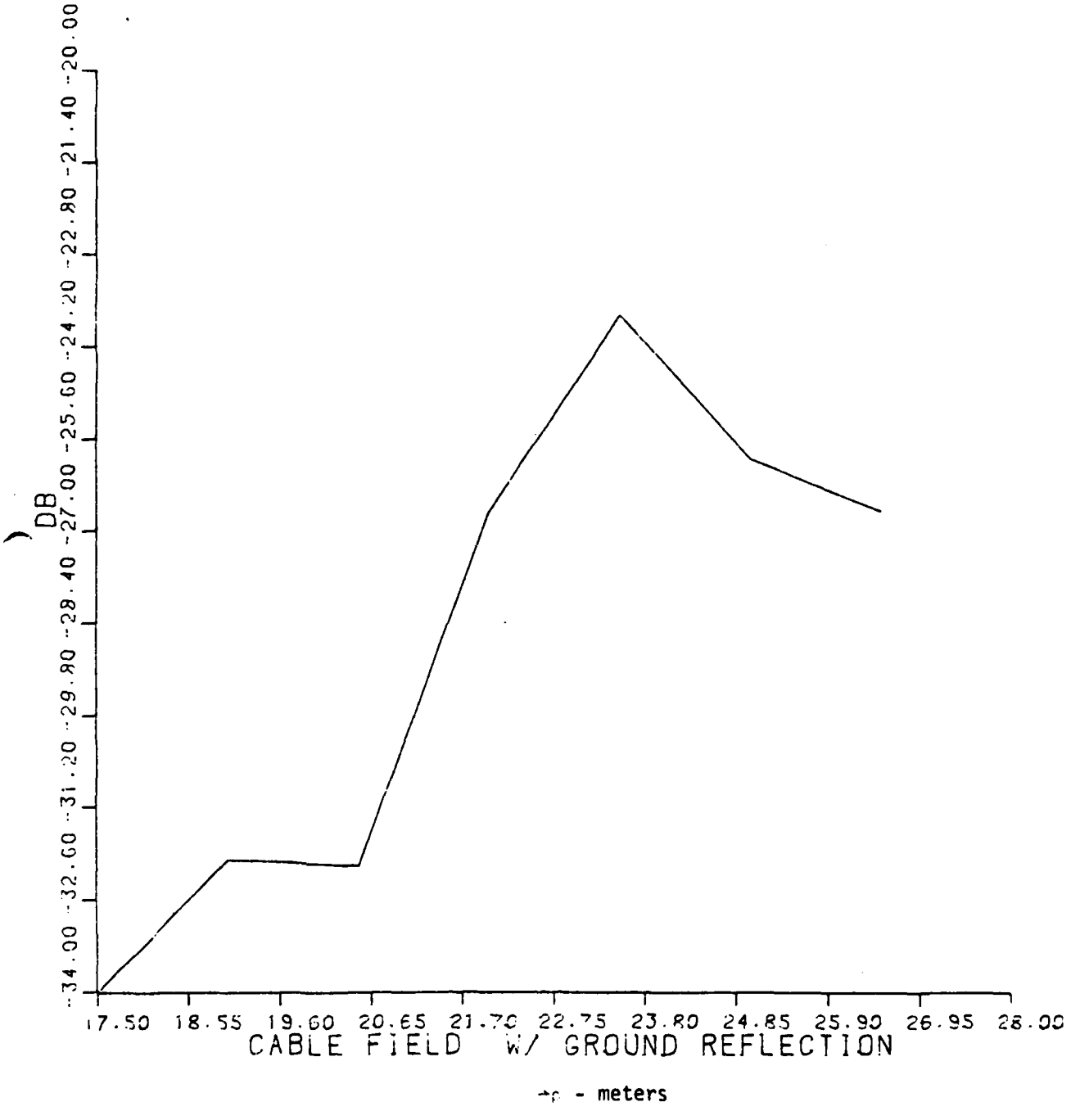

Figure 11.16

$|E_y|$ dB vs. ρ

$\phi = 270^0$

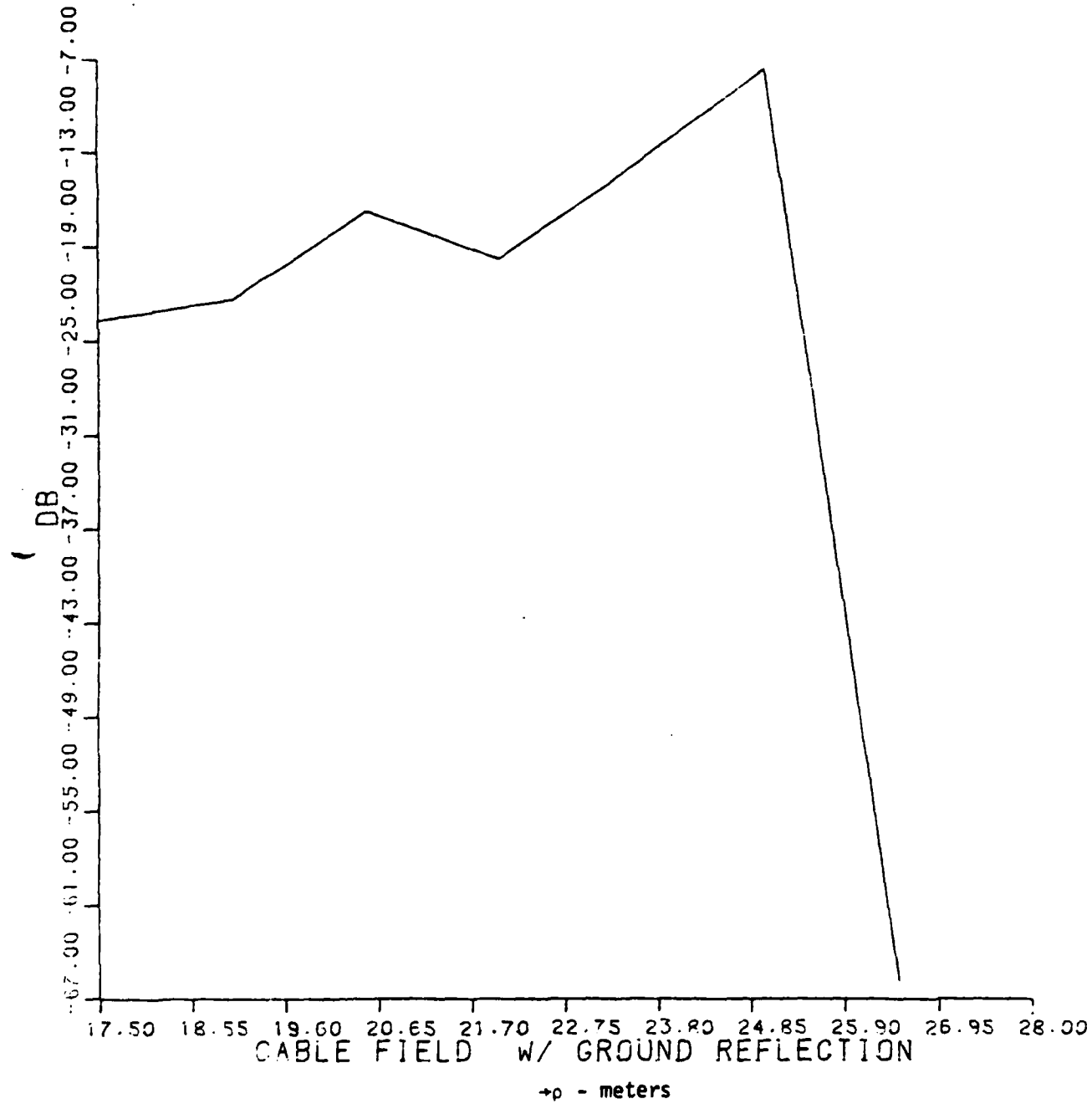

Figure 11.17

$|E_y|$dB vs. ρ_s

$\phi_s = 0^o$

Upright Man

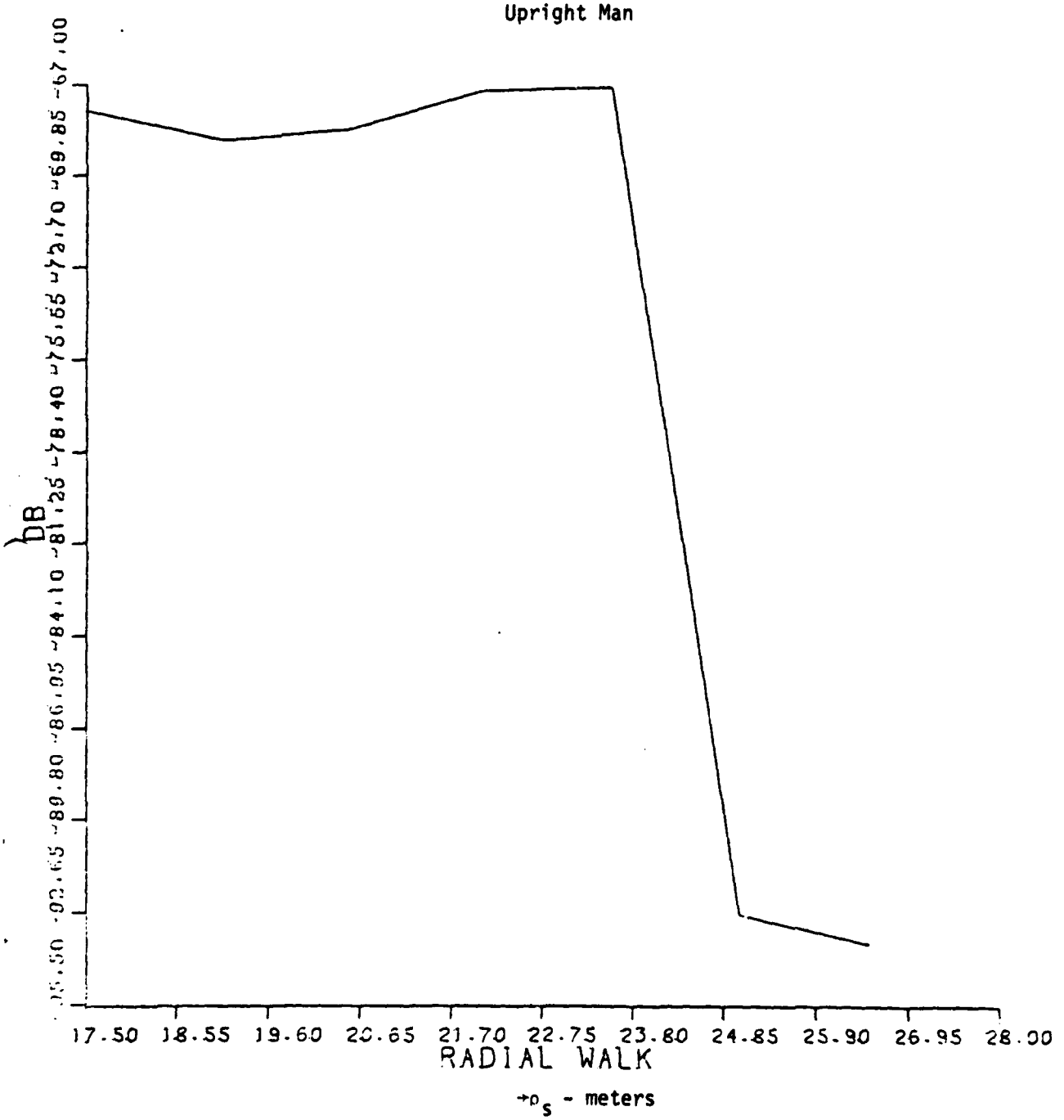

Figure 11.18

$|E_z|$ dB vs. ρ_s

$\phi_s = 0^o$

Upright Man

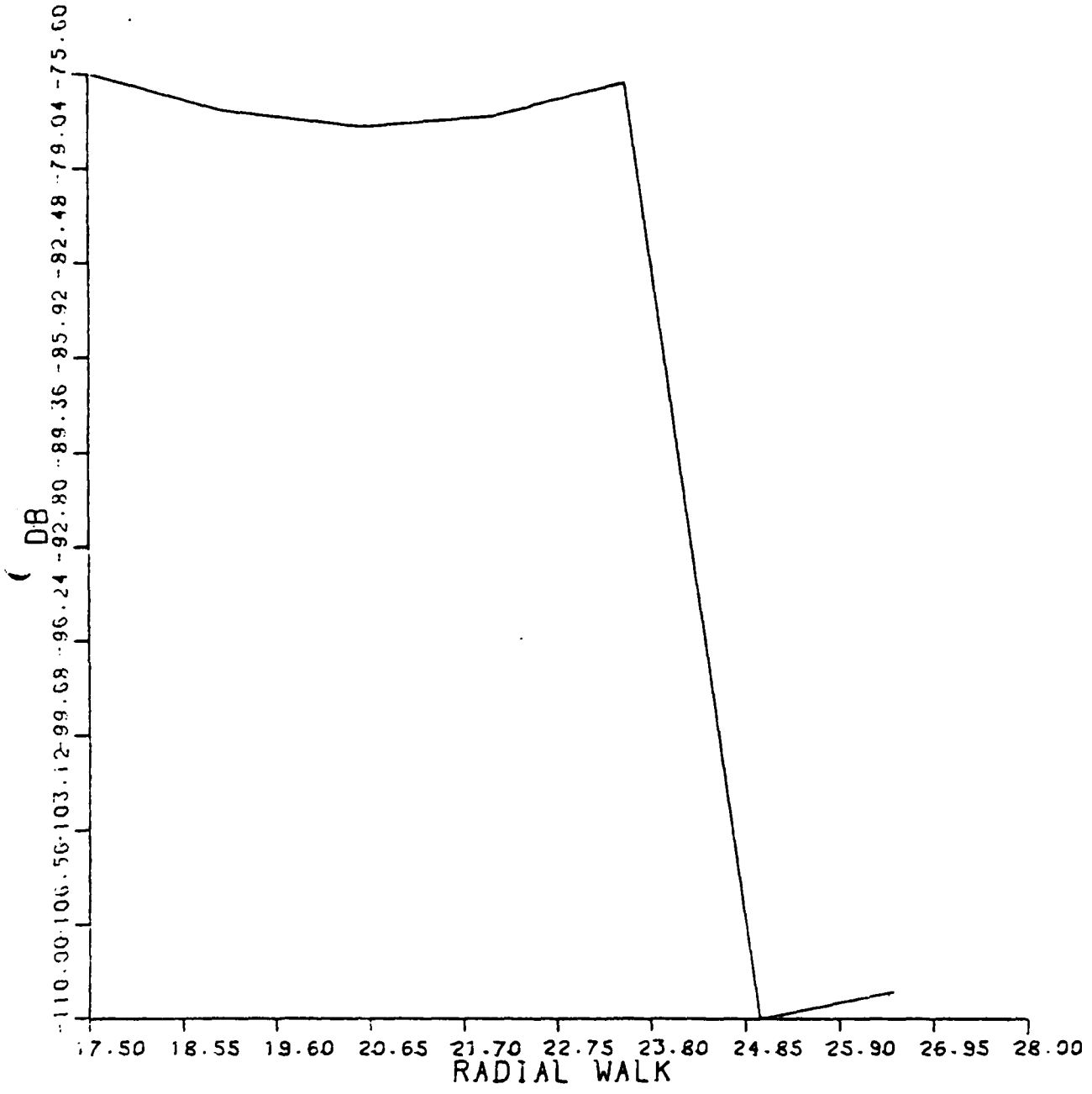

$\rightarrow \rho_s$ - meters

Figure 11.19

$|E_x|$dB vs. ρ_s

$\phi_s = 90^o$

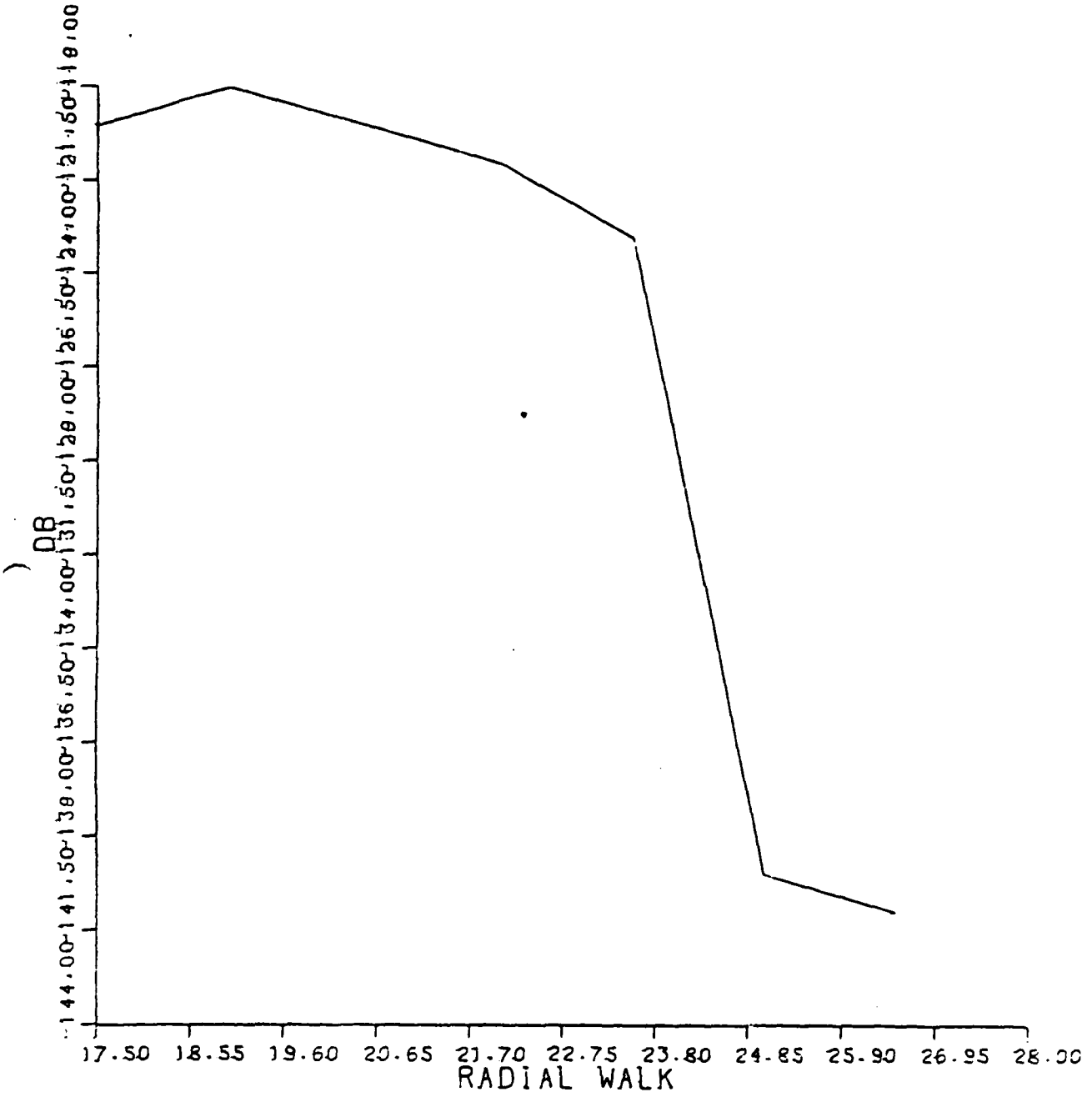

Figure 11.20

$|E_{\hat{x}}|$dB vs. ρ_s

$\phi_s = 180^0$

Upright Man

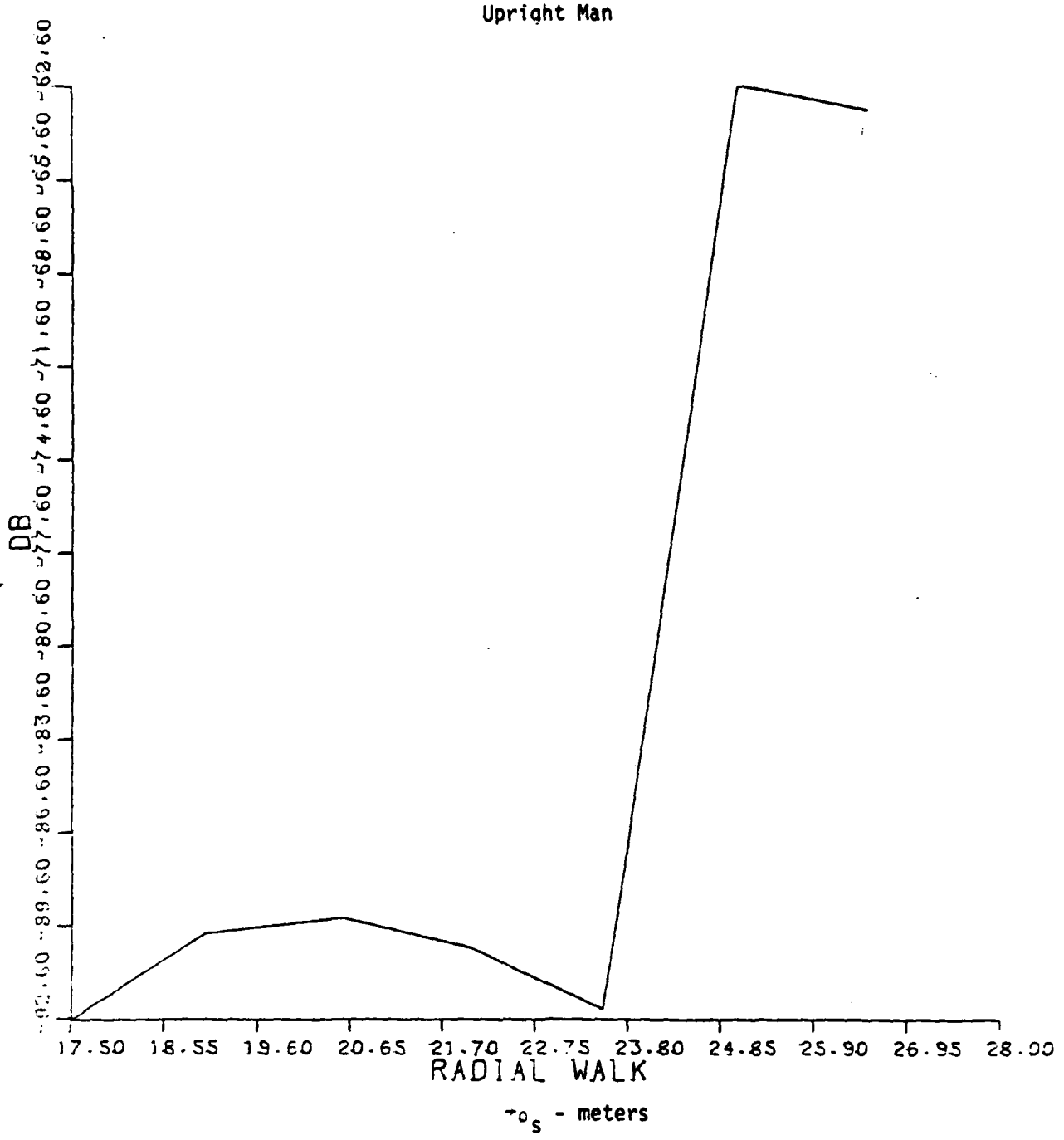

Figure 11.21

$|E_y|$dB vs. ρ_s

$\phi_s = 180^0$

Upright Man

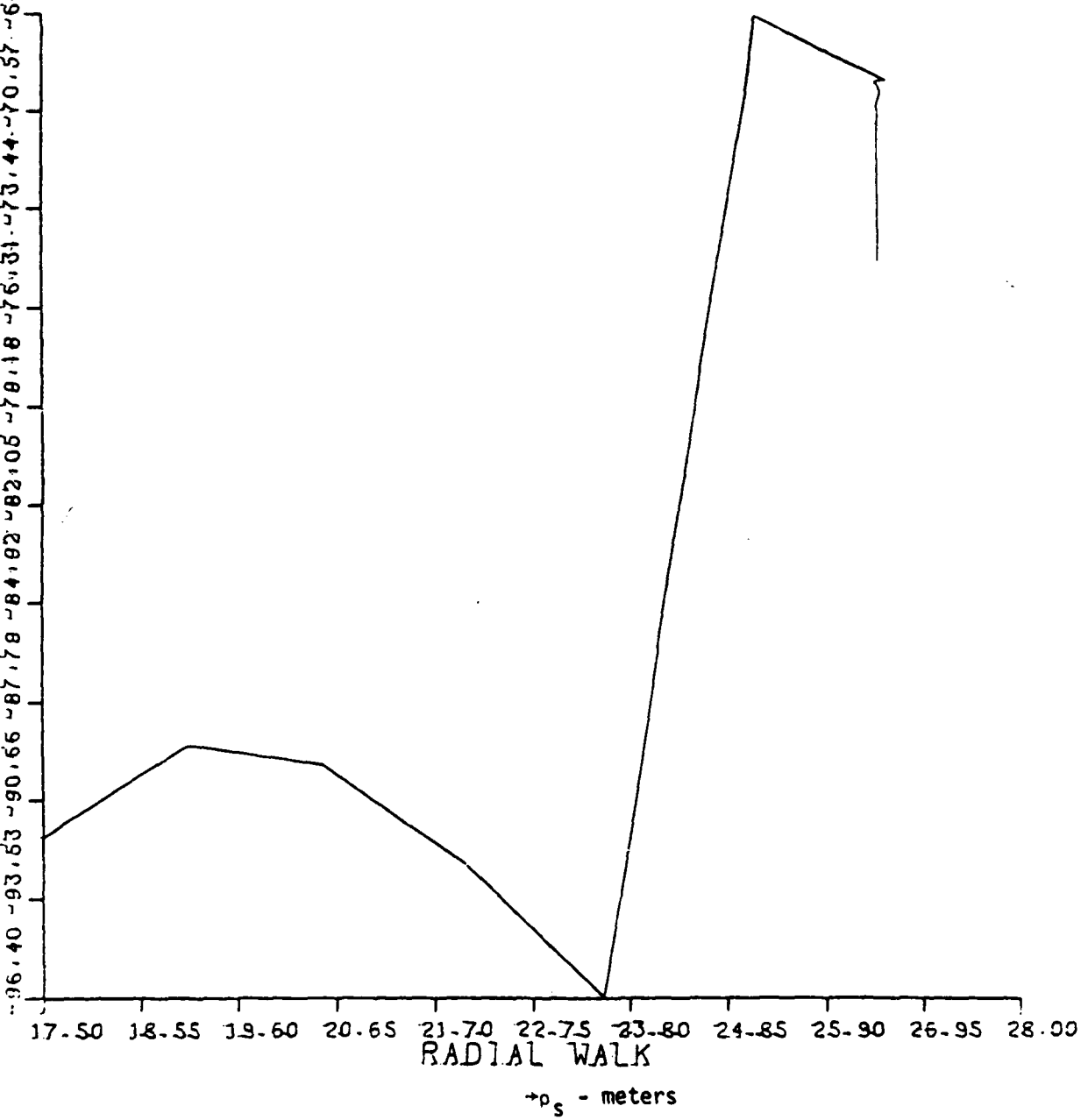

Figure 11.22

$|E_z|$dB vs. ρ_s

$\phi_s = 270^0$

Upright Man

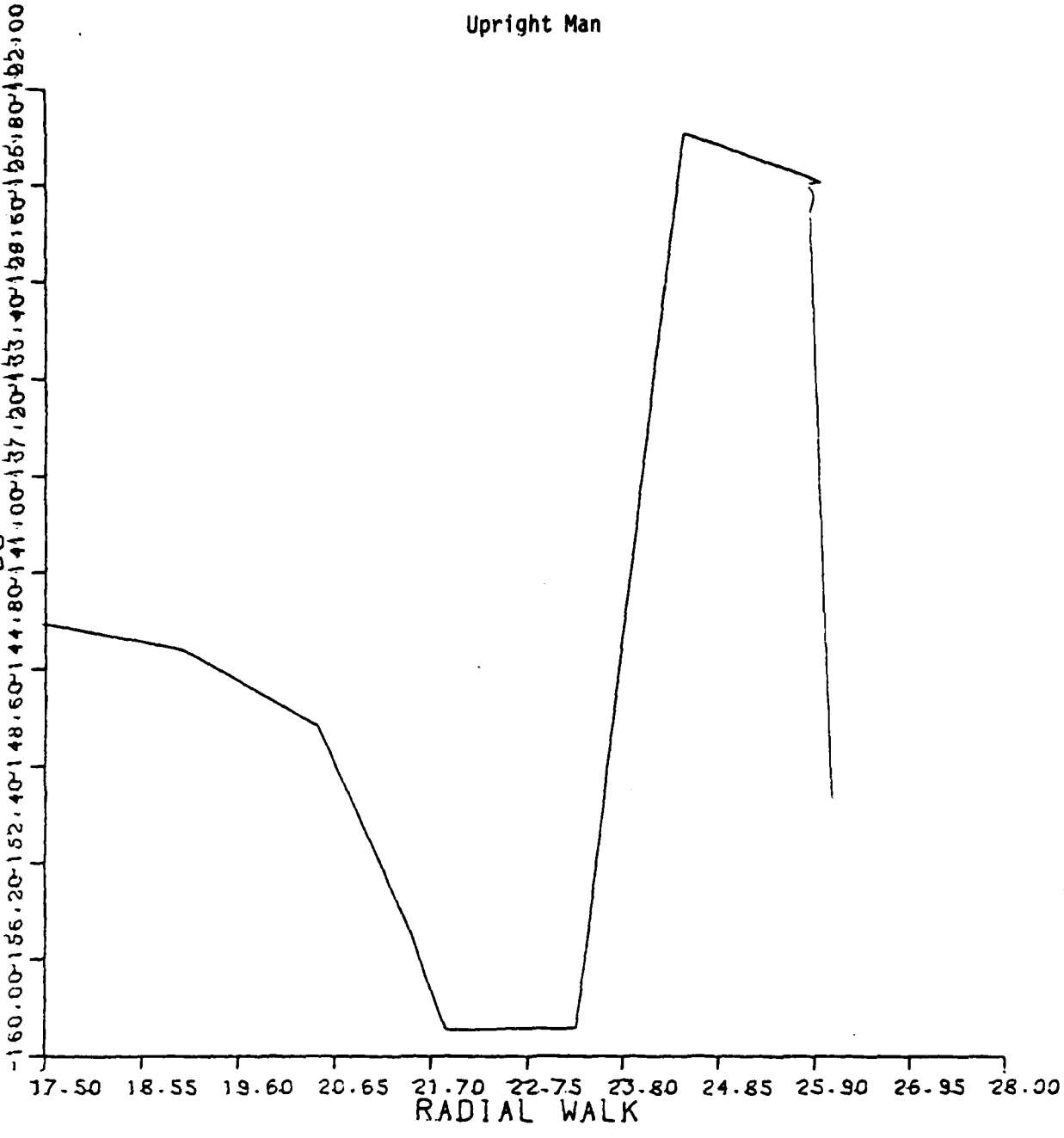

$\rightarrow \rho_s$ - meters

Figure 11.23

$|E_z|$dB vs. ρ_s

$\phi_s = 270^0$

Upright Man

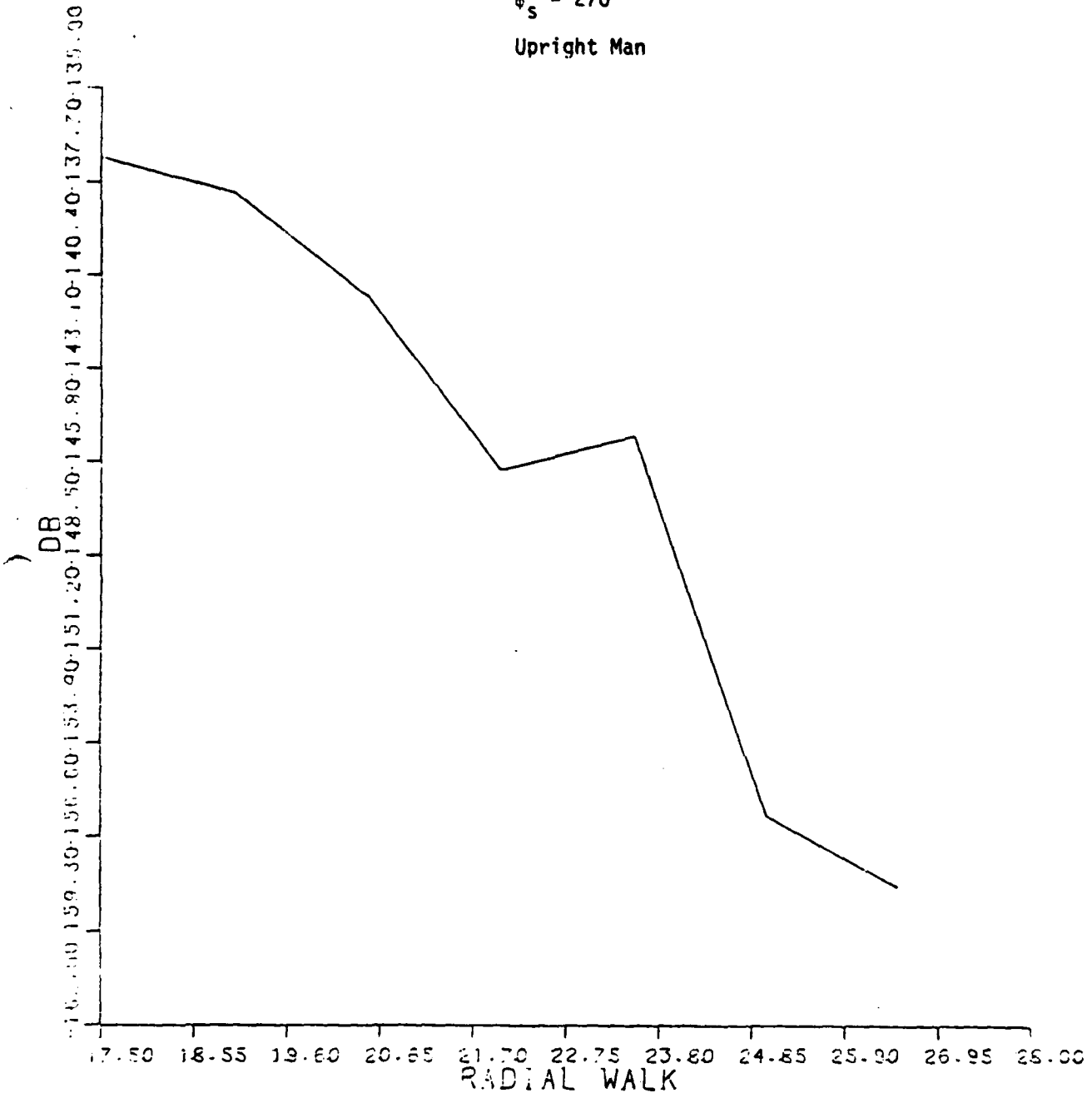

$\rightarrow \rho_s$ - meters

Figure 11.24

$|E_x|$dB vs. ℓ_s

$\rho_s = 22.0$, $\phi_s = 0^o$

Elevated Upright Man

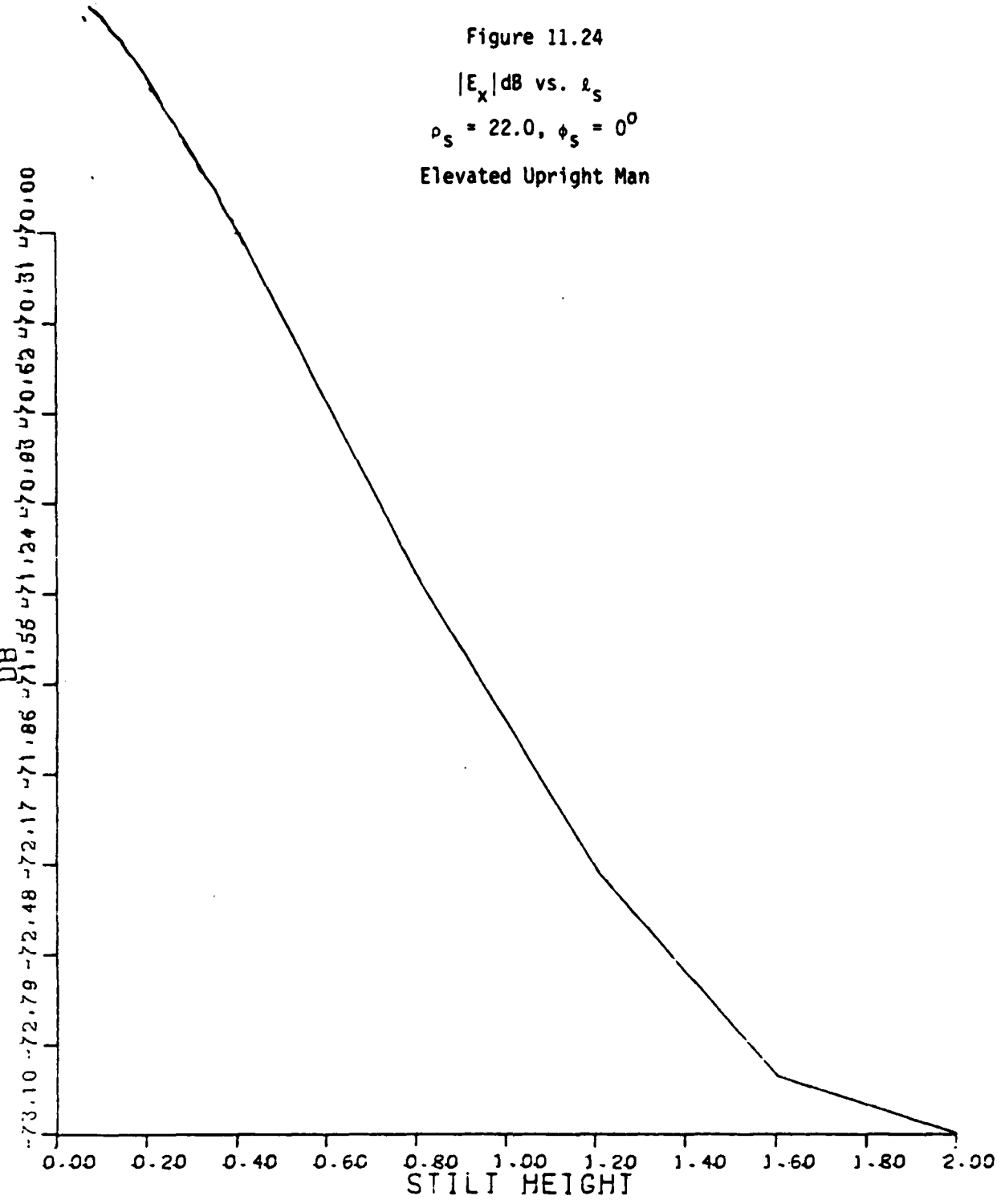

Figure 11.25

$|E_y|$dB vs. ℓ_s

$\rho_s = 22.0$, $\phi_s = 0^o$

Elevated Upright Man

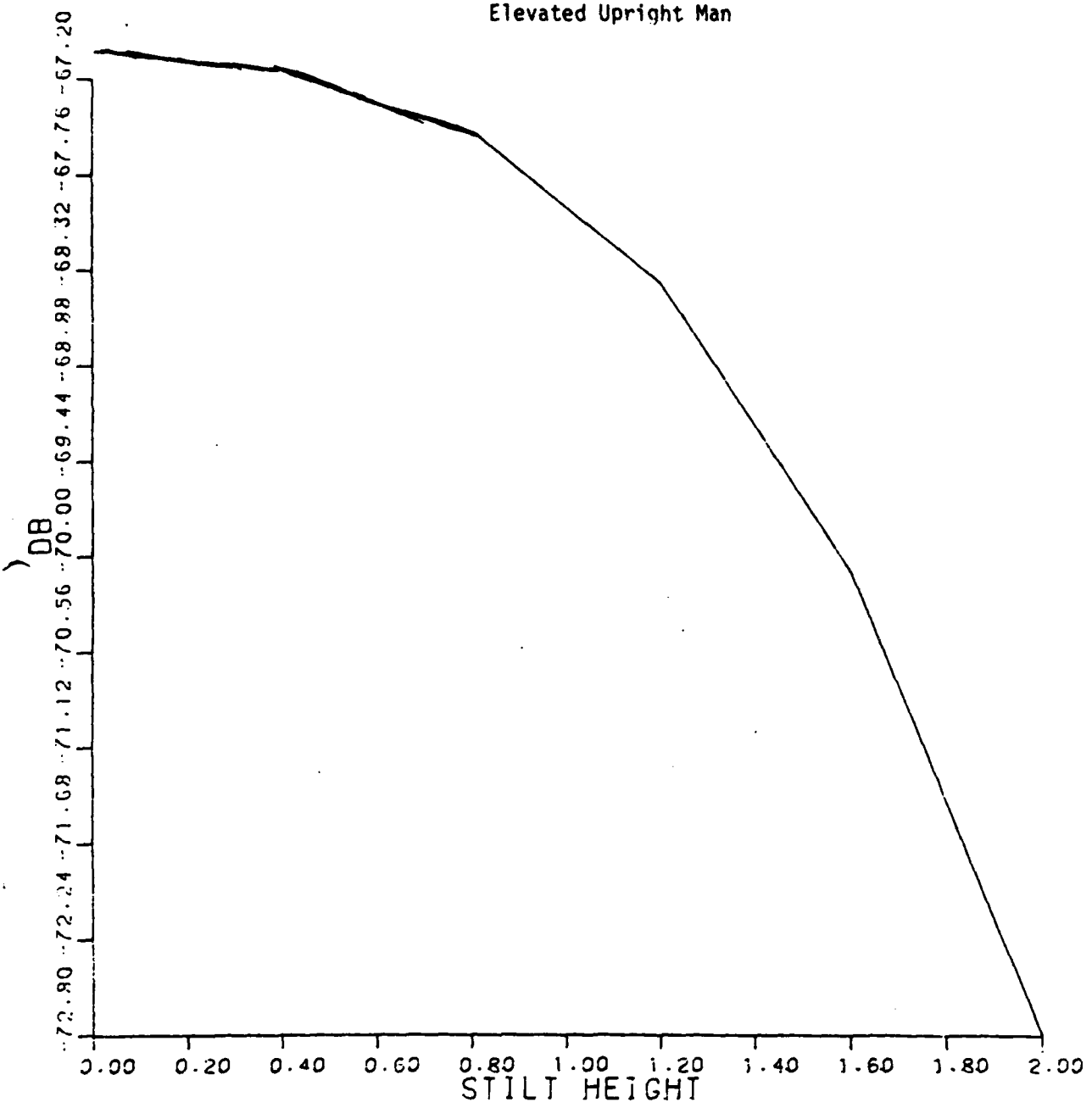

Figure 11.26

$|E_y|$dB vs. ℓ_s

$\rho_s = 23.5$, $\phi_s = 0^0$

Elevated Upright Man

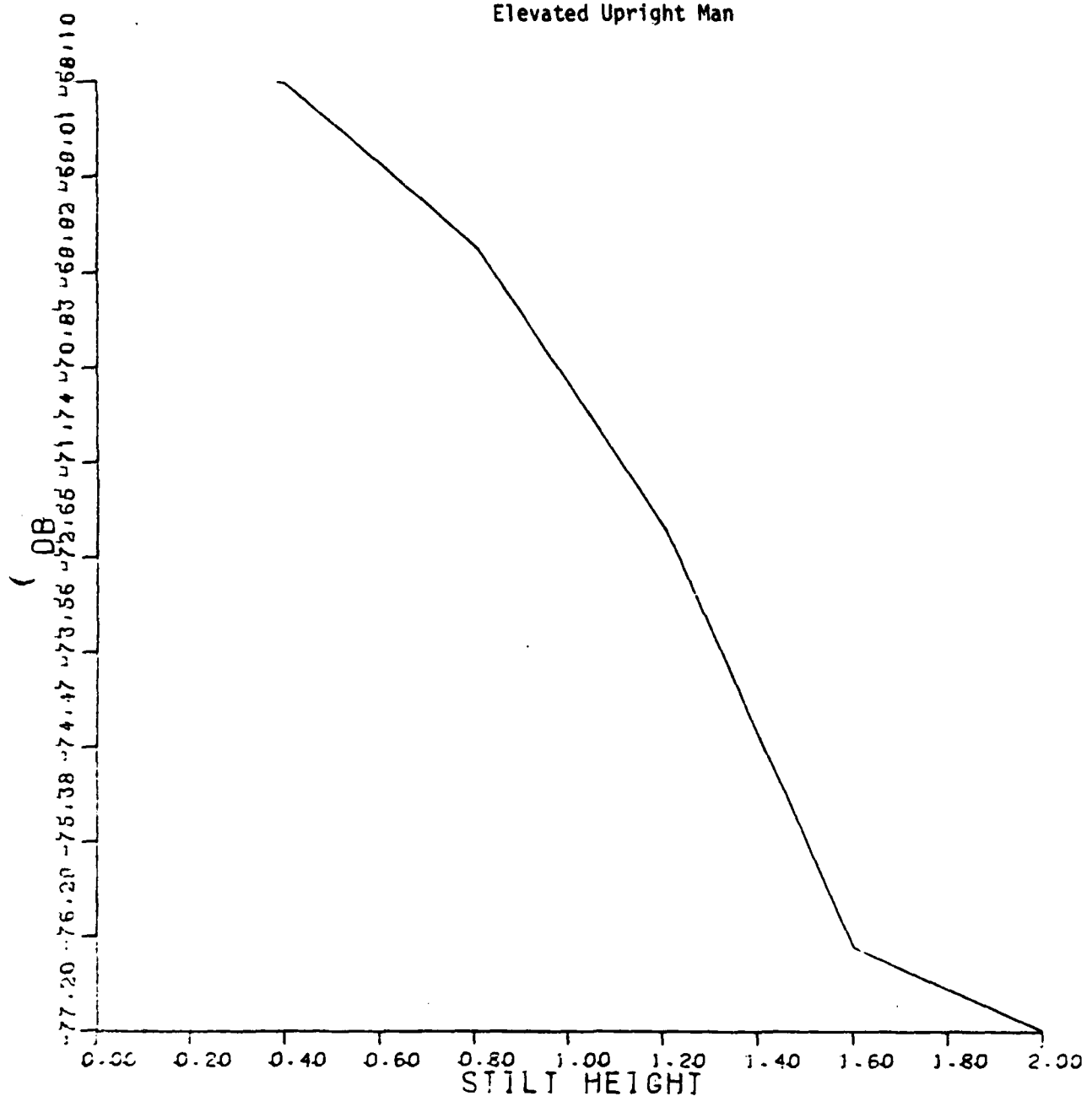

Figure 11.27

$|E_x|$ dB vs. ℓ_s

$\rho_s = 25.0$, $\phi_s = 0^0$

Elevated Upright Man

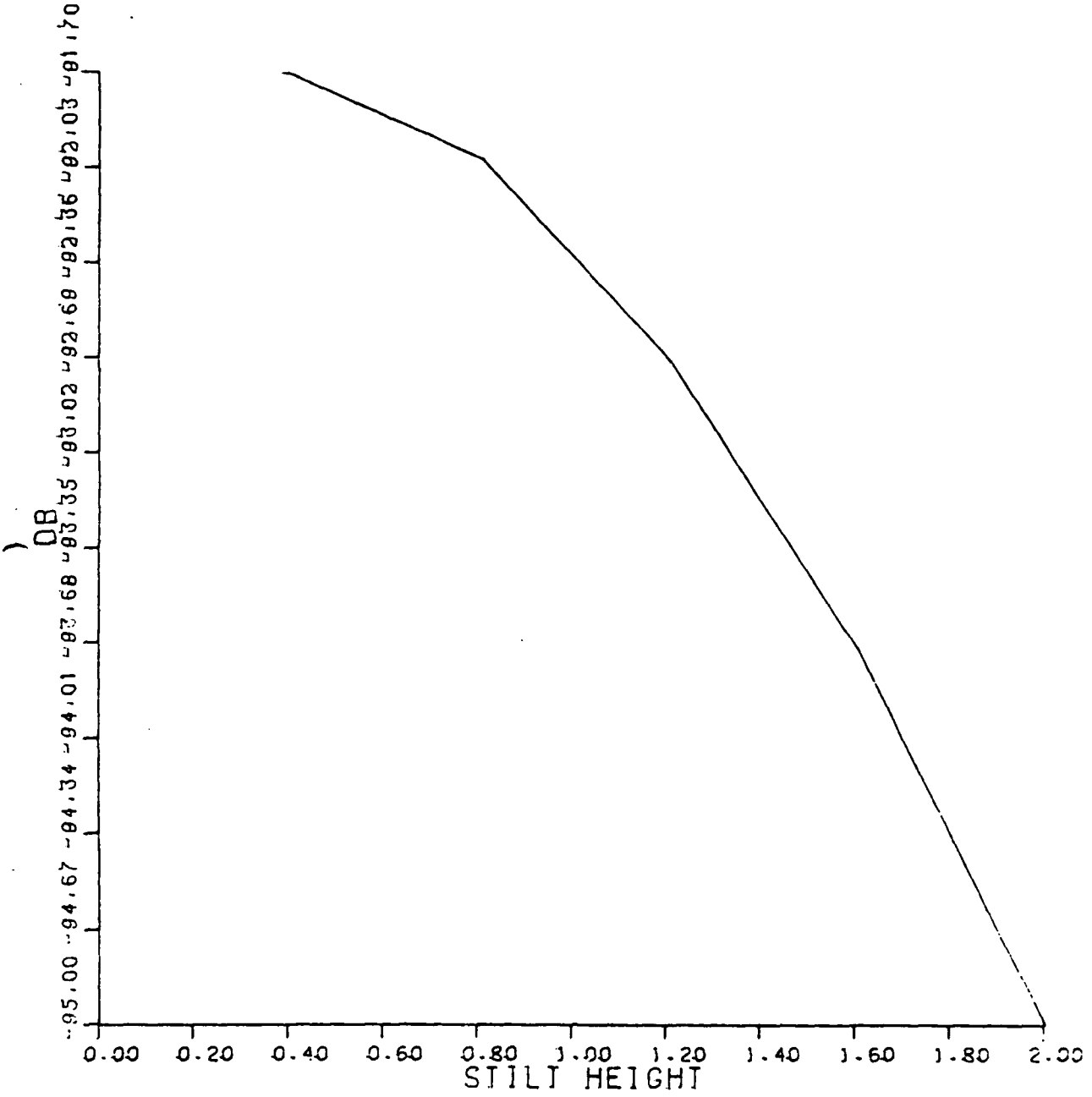

Figure 11.28

$|E_z|$dB vs. ℓ_s

$\rho_s = 25.0$, $\phi_s = 0^0$

Elevated Upright Man

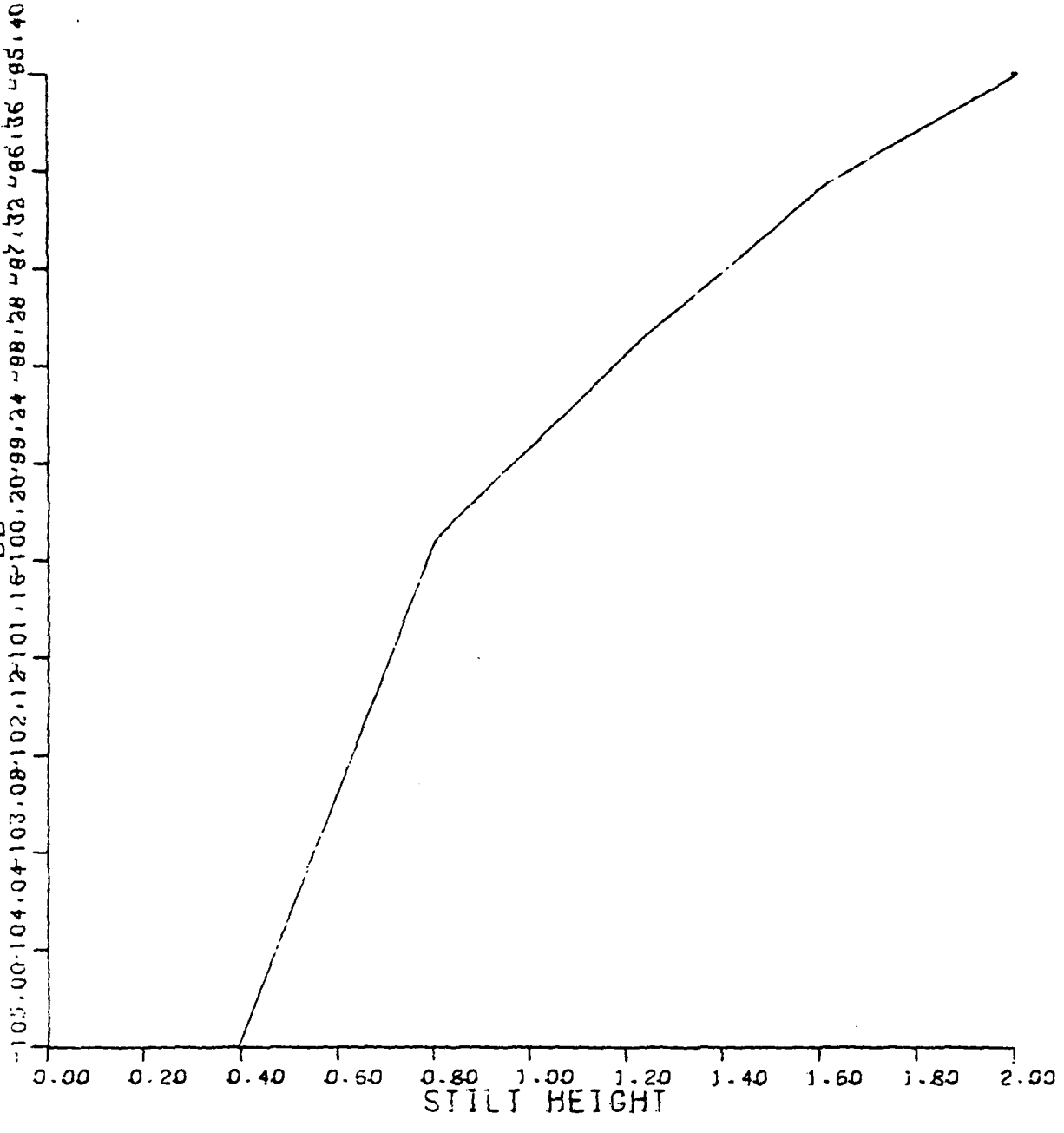

Figure 11.29

$|E_y|$ dB vs. L_s

ρ_s - 22.0, $\phi_s = 0^o$

Height Variation

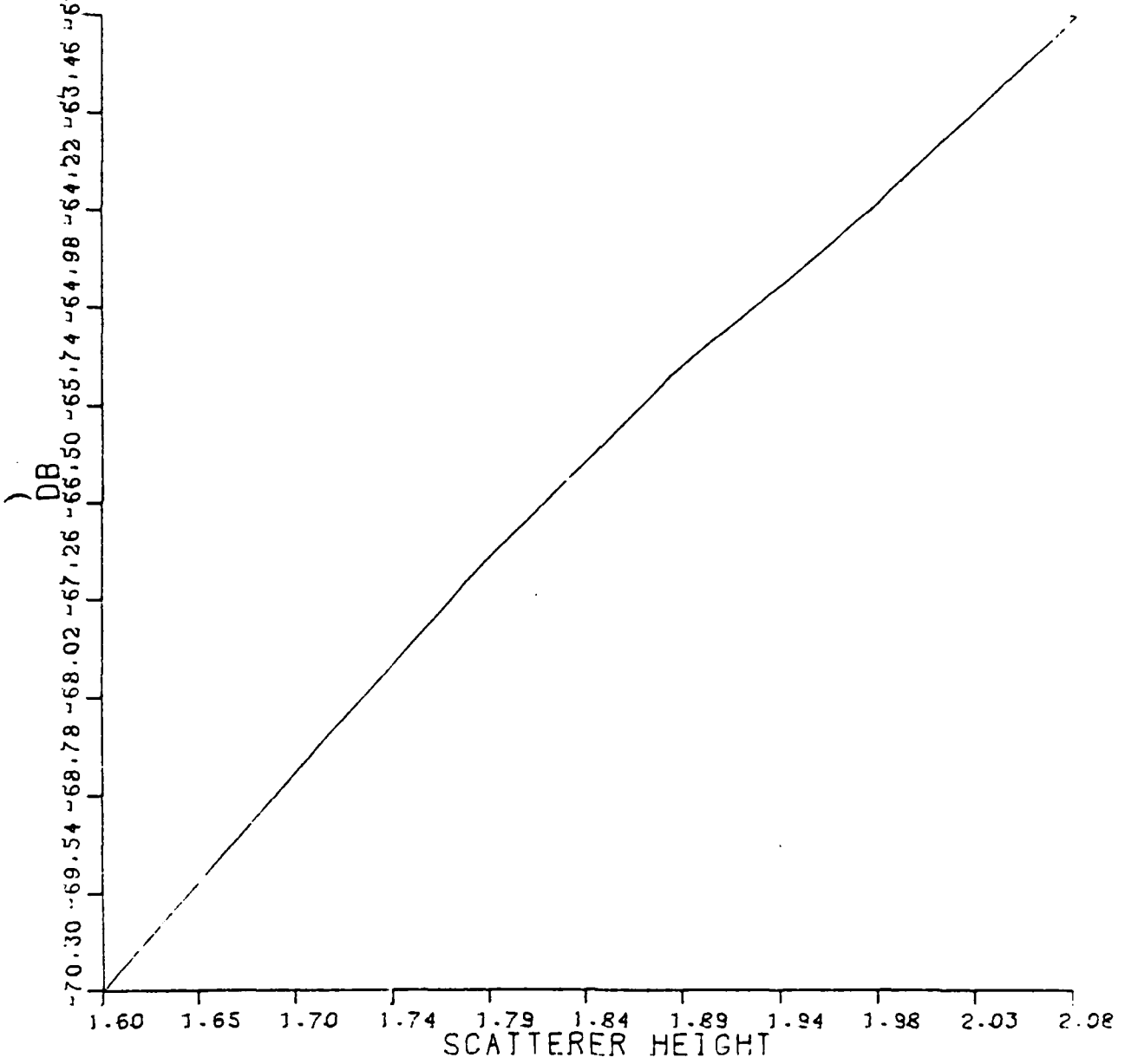

Figure 11.30

$|E_z|$dB vs. L_s

$\rho_s = 22.0$, $\phi_s = 0^o$

Height Variation

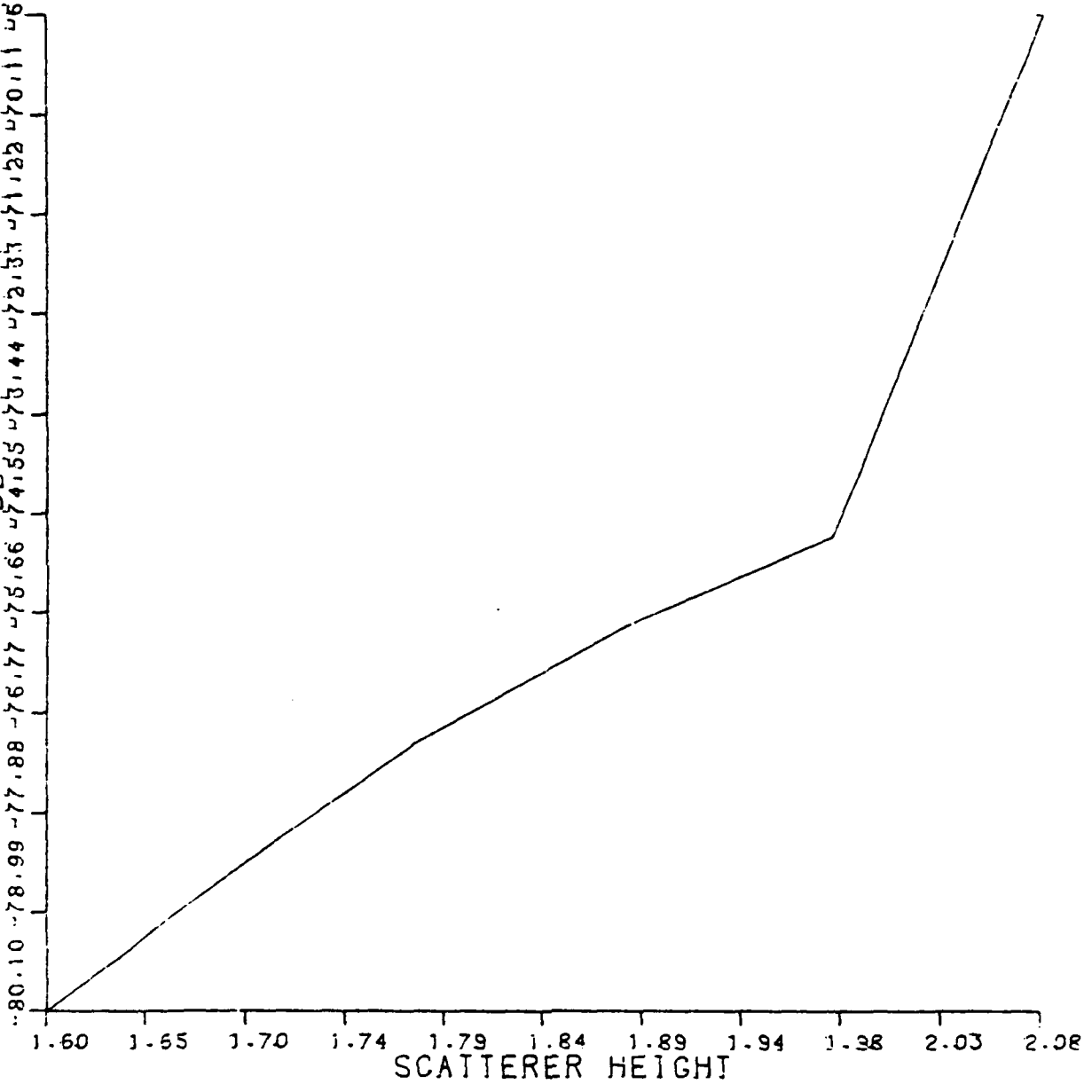

Figure 11.31

$|E_y|$dB vs. L_s

$\rho_s = 23.5$, $\phi_s = 0^o$

Height Variation

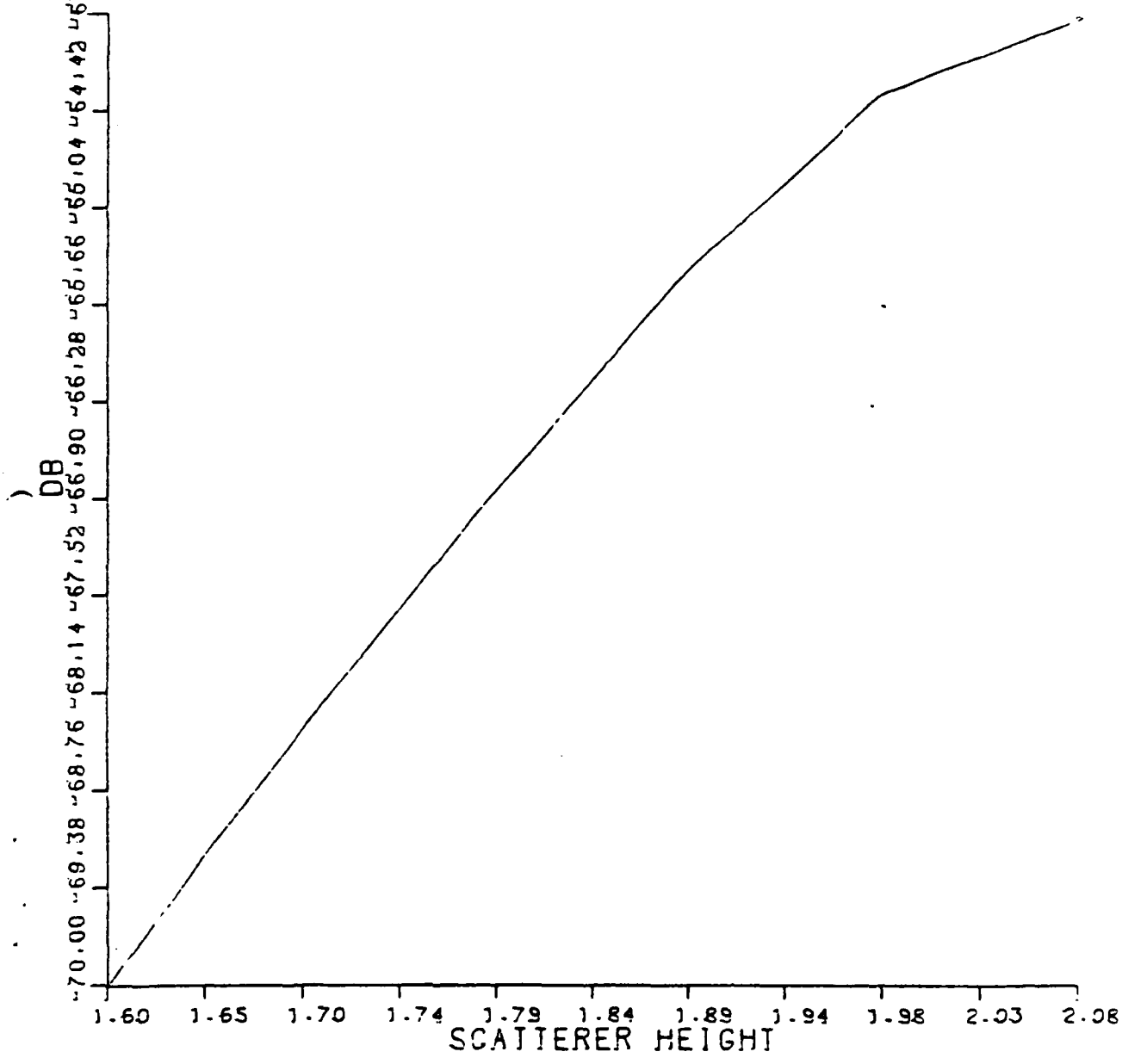

Figure 11.32

$|E_z|$dB vs. L_s

$\rho_s = 23.5$, $\phi_s = 0^o$

Height Variation

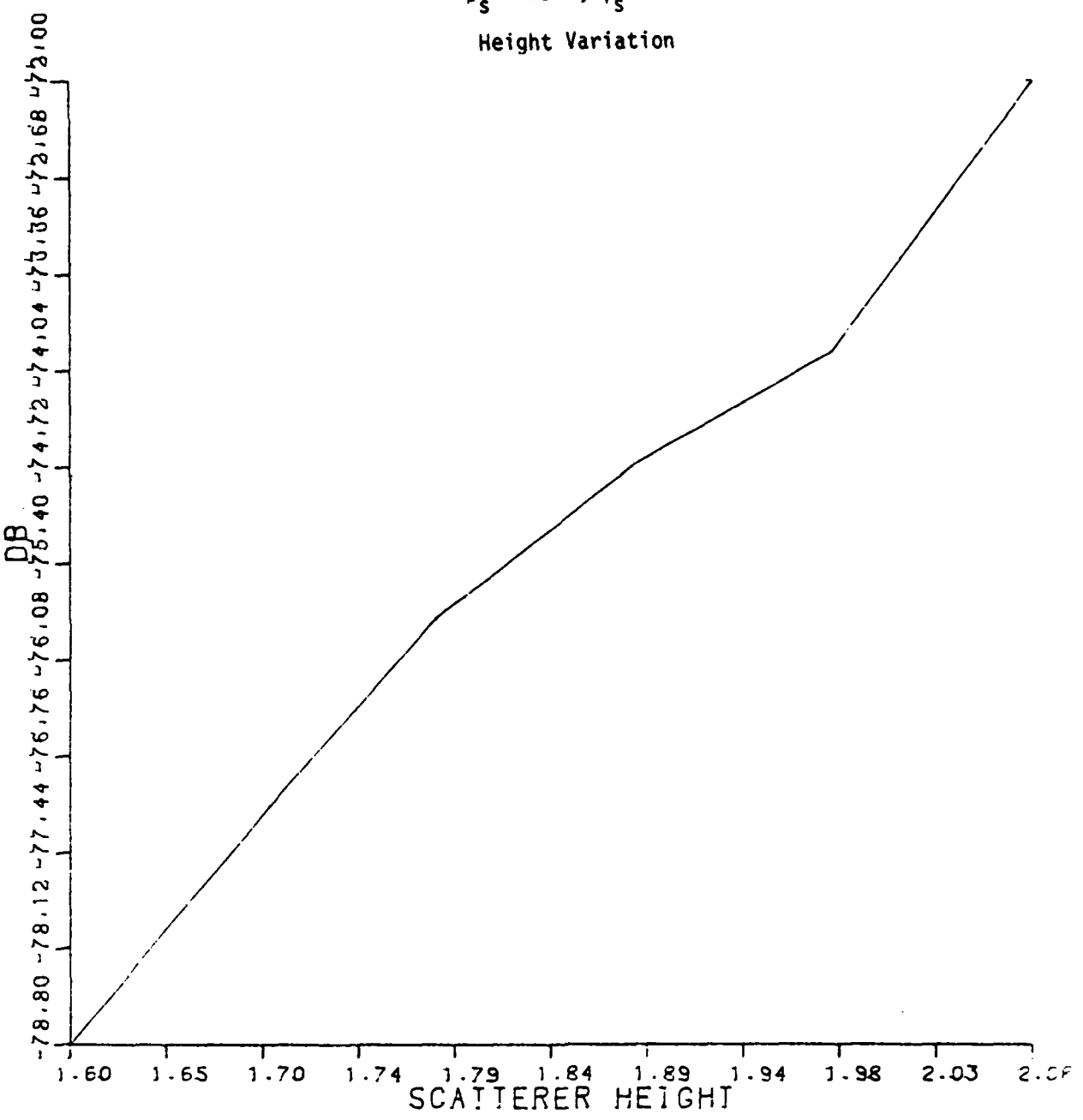

Figure 11.33

$|E_x|$dB vs. L_s

$\rho_s = 25.0$, $\phi_s = 0^o$

Height Variation

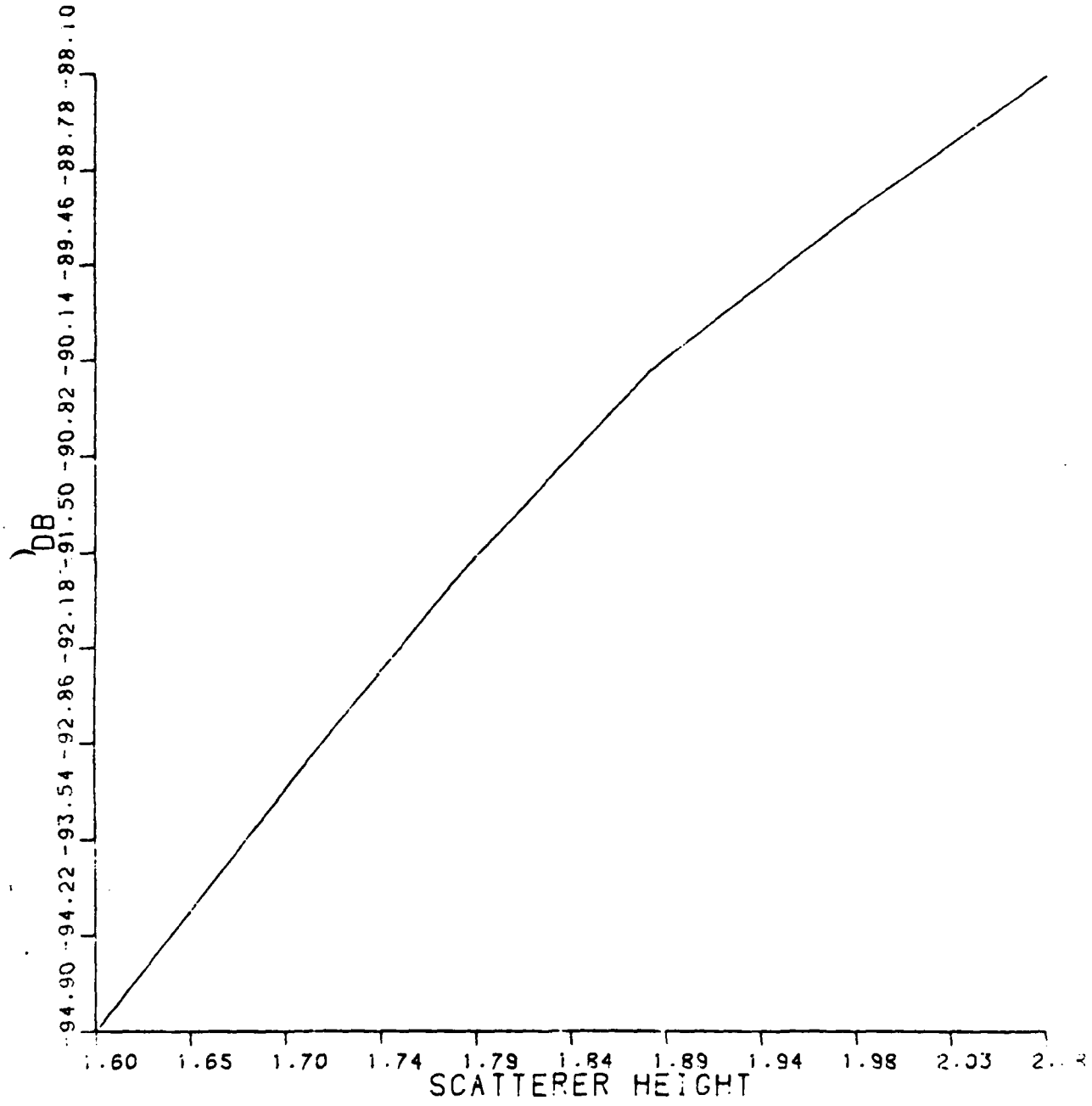

Figure 11.34

$|E_y|$dB vs. L_s

$\rho_s = 25.0$, $\phi_s = 0^0$

Height Variation

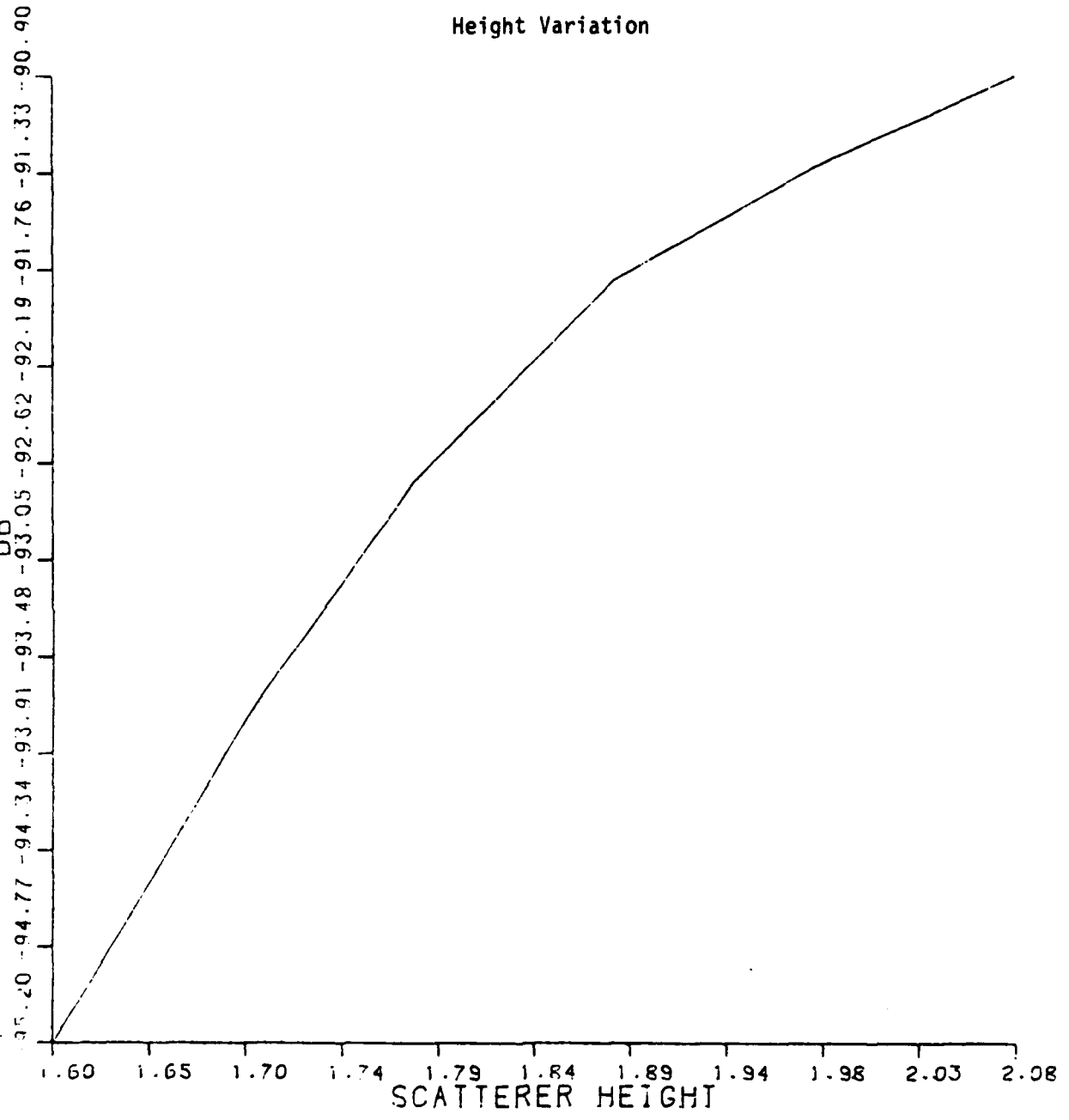

Figure 11.35

$|E_z|$dB vs. L_s

$\rho_s = 25.0$, $\phi_s = 0^o$

Height Variation

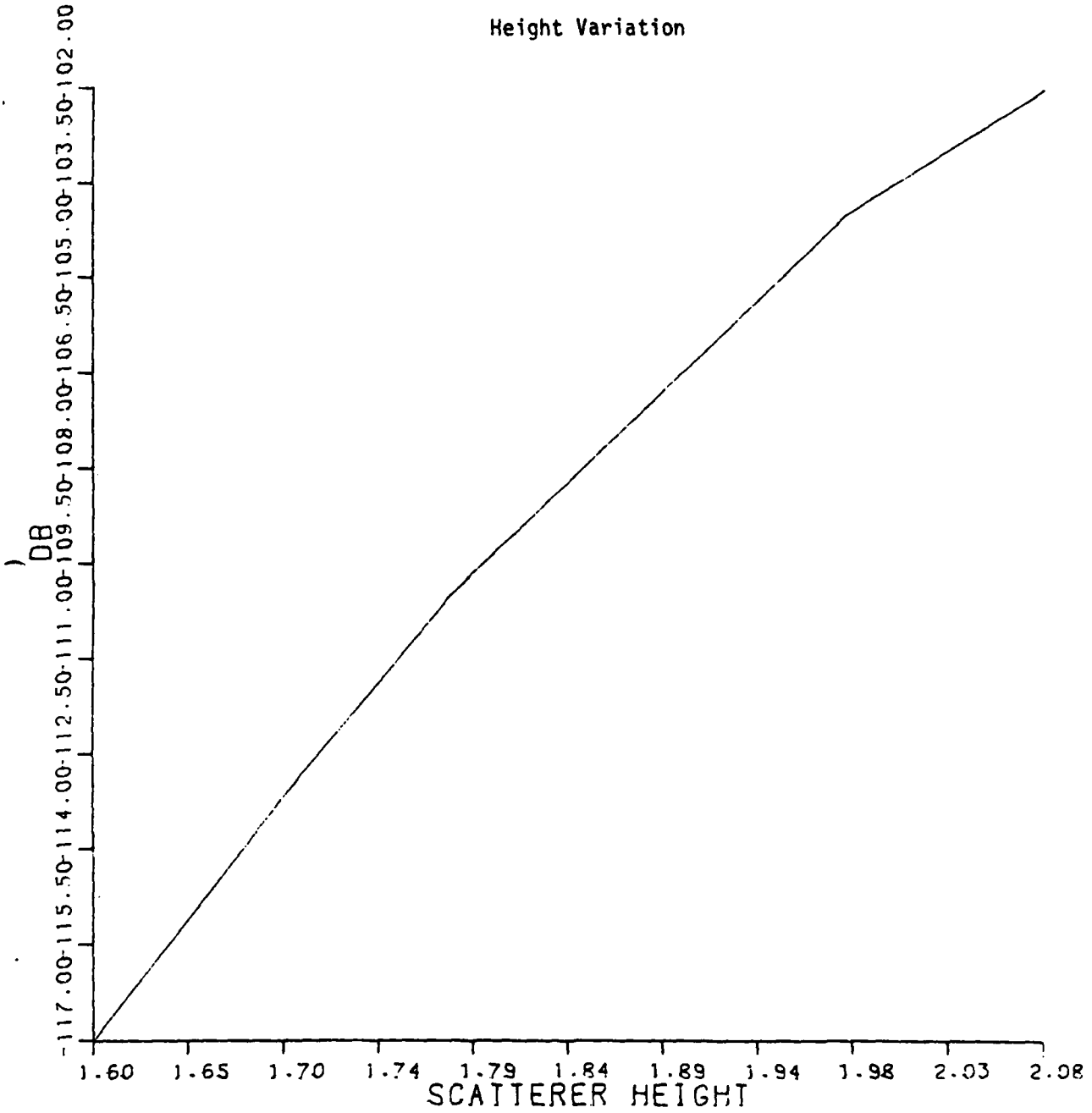

Figure 11.36

$|E_x|$dB vs. ρ_s

$\phi_s = 0^0$

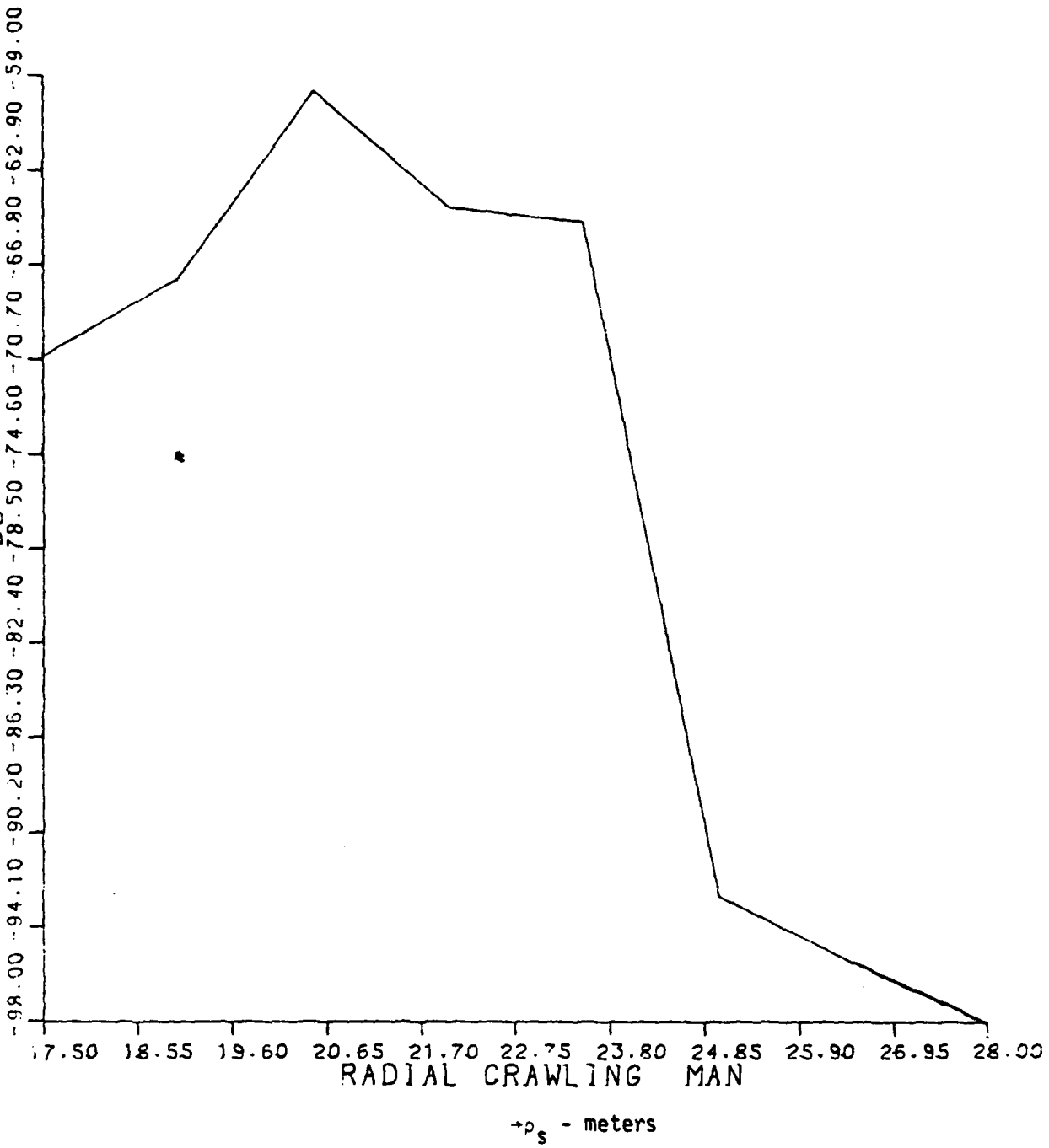

Figure 11.37

$|E_y|$ dB vs. ρ_s

$\phi_s = 0^0$

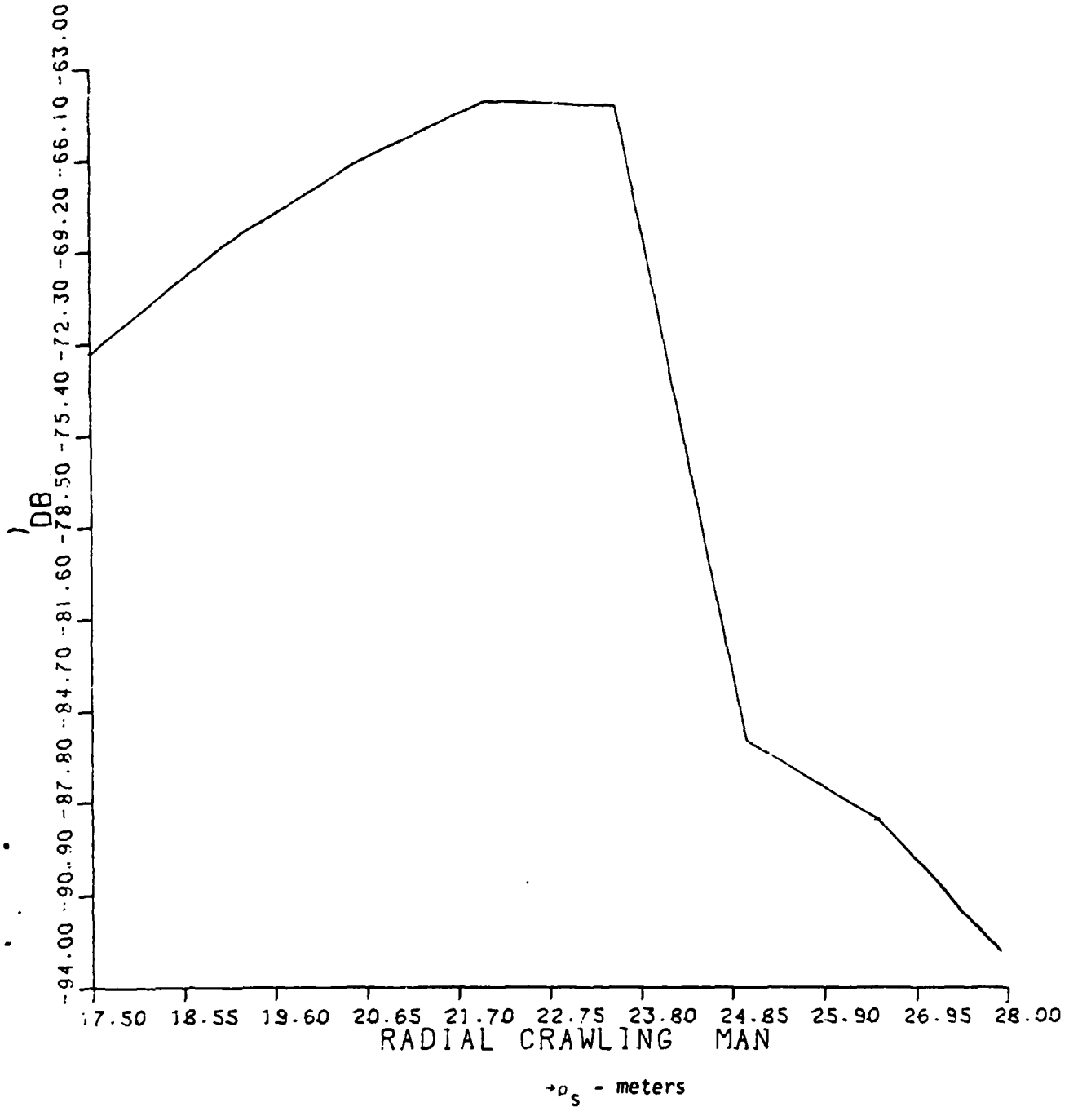

Figure 11.38

$|E_x|$dB vs. ρ_s

$\phi = 90^o$

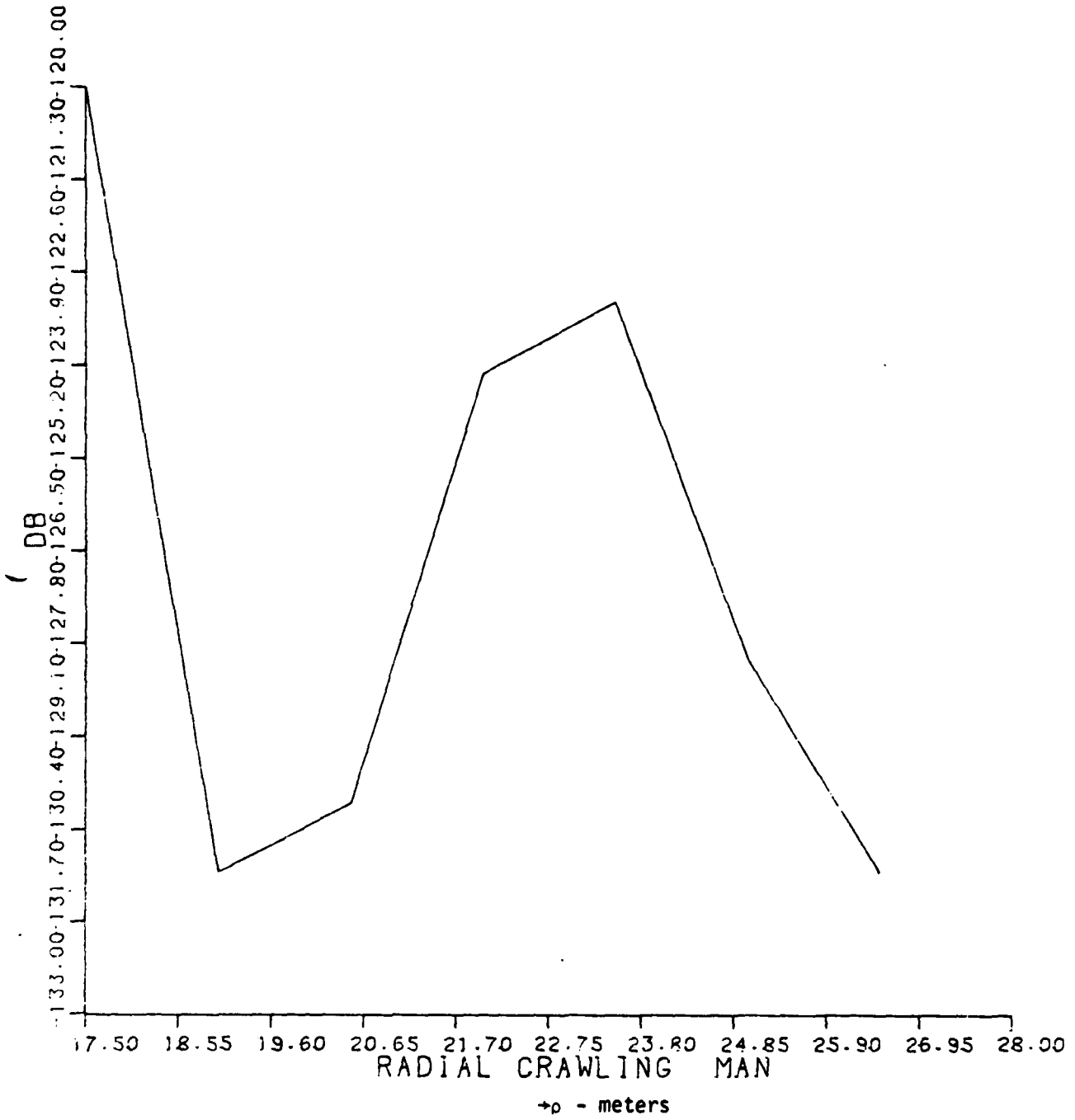

Figure 11.39

$|E_y|$dB vs. ρ_s

$\phi_s = 90^o$

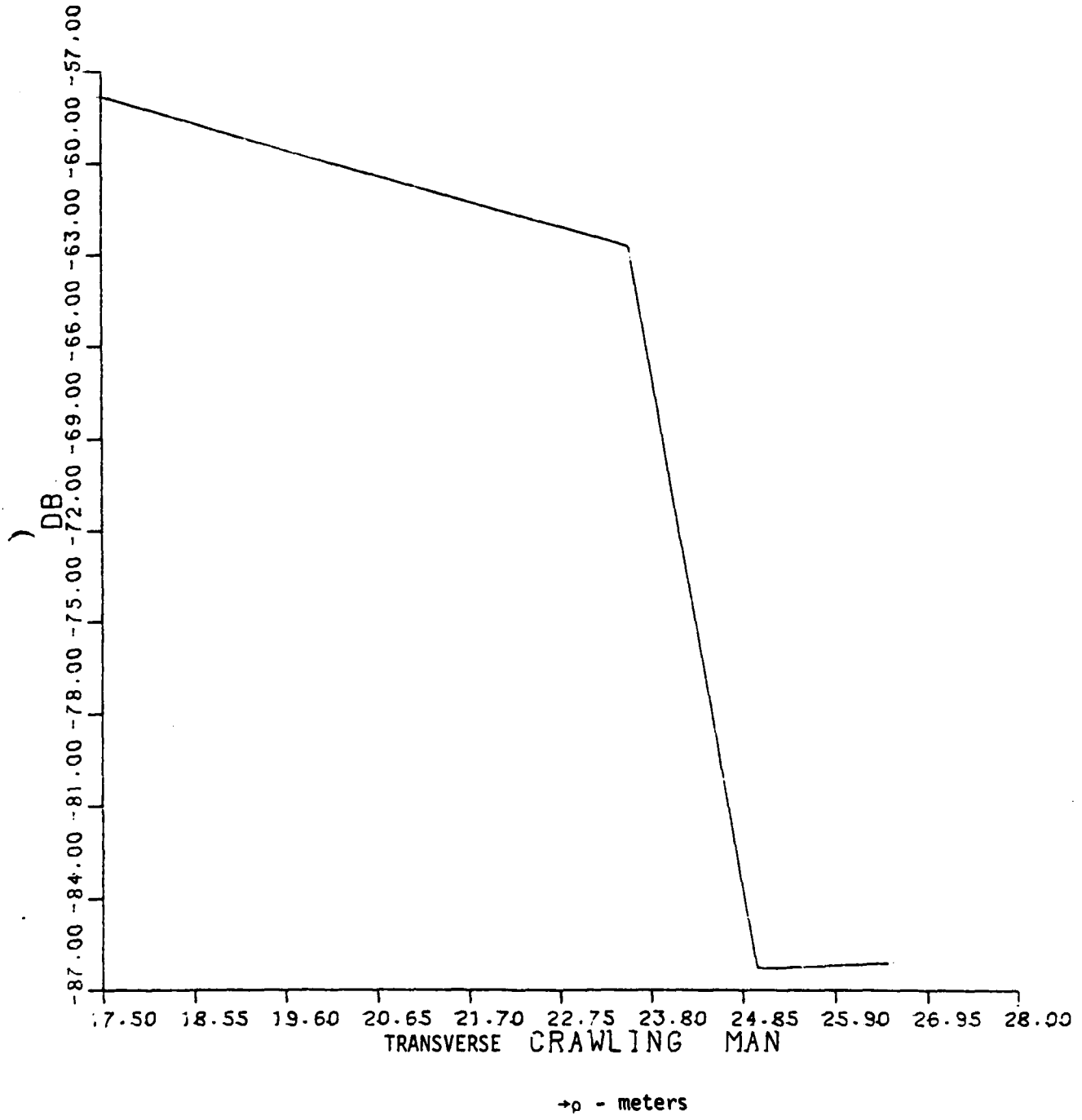

REFERENCES

A. General Ref.

(Used directly in formulating the general theory behind the analysis)

A.1 J. A. Stratton, "Electromagnetic Theory", McGraw-Hill, New York, 1941.

A.2 P. C. Clemmow, "The Plane Wave Spectrum Representation of Electromagnetic Fields", Oxford, New York, Pergamon Press, 1966.

A.3 R. E. Collin, "Foundations for Microwave Engineering", Mc-Graw Hill, New York, 1966.

A.4 M. R. Spiegel, "Mathematical Handbook of Formulas and Tables", (Schaum's Outline), McGraw-Hill, 1968.

A.5 C. Bender and S. Orszag, "Advanced Mathematical Methods for Scientists and Engineers", McGraw-Hill, 1978.

B. RF Intrusion Sensing Systems

(Primarily government reports received from the contract monitor on a class of systems similar to or related to that under investigation on this project.)

B.1 N. V. Karas, P. Franchi, R. L. Fante, and J. L. Poirier, "An RF Intrusion Sensor for Isolated Resources", RADC-TR-77-118, In-House Report, March 1977.

B.2 J. L. Poirier, N. V. Karas, J. A. Antonucci, and M. Szczytko, "VHF Intrusion Detection: A Technique for Parked Aircraft", RAD-TR-77-384, In-House Report, November 1977.

B.3 N. V. Karas, J. L. Poirier, J. Antonucci and M. Szczytko, "A VHF Intrusion Detection Technique for Isolated Resources", RADC-TR-78-177, In-House Report, July 1978.

B.4 N. V. Karas, J. A. Antonucci, and M. Szczytko, "A VHF Intruder Detection System: Tests on a C-5A Aircraft", RADC-TR-78-230, In-House Report, November 1978.

B.5 J. S. Rochefort, R. Sukys and N. C. Poirier, "An Area Intrusion Detection and Alarm System", RADC-TR-78-258, Final Technical Report, November 1978.

B.6 J. L. Poirier and M. Kushner, "Analysis of the Response of an RF Intruder Protection System", RADC-TR-79-17, In-House Report, January, 1979.

B.7 J. L. Poirier, "Effect on Multiple Receiving Antennas on the Response of an RF Intrusion Sensor", RADC-TR-79-42, In-House Report, February 1979.

B.8 J. L. Poirier, "An Evaluation of Some Factors Affecting the Choice of Operating Frequency of a Guided Wave Radar for Intruder Detection", RADC Report, 1979.

B.9 J. L. Poirier, "Estimation of the Zone of Detection of the Single Wire Individual Resource Protection Sensor", RADC Report, 1979.

C. Leaky Cables

(Theoretical and empirical studies of cables similar to that used as the source of RF wave energy in the system under investigation on this project. Useful background material, although the results were not used directly in our analysis.)

C.1 G. Goubau, "Surface waves and their application to transmission lines", J. Appl. Phys., 21, No. 11, November 1950, pp. 1119-1128.

C.2 H. M. Barlow and J. Brown, "Radio Surface Waves", International Monographs on Radio, Oxford at the Clarendon Press, 1962.

C.3 Veena Rawat, "Unorthodox Transmission Lines for Continuous Access Guided Communication (CAGC)", Ph.D. Thesis, Queen's University, Kingston, Ontario, Canada, July 1973.

C.4 P. Yoh, R. Esposito, R. Gagnon and R. Kodis, "Measurements of leaky coaxial cables and possible applications to train communications", Report No. FRA-ORO and 0-74-43, U.S. Dept. of Transportation, May 1974.

C.5 D. J. Cree and L. J. Giles, "Practical performance of radiating cables", The Radio and Electronic Engineer, 45, No. 5, May 1975, pp. 215-223.

C.6 P. P. Delogne and M. Safak, "Electromagnetic theory of the leaky coaxial cable", The Radio and Electronic Engineer, 45, No. 5, May 1975, pp. 233-240.

C.7 D. J. R. Martin, "A general study of the leaky feeder principle", The Radio and Electronic Engineer, 45, No. 5, May 1975, pp. 205-214.

C.8 J. R. Wait and D. A. Hill, "Propagation along a braided coaxial cable in a circular tunnel", IEEE Trans. on Microwave Theory and Techniques, MTT-23, No. 5, May 1975, pp. 401-405.

C.9 D. C. Chang, "A general theory on small, radiating apertures in the outer sheath of coaxial cable", Scientific Report No. 19, ONR Contract No. N0014-76-C-0318, July 1976.

C.10 D. C. Chang, "Some comments on the time-causal characteristics of leaky and surface waves", RADC TR-76-374, Interim Technical Report, December 1976.

C.11 D. C. Chang, "Modal Characteristics of Single and Dual Wires Located Over a Dissipative Earth", RADC-TR-77-108, Final Report, March 1972.

C.12 J. L. Mason, "Performance Characteristics of Leaky Coaxial Cables", Status Report No. 3, September 26, 1978, and Status Report No. 4, December 28, 1978, USAF Contract No. F 19628-77-C-0249, CCC Contract Serial No. 7SU77-00317.

C.13 A. S. de C. Fernandes, "Propagation characteristics of a loose braid coaxial cable in free space", The Radio and Electronic Engineer, Vol. 49, No. 5, May 1979, pp. 255-260.

C.14 Bulletin 1058A, Radiax Slotted Coaxial Cable, Andrew Corp., Oakland Park, Illinois.

D. Scattering from Bodies Used as Models for Human and Animal Frames

(There are thousands of references on electromagnetic scattering in general and scattering from spheres, spheroids, etc. The list below confines itself primarily to those concerning scattering from biological bodies, with particular emphasis on prolate spheroids. That shape is very popular with researchers in biomedical engineering interested primarily in absorption and usually secondarily in scattering. However, the scattering theory is contained in their analysis. The list below contains the background references on the theory behind the "Barber Program" (Section 7) used in this project.)

D.1 D. S. Saxon, "Tensor scattering matrix for the electromagnetic field", Phys. Rev. Vol. 100, No. 6, December 1955, pp. 1771-1775.

D.2 A. Anne, "Scattering and absorption of microwaves by dielectric objects: The biological significance and hazards to mankind", Ph.D. Thesis, Univ. of Pennsylvania, July 1963.

D.3 A. C. Lind, R. T. Wang and J. M. Greenberg, "Microwave scattering by nonspherical particles", Applied Optics, Vol. 4, No. 12, December 1965, pp. 1555-1561.

D.4 P. C. Waterman, "Symmetry, unitarity and geometry in electromagnetic scattering", Phys. Rev. D.3, 1971, pp. 825-839.

D.5 C. C. Johnson and A. W. Guy, "Nonionizing electromagnetic wave effects in biological materials and systems", Proc. IEEE, Vol. 60, 1972, pp. 692-718.

D.6 A. J. Poggio and E. K. Miller, "Integral equation solutions of three-dimensional scattering problems", Computer Techniques for Electromagnetics, R. Mittra, Ed., Pergamon Press, New York, 1973, pp. 159-264.

D.7 W. T. Joines and R. J. Spiegel, "Resonance absorption of microwaves by the human skull", IEEE Trans. on Biomedical Engineering, Vol. BME-21, 1974, pp. 46-48.

D.8 O. P. Gandhi, "Polarization and frequency effects on whole animal absorption of RF energy", Proc. IEEE, Vol. 62, No. 8, August 1974, pp. 1171-1175.

D.9 B. Peterson and S. Strom, "T-matrix formulation of electromagnetic scattering from multilayered scatterers", Phys. Rev. D., Vol. 10, No. 8, pp. 2670-2684, October 15, 1974.

D.10 S. Asano and G. Yamamoto, "Light scattering by a spheroidal particle", Applied Optics, January 1975, pp. 29-49.

D.11 C. H. Durney, C. C. Johnson and H. Massoudi, "Long-wavelength analysis of plane-wave irradiation of a prolate spheroid model of man", IEEE Trans. on Microwave Theory and Techniques, Vol. MTT-23, No. 2, February 1975, pp. 246-253.

D.12 D. E. Beischer and V. R. Reno, "Microwave energy distribution measurements in proximity to man and their practical applications", Annals of N. Y. Acad. Sci., Vol. 247, February 28, 1975, pp. 473-480.

D.13 P. W. Barber, "Numerical study of electromagnetic power deposition in biological tissue bodies", presented URSI Annual Meeting, Boulder, Colorado, 1975.

D.14 G. W. Hohmann, "Three-dimensional polarization and electromagnetic modeling", Geophysics, Vol. 40, 1975, pp. 309-324.

D.15 C. C. Johnson, C. H. Durney, and H. Massoudi, "Long wavelength electromagnetic power absorption in prolate spheroidal models of man and animals", IEEE Trans. on Microwave Theory and Techniques, Vol. MTT-23, September 1975, pp. 739-747.

D. 16 O. P. Gandhi, "Frequency and orientation effects on whole animal absorption of EM waves", IEEE Trans. on Biomedical Engineering, Vol. BME 22, No. 11, November 1975, p. 536.

D.17 P. Barber and C. Yeh, "Scattering of light by arbitrarily shaped dielectric bodies", Applied Optics, Vol. 14, December, 1975, pp. 2864-2872.

D.18 C. C. Johnson, C.H. Durney, P. W. Barber, H. Massoudi, S. J. Allen and J. C. Mitchell, "Radio Frequency Radiation Dosimetry Handbook", USAF Report SAM-TR-76-35, 1976.

D.19 P. W. Barber, "Numerical study of electromagnetic power deposition in biological tissue bodies", and "Biological effects of electromagnetic waves", Vol. II, U. S. Government Printing Office, 1976, pp. 119-134.

D.20 K. M. Chen and B. S. Guru, "Induced EM field and absorbed power density inside human torsos by 1 to 500 MHz EM waves", Technical Report No. 1, NSF Grant ENG 74-12603, 1976.

D.21 H. E. King and J. L. Wong, "Effects of a human body on a dipole antenna at 450 and 900 MHz", IEEE Trans. on Antennas and Propagation, Vol. AP-25, No. 3, May 1977, pp. 376-379.

D.22 P. W. Barber, "Resonance electromagnetic absorption by nonspherical dielectric objects", IEEE Trans. Microwave Theory and Techniques, Vol. MTT-25, May 1977, pp. 373-381.

D.23 K. M. Chen and B. S. Guru, "Internal EM field and absorbed power density on human torsos induced by 1-500 MHz EM waves", IEEE Trans. on Microwave Theory and Techniques, Vol. MTT-25, September 1977, pp. 746-756.

D.24 P. W. Barber, "Electromagnetic power deposition in prolate spheroid models of man and animals at resonance", IEEE Trans. on Biomedical Engineering, Vol. BME 24, September 1977, pp. 513-521.

D.25 M. J. Hagmann, O. P. Gandhi, and C. H. Durney, "Upper bound on cell size for moment-method solutions", IEEE Trans. on Microwave Theory and Techniques, Vol. MTT-25, October 1977, pp. 831-832,

D.26 M. J. Hagmann, O. P. Gandhi and C. H. Durney, "Numerical calculation of electromagnetic energy deposition for a realistic model of man", URSI International Symposium on Biological Effects of Electromagnetic Waves, Airlie, Va., October 1977.

D.27 D. [illegible]. Nyquist, K. M. Chan, and B. S. Guru, "Coupling between small thin-wire antennas and a biological body", IEEE Trans. on Antennas and Propagation, Vol. AP-25, No. 6, Nov. 1977, pp. 863-866.

D.28 O. P. Gandhi, E. L. Hunt and J. A. D'Andrea, "Electromagnetic power deposition in man and animals with and without ground and reflector effects", Radio Science, Vol. 12, November/December 1977, pp. 39-47.

D.29 P. W. Barber, "Scattering and absorption efficiencies for nonspherical dielectric objects - biological models", IEEE Trans. on Biomedical Engineering, Vol. BMS-25, No. 2, March 1978, pp. 155-159.

D.30 C. H. Durney, C. C. Johnson, P. W. Barber, H. Massoudi, M. F. Iskandor, J. L. Lords, D. K. Ryser, S.J. Allen, J. C. Mitchell, "Radio Frequency Radiation Dosimetry Handbook", (Second Edition), SAM-TR-78-22, June 1978.

D.31 M. J. Hagmann, "Numerical Studies of Electromagnetic Energy by Man", Ph.D. Thesis, University of Utah, 1978.

D.32 M. J. Hagmann, O. P. Gandhi, and C. H. Durney, "Improvement of convergence in moment-method solutions by the use of interpolants", IEEE Trans. on Microwave Theory and Techniques, Vol. MTT-26, No. 11, November 1978, pp. 904-908.

D.33 P. W. Barber, O. P. Gandhi, M. J. Hagmann and I. Chatterjee, "Electromagnetic absorption in a multilayered model of man", IEEE Trans. on Biomedical Engineering, Vol. BME-26, No. 7, July 1979, pp. 400-405.

D.34 P. W. Barber, "Electromagnetic power deposition in an inhomogeneous man model", Final Report, NSF Award Number 76-15641, Bioengineering, Award Period: 9-1-76 to 8-31-79.

D.35 V. K. Tripathi and H. Lee, "Absorption characteristics of prolate spheroidal model of man and animals at and near resonance", EPA-600/1-79-025, U. S. Environmental Protection Agency, Research Triangle Park, North Carolina, 1979, p. 21.

D.36 P. O. Gandhi, "State of the knowledge for electromagnetic absorbed dose in man and animals", Proc. IEEE, Vol. 68, No. 1, January 1980, pp. 24-32.

D.37 C. H. Durney, "Electromagnetic dosimetry for models of humans and animals: a review of theoretical and numerical techniques", Proc. IEEE, Vol. 69, No. 1, January 1980, pp. 33-49.

Appendix I: KIRCHHOFF-HUYGHENS (OR STRATTON-CHU) INTEGRAL FORMULAS FOR FIELDS FROM APERTURES

The Kirchhoff-Huyghens Formula[A-1] for the fields from an aperture with area $\Delta S'$ in an unbounded charge-free, current-free linear, homogeneous, isotropic medium (neglecting contributions from the aperture edges) is (see Figure I-1):

$$\underset{\rightarrow}{V}(\underset{\rightarrow}{r}) = -\frac{1}{4\pi}\iint_{\Delta S'} dS'\left[\underset{\rightarrow}{V}(\underset{\rightarrow}{r}')\,\hat{\underset{\rightarrow}{n}}'\cdot\nabla'\left(\frac{e^{jkR}}{R}\right) - \frac{e^{jkR}}{R}\frac{\partial \underset{\rightarrow}{V}}{\partial \underset{\rightarrow}{n}'}(\underset{\rightarrow}{r}')\right] \quad \text{(I-1)}$$

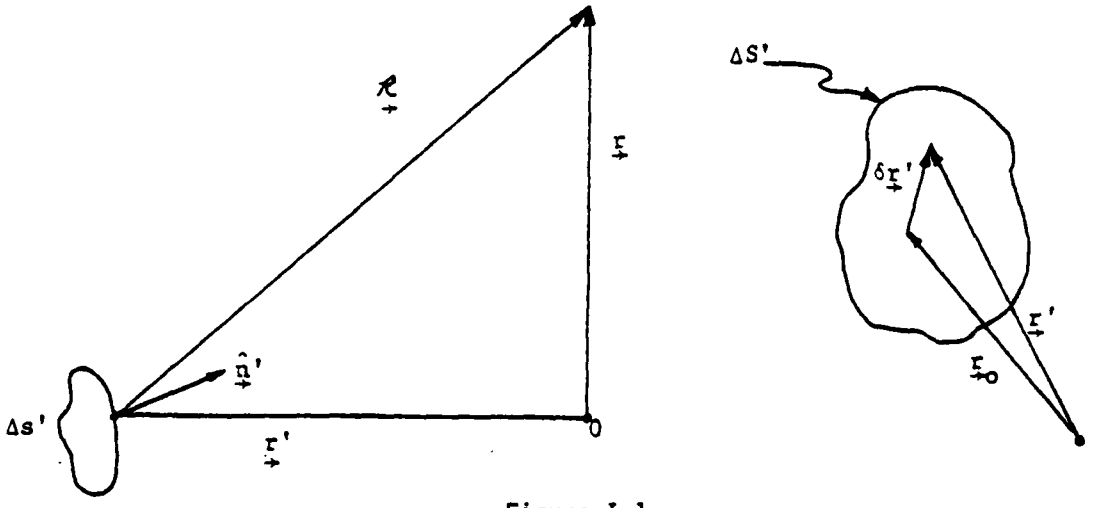

Figure I-1

Geometry for Integral Formulas

where

$\Delta S'$ is the aperture area

$dS' = d\zeta_1\, d\zeta_2$ = aperture area element, where ζ_1 and ζ_2 are orthogonal coordinates along the aperture

$\underset{\rightarrow}{V}(\underset{\rightarrow}{r})$ = generic vector indicating electric field vector $\underset{\rightarrow}{E}(\underset{\rightarrow}{r})$ or magnetic field vector $\underset{\rightarrow}{H}(\underset{\rightarrow}{r})$

0 = origin or coordinates

$\underset{\rightarrow}{r}$ = field-point vector = $\hat{\underset{\rightarrow}{x}}x + \hat{\underset{\rightarrow}{y}}y + \hat{\underset{\rightarrow}{z}}z$

$\underset{\rightarrow}{r}'$ = source-point vector (on aperture) = $\hat{\underset{\rightarrow}{x}}x' + \hat{\underset{\rightarrow}{y}}y' + \hat{\underset{\rightarrow}{z}}z'$

$\hat{\underset{\rightarrow}{n}}'$ = outward normal unit vector

$$\nabla' = \hat{\underset{\rightarrow}{x}} \frac{\partial}{x'} + \hat{\underset{\rightarrow}{y}} \frac{\partial}{y'} + \hat{\underset{\rightarrow}{z}} \frac{\partial}{z'}$$

$$\frac{\partial}{\partial n'} = \hat{\underset{\rightarrow}{n}}' \cdot \nabla' = \text{normal derivative operator}$$

$$\underset{\rightarrow}{R} = \underset{\rightarrow}{r} - \underset{\rightarrow}{r}'$$

$$R = |\underset{\rightarrow}{R}|$$

Note that

$$\underset{\rightarrow}{r}' = \underset{\rightarrow}{r}'_0 + \delta\underset{\rightarrow}{r}' \qquad \text{(I-2)}$$

where r'_0, position vector of aperture center $= \hat{\underset{\rightarrow}{x}}x'_0 + \hat{\underset{\rightarrow}{y}}y'_0 + \hat{\underset{\rightarrow}{z}}z'_0$

$\delta\underset{\rightarrow}{r}'$ = vector from the center $\underset{\rightarrow}{r}'_0$ to a point on the aperture

$$= \hat{\underset{\rightarrow}{x}}\delta x'_0 + \hat{\underset{\rightarrow}{y}}\delta y'_0 + \hat{\underset{\rightarrow}{z}}\delta z'_0 = [\hat{\underset{\rightarrow}{\xi}}_1 \zeta_1 + \hat{\underset{\rightarrow}{\xi}}_2 \zeta_2 + \hat{\underset{\rightarrow}{n}}' n']_{n'=0}$$

where $(\hat{\xi}_1, \hat{\zeta}_2)$ are the unit basis vectors in the ζ_1 and ζ_2 directions respectively, and n' is the coordinate in the $\underset{\rightarrow}{n}'$ direction (which is set to zero along the aperture).

Note that Eq. (I-1) applies to either the electric field vector $\underset{\rightarrow}{E}(\underset{\rightarrow}{r})$ or the magnetic field vector $\underset{\rightarrow}{H}(\underset{\rightarrow}{r})$.

Another integral formula similar to (and equivalent to) Eq. (I-1) is sometimes referred to as the Stratton-Chu integral formula [Stratton, p. 466].

$$\underset{\rightarrow}{E}(\underset{\rightarrow}{r}) = -\frac{1}{4\pi}\iint_{\Delta S'} dS'[j\omega\mu_o(\hat{\underset{\rightarrow}{n}}' \times \underset{\rightarrow}{H}(\underset{\rightarrow}{r}')) \frac{e^{jkR}}{R} \tag{I-3a}$$

$$+ (\hat{\underset{\rightarrow}{n}}' \times \underset{\rightarrow}{E}(\underset{\rightarrow}{r}')) \times \nabla'(\frac{e^{jkR}}{R}) + (\hat{\underset{\rightarrow}{n}}' \cdot \underset{\rightarrow}{E}(\underset{\rightarrow}{r}')) \nabla'(\frac{e^{jkR}}{R})] \tag{I-3a}$$

$$\underset{\rightarrow}{H}(\underset{\rightarrow}{r}) = \frac{1}{4\pi}\iint_{\Delta S'} dS'[j\omega\varepsilon_o(\hat{\underset{\rightarrow}{n}}' \times \underset{\rightarrow}{E}(\underset{\rightarrow}{r}')) \frac{e^{jkR}}{R}$$

$$- (\hat{\underset{\rightarrow}{n}}' \times \underset{\rightarrow}{H}(\underset{\rightarrow}{r}')) \times \nabla'(\frac{e^{jkR}}{R}) - (\hat{\underset{\rightarrow}{n}}' \cdot \underset{\rightarrow}{H}(\underset{\rightarrow}{r}')) \nabla'(\frac{e^{jkR}}{R})] \tag{I-3b}$$

Where in Eqs. (I-3a,b) we neglect contributions from aperture edges [Stratton, p. 469] and assuming volume current and charge densities to be zero.

We can easily derive an alternative form for Eqs. (I-3a,b) in which the gradients are taken with respect to the field point (unprimed) coordinates rather than the source point (primed) coordinates. We recognize that

$$\nabla'(\frac{e^{jkR}}{R}) = -\nabla(\frac{e^{jkR}}{R}) \tag{I-4}$$

and

$\underset{\rightarrow}{E}(\underset{\rightarrow}{r}')$, $\underset{\rightarrow}{H}(\underset{\rightarrow}{r}')$, $\hat{\underset{\rightarrow}{n}}'$ are all independent of the field point (unprimed) coordinates (I-5)

Using Eqs. (I-4) and (I-5) in Eq. (I-3a,b), we have

$$\underset{\rightarrow}{E}(\underset{\rightarrow}{r}) = -\frac{1}{4\pi}\{\iint_{\Delta S'} dS'\, j\omega\mu_o(\hat{\underset{\rightarrow}{n}}' \times \underset{\rightarrow}{H}(\underset{\rightarrow}{r}))\frac{e^{jkR}}{R}$$

$$-\nabla \times \left(\iint_{\Delta S'} dS'(\hat{\underset{\rightarrow}{n}}' \times \underset{\rightarrow}{E}(\underset{\rightarrow}{r}'))\frac{e^{jkR}}{R}\right) \qquad \text{(I-6a)}$$

$$+\nabla\left(\iint_{\Delta S'} dS'(\hat{\underset{\rightarrow}{n}}\cdot\underset{\rightarrow}{E}(\underset{\rightarrow}{r}'))\frac{e^{jkR}}{R}\right)\}$$

$$\underset{\rightarrow}{H}(\underset{\rightarrow}{r}) = \frac{1}{4\pi}\{\iint_{\Delta S'} dS'\, j\omega\varepsilon_o(\hat{\underset{\rightarrow}{n}}' \times \underset{\rightarrow}{E}(\underset{\rightarrow}{r}'))\frac{e^{jkR}}{R} \qquad \text{(I-6b)}$$

$$-\nabla \times \left(\iint_{\Delta S'} dS'(\hat{\underset{\rightarrow}{n}}' \times \underset{\rightarrow}{H}(\underset{\rightarrow}{r}'))\frac{e^{jkR}}{R}\right)$$

$$+\nabla\left(\iint_{\Delta S'} dS'(\hat{\underset{\rightarrow}{n}}\cdot\underset{\rightarrow}{H}(\underset{\rightarrow}{r}'))\frac{e^{jkR}}{R}\right)\}$$

Appendix II: PLANE-WAVE SPECTRAL REPRESENTATION OF FIELDS

The representation of electric and magnetic fields as a superposition of plane waves is amply covered in the literature.[A-1,A-2] It is a well-established technique for dealing with arbitrary electric and magnetic fields in a homogeneous medium. In principle, it involves no more than the three-dimensional spatial Fourier transformation of the field vector or one of its components.

As in Figure II-1, consider a right-handed rectangular coordinate system (x,y,z) with unit vectors $(\hat{x},\hat{y},\hat{z})$. Assume harmonic time dependence $e^{-j\omega t}$. The vector $\underset{\rightarrow}{r} = x\hat{x} + y\hat{y} + z\hat{z}$ is the position vector referred to the origin of coordinates 0. Electric or magnetic field vectors are denoted generically by $\underset{\rightarrow}{V}(\underset{\rightarrow}{r})$ and their three-dimensional spatial Fourier transforms by $\tilde{\underset{\rightarrow}{V}}(\underset{\rightarrow}{\beta})$. The vector $\underset{\rightarrow}{k}$ is the propagation vector associated with a plane wave propagating in a particular direction. The angle between $\underset{\rightarrow}{r}$ and $\underset{\rightarrow}{k}$ is denoted by γ.

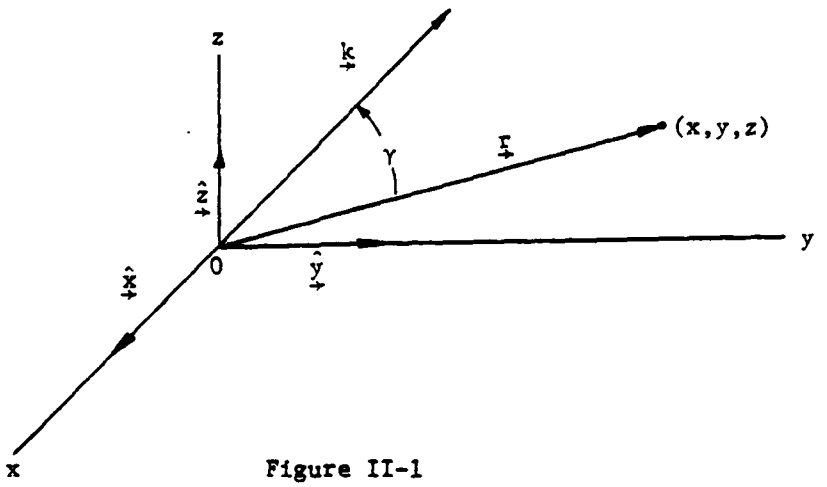

Figure II-1

Geometry for Plane-Wave Spectral Representative of Fields

The propagation vector is denoted by

$$\underset{\rightarrow}{k} = k\underset{\rightarrow}{\beta} \qquad \text{(II-1)}$$

where $k = \frac{\omega}{v}$ = propagation constant of the medium, where ω = angular frequency, v = velocity of electromagnetic waves in the medium, which in the case of free-space is $c = 3(10^8)$ meter/second and which in general could be real (in a non dissipative medium) or complex (in a dissipative medium, e.g., the earth), and $\underset{\rightarrow}{\beta}$ is the direction vector, given by

$$\underset{\rightarrow}{\beta} = \underset{\rightarrow}{\beta}_h + \hat{z}\beta_z \qquad \text{(II-2)}$$

where

$$\underset{\rightarrow}{\beta}_h = \beta_x\hat{x} + \beta_y\hat{y}$$

and where the quantities in Eq. (II-2) are given in terms of angles by the relationships

$$\beta_x = \sin\theta_\beta \cos\phi_\beta \qquad \text{(II-2-1)'}$$

$$\beta_y = \sin\theta_\beta \sin\phi_\beta \qquad \text{(II-2-2)'}$$

$$\beta_h = \sqrt{\beta_x^2 + \beta_y^2} = \sin\theta_\beta \qquad \text{(II-2-3)'}$$

$$\beta_z = \cos\theta_\beta = \pm\sqrt{1 - \beta_h^2}\ ; \quad \begin{matrix} + \text{ if } 0 \le \theta_\beta < \frac{\pi}{2} \\ - \text{ if } \frac{\pi}{2} \le \theta_\beta \le \pi \end{matrix} \qquad \text{(II-2-4)'}$$

θ_β = spherical polar angle of propagation direction (II-2-5)'

ϕ_β = azimuthal angle of propagation direction (II-2-6)'

and the plus and minus signs correspond to upward and downward propagation, respectively.

Integration over all direction angles results in the representation

$$\underset{\rightarrow}{V}(\underset{\rightarrow}{r}) = \underset{\rightarrow}{V}(\underset{\rightarrow}{\rho},z) = \iint_{-\infty}^{\infty} d^2\,\underset{\rightarrow}{\beta}_h\, e^{jk\underset{\rightarrow}{\beta}_h\cdot\underset{\rightarrow}{\rho}} \{e^{-jk|\beta_z|z}\,\underset{\rightarrow}{\tilde{V}}_-(\underset{\rightarrow}{\beta}_h)$$

$$+ e^{jk|\beta_z|z}\,\tilde{V}_+(\underset{\rightarrow}{\beta}_h)\} \qquad \text{(II-3)}$$

where $d^2\underset{\rightarrow}{\beta}_h = d\beta_x\, d\beta_y$, $\underset{\rightarrow}{\rho} = \hat{x}x + \hat{y}y$, $V_-(\underset{\rightarrow}{\beta}_h)$ and $V_+(\underset{\rightarrow}{\beta}_h)$ denote the two-dimensional spatial Fourier transforms for downward and upward propagation respectively and where the z-component β_z has been eliminated in the arguments of $\tilde{V}_-$ and $\tilde{V}_+$ by invoking the relationship (II-2-4)', by virtue of which β_z can be expressed as a function of β_x and β_y.

By differentiating Eq. (II-3) with respect to z and setting z equal to zero, we obtain

$$\underset{\rightarrow}{V}(\underset{\rightarrow}{\rho},0) = \iint_{-\infty}^{\infty} d^2\,\underset{\rightarrow}{\beta}_h\, e^{jk\underset{\rightarrow}{\beta}_h\cdot\underset{\rightarrow}{\rho}} \{\tilde{\underset{\rightarrow}{V}}_+(\underset{\rightarrow}{\beta}_h) + \tilde{V}_-(\underset{\rightarrow}{\beta}_h)\} \qquad \text{(II-4a)}$$

$$\left[\frac{\partial \underset{\rightarrow}{V}}{\partial z}(\underset{\rightarrow}{\rho},z)\right]_{z=0} = jk \iint_{-\infty}^{\infty} d^2\,\underset{\rightarrow}{\beta}_h\, e^{jk\underset{\rightarrow}{\beta}_h\cdot\underset{\rightarrow}{\rho}} |\beta_z| \{\tilde{\underset{\rightarrow}{V}}_+(\underset{\rightarrow}{\beta}_h) - \tilde{V}_-(\underset{\rightarrow}{\beta}_h)\} \qquad \text{(II-4b)}$$

It is easily shown from Eq. (II-4a) (by multiplying by $e^{-jk\underset{\rightarrow}{\beta}'_h\cdot\underset{\rightarrow}{\rho}}$ and integrating on x and y) that

$$\tilde{\underset{\rightarrow}{V}}_{+}(\underset{\rightarrow}{\beta}_h) = \frac{\left(\frac{k}{2\pi}\right)^2}{(1 + |\beta_z|)} \iint_{-\infty}^{\infty} d^2\underset{\rightarrow}{\rho} \{ |\beta_z| \underset{\rightarrow}{V}(\underset{\rightarrow}{\rho},0) - \frac{j}{k} \left[\frac{\partial \underset{\rightarrow}{V}}{\partial z}(\underset{\rightarrow}{\rho},z) \right]_{z=0} \} e^{-jk\underset{\rightarrow}{\beta}_h \cdot \underset{\rightarrow}{\rho}} \tag{II-5a}$$

$$\tilde{\underset{\rightarrow}{V}}_{-}(\underset{\rightarrow}{\beta}_h) = \frac{\left(\frac{k}{2\pi}\right)^2}{(1 + |\beta_z|)} \iint_{-\infty}^{\infty} d^2\underset{\rightarrow}{\rho} \{ |\beta_z| \tilde{\underset{\rightarrow}{V}}(\underset{\rightarrow}{\rho},0) + \frac{j}{k} \left[\frac{\partial \underset{\rightarrow}{V}}{\partial z}(\underset{\rightarrow}{\rho},z) \right]_{z=0} \} e^{-jk\underset{\rightarrow}{\beta}_h \cdot \underset{\rightarrow}{\rho}} \tag{II-5b}$$

where $d^2\underset{\rightarrow}{\rho} = dx\, dy$.

An alternative representation equivalent to Eq. (II-3) in terms of the spherical angles of the wave vector and the spherical coordinates of r (given by r, θ, ϕ) is:

$$\underset{\rightarrow}{V}(\underset{\rightarrow}{r}) = \int_0^{2\pi} d\phi_\beta \left\{ \int_0^{\pi/2} d\theta_\beta \sin\theta_\beta \, \tilde{\tilde{V}}_{-}(\theta_\beta, \phi_\beta) \, e^{jkr\cos\gamma} \right.$$

$$\left. + \int_{\pi/2}^{\pi} d\theta_\beta \sin\theta_\beta \, \tilde{\tilde{\underset{\rightarrow}{V}}}_{+}(\theta_\beta, \phi_\beta) \, e^{jkr\cos\gamma} \right. \tag{II-6}$$

where

$$\cos\gamma = \cos\theta\cos\theta_\beta + \sin\theta\sin\theta_\beta\cos(\phi - \phi_\beta) \tag{II-7}$$

and

$$\tilde{\tilde{\underset{\mp}{V}}}(\theta_\beta, \phi_\beta) = [\tilde{\underset{\mp}{V}}(\underset{\rightarrow}{\beta}_h)]_{\substack{\beta_x = \sin\theta_\beta\cos\phi_\beta \\ \beta_y = \sin\theta_\beta\sin\phi_\beta}}$$

Appendix III: PLANE-WAVE SPECTRAL REPRESENTATION OF THE FIELDS FROM AN APERTURE

The spherical wave function $\frac{e^{jkR}}{R}$ -- appearing in Eqs. (I.1), (I.3 a,b) and (I.6.a,b) has a modified plane-wave spectral representation [from a modification of Stratton, Chapter IX, Eqs. (23), (24), (25), (26), pp. 577, 578]*.

$$\frac{e^{jkR}}{R} = \frac{jk}{2\pi}\int_0^{2\pi} d\phi'_\beta \int_0^{\pi} d\theta'_\beta \sin\theta'_\beta\, e^{jkR\cos\theta'_\beta}\, f(\underset{\rightarrow}{\beta}, \underset{\rightarrow}{R}) \qquad \text{(III.1)}$$

where it is recalled that $R = |\underset{\rightarrow}{R}| = |\underset{\rightarrow}{r} - \underset{\rightarrow}{r}'|$, where $(\theta'_\beta, \phi'_\beta)$ are the spherical coordinate direction angles of $\underset{\rightarrow}{\beta}$ referenced to a z-coordinate in the direction of R, and where**

$$f(\underset{\rightarrow}{\beta}, \underset{\rightarrow}{R}) = \frac{1}{2}\left[1 + \cos\theta'_\beta + \frac{1}{jkR}\right]$$

Noting that $e^{jkR\cos\theta'_\beta} = e^{jk\underset{\rightarrow}{\beta}\cdot\underset{\rightarrow}{R}}$, it follows that $\nabla(e^{jk\underset{\rightarrow}{\beta}\cdot\underset{\rightarrow}{R}}) = jk\underset{\rightarrow}{\beta}\, e^{jk\underset{\rightarrow}{\beta}\cdot\underset{\rightarrow}{R}}$ and hence, taking the gradient of (III.1) (differentiating under the integral sign) we have

$$\nabla\left(\frac{e^{jkR}}{R}\right) = -\nabla'\left(\frac{e^{jkR}}{R}\right) = \frac{(jk)^2}{2\pi}\int_0^{2\pi} d\phi'_\beta \int_0^{\pi} d\theta'_\beta \sin\theta'_\beta \text{ ----}$$

$$\ldots\, e^{jkR\cos\theta'_\beta}\left\{\underset{\rightarrow}{\beta} f(\underset{\rightarrow}{\beta},\underset{\rightarrow}{R}) + \frac{1}{jk}\nabla f(\underset{\rightarrow}{\beta}, \underset{\rightarrow}{R})\right\} \qquad \text{(III.2)}$$

*The relationship appearing in Stratton requires the use of complex values of the components of $\underset{\rightarrow}{\beta}$, the propagation vector, for its implementation. The present form, confining itself to real values of the β components, contains a dependence on $\underset{\rightarrow}{R}$. Hence it is a modified plane-wave spectral representation where the compound waves have phase factors $e^{jk\underset{\rightarrow}{\beta}\cdot\underset{\rightarrow}{R}}$ as do plane waves, but are weighted with a factor that is dependent on the space coordinates.

**The derivation of (III.1) is easily accomplished by recognizing that $\frac{jkR}{2}\int_0^{\pi} d\theta'_\beta \sin\theta'_\beta\, e^{jkR\cos\theta'_\beta} = j\sin kR$. Differentiation of $\sin kR$ then produces the result $\cos kR = \frac{1}{2}\int_0^{\pi} d\theta'_\beta \sin\theta'_\beta\, e^{jkR\cos\theta'_\beta}\{1+jkR\cos\theta'_\beta\}$. Adding $\cos kR$ and $j\sin kR$, dividing by R and noting that the integrand is independent of ϕ'_β, implying that $\int_0^{2\pi} d\phi'_\beta = 2\pi$, we obtain III.1.

Revising (III.1) and (III.2) to include the separation into upward and downward waves and transforming from the spherical coordinate system with z-axis in the R direction to our ground frame, we have

$$\left(\frac{e^{jkR}}{R}\right)_{\pm} = \frac{jk}{2\pi}\iint_{\varpi} d^2\beta_h\, e^{jk\beta_{\pm}\cdot R} f(\beta_{\pm}, R) \qquad \text{(III.1)'}$$

$$\nabla\left(\frac{e^{jkR}}{R}\right)_{\pm} = -\nabla'\left(\frac{e^{jkR}}{R}\right) = \frac{(jk)^2}{2\pi}\iint_{\varpi} d^2\beta_h\, e^{jk\beta_{\pm}\cdot R}\left\{f(\beta_{\pm}, R)\beta_{\pm} - \frac{1}{2(jkR)^2}\frac{R}{R}\right\} \qquad \text{(III.2)'}$$

where $\beta_{\pm} = \beta_h \pm \hat{z}\,|\beta_z|$.

We now simplify the notation by denoting $f(\beta_{\pm}, R)$ by $f^{\pm}$, neglect the $\frac{R}{R}$ term in (III.2)'*, neglect the field contributions due to line currents around the aperture edge, assume that the ambient medium is free space, and then substitute (III.1)' and (III.2)' into Eqs. (I.3-a,b), interchanging the order of integration. The results of these operations are:

$$E(r) = -\frac{(j k_0)^2}{4\pi}\iint_{-\infty}^{\infty} d^2\beta_h \iint_{\Delta S'} dS'\, e^{jk\beta^{\pm}\cdot R}\{-Z_0[\hat{n}' \times H(r')] - [\beta^{+} \times (\hat{n}' \times E(r')) - (\hat{n}'\cdot E(r'))\,\beta^{\pm}]\} f^{\pm} \qquad \text{(III.3a)}$$

* This term is not included in the analysis in Sections 3 and 4, but it is approximately accounted for in the computations. It is negligibly small except at positions extremely close to the source.

where $Z_o = \sqrt{\frac{\mu_o}{\varepsilon_o}}$ = wave impedance of free-space and the + and - superscripts represent upward and downward propagation, respectively.

$$\underset{\rightarrow}{H}(\underset{\rightarrow}{r}) = -\frac{(j\,k_o)^2}{4\pi} \iint_{-\infty}^{\infty} d^2\,\underset{\rightarrow}{\beta}_h \iint_{\Delta S'} e^{jk_o \underset{\rightarrow}{\beta}^{\pm} \cdot \underset{\rightarrow}{R}'} \{Y_o[\hat{n}' \times \underset{\rightarrow}{E}(\underset{\rightarrow}{r})']$$

$$- [\underset{\rightarrow}{\beta}^{\pm} \times (\hat{n}' \times \underset{\rightarrow}{H}(\underset{\rightarrow}{r}'))] - (\hat{n}' \cdot \underset{\rightarrow}{H}(\underset{\rightarrow}{r}'))\,\underset{\rightarrow}{\beta}^{\pm}]\}\, f' \qquad \text{(III.3b)}$$

where $Y_o = \sqrt{\frac{\varepsilon_o}{\mu_o}} = \frac{1}{Z_o}$ = wave admittance of free-space and + and - superscripts have the same meaning as in Eq. (III.3a).

We now express $\underset{\rightarrow}{E}(\underset{\rightarrow}{r})$ and $\underset{\rightarrow}{H}(\underset{\rightarrow}{r})$ in the form (II.3) as follows:

$$\underset{\rightarrow}{E}(\underset{\rightarrow}{r}) = \underset{\rightarrow}{E}^{+}(\underset{\rightarrow}{r}) + \underset{\rightarrow}{E}^{-}(\underset{\rightarrow}{r}) \qquad \text{(III.4a)}$$

$$\underset{\rightarrow}{H}(\underset{\rightarrow}{r}) = \underset{\rightarrow}{H}^{+}(\underset{\rightarrow}{r}) + \underset{\rightarrow}{H}^{-}(\underset{\rightarrow}{r}) \qquad \text{(III.4b)}$$

where

$$\underset{\rightarrow}{E}^{\pm}(\underset{\rightarrow}{r}) = \iint_{-\infty}^{\infty} d^2\,\underset{\rightarrow}{\beta}_h\, e^{jk_o(\underset{\rightarrow}{\beta}_h \cdot \underset{\rightarrow}{\rho}^{\pm} \mp |\beta_z| z)}\, \underset{\rightarrow}{\tilde{E}}_{\pm}(\underset{\rightarrow}{\beta}_h)$$

$$\underset{\rightarrow}{H}^{\pm}(\underset{\rightarrow}{r}) = \iint_{-\infty}^{\infty} d^2\,\underset{\rightarrow}{\beta}_h\, e^{jk_o(\underset{\rightarrow}{\beta}_h \cdot \underset{\rightarrow}{\rho}^{\pm} \mp |\beta_z| z)}\, \underset{\rightarrow}{\tilde{H}}_{\pm}(\underset{\rightarrow}{\beta}_h)$$

and where, from Eqs. (III.3a,b),

$$\underset{\rightarrow}{\tilde{E}}_{\pm}(\underset{\rightarrow}{\beta}_h) = \frac{-(j\,k_o)^2}{4\pi} \iint_{\Delta S'} dS'\, e^{-jk_o(\underset{\rightarrow}{\beta}_h \pm \hat{z}|\beta_z|) \cdot \underset{\rightarrow}{r}'}\, \{-Z_o[\hat{n}' \times \underset{\rightarrow}{H}(\underset{\rightarrow}{r}')]$$

$$- [(\underset{\sim}{\rho}_{sh} + \hat{z}|z_i|) \times (\hat{n}' \times \underset{\sim}{E}(\underset{\sim}{r}')) - (\hat{n}' \cdot \underset{\sim}{E}(\underset{\sim}{r}'))(\underset{\sim}{\rho}_{sh} + \hat{z}|z_i|)]\, f^{\pm} \tag{III.5a}$$

$$\underset{\sim}{H}_{\pm}(\underset{\sim}{\rho}_{sh}) = \frac{-(j k_o)^2}{-4\pi} \iint_{AS'} dS'\, e^{-jk_o(\underset{\sim}{\rho}_{sh} \pm \hat{z}|z_i|)\cdot \underset{\sim}{r}'} \{Y_o[\hat{n}' \times \underset{\sim}{E}(\underset{\sim}{r}')]$$

$$- [(\underset{\sim}{\rho}_{sh} \pm \hat{z}|z_i|) \times (\hat{n}' \times \underset{\sim}{H}(\underset{\sim}{r}')) - (\hat{n}' \cdot \underset{\sim}{H}(\underset{\sim}{r}'))(\underset{\sim}{\rho}_{sh} \pm \hat{z}|z_i|)]\}\, f^{\pm} \tag{III.5b}$$

An important point arises at this juncture. It is necessary that $\underset{\sim}{\tilde{E}}_{\pm}(\underset{\sim}{\rho}_{sh})$ and $\underset{\sim}{\tilde{H}}_{\pm}(\underset{\sim}{\rho}_{sh})$ be interrelated through the Maxwell equations, i.e.,

$$\underset{\sim}{\tilde{E}}_{\pm}(\underset{\sim}{\rho}_{sh}) = -Z_o[\underset{\sim}{\beta}^{\pm} \times \underset{\sim}{\tilde{H}}_{\pm}(\underset{\sim}{\rho}_{sh})] \tag{III.6a}$$

$$\underset{\sim}{\tilde{H}}_{\pm}(\underset{\sim}{\rho}_{sh}) = Y_o[\underset{\sim}{\beta}^{\pm} \times \underset{\sim}{\tilde{E}}_{\pm}(\underset{\sim}{\rho}_{sh})] \tag{III.6b}$$

$$\underset{\sim}{\beta}^{\pm} \cdot \underset{\sim}{\tilde{E}}(\underset{\sim}{\rho}_{sh}) = 0 \tag{III.6c}$$

$$\underset{\sim}{\beta}^{\pm} \cdot \underset{\sim}{\tilde{H}}(\underset{\sim}{\rho}_{sh}) = 0 \tag{III.6d}$$

Since Eqs. (III.6a) and (III.6b) imply Eqs. (III.6c) and (III.6d), respectively, and Eq. (III.6a) [with the aid of (III.6d)] implies Eq. (III.6b), it follows that if Eqs. (III.5a,b) are consistent with either Eq. (III.6a) or (III.6b), then Eqs. (III.5a,b) are consistent with the entire system of Eqs. (III.6a,b,c,d).

To test this consistency, we apply the $(-Z_o\, \underset{\sim}{\beta}^{\pm} \times \ldots)$ operation to Eqs. (III.5)-(III.6), resulting, after some manipulation (using the vector identity

$\underset{\rightarrow}{a} \times (\underset{\rightarrow}{b} \times \underset{\rightarrow}{c}) = \underset{\rightarrow}{b}(\underset{\rightarrow}{a} \cdot \underset{\rightarrow}{c}) - \underset{\rightarrow}{c}(\underset{\rightarrow}{a} \cdot \underset{\rightarrow}{b})$ and the fact that $\hat{\beta}^{\pm} \times \hat{\beta}^{\pm} = 0$, $\hat{\beta}^{\pm} \cdot \hat{\beta}^{\pm} = 1$), in the expression

$$-Z_o \hat{\beta}^{\pm} \times \tilde{\underline{\underline{H}}}_{t}(\beta_h) = \frac{-(j k_o)^2}{4\pi} \iint_{\Delta S'} dS' \, e^{-jk_o \hat{\beta}^{\pm} \cdot \underset{\rightarrow}{r}'} \{(-Z_o \hat{n}' \times \underset{\rightarrow}{H}(\underset{\rightarrow}{r}'))$$

$$- [\hat{\beta}^{\pm} \times (\hat{n}' \times \underset{\rightarrow}{E}(\underset{\rightarrow}{r}')) - \hat{\beta}^{\pm}(\hat{n}' \cdot \underset{\rightarrow}{E}(\underset{\rightarrow}{r}'))]$$

$$+ \hat{\beta}^{\pm} \hat{n}' \cdot [-Z_o(\hat{\beta}^{\pm} \times \underset{\rightarrow}{H}(\underset{\rightarrow}{r}')) - \underset{\rightarrow}{E}(\underset{\rightarrow}{r}'))]\} f^{\pm} \qquad \text{(III.7)}$$

Expressing $\underset{\rightarrow}{E}(\underset{\rightarrow}{r}')$ and $\underset{\rightarrow}{H}(\underset{\rightarrow}{r}')$ in the last square-bracketed quantity in Eq. (III.7) in terms of its spectral representation, we have

$$-Z_o[\hat{\beta}^{\pm} \times \underset{\rightarrow}{H}(\underset{\rightarrow}{r}')] - \underset{\rightarrow}{E}(\underset{\rightarrow}{r}')$$

$$= \iint d^2 \underset{\rightarrow}{\beta}_h' \, e^{jk_o \hat{\beta}'^{\pm} \cdot \underset{\rightarrow}{r}'} [-Z_o(\hat{\beta}^{\pm} \times \tilde{\underline{\underline{H}}}_{t}(\beta_h')) - \tilde{\underline{\underline{E}}}_{t}(\beta_h')] f^{\pm} \qquad \text{(III.8)}$$

When we evaluate the integral

$$I = \iint_{\Delta S'} dS' \, e^{jk_o(\hat{\beta}'^{\pm} - \hat{\beta}^{\pm}) \cdot \underset{\rightarrow}{r}'} \qquad \text{(III.9)}$$

which arises in Eq. (III.7), if $\Delta S'$ were an infinitely large surface, then

$$I \propto \delta(\hat{\beta}'^{\pm} - \hat{\beta}^{\pm}) \qquad \text{(III.10)}$$

which implies that

$$\hat{\beta}^{\pm\prime} = \hat{\beta}^{\pm} \qquad \text{(III.11)}$$

If Eq. (III.11) holds, then the RHS of Eq. (III.8) must vanish, since the vanishing of the integrand on the RHS of Eq. (III.8) is implied by the plane-wave Maxwell equation (III.6a). Thus, the LHS of Eq. (III.8) must also vanish, which implies that the RHS of Eq. (III.7) is equivalent to $\vec{E}_q(\rho_h)$ as given by Eq. (III.5a). This completes the demonstration that Eqs. (III.5a,b) are consistent with Eqs. (III.6a,b,c,d).

Of course, the "infinitely large surface" assumption on which Eq. (III.10) is based is not really valid here. However, for Eqs. (I.3a,b) (on which this entire analysis is based) to be truly valid, it is necessary that the surface be closed. In the present model, the fields are assumed to be negligibly small except on the slots; however, the surface still includes the cable area outside the slots and the integral I of Eq. (III.9) still can be considered as an integral over a closed surface. Such an integral will vanish unless $\vec{\rho}'^{+}_{-}$ is equal to $\vec{\rho}^{+}_{-}$; hence Eq. (III.11) holds.

Also, as remarked earlier, we have neglected , in the above analysis, the $\frac{\vec{R}}{R^2}$ term arising in the gradient of $\frac{e^{jkR}}{R}$. This term is only significant at positions extremely close to the source. It will be included in the computations.

Appendix IV: ELECTROMAGNETIC WAVE PROPAGATION ALONG A COAXIAL CABLE

The theory of electromagnetic wave propagation along a coaxial cable is well-known; consequently we will invoke standard references[A-3] in developing the theory in the context of the specific problem that is the subject of this report.

First, consider the modes of propagation down a guiding structure with circular cross-section. Using cylindrical coordinates (r", ϕ", z") and corresponding unit base vectors ($\hat{\underset{\rightarrow}{r}}$", $\hat{\underset{\rightarrow}{\phi}}$", $\hat{\underset{\rightarrow}{z}}$"), we have in general a set of TE (transverse electric) and TM (transverse magnetic) modes of propagation. The fields between r" = a and r" = b, where a and b are inner and outer radii respectively, can be expressed as a superposition of TE and TM modes. The field vectors have the forms (where harmonic time dependence $e^{-j\omega t}$ has been assumed)

$$\begin{bmatrix} \underset{\rightarrow}{E}(r",\phi",z") \\ \underset{\rightarrow}{H}(r",\phi",z") \end{bmatrix} = \sum_{n=-\infty}^{\infty} \{ \begin{matrix} \underset{\rightarrow}{C}_{nE}^{(TE)} \\ C_{nH}^{(TE)} \end{matrix} (r") \; e^{jn\phi"} \cdot e^{jk_o(\hat{k}_{zn})_{TE} z"} \qquad \text{(IV.1)}$$

$$+ \begin{matrix} \underset{\rightarrow}{C}_{nE}^{(TM)} \\ C_{nH}^{(TM)} \end{matrix} (r") \; e^{jn\phi"} \cdot e^{jk_o(\hat{k}_{zn})_{TM} z"} \}$$

where in general

$$\hat{k}_{zn} = k_{zn}/k_o$$

$$(\hat{k}_{zn})_{\substack{TE \\ TM}} = (\hat{k}_{znR})_{\substack{TE \\ TM}} + j(\alpha_n)_{\substack{TE \\ TM}}$$

and where

$$(\hat{k}_{znR})_{\substack{TE \\ TM}} = \frac{\omega}{k_o (v_{pn})_{\substack{TE \\ YM}}} = \frac{c}{(v_{pn})_{\substack{TE \\ TM}}}$$

$$(\hat{\alpha}_n)_{\substack{TE \\ TM}} = \frac{(\alpha_n)_{\substack{TE \\ TM}}}{k_o}$$

$(v_{pn})_{TE}$ = phase velocity in meters/sec for TE_n mode

$(v_{pn})_{TM}$ = phase velocity in meters/sec for TM_n mode

$(\alpha_n)_{TE}$ = attenuation in nepers/meter for TE_n mode

$(\alpha_n)_{TM}$ = attenuation in nepers/meter for TM_n mode

From Reference A-3, Chapter 3, we can write the general forms of the vectors $\vec{C}^{\substack{TE \\ TM}}_{\substack{nE \\ nH}}(r)$, as follows:

TE modes $[\overline{E}^{(n)}_{z''}(r'') = 0]$

$$\vec{C}^{TE}_{nE}(r'') = \hat{r}'' \, \overline{E}^{(n)}_{r''}(r'') + \hat{\phi}'' \, \overline{E}^{(n)}_{\phi''}(r'') \qquad \text{(IV.2a)}$$

$$\vec{C}^{TE}_{nH}(r'') = \hat{r}'' \, \overline{H}^{(n)}_{r''}(r'') + \hat{\phi}'' \, \overline{H}^{(n)}_{\phi''}(r'') + \hat{z}'' \, \overline{H}^{(n)}_{z''}(r'') \qquad \text{(IV.2b)}$$

where

$$\bar{H}_{z''}^{(n)}(r'') = A^{TE_n} J_n(k_{cn}\, r'') + B^{TE_n} N_n(k_{cn}\, r'')$$

$$\bar{H}_{r''}^{(n)}(r'') = \frac{j\, \hat{k}_{zn}}{\hat{k}_{cn}} \left[A^{TE_n} J_n'(k_{cn}\, r'') + B^{TE_n} N_n'(k_{cn}\, r'')\right]$$

$$\bar{H}_{\phi''}^{(n)}(r'') = \frac{j\, n\, \hat{k}_{zn}}{\rho\, \hat{k}_{cn}} \left[A^{TE_n} J_n(k_{cn}\, r'') + B^{TE_n} N_n(k_{cn}\, r'')\right]$$

$$\bar{E}_{r''}^{(n)}(r'') = \frac{1}{Y_w^{TE_n}} \bar{H}_{\phi''}^{(n)}(r'')$$

$$\bar{E}_{\phi''}^{(n)}(r'') = -\frac{1}{Y_w^{TE_n}} \bar{H}_{r''}^{(n)}(r'')$$

and where

$\rho = k_{cn}\, r''$

$J_n(k_{cn}\, r'')$ = Bessel function of first kind and order n

$N_n(k_{cn}\, r'')$ = Bessel function of second kind and n^{th} order

$Y_w^{TE_n}$ = wave admittance for TE_n mode = $\dfrac{k_{zn}}{\omega\, \mu_o}$

k_{zn} and $\hat{k}_{zn}$ are given below Eq. (IV.1)

$$k_{cn} = \sqrt{k_{ca}^2 - k_{zn}^2} = k_o \sqrt{\hat{k}_{ca}^2 - \hat{k}_{zn}^2} = k_o \hat{k}_{cn}$$

$$k_{ca} = k_o \sqrt{\hat{\varepsilon}_{cac}} \quad ; \quad \hat{k}_{ca} = \sqrt{\hat{\varepsilon}_{cac}}$$

$$\hat{\varepsilon}_{cac} = \frac{\varepsilon_{cac}}{\varepsilon_o} = \hat{\varepsilon}_{ca} + \frac{j\,\sigma_{ca}}{\omega\,\varepsilon_o} = \text{complex dielectric constant of cable material}$$

$$\hat{\varepsilon}_{ca} = \frac{\varepsilon_{ca}}{\varepsilon_o} \text{ , where } \varepsilon_{ca} = \text{permittivity of cable material}$$

σ_{ca} = conductivity of cable material

A^{TE_n} = amplitude of $J_n(\rho)$ term of TE_n mode

B^{TE_n} = amplitude of $N_n(\rho)$ term of TE_n mode

$$J_n'(k_{cn}\, r'') = \left(\frac{d\, J_n(\rho)}{d\rho}\right)_{\rho = k_{cn} r''}$$

$$N_n'(k_{cn}\, r'') = \left(\frac{d\, N_n(\rho)}{d\rho}\right)_{\rho = k_{cn} r''}$$

TM Modes $[\overline{H}_{z''}^{(n)}(r'') = 0]$

$$\underset{\rightarrow}{C}_{nE}^{TM}(r'') = \hat{\underset{\rightarrow}{r}}''\, \overline{E}_{r''}^{(n)}(r'') + \hat{\underset{\rightarrow}{\phi}}''\, \overline{E}_{\phi''}^{(n)}(r'') + \hat{\underset{\rightarrow}{z}}''\, \overline{E}_{z''}^{(n)}(r'') \qquad \text{(IV.3a)}$$

$$\underset{\rightarrow}{C}_{nH}^{TM}(r'') = \hat{\underset{\rightarrow}{r}}'' \, \overline{H}_{r''}^{(n)}(r'') + \hat{\underset{\rightarrow}{\phi}}'' \, \overline{H}_{\phi''}^{(n)}(r'') \qquad \text{(IV.3b)}$$

where

$$\overline{E}_{z''}^{(n)}(r'') = A^{TM_n} J_n(k_{cn} r'') + B^{TM_n} N_n(k_{cn} r'')$$

$$\overline{E}_{r''}^{(n)}(r'') = \frac{j \hat{k}_{zn}}{\hat{k}_{cn}} [A^{TM_n} J_n'(k_{cn} r'') + B^{TM_n} N_n'(k_{cn} r'')]$$

$$\overline{E}_{\phi''}^{(n)}(r'') = \frac{j n \hat{k}_{zn}}{\rho \hat{k}_{cn}} [A^{TM_n} J_n(k_{cn} r'') + B^{TM_n} N_n(k_{cn} r'')]$$

$$\overline{H}_{r''}^{(n)}(r'') = -Y_w^{TM_n} \overline{E}_{\phi''}^{(n)}(r'')$$

$$\overline{H}_{\phi''}^{(n)}(r'') = Y_w^{TM_n} \overline{E}_{r''}^{(n)}(r'')$$

where all quantities used in Eqs. (IV.3a,b) were defined below Eqs. (IV.2a,b) with the exceptions

A^{TM_n} = amplitude of $J_n(\rho)$ term of TM_n mode

B^{TM_n} = amplitude of $N_n(\rho)$ term of TM_n mode

$Y_w^{TM_n}$ = wave admittance of TM_n mode = $\dfrac{\omega \epsilon_{ca}}{k_{zn}}$

The TEM (standard coaxial) mode $[\overline{E}_{z''}^{(n)}(r'') = \overline{H}_{z''}^{(n)}(r'') = 0]$

At low frequencies we can limit propagation in a coaxial line to the transverse electromagnetic (TEM) mode, which has the form

$$\underset{\rightarrow}{E}(r'', \phi'', z'') = \hat{\underset{\rightarrow}{r}}'' \, E_{r''}^{(n)}(r'') = \hat{\underset{\rightarrow}{r}}'' \, \frac{V_o}{\ell n(b/a) r''} \, e^{jk_{ca}z''} \qquad \text{(IV.4a)}$$

$$\underset{\rightarrow}{H}(r'', \phi'', z'') = \hat{\underset{\rightarrow}{\phi}}'' \, H_{\phi''}^{(n)}(r'') = \hat{\underset{\rightarrow}{\phi}}'' \, \frac{Y_{ca} V_o}{\ell n(b/a) r''} \, e^{jk_{ca}z''} \qquad \text{(IV.4b)}$$

where k_{ca} is defined below Eqs. (IV.2a,b) and where

a = inner radius of cable

b = outer radius of cable

V_o = voltage between $r'' = a$ and $r'' = b$

$Y_{ca} = \sqrt{\frac{\epsilon_{ca}}{\mu_o}}$ = wave admittance of cable material

Equations (IV.4a,b) constitute a complete solution for the TEM fields. Equations (IV.2a,b) and (IV.3a,b) require the imposition of boundary conditions at $r'' = a$ and $r'' = b$ for completion. In the actual cable that is used in the configuration under study on this project, the inner boundary at $r'' = a$ may be well approximated by a perfect conductor. The outer boundary at $r'' = b$, since it contains the slots, may be approximated as a perfect conductor except in the slot region. An exact analysis would require consideration of a boundary, that is <u>not</u> cylindrically symmetric, i.e., partially

free space. Such an analysis would not be feasible within the time limitations of the project; hence, the fields are being approximated as if the cable had perfectly conducting inner and outer boundaries.

The result of these approximations is the condition that the tangential electric fields must vanish at both r" = a and r" = b; hence,

$$\bar{E}_{\phi''}^{(n)}(a) = \bar{E}_{\phi''}^{(n)}(b) = \bar{E}_{z''}^{(n)}(a) = \bar{E}_{z''}^{(n)}(b) = 0 \qquad \text{(IV.5)}$$

for both TE and TM modes.

Applying the conditions (IV.5) to Eqs. (IV.2a,b) and (IV.3a,b), we obtain the following results:

TE Modes

$$J_n'(k_{cn}\, a) + D^{TE_n} N_n'(k_{cn}\, a) = 0 \qquad \text{(IV.6a)}$$

$$J_n'(k_{cn}\, b) + D^{TE_n} N_n'(k_{cn}\, b) = 0 \qquad \text{(IV.6b)}$$

where

$$D^{TE_n} = \frac{B^{TE_n}}{A^{TE_n}}$$

TM Modes

$$J_n(k_{cn}\, a) + D^{TM_n} N_n(k_{cn}\, a) = 0 \qquad \text{(IV.7a)}$$

$$J_n(k_{cn}\, b) + D^{TM_n} N_n(k_{cn}\, b) = 0 \qquad \text{(IV.7b)}$$

where

$$D^{TM_n} = \frac{B^{TM_n}}{A^{TM_n}}$$

From Eqs. (IV.6a) and (IV.6b), we obtain the conditions required to determine k_{cn} for TE and TM modes respectively. Dividing Eq. (IV.6a) by Eq. (IV.6b) and Eq. (IV.7a) by Eq. (IV.7b), we obtain:

For TE modes

$$J_n'(k_{cn}\, a)\, N_n'(k_{cn}\, b) - J_n'(k_{cn}\, b)\, N_n'(k_{cn}\, a) = 0 \qquad \text{(IV.8a)}$$

and for TM modes

$$J_n(k_{cn}\, a)\, N_n(k_{cn}\, b) - J_n(k_{cn}\, b)\, N_n(k_{cn}\, a) = 0 \qquad \text{(IV.8b)}$$

In the configuration under investigation, a and b are extremely small compared with wavelength. Under the very plausible assumption that k_{cn} is of at least the same order of magnitude as k_o or at the very least no greater than one order of magnitude greater than k_o, a study of parameter values indicates that the argument k_{cn} a and k_{cn} b appearing in Eqs. (IV.8a,b) are all very small compared with unity. Hence the first few terms of the power series for the Bessel functions with small arguments can be used to put Eqs. (IV.8a,b) in a form where they can be easily solved for k_{cn}.

Also, it follows from either Eq. (IV.6a) or (IV.6b) that

$$D^{TE_n} = -\frac{J_n'(k_{cn}\,a)}{N_n'(k_{cn}\,a)} = -\frac{J_n'(k_{cn}\,b)}{N_n'(k_{cn}\,b)} \tag{IV.9a}$$

and from either Eqs. (IV.7a) or (IV.7b) that

$$D^{TM_n} = -\frac{J_n(k_{cn}\,a)}{N_n(k_{cn}\,a)} = -\frac{J_n(k_{cn}\,b)}{N_n(k_{cn}\,b)} \tag{IV.9b}$$

The fields on the slots are those corresponding to r" = b. Since those are the fields that must be evaluated in our problem, we will focus on them at this point.

From Eqs. (IV.2a,b), (IV.3a,b) and (IV.9a,b), we have, for the fields at r" = b:

TE Modes

$$\overline{H}_{z''}^{(n)}(b) = \frac{A^{TE_n}}{N_n'(k_{cn}\,b)}\, L_n(k_{cn}\,b) \tag{IV.10a}$$

$$\overline{H}_{r''}^{(n)}(b) = \overline{E}_{\phi''}^{(n)}(b) = \overline{E}_{z''}^{(n)}(b) = 0 \tag{IV.10b}$$

$$\overline{H}_{\phi''}^{(n)} = \frac{A^{TE_n}}{N_n'(k_{cn}\,b)}\,\frac{j\,n\,\hat{k}_{zn}}{b\,\hat{k}_{cn}^2}\, L_n(k_{cn}\,b) \tag{IV.10c}$$

$$\overline{E}_{r''}^{(n)}(b) = \frac{1}{Y_w^{TE_n}}\,\overline{H}_{\phi''}^{(n)}(b) \tag{IV.10d}$$

where

$$L_n(\rho) = J_n(\rho)\, N_n'(\rho) - N_n(\rho)\, J_n'(\rho)$$

TM Modes

$$\overline{E}_{z''}^{(n)}(b) = \overline{E}_{\phi''}^{(n)}(b) = \overline{H}_{z''}^{(n)}(b) = \overline{H}_{r''}^{(n)}(b) = 0 \qquad \text{(IV.11a)}$$

$$\overline{E}_{r''}^{(n)}(b) = \frac{-A^{TM_n}}{N_n(k_{cn}\, b)} \frac{j\, \hat{k}_{zn}}{\hat{k}_{cn}} L_n(k_{cn}\, b) \qquad \text{(IV.11b)}$$

$$\overline{H}_{\psi''}^{(n)}(b) = Y_w^{TM_n}\, \overline{E}_{r''}^{(n)}(b) \qquad \text{(IV.11c)}$$

The Bessel function series[A-4] have been evaluated to fourth order in the argument ρ, based on the observation that $(k_{cn}\, b) \ll 1$ in our problem. The results are:

$$J_0(\rho) \simeq 1 - \left(\frac{\rho}{2}\right)^2 + \frac{1}{4}\left(\frac{\rho}{2}\right)^4 \qquad \text{(IV.12a)}$$

$$J_1(\rho) \simeq \frac{\rho}{2}\left\{1 - \frac{1}{2}\left(\frac{\rho}{2}\right)^2 + \frac{1}{12}\left(\frac{\rho}{2}\right)^4\right\} \qquad \text{(IV.12b)}$$

$$J_2(\rho) \simeq \frac{\rho^2}{4}\left\{1 - \frac{\rho^2}{12} + \frac{\rho^4}{384}\right\} \qquad \text{(IV.12c)}$$

For $n \geq 3$

$$J_n(\rho) \simeq \frac{\rho^n}{2^n\, n!}\left\{1 - \frac{\rho^2}{2(2n+2)} + \frac{\rho^4}{2.4(2n+2)(2n+4)} - \ldots\right\} \qquad \text{(IV.12d)}$$

$$J_0'(\rho) \simeq -\frac{\rho}{2} + \frac{1}{2}\left(\frac{\rho}{2}\right)^3 \qquad \text{(IV.13a)}$$

$$J_1'(\rho) \simeq \frac{1}{2}\left\{1 - \frac{3}{2}\left(\frac{\rho}{2}\right)^2 + \frac{5}{12}\left(\frac{\rho}{2}\right)^4\right\} \qquad \text{(IV.13b)}$$

$$J_2'(\rho) \simeq \frac{\rho}{2}\left\{1 - \frac{\rho^2}{6} + \frac{\rho^4}{128}\right\} \qquad \text{(IV.13c)}$$

For $n \geq 3$

$$J_n'(\rho) \cong \frac{\rho^{n-1}}{2^n\, n!}\left\{n - \frac{(n+2)\rho^2}{2(2n+2)} + \frac{(n+4)\rho^4}{2.4(2n+2)(2n+4)}\right\} \qquad \text{(IV.13d)}$$

$$N_0(\rho) \simeq \frac{2}{\pi}\left\{\ell n\,\frac{\rho}{2} + \gamma\right\} J_0(\rho) + \frac{2}{\pi}\left\{\left(\frac{\rho}{2}\right)^2 - \frac{3}{8}\left(\frac{\rho}{2}\right)^4\right\}$$

$$= \frac{2}{\pi}\left\{\ell n\left(\frac{\rho}{2}\right)\left[1 - \left(\frac{\rho}{2}\right)^2 + \frac{1}{4}\left(\frac{\rho}{2}\right)^4\right]\right.$$

$$\left. + \left[\gamma + \left(\frac{\rho}{2}\right)^2(1-\gamma) + \frac{1}{8}\left(\frac{\rho}{2}\right)^4(2\gamma - 3)\right]\right\} \qquad \text{(IV.14a)}$$

where $\gamma = 0.5772156$

$$N_1(\rho) \simeq -\frac{2}{\pi\rho} \qquad \text{(IV.14b)}$$

$$N_2(\rho) \simeq -\frac{2}{\pi\rho}\left(\frac{2}{\rho}\right)\left\{1 + \left(\frac{\rho}{2}\right)^2\right\} \qquad \text{(IV.14c)}$$

For $n \geq 3$

$$N_n(\rho) \simeq -\frac{1}{\pi}\left(\frac{2}{\rho}\right)^n\{(n-1)! + (n-2)!\left(\frac{\rho}{2}\right)^2 + \frac{(n-3)!}{2}\left(\frac{\rho}{2}\right)^4\} \tag{IV.14d}$$

$$N_0'(\rho) \simeq \frac{2}{\pi}\left(\frac{1}{\rho}\right) J_0(\rho) + \frac{2}{\pi}\{\ell n\left(\frac{\rho}{2}\right) + \gamma\} J_0'(\rho) + \frac{2}{\pi}\{\left(\frac{\rho}{2}\right) - \frac{3}{4}\left(\frac{\rho}{2}\right)^3\}$$

$$= \frac{2}{\pi}\{\ell n\left(\frac{\rho}{2}\right)[-\left(\frac{\rho}{2}\right) + \frac{1}{2}\left(\frac{\rho}{2}\right)^3] + \frac{1}{\rho}$$

$$+ \left(\frac{\rho}{2}\right)\left(\frac{1-2\gamma}{2}\right) + \left(\frac{\rho}{2}\right)^3\left(\frac{4\gamma-5}{8}\right)\} \tag{IV.15a}$$

$$N_1'(\rho) \simeq \frac{2}{\pi\rho^2} \tag{IV.15b}$$

$$N_2'(\rho) \simeq \frac{1}{\pi}\left(\frac{2}{\rho}\right)^3 \tag{IV.15c}$$

For $n \geq 3$

$$N_n'(\rho) \simeq -\frac{1}{2\pi}\left(\frac{2}{\rho}\right)^{n+1}\{-n! + (n-2)!(2-n)\left(\frac{\rho}{2}\right)^2$$

$$+ \frac{(n-3)!(4-n)}{2}\left(\frac{\rho}{2}\right)^4\} \tag{IV.15d}$$

From Eqs. (IV.12a) through (IV.15d),

$$L_0(\rho) = J_0(\rho)\, N_0'(\rho) - J_0'(\rho)\, N_0(\rho) \simeq \frac{2}{\pi\rho} \tag{IV.16a}$$

$$\mathcal{L}_1(\rho) = J_1(\rho)\, N_1'(\rho) - J_1'(\rho)\, N_1(\rho)$$

$$\simeq \frac{2}{\pi\rho}\left\{1 - \left(\frac{\rho}{2}\right)^2 + \frac{1}{4}\left(\frac{\rho}{2}\right)^4\right\} \qquad \text{(IV.16b)}$$

$$\mathcal{L}_2(\rho) = J_2(\rho)\, N_2'(\rho) - J_2'(\rho)\, N_2(\rho)$$

$$\simeq \frac{2}{\pi\rho}\left\{1 - \frac{1}{4}\left(\frac{\rho}{2}\right)^4\right\} \qquad \text{(IV.16c)}$$

For $n \geq 3$

$$\mathcal{L}_n(\rho) = J_n(\rho)\, N_n'(\rho) - J_n'(\rho)\, N_n(\rho)$$

$$\simeq \frac{2}{\pi\rho}\left\{1 - \frac{1}{(n^2-1)}\left(\frac{\rho}{2}\right)^2 + \frac{1}{2(n^2-4)(n^2-1)}\left(\frac{\rho}{2}\right)^4\right\} \qquad \text{(IV.16d)}$$

The forms (IV.12a) through (IV.16d) are those actually used in the computer program. In view of the small values of ρ applicable to our problem, these forms are adequate approximations for these functions.

An aspect of this analysis we have not yet discussed is the determination of the attenuation α_n for each mode. The usual analytical procedure for the case of nearly perfectly conducting walls is as follows:[A-3] (a) Ignore the departure from the perfectly conducting wall case in calculating the fields inside the (possibly lossy) dielectric; (b) Consider the actual conductivity of the wall material and calculate the "surface impedance" along the walls; (c) Calculate the "surface current" $\vec{J}_S = \vec{n} \times \vec{H}$, where $\vec{H}$ is the loss-free magnetic field at the surface and $\vec{n}$ the normal unit vector; (d) Using the surface impedance and surface current, calculate the power loss per unit leng[illegible]

of line due to ohmic losses along the wall surface; (e) Using the Poynting theorem, calculate the losses due to the nonzero conductivity of the lossy dielectric material, assuming of course that the conductivity is nonzero; (f) Add the power loss per unit length due to both mechanisms (d) and (e) and calculate the resulting total attenuation α_n.

It was originally planned to carry out the procedures (a) through (f) above for each mode and thereby evaluate the attenuation α_n by purely analytical means. It was decided later that the degree of approximation of those calculations was even greater than that associated with the evaluation of the fields in the cable as if the walls were perfectly conducting. Also, in the actual cable, the slots should play a prominent role in the introduction of another source of energy loss. Obviously these slots will also perturb the magnitude and direction of the field vectors, but that effect is probably not as severe as the degree to which they will affect the attenuation. All of this is speculation of course, but based on such speculation and the computer time and other limitations on the project, it was decided to use empirically determined values of attenuation. That is what was done in the computer program.

Another issue that has not yet been discussed in detail is that of the determination of k_{cn} for each mode. This can be determined theoretically by solving the equations (IV.8a,b) for k_{cn}. We invoke the assumptions:

$$|k_{cn}\, a| \ll 1 \qquad \text{(IV.17a)}$$

$$|k_{cn}\, b| \ll 1 \qquad \text{(IV.17b)}$$

thereby justifying the use of the approximations leading to Eqs. (IV.12a)

through (IV.15d) in constructing the expressions on the left hand side of Eq. (IV.8a,b). We then construct these expressions and truncate the resulting series beyond the fourth power in k_{cn}. The results of these operations are two quadratic equations in k_{cn}^2, as follows:

TM Modes

$$A_n k_{cn}^4 + B_n k_{cn}^2 + C_n = 0 \qquad \text{(IV.18a)}$$

TE Modes

$$D_n k_{cn}^4 + E_n k_{cn}^2 + F_n = 0 \qquad \text{(IV.18b)}$$

where

$$A_o = \frac{1}{128} \{2 \ell n(\frac{b}{a})[a^4 + b^4 + 4a^2 b^2] + 3[a^4 - b^4]\}$$

$$B_o = \frac{1}{4} \{(b^2 - a^2) - (a^2 + b^2) \ell n(\frac{b}{a})\}$$

$$C_o = \ell n(\frac{b}{a})$$

$$D_o = a^2 b^2[(a^2 - b^2) + (a^2 + b^2) \ell n(\frac{b}{a})]$$

$$E_o = -[2(a^4 - b^4) + a^2 b^2 \ell n(\frac{b}{a})]$$

$$F_o = 16(a^2 - b^2)$$

$$A_1 = \frac{1}{192}\,(a^4 + b^4 + a^2\,b^2)$$

$$B_1 = -\,\frac{1}{8}\,(a^2 + b^2)$$

$$C_1 = 1$$

$$D_1 = \frac{5}{192}\,(a^4 + b^4 + a^2\,b^2)$$

$$E_1 = -\,\frac{3}{8}\,(a^2 + b^2)$$

$$F_1 = 1$$

$$A^2 = \frac{1}{384}\,(a^2 + b^2)[a^4 + b^4 + 8a^2\,b^2]$$

$$B_2 = -\,\frac{1}{12}\,(a^4 + b^4 + 4a^2\,b^2)$$

$$C_2 = a^2 + b^2$$

$$D_2 = \frac{1}{128}\,(a^2 + b^2)(a^4 + b^4)$$

$$E_2 = -\,\frac{1}{6}\,(a^4 + b^4 + a^2\,b^2)$$

$$F_2 = a^2 + b^2$$

For $n \geq 3$

$$A_n = \frac{1}{32n(n^2 - 4)(n^2 - 1)(ab)^n} \text{ -----}$$

$$\text{--- } \{(b^{2n} - a^{2n})\, n^2(a^2 - b^2)^2 + 3n(a^4 - b^4)(b^{2n} + a^{2n})$$

$$+ 2(a^4 + b^4 + 4a^2 b^2)(b^{2n} - a^{2n})\}$$

$$B_n = \frac{1}{4n(n^2 - 1)(ab)^n} \{(a^{2n} + b^{2n})\, n(a^2 - b^2) + (b^{2n} - a^{2n})(a^2 + b^2)\}$$

$$C_n = \frac{1}{n(ab)^n} [b^{2n} - a^{2n}]$$

$$D_n = \frac{1}{32n(n^2 - 4)(n^2 - 1)(ab)^n} \text{ -----}$$

$$\text{--- } \{(b^{2n} - a^{2n})[-n^4(a^2 - b^2)^2 + 10n^2(a^4 + b^4 - a^2 b^2)$$

$$+ 8a^2 b^2] + (b^{2n} + a^{2n})[n^3(a^4 - b^4) + 8n(a^4 - b^4)]\}$$

$$E_n = -nB_n + \frac{(b^{2n} - a^{2n})(a^2 + b^2)}{4(ab)^n}$$

$$F_n = -n^2 C_n$$

Equations (IV.18a,b) can be solved for k_{cn}. The solutions are:

$$(k_{cn})_{TM_n \text{ mode}} = \pm\sqrt{\frac{-B_n \pm \sqrt{B_n^2 - 4A_n C_n}}{2A_n}} \qquad \text{(IV.19a)}$$

$$(k_{cn})_{TM_n \text{ mode}} = \pm\sqrt{\frac{-E_n \pm \sqrt{E_n^2 - 4D_n F_n}}{2D_n}} \qquad \text{(IV.19b)}$$

A small program was written to implement the calculations embodied in Eqs. (IV.18a,b) and (IV.19a,b). From the k_{cn} values and the equation

$$k_{zn} = \sqrt{k_c^2 - k_{cn}^2} \qquad \text{(IV.20)}$$

we can determine the values of k_{zn}, the complex propagation constant for a particular mode.

Since the real part of k_{zn} is ω/v_p, where v_p is the phase velocity, and the imaginary part is a portion of the attenuation α_n (it does not include attenuation due to wall losses), it would seem that the calculations represented by Eqs. (IV.18a,b), (IV.19a) and (IV.20) would be sufficient to determine the propagation and attenuation (exclusive of wall losses, discussed elsewhere) properties of a TE_n or TM_n mode.

In the numerical computations presented in this report, we have not used the above formalism to obtain the propagation constants k_{zn}. Instead, we have used empirically determined values of the phase velocity and the attenuation, which circumvents the need for these computations.

However, the computation of both phase velocity and attenuation for each mode directly from the theory is quite feasible and simple to carry out. If there were justification for carrying out these computations in a practical

problem (i.e., if it were known that a number of higher order modes were propagating and if their relative amplitudes could be determined), it would be very easy to add this capability to our general computer program. At the relatively low frequencies of interest in this particular problem, most of the higher order modes would be highly evanescent and would contribute energy only from those slots near the power source; hence, they would not be very important contributors to the fields incident on the scatterer or the fields at the antenna.

MISSION
of
Rome Air Development Center

RADC plans and executes research, development, test and selected acquisition programs in support of Command, Control Communications and Intelligence (C^3I) activities. Technical and engineering support within areas of technical competence is provided to ESD Program Offices (POs) and other ESD elements. The principal technical mission areas are communications, electromagnetic guidance and control, surveillance of ground and aerospace objects, intelligence data collection and handling, information system technology, ionospheric propagation, solid state sciences, microwave physics and electronic reliability, maintainability and compatibility.

Printed by
United States Air Force
Hanscom AFB, Mass. 01731


FILMED
8